



# Extraction liquid-liquide modulée électrochimiquement et microextraction en phase solide de composés pharmaceutiques sélectionnés

Maizatul Najwa Jajuli

## ► To cite this version:

Maizatul Najwa Jajuli. Extraction liquid-liquide modulée électrochimiquement et microextraction en phase solide de composés pharmaceutiques sélectionnés. Chimie. Université de Lorraine; Universiti Sains Malaysia (Malaisie), 2019. Français. NNT : 2019LORR0127 . tel-02479399

**HAL Id: tel-02479399**

**<https://hal.univ-lorraine.fr/tel-02479399>**

Submitted on 14 Feb 2020

**HAL** is a multi-disciplinary open access archive for the deposit and dissemination of scientific research documents, whether they are published or not. The documents may come from teaching and research institutions in France or abroad, or from public or private research centers.

L'archive ouverte pluridisciplinaire **HAL**, est destinée au dépôt et à la diffusion de documents scientifiques de niveau recherche, publiés ou non, émanant des établissements d'enseignement et de recherche français ou étrangers, des laboratoires publics ou privés.



## AVERTISSEMENT

Ce document est le fruit d'un long travail approuvé par le jury de soutenance et mis à disposition de l'ensemble de la communauté universitaire élargie.

Il est soumis à la propriété intellectuelle de l'auteur. Ceci implique une obligation de citation et de référencement lors de l'utilisation de ce document.

D'autre part, toute contrefaçon, plagiat, reproduction illicite encourt une poursuite pénale.

Contact : [ddoc-theses-contact@univ-lorraine.fr](mailto:ddoc-theses-contact@univ-lorraine.fr)

## LIENS

Code de la Propriété Intellectuelle. articles L 122. 4

Code de la Propriété Intellectuelle. articles L 335.2- L 335.10

[http://www.cfcopies.com/V2/leg/leg\\_droi.php](http://www.cfcopies.com/V2/leg/leg_droi.php)

<http://www.culture.gouv.fr/culture/infos-pratiques/droits/protection.htm>

# Thèse

Présentée et soutenue publiquement pour l'obtention du titre de

DOCTEUR de L'UNIVERSITÉ DE LORRAINE

Spécialité : Chimie

Présentée par :

**MAIZATUL NAJWA BINTI JAJULI**

## **Extraction liquid-liquide modulée électrochimiquement et microextraction en phase solide de composés pharmaceutiques sélectionnés**

Thèse soutenue publiquement le 22 août 2019 à Penang (Malaisie) devant le jury composé de :

Isabelle, BILLARD	Directeur de Recherche CNRS, Université de Grenoble Alpes	Rapporteurs
Zulkarnain ZAINAL	Professeur, Universiti Putra Malaysia	Rapporteurs
Sabariah ISMAIL	Professeur USM	Examineurs
Noor Hana Hanif ABU BAKAR	Maitre de Conférence, USM	Examineurs
Gregoire HERZOG	Chargé de Recherche, CNRS LCPME	Examineurs
Bahrudin SAAD	Professeur, Universiti Teknologi Petronas	Examineurs
Marc HEBRANT	Professeur, UL LCPME, Directeur de thèse	Membres invités
Afidah ABDUL RAHIM	Professeur, USM, Malaysia	Membres invités
Mohd. Hazwan HUSSIN	Maitre de Conférence, USM, Directeur de thèse	Membres invités
Rohana ADNAN	Professeur, Dean USM	Membres invités

*Laboratoire de Chimie Physique et Microbiologie pour les Matériaux et l'Environnement*

*(LCPME), UMR CNRS-UL 7564 - 405 rue de Vandoeuvre, 54600, Villers-lès-Nancy, France*

## ACKNOWLEDGEMENT

First and foremost, my sincere glorifications and adorations go to Almighty Allah for his guidance, protection and strength over me to complete my co-tutelle research study between Universiti Sains Malaysia (USM) and Universite de Lorraine (UL). I would like to express my sincere gratitude to my supervisors, Dr. Mohd. Hazwan Hussin, Professor Bahruddin Saad and Professor Afidah Abdul Rahim from USM and Professor Marc Hebrant and Dr. Gregoire Herzog from UL for their supervision and insightful guidance throughout the entire period of my research. I will forever remain grateful for the continued help and wise counselling. The time, which they have invested in me, resulted in my tremendous personal development – I am in their debt.

My sincere appreciation goes to USM for its financial support under Graduate Research Assistance (GRA) and USM Short Term Grant (304/PKIMIA/6313303). I am also grateful for Campus France and Agence National de la Recherche Grant (ANR-14-CE14-002-01) for financial support in France.

Next, I would like to address my appreciation to the colleagues who contributed in this work Dr. Alonso Gamero-Quijano, and Dr. Mazidatul Akmam for the help and discussions. I would also like to thank my colleagues, Nur Hidayah, Nadhiratul Farihin, Syaza Atikah, Umie Fatihah and Nor Amira for their emotional support. Thank you to Martha Collins and Cheryl Karman, the ultimate lab and lunch partner. Also, other labmates Tauqir Nasir, Maciej Mierzwa, Lin Zhang, Christelle Ghazally, Salima Mesli, and others. Furthermore, thank you for the people who have helped me in the laboratory. Mr Zamri for the HPLC, Jaun Paul and Claire Genois for the technical assistance in LCPME.

My sincere gratitude and love go to my dear parents, Jajuli bin Marzuki and Hafisah binti Rafiee and the entire family for the consistent love, support, encouragement and guidance shown to me during the course of my study. To all my dear friends (especially KK12) whom I am so lucky to have, thanks for all your contributions both directly and indirectly towards my project and the entire PhD's programme.

***Maizatul Najwa Binti Jajuli, 2019***

## TABLE OF CONTENTS

<b>ACKNOWLEDGEMENT</b>	ii
<b>TABLE OF CONTENTS</b>	iv
<b>LIST OF TABLES</b>	viii
<b>LIST OF FIGURES</b>	x
<b>LIST OF ABBREVIATIONS</b>	xviii
<b>LIST OF SYMBOLS</b>	xxi
<b>ABSTRAK</b>	xxii
<b>ABSTRACT</b>	xxiv
<b>RÉSUMÉ</b>	xxvi
<b>CHAPTER 1 INTRODUCTION</b>	1
1.1 Sample preparation	1
1.1.1 Liquid-liquid extraction (LLE)	2
1.1.2 Solid phase extraction (SPE)	3
1.2 Solid phase microextraction	4
1.2.1 Adsorbents	11
1.3 Liquid phase micro-extraction (LPME)	13
1.3.1 Electrified interface between two immiscible electrolytes solutions	17
1.3.2 Pseudo Nernst equation on ITIES	18
1.3.3 Polarizable and non-polarizable liquid-liquid interfaces	20
1.3.4 Charge transfer at the ITIES	21
1.3.5 Electrochemically modulated liquid-liquid extraction	23
1.4 Target analytes	26
1.4.1 Biguanides (Metformin, Buformin, Phenyl biguanide,	27

Phenformin)	
1.4.2 Beta -blocker drug (Propranolol)	29
1.5 General problem statements	30
1.6 Objectives	32
1.7 Scope of study	33
<b>CHAPTER 2 GENERAL EXPERIMENTAL METHOD</b>	<b>34</b>
2.1 Experimental method I (Chapter 3 & 4)	34
2.1.1 Chemicals & reagents	34
2.1.2 Instrumentation	35
2.1.3 Cyclic voltammetry	36
2.1.4 Preparation of standard solution, aqueous and organic phase	38
2.1.5 Preparation of organic salt (BTTPA <sup>+</sup> TPBCl <sup>-</sup> )	38
2.2 Cyclic voltammetry studies	39
2.3 Experimental method II (Chapter 5)	44
2.3.1 Chemicals & reagents	44
2.3.2 Instrumentation	45
<b>CHAPTER 3 ELECTROCHEMICALLY MODULATED LIQUID-LIQUID EXTRACTION BASED ON POTENTIOSTATIC METHOD</b>	<b>46</b>
3.1 Methodology	46
3.1.1 Experimental strategy	46
3.1.2 Sample preparation by applying potential using potentiostat	46
3.2 Results and discussion	48
3.2.1 Optimization of HPLC method	48
3.2.2 Cyclic voltammetry study of targeted compounds	50

3.2.3 Hydrodynamic cell	55
3.2.4 Electrochemical extraction as sample preparation	64
3.3 Conclusion	71
<b>CHAPTER 4 ELECTROCHEMICALLY MODULATED LIQUID-LIQUID EXTRACTION BASED ON POTENTIOSTATIC-FREE METHOD</b>	72
4.1 Methodology	72
4.1.1 Cyclic voltammetry of rotating paddle in static ITIES cell	72
4.1.2 Preparation of standard solution, aqueous and organic phase	72
4.1.3 Preparation of organic salt ( $\text{TMA}^+\text{TPBCl}^-$ )	73
4.1.4 Preparation of urine samples	73
4.1.5 Sample preparation by interfacial potential difference by common ion	74
4.1.6 Method validation	75
4.2 Results and Discussion	77
4.2.1 Sample preparation using interfacial potential	77
4.2.2 Method of validation	99
4.3 Comparison to previously reported analytical methods	102
4.4 Conclusion	106
<b>CHAPTER 5 GRAPHENE AND ZEOLITE AS ADSORBENTS IN BAR-MICRO-SOLID PHASE EXTRACTION FOR THE HPLC DETERMINATION OF SELECTED PHARMACEUTICAL COMPOUNDS</b>	107
5.1 Methodology	107
5.1.1 Preparation of standard solutions	107
5.1.2 Urine samples	107
5.1.3 Preparation of bar-micro-solid phase extraction (bar- $\mu$ -SPE)	107

5.1.4 Bar- $\mu$ -SPE procedure	109
5.1.5 Method validation of bar- $\mu$ -SPE- HPLC method	111
5.1.6 Extraction efficiency (EE %) and enrichment factor (EF)	112
5.2 Results and discussion	113
5.2.1 Optimization of HPLC method	113
5.2.2 Type of adsorbents	115
5.2.3 Mixed-adsorbent	139
5.2.4 Comparison of performance between individual and mixed adsorbent	145
5.2.5 Comparison with previously reported analytical methods	147
5.3 Conclusion	150
<b>CHAPTER 6 GENERAL CONCLUSIONS AND SUGGESTIONS FOR FUTURE STUDIES</b>	151
6.1 Conclusion	151
6.2 Suggestions for future studies	154
<b>REFERENCES</b>	156
<b>APPENDICES</b>	
<b>LIST OF PUBLICATION</b>	

## LIST OF TABLES

		<b>Page</b>
Table 1.1	Steps involved in LLE, SPE and SPME as sample preparation method (Alpendurada, 2000)	5
Table 1.2	Techniques that are related to SPME method	7
Table 1.3	Relative permittivity, $\epsilon$ of solvents at 25°C	18
Table 1.4	Standard ion-transfer potentials, $\Delta_w^\circ\phi$ for different cations across interface of 1,2- dichloroethane and water	21
Table 1.5	Standard ion-transfer potentials, $\Delta_w^\circ\phi$ for different anions across interface of 1,2- dichloroethane and water	22
Table 1.6	Analytes of interest on ITIES applications	24
Table 1.7	Chemical structure, pKa, log $P_0$ values for biguanide compounds	27
Table 1.8	Chemical structure, pKa, log $P_0$ values for PROP	29
Table 3.1	Transfer potential, pKA, and log $P_0$ for each drug	52
Table 3.2	Current density for each electrochemical cell	62
Table 4.1	Equations of various boundary lines with coordinates of their end points a) MET b) PHEBI c) PHEN. The equations given correspond to the boundary lines shown in Figures 4.3-4.5. For all calculations, we have considered $V_{org} = V_{aq}$	82
Table 4.2	Equations of various boundary lines with coordinates of their end points for PROP. The equations given correspond to the boundary lines shown in Figures 4.6. For all calculations, we have considered $V_{org} = V_{aq}$	83
Table 4.3	Variation of conditions for the extraction step. Optimised parameters are in bold	91
Table 4.4	Variation of conditions for the back-extraction step. Optimised parameters are shown in bold	91
Table 4.5	Composition of the different phases for the control experiments 1-3	92

Table 4.6	Analytical parameters for the proposed method for MET, PHEBI and PHEN	102
Table 4.7	Comparison of the analytical performances of published extraction procedures with the method reported here	104
Table 5.1	Summary of the adopted conditions of bar- $\mu$ -SPE-HPLC method using graphene and zeolite as adsorbent	137
Table 5.2	Analytical parameters for the bar-uSPE-HPLC method using graphene as adsorbent	138
Table 5.3	Analytical parameters for the bar-uSPE-HPLC method using zeolite as adsorbent	138
Table 5.4	Recovery for urine that was spiked with 950 $\mu\text{g L}^{-1}$ of drugs mixture (n = 6)	139
Table 5.5	Summary of the final adopted conditions of bar- $\mu$ -SPE-HPLC method using mixed-adsorbent	142
Table 5.6	Analytical parameters for the bar-uSPE-HPLC method using mixed-adsorbent	143
Table 5.7	Intraday precision of the method using mixed-adsorbent (n=6)	144
Table 5.8	Interday precision of the method using mixed-adsorbent (n=6)	144
Table 5.9	Recovery of urine sample for using mixed-adsorbent (n=6)	144
Table 5.10	Comparison of previously determination method for MET, BUF, PHEN and PROP with this work	148

## LIST OF FIGURES

		<b>Page</b>
Figure 1.1	Configuration of sorbent in RDSE, SRSE, SCSE, A $\mu$ E and $\mu$ SPE method (Gilart et al., 2014; Sajid, 2017)	10
Figure 1.2	Summary on types of commercial adsorbents	11
Figure 1.3	Illustration of SDME methods (Tang et al., 2018)	14
Figure 1.4	Illustration of two- and three-phases of HF-LPME method (Vičkačkaitė and Padarauskas, 2012)	15
Figure 1.5	Illustration of DLLME method (Vičkačkaitė and Padarauskas, 2012)	16
Figure 2.1	Custom made electrochemical cells a) Static ITIES cell b) Rotating paddle in ITIES cell c) Rotating disk electrode with PET membrane supported ITIES for ion transfer studies. RE <sub>org</sub> : Reference electrode for the organic phase; RE <sub>aq</sub> : Reference electrode for the aqueous phase; CE <sub>aq</sub> : Counter electrode for the aqueous phase; CE <sub>org</sub> : counter electrode for the organic phase	35
Figure 2.2	Metathesis reaction of BTPPA <sup>+</sup> TPBCl <sup>-</sup>	38
Figure 2.3	Custom made electrochemical cell or ITIES cell for ion transfer studies. RE <sub>org</sub> : Reference electrode for the organic phase; RE <sub>aq</sub> : Reference electrode for the aqueous phase; CE <sub>aq</sub> : Counter electrode for the aqueous phase; CE <sub>org</sub> : counter electrode for the organic phase	39
Figure 2.4	Voltammogram for blank solution. Aquoues phase: 10 mm LiCl, Organic phase: 10 mM BTPPA <sup>+</sup> TPBCl <sup>-</sup> in 1,2- DCE, Reference electrode: Ag/AgCl, Counter electrodes: Pt, Scan rate: 5mV s <sup>-1</sup> . Blue region: Water, Yellow region: DCE	40
Figure 2.5	Voltammogram for blank solution containing MET. Aquoues phase: 10 mm LiCl, Organic phase: 10 mM BTPPA <sup>+</sup> TPBCl <sup>-</sup> in 1,2- DCE, Reference electrode: Ag/AgCl, Counter electrodes: Pt, Scan rate: 5mV s <sup>-1</sup> . Blue region: Water, Yellow region: DCE	42
Figure 2.6	Direction of ion transfer. C <sup>+</sup> : Cation, A <sup>-</sup> : Anion	43

Figure 3.1	Experimental procedure of the electrochemically modulated liquid-liquid extraction. Target cations are extracted from the aqueous sample to organic phase before being back-extracted to a final aqueous phase. The numbers 1, 2 and 3 correspond to the initial, intermediate and final stages at which the aqueous phases are analysed by HPLC	47
Figure 3.2	Chromatogram of MET, PHEBI, PHEN and PROP. Mobile phase: Phosphate buffer, 50: ACN, 50: triethylamine, 0.2. Column: Zorbax TMS (250 x 4.6 mm). Flow rate: 1.3 mL min <sup>-1</sup> . Injection volume: 20 µL. Column temperature: 40 °C. Wavelength: 230 nm. Concentration of analytes: 16.4 µM	49
Figure 3.3	Calibration curves for MET, PHEBI, PHEN and PROP obtained by HPLC. Mobile phase: Phosphate buffer, 50: ACN, 50: triethylamine, 0.2. Column: Zorbax TMS (250 x 4.6 mm). Flow rate: 1.3 mL min <sup>-1</sup> . Injection volume: 20 µL. Column temperature: 40 °C. Wavelength: 230 nm. Concentration of analytes: 0.8 -16 µM. MET (blue squares), PHEBI (grey circles), PHEN (orange triangles) and PROP (pink diamond)	50
Figure 3.4	Cyclic voltammograms of 170 µM MET (blue curve), PHEBI (grey curve), PHEN (orange curve) and PROP (pink curve) transferring across the ITIES. Electrochemical cell 1, Scan rate= 5 mV s <sup>-1</sup> . a) pH 6 b) pH 2. Experimental conditions: Aqueous phase: 10 mM LiCl. pH of aqueous phase: 6. Organic phase: 10 mM of BTPPA <sup>+</sup> TPBCl <sup>-</sup> in DCE. Scan rate: 5 mV s <sup>-1</sup> . Cell: Static ITIES cell	51
Figure 3.5	Graph of Galvanic transfer potential versus log P <sub>o</sub> for each drug	53
Figure 3.6	Effect of scan rate of on MET transfer. Experimental conditions: Aqueous phase: 10 mM LiCl. pH of aqueous phase: 6. Organic phase: 10 mM of BTPPA <sup>+</sup> TPBCl <sup>-</sup> in DCE. Scan rate: 5 - 25 mV s <sup>-1</sup> . Cell: Static ITIES cell. [MET] :0.280 mM	54
Figure 3.7	Peak current vs squares root of scan rate of MET. Experimental conditions: Aqueous phase: 10 mM LiCl. pH of aqueous phase: 6. Organic phase: 10 mM of BTPPA <sup>+</sup> TPBCl <sup>-</sup> in DCE. Scan rate: 5 - 25 mV s <sup>-1</sup> . Cell: Static ITIES cell. [MET] :0.280 mM	55

Figure 3.8	Effect of the concentration of MET. Experimental conditions: Aqueous phase: 10 mM LiCl. pH of aqueous phase: 6. Organic phase: 10 mM of BTPPA <sup>+</sup> TPBCl <sup>-</sup> in DCE. Scan rate: 5 mV s <sup>-1</sup> . Rotation speed: 100 rpm	56
Figure 3.9	A) Effect of the concentration of TEA <sup>+</sup> . Rotation speed= 100 and 200 rpm. B) Effect of the concentration of PROP. Rotation speed= 100 rpm. Experimental conditions: Aqueous phase: 10 mM LiCl. pH of aqueous phase: 6. Organic phase: 10 mM of BTPPA <sup>+</sup> TPBCl <sup>-</sup> in NPOE. Scan rate: 5 mV s <sup>-1</sup>	58
Figure 3.10	A) Effect of 0.029 mM TEA <sup>+</sup> B) Effect of the rotation speed (25-150 rpm). Experimental conditions: Aqueous phase: 10 mM LiCl. pH of aqueous phase: 6. Organic phase: 10 mM of BTPPA <sup>+</sup> TPBCl <sup>-</sup> in DCE. Scan rate: 5 mV s <sup>-1</sup>	60
Figure 3.11	Schematic to illustrate the flow lines at interface	61
Figure 3.12	Calibration curve of 1/I <sub>lim</sub> versus the inverse squares root of the rotation speed at 0.55 V	62
Figure 3.13	Effect of the type of cells on the current density. A) 10 mM LiCl B) TEA in 10 mM LiCl. Experimental conditions: Aqueous phase: 10 mM LiCl. pH of aqueous phase: 6. Organic phase: 10 mM of BTPPA <sup>+</sup> TPBCl <sup>-</sup> in DCE. Scan rate: 5 mV s <sup>-1</sup>	63
Figure 3.14	Chronoamperometry for different applied potential in the absence and in the presence of target analytes. Experimental conditions: Aqueous phase: 10 mM LiCl. Organic phase: 100 µL of 10 mM of BTPPA <sup>+</sup> TPBCl <sup>-</sup> in DCE. [Target analytes]: 0.164 mM. Scan rate: 5 mV s <sup>-1</sup> . Extraction time: 900 s. Rotation speed: 150 rpm. Cell: Rotating paddle in ITIES cell	65
Figure 3.15	Chronoamperometry for potential driven extraction of analytes. Experimental conditions: Aqueous phase: 10 mM LiCl. Organic phase: 100 µL of 10 mM of BTPPA <sup>+</sup> TPBCl <sup>-</sup> in DCE. [Target analytes]: 0.164 mM. Scan rate: 5 mV s <sup>-1</sup> . Time extraction: 900 s. Rotation speed: 150 rpm. Cell: Rotating paddle in ITIES cell	66

Figure 3.16	Graph of charge versus potential extraction of analytes, A) individually MET (blue curve), PHEBI (grey curve), PROP (pink curve) and mixed-drug (green curve). B) mixed-drugs simultaneously. Experimental conditions: Aqueous phase: 10 mM LiCl. Organic phase: 100 $\mu$ L of 10 mM of BTPPA <sup>+</sup> TPBCl <sup>-</sup> in DCE. [Target analytes]: 0.164 mM. Scan rate: 5 mV s <sup>-1</sup> . Time extraction: 900 s. Rotation speed: 150 rpm. Cell: Rotating paddle in ITIES cell	67
Figure 3.17	Comparison of faradaic and real extraction yield. Experimental conditions: Aqueous phase: 10 mM LiCl. Organic phase: 100 $\mu$ L of 10 mM of BTPPA <sup>+</sup> TPBCl <sup>-</sup> in DCE. [MET] = 0.164 mM. Time of extraction: 900 s. Potential applied: + 0.8 V. Rotation speed: 150 rpm. Cell: Rotating paddle in ITIES cell	69
Figure 3.18	Graph of moles extracted against back-extraction step. Experimental conditions: Aqueous phase: 100 $\mu$ L of H <sub>2</sub> O. Organic phase: 100 $\mu$ L of 10 mM of BTPPA <sup>+</sup> TPBCl <sup>-</sup> in DCE. [MET]: 0.164 mM. Vortex time: 90 s. Centrifuge time: 3 mins. Cell: Rotating paddle in ITIES cell	70
Figure 3.19	Graph of moles detected by HPLC against waiting time after extraction. Experimental conditions: Aqueous phase: 10 mM LiCl. Organic phase: 10 mM of BTPPA <sup>+</sup> TPBCl <sup>-</sup> in DCE. [MET] = 0.164 mM. Time extraction: 900 s. Potential applied: +0.8 V. Rotation speed: 150 rpm. Cell: Rotating paddle in ITIES cell	71
Figure 4.1	Metathesis reaction of TMA <sup>+</sup> TPBCl <sup>-</sup>	73
Figure 4.2	Distribution of the monocationic form (AH <sup>+</sup> ) of MET (blue curve), PHEBI (gray curve) and PHEN (orange curve) as a function of pH	78
Figure 4.3	Ionic partition diagram for MET	78
Figure 4.4	Ionic partition diagram for PHEBI	79
Figure 4.5	Ionic partition diagram for PHEN	79
Figure 4.6	Ionic partition diagram for PROP	80
Figure 4.7	Experimental procedure of the electrochemically modulated liquid-liquid extraction. Target cations are extracted from	84

the aqueous sample to organic phase before being back-extracted to a final aqueous phase. The numbers 1, 2 and 3 correspond to the initial, intermediate and final stages at which the aqueous phases are analysed by HPLC

Figure 4.8	Chromatograms obtained for a sample containing MET, PHEBI and PHEN at (A) 164 $\mu\text{M}$ each and at (B) 1.64 $\mu\text{M}$ each before (1) and after (2) extraction, in the aqueous back-extraction phase (3). Extraction conditions were $[\text{TMA}^+]_o = 10 \text{ mM}$ , $[\text{TMA}^+]_w = 0.001 \text{ mM}$ , pH 11, $V_{\text{DCE}} = 2 \text{ mL}$ , Rotation speed= 900 rpm, $t_{\text{ext}} = 15 \text{ min}$	85
Figure 4.9	Extraction efficiency as a function of (A) time and (B) rotation speed. Other experimental parameters were: $[\text{TMA}^+]_o = 10 \text{ mM}$ , $[\text{TMA}^+]_w = 0.001 \text{ mM}$ , pH 11, $V_{\text{DCE}} = 2 \text{ mL}$	88
Figure 4.10	A) Dependence of $\zeta_{\text{total}}$ as a function of the interfacial potential difference, $\Delta_o^w\phi$ , for extraction conditions of Figure 4.8. $[\text{Analyte}] = 164 \mu\text{M}$ for the blue curve and 1.64 $\mu\text{M}$ for the orange curve. B) Extraction efficiency as a function of initial concentration targeted analytes. Other experimental parameters were: $[\text{TMA}^+]_o = 10 \text{ mM}$ , $[\text{TMA}^+]_w = 0.001 \text{ mM}$ , pH 9, $V_{\text{DCE}} = 2 \text{ mL}$	90
Figure 4.11	Enrichment factors for 10 $\mu\text{M}$ MET, PHEBI and PHEN achieved for control experiments 1-3 and the extraction method proposed here. Experimental conditions for control 1-3 are given in Figure 4.5. Experimental conditions for the extraction method are the optimal conditions	92
Figure 4.12	Extraction efficiency as a function of Galvanic transfer potential. Other experimental parameters were: $[\text{TMA}^+]_o = 10 \text{ mM}$ , $[\text{TMA}^+]_w = 0.001 \text{ mM}$ , pH 11, $V_{\text{DCE}} = 0.3 \text{ mL}$	93
Figure 4.13	A) Enrichment factor as a function of Galvanic back-transfer potential. Other experimental parameters for back-extraction were: $[\text{TMA}^+]_o = 10 \text{ mM}$ , $[\text{TMA}^+]_{\text{back}} = 50 \text{ mM}$ , pH 2, $V_{\text{DCE}} = 2 \text{ mL}$ . B) Enrichment factor vs final volume of aqueous phase	95
Figure 4.14	%Extraction as a function of the enrichment factor for MET, (blue triangles) PHEBI (grey circles) and PHEN (orange	96

squares). The solid line represents the enrichment factor expected if back-extraction efficiency is 100 %

Figure 4.15	%Extraction yield of MET, (blue triangles) PHEBI (grey circles) and PHEN (orange squares) as a function of the interfacial potential difference at equilibrium $\Delta_o^w \phi_{Eq}^{Ext}$ . These experimental points were obtained for a variety of parameters. Solid lines are the expected extraction yields for each of the drugs according to Nernst equation	98
Figure 4.16	%Extraction vs $\Delta_o^w \phi_{Eq}^{Ext}$ for the extraction of propranolol. %Extraction vs EF	99
Figure 4.17	Chromatograms MET, PHEBI and PHEN after sample enrichment using the optimised conditions (shown in Tables 4.3 and 4.4). Concentrations ranged from 16 nM to 1.6 $\mu$ M	100
Figure 4.18	Chromatograms before (1) and after (2) extraction and after back-extraction (3). $[TMA^+]_o = 10$ mM, $[TMA^+]_w = 0.001$ mM, pH 6, $V_{DCE} = 2$ mL, rotation speed= 600 rpm, $t_{ext} = 15$ min. The chromatograms were obtained for sample pre-treated by dilution 1:4 in DI water	101
Figure 5.1	Preparation of bar- $\mu$ -SPE. a) Preparation of PP bag b) Insertion of metal rod in PP bag c) heat-sealed of edges d) completed device	108
Figure 5.2	Protocol of extraction and desorption steps	110
Figure 5.3	Chromatogram for the separation of analytes. HPLC conditions: mobile phase, 20 mM phosphate buffer (pH 6.2): ACN: trimethylamine (45:55:0.2, v/v) Column: Zorbax TMS (250 x 4.6 mm). Flow rate, 1.3 mL min <sup>-1</sup> : Injection volume, 20 $\mu$ L. Wavelength: 230 nm. Concentration of analytes: 1 mg L <sup>-1</sup>	114
Figure 5.4	Effect of type of adsorbents on extraction. Experimental conditions: Conditioning solvent: ACN, $V_{solution}$ : 20 mL, pH <sub>solution</sub> : 6, amount of adsorbent: 20 mg, time of extraction: 60 mins, rotation speed: 800 rpm	116
Figure 5.5	Effect of conditioning solvents on the extraction of drugs. Experimental conditions: $V_{solution}$ : 20 mL, pH <sub>solution</sub> : 6,	118

amount of adsorbent: 20 mg, time of extraction: 60 mins,  
rotation speed: 800 rpm

Figure 5.6	Effect of pH solution on the extraction of drugs. Experimental conditions: Conditioning solvent: ACN, $V_{\text{solution}}$ : 20 mL, amount of adsorbent: 20 mg, time of extraction: 60 mins, rotation speed: 800 rpm	120
Figure 5.7	Effect of amount of adsorbent on the extraction of drug. Experimental conditions: Conditioning solvent: ACN, $V_{\text{solution}}$ : 20 mL, pH <sub>solution</sub> : pH 10 (Graphene) and pH 3 (Zeolite), time of extraction: 60 mins, rotation speed: 800 rpm	122
Figure 5.8	Effect of volume of solution on the extraction of drugs. Experimental conditions: Conditioning solvent: ACN, pH <sub>solution</sub> : pH 10 (Graphene) and pH 3 (Zeolite), amount of adsorbent: 10 mg (Graphene) and 25 mg (Zeolite), time of extraction: 60 mins, rotation speed: 800 rpm	124
Figure 5.9	Effect of rotation speed on the extraction of drugs. Experimental conditions: Conditioning solvent: ACN, $V_{\text{solution}}$ : 10 mL, pH <sub>solution</sub> : pH 10 (Graphene) and pH 3 (Zeolite), amount of adsorbent: 10 mg (Graphene) and 25 mg (Zeolite), time of extraction: 60 mins	126
Figure 5.10	Effect of time of extraction of drugs. Experimental conditions: Conditioning solvent: ACN, $V_{\text{solution}}$ : 10 mL, pH <sub>solution</sub> : pH 10 (Graphene) and pH 3 (Zeolite), amount of adsorbent: 10 mg (Graphene) and 25 mg (Zeolite), rotating speed: 800 rpm	128
Figure 5.11	Effect of ionic strength, NaCl on the extraction of drugs. Experimental conditions: Conditioning solvent: ACN, $V_{\text{solution}}$ : 10 mL, pH <sub>solution</sub> : pH 10 (Graphene) and pH 3 (Zeolite), amount of adsorbent: 10 mg (Graphene) and 25 mg (Zeolite), time of extraction: 90 mins (Graphene) and 120 mins (Zeolite), rotating speed: 800 rpm	130
Figure 5.12	Effect on desorption solvents. Experimental conditions; $V_{\text{desorption solvent}}$ : 0.6 mL, sonication time: 30 mins. MET (vertical lines), BUF (horizontal lines), PHEN (cross), PROP (dots). Ion-pair reagent (IP): Sodium heptanesulphonate	132

Figure 5.13	Effect on time of desorption. Experimental conditions; $V_{\text{desorption solvent}}$ : 0.6 mL, Desorption solvents: 0.1 M IP in IPA, 0.1 M IP in ACN, sonication time: 30 mins. Ion-pair reagent (IP): Sodium heptanesulphonate. MET (red squares), BUF (blue circles), PHEN (yellow triangles), PROP (green stars)	134
Figure 5.14	Effect on desorption solvents volume. Experimental conditions; $V_{\text{desorption solvent}}$ : 0.6 mL, desorption solvents: 0.1 M IP in IPA, 0.1 M IP in ACN, sonication time: 30 mins. Ion-pair reagent (IP): Sodium heptanesulphonate. MET (red squares), BUF (blue circles), PHEN (yellow triangles), PROP (green stars)	136
Figure 5.15	% extraction vs % zeolite:graphene ratio. Experimental conditions: Conditioning solvent: ACN, $\text{pH}_{\text{solution}}$ : 6, time of extraction: 120 mins, rotation speed: 800 rpm	140
Figure 5.16	Effect of pH on extraction of drugs. Experimental conditions: Conditioning solvent: ACN, $V_{\text{solution}}$ : 10 mL, Zeolite: Graphene: 7:3, time of extraction: 120 mins, rotation speed: 800 rpm	141
Figure 5.17	Effect of desorption solvent on mixed-adsorbent. Experimental conditions: $V_{\text{Desorption solvent}}$ : 0.60 mL, sonication time: 30 mins	142
Figure 5.18	Typical chromatogram of urine sample that were spiked with the drug ( $950 \mu\text{g L}^{-1}$ ) using the bar- $\mu$ -SPE-HPLC method	145
Figure 5.19	EE % for different type of adsorbents studied	146
Figure 5.20	EF for different types of adsorbents studied	146

## LIST OF ABBREVIATIONS

$\mu$ -SPE	Micro-solid phase extraction
1,2-DCE	1,2-dichloroethane
A $\mu$ E	Adsorptive micro extraction
AAS	Atomic absorption spectroscopy
ACN	Acetonitrile
BTPPA	Bis(triphenylphosphoranylidene) ammonium
BUF	Buformin
CE	Capillary electrophoresis
CE	Counter electrode
CTC	Chlorotetracycline
CV	Cyclic voltammetry
CNT	Carbon nanotubes
D- $\mu$ -SPE	Dispersive micro-solid phase extraction
DI	Direct immersion
DLLME	Dispersive liquid-liquid micro-extraction
EE	Extraction efficiency
EF	Enrichment factor
ELMME	Electrochemically modulated liquid-liquid extraction
GC	Gas chromatography
GO	Graphene oxide
HF-LPME	Hollow -fibre liquid-phase micro-extraction
HPLC	High performance liquid chromatography
HS	Headspace
HS-SPME	Headspace-solid phase micro emission

IP	Ion-pair
IPA	2-Propranol
ITIES	Interface between two electrolyte solution
LiCl	Lithium chloride
LLE	Liquid-liquid extraction
LPME	Liquid phase micro extraction
LTL	Linde Type L
LOD	Limit of detection
Log P	Logarithm of partition coefficient
LOQ	Limit of quantification
MeOH	Methanol
MEPS	Microextraction by packed sorbent
MET	Metformin
MOF	Metal-organic frameworks
MWCNT	Multi-walled carbon nanotubes
NPOE	Nitrophenyl octyl ether
OTC	Oxytetracycline
PAH	Polyaromatic hydrocarbon
PE	Percentage of extraction
PET	Polyethyleneterephthalate
PHEBI	Phenyl biguanide
PHEN	Phenformin
PP	Polypropylene
PROP	Propranolol
Pt	Platinum
RE	Reference electrode

RDSE	Rotating disk sorbent extraction
SALLE	Salting out liquid-liquid extraction
SBSE	Stir bar sorptive extraction
SCSE	Stir-cake sorptive extraction
SDME	Single drop micro-extraction
SLM	Supporting liquid membrane
SPE	Solid phase extraction
SPME	Solid phase micro extraction
SRSE	Stir rod sorptive extraction
TC	Tetracycline
TEA	Tetraethylammonium
THF	Tetrahydrofuran
TMA	Tetramethylammonium
TPA	Tetrapropylammonium
TPBCl	Tetrakis(4-chlorophenylborate)
VALLME	Vortex assisted liquid-liquid extraction
β-blocker	Beta-blocker

## LIST OF SYMBOLS

$\varepsilon$	Relative permittivity
$a_i$	Activity of ion
$c_i$	Concentration of ion
$Z$	Charge
$F$	Faraday's constant
$R$	Gas constant
$T$	Temperature
$\Delta_o^w \phi$	Standard transfer potential
$\Delta_o^w \phi_i^{o'}$	Formal transfer potential

**KAEDAH PENGEKSTRAKAN CECAIR-CECAIR TERMODULASI  
ELEKROKIMIA DAN PENGEKSTRAKAN MIKRO FASA PEPEJAL BAGI  
PENENTUAN SEBATIAN FARMASEUTIKAL TERPILIH**

**ABSTRAK**

Kaedah penyediaan sampel konvensional bagi penentuan sebatian berkutub seperti pengekstrakan cecair-cecair (LLE) dan pengekstrakan fasa pepejal (SPE) secara umumnya diketahui tidak berkesan kerana melibatkan pelbagai langkah, pemulihan yang rendah dan penggunaan pelarut organik yang tinggi. Oleh yang demikian, tesis ini terkait dengan pembangunan kaedah penyediaan sampel baru, iaitu, pengekstrakan cecair-cecair termodulasi elektrokimia (EMLLE) dan pengekstrakan fasa pepejal mikro-batang ( $\mu$ -SPE-batang) bagi penentuan sebatian farmaseutikal terpilih, iaitu metformin (MET), buformin (BUF), penformin (PHEN), dan propranolol (PROP) yang mempunyai lipofilisiti yang berbeza dalam sampel biologi. Dalam kaedah EMLLE, bantuan medan elektrik telah digunakan untuk mengekstrak sebatian farmaseutikal di antara dua larutan elektrolit (ITIES). ITIES terbentuk apabila dua fasa pelarut pual (litium klorida) dan fasa organik (I, 2-dikloroetana), kedua-duanya mengandungi elektrolit bersentuh bersama. Keupayaan pindahan untuk setiap analit dianalisa menggunakan voltammetri. Corak keupayaan pemindahan mengikuti lipofilisiti adalah; propranolol <penformin <phenil biguanida<metformin. Pengekstrakan analit telah dilakukan dengan menggunakan keupayaan yang tetap bagi sistem dua fasa menggunakan potentiostat selama 15 minit. Prestasi pengekstrakan adalah lemah. Penetapan sel ITIES yang lain dan penetapan keupayaan antara muka oleh kekutuban kimia boleh dilakukan bagi meningkatkan prestasi pengekstrakan

menggunakan kaedah ini. Oleh yang demikian, teknik EMLLE adalah berdasarkan pada aplikasi keupayaan antara muka disebabkan kehadiran kepekatan ion tetramethylammonium ( $\text{TMA}^+$ ) yang berbeza seperti ion biasa dalam setiap fasa telah dikaji. Keadaan pengekstrakan optimum untuk kaedah ini adalah,  $[\text{TMA}^+]_o = 10 \text{ mM}$ ,  $[\text{TMA}^+]_w = 0.001 \text{ mM}$ ,  $V_{org} = 2 \text{ mL}$ ,  $pH_{sampel} = 9$ , kelajuan pusingan = 900 rpm, masa pengekstrakan = 600 s. Parameter yang dioptimumkan untuk pengekstrakan semula adalah:  $[\text{TMA}^+]_{kembali} = 50 \text{ mM}$ ,  $V_{akhir} = 0.1 \text{ mL}$ ,  $pH_{kembali} = 2$ . Hampir 100 % pengekstrakan analit sasaran telah dicapai, dan faktor pemerkayaan diperolehi sehingga  $\sim 60$  kali ganda bagi sebatian biguanida. Dalam kaedah  $\mu$ -SPE-batang, (penjerap dan rod logam kecil diletakkan dalam beg membran polipropilena). Berdasarkan pelbagai penjerap, grafin dan zeolit menunjukkan kebolehpayaan. Oleh yang demikian, keadaan pengekstrakan untuk setiap penjerap dan campuran penjerap telah dioptimumkan. Walaupun pengoptimuman dilakukan, pengekstrakan diketahui adalah rendah (5.03-39.2 %). Walau bagaimanapun, faktor pemerkayaan sebanyak 1.49 -14.9 telah diperolehi. Kedua-dua kaedah yang dicadangkan telah diaplikasikan bagi penentuan analit dalam air kencing. Pada keseluruhannya, kaedah baru yang dicadangkan ini adalah mudah dan mengurangkan penggunaan pelarut organik dengan ketara.

**ELECTROCHEMICALLY MODULATED LIQUID-LIQUID EXTRACTION  
AND MICRO-SOLID PHASE EXTRACTION METHODS FOR  
DETERMINATION OF SELECTED PHARMACEUTICAL COMPOUNDS**

**ABSTRACT**

Conventional sample preparation methods for the determination of polar compounds such as liquid-liquid extraction (LLE) and solid phase extraction (SPE) are generally not effective because of their multiple steps, low recovery and high consumption of organic solvents. Thus, this thesis deals with the development of new sample preparation methods, i.e, electrochemically modulated liquid-liquid extraction (EMLLE) and bar-micro solid phase extraction (bar- $\mu$ -SPE) to determine selected pharmaceutical compounds, i.e., metformin (MET), buformin (BUF), phenformin (PHEN), and propranolol (PROP) having varied lipophilicity in biological samples. In the EMLLE method, the aid of electric field was utilized to extract the pharmaceutical compounds across the interface between two immiscible electrolyte solutions (ITIES). ITIES formed when two bulk solvents aqueous phase (lithium chloride) and organic phase (1,2-dichloroethane), both containing electrolytes are brought into contact. Transfer potential for each analyte was analysed by voltammetry. The trend of transfer potential followed their lipophilicity; propranolol < phenformin < phenyl biguanide < metformin. Extraction of the analytes was performed by applying fixed potential to the biphasic system using potentiostat for 15 mins. The extraction performance was poor. Design of another ITIES cell and imposing interfacial potential by chemical polarization was done to enhance the extraction performance of this method. Thus, the EMLLE technique based on application of interfacial potential due to the presence of

different concentrations of tetramethylammonium ion ( $\text{TMA}^+$ ) as common ion in each phase was studied. The optimum extraction conditions for this method are,  $[\text{TMA}^+]_o = 10 \text{ mM}$ ,  $[\text{TMA}^+]_w = 0.001 \text{ mM}$ ,  $V_{org} = 2 \text{ mL}$ ,  $pH_{sample} = 9$ , rotation speed = 900 rpm, extraction time = 600 s. The optimised parameters for back-extraction are:  $[\text{TMA}^+]_{back} = 50 \text{ mM}$ ,  $V_{final} = 0.1 \text{ mL}$ ,  $pH_{back} = 2$ . Nearly 100 % extraction of targeted analytes was achieved, and the enrichment factor obtained was up to  $\sim 60$  for biguanide compounds. In the bar- $\mu$  -SPE method, adsorbent and a tiny metal rod was placed in a polypropylene membrane bag. Among the various adsorbents studied, graphene and zeolite showed some potential. Thus, extraction conditions were optimised for each adsorbent and adsorbent mixture. Despite the optimisations, the extraction was low (5.03-39.2 %). Nevertheless, enrichment factors of 1.49 -14.9 were obtained. Both proposed methods were applied to the determination of the analytes in urine. On the whole, the newly proposed methods are simple and markedly reduced consumption of organic solvents.

**EXTRACTION LIQUIDE-LIQUIDE MODULEE**  
**ÉLECTROCHIMIQUEMENT ET MICRO-EXTRACTION EN PHASE**  
**SOLIDE POUR LA DÉTERMINATION DE COMPOSÉS**  
**PHARMACEUTIQUES**

**RÉSUMÉ**

Les méthodes classiques de préparation d'échantillons pour la détermination de composés polaires, telles que l'extraction liquide-liquide (LLE) et l'extraction en phase solide (SPE), ne sont généralement pas efficaces en raison de multiples étapes, d'une faible récupération et d'une consommation élevée de solvants organiques. Cette thèse traite du développement de nouvelles méthodes de préparation d'échantillons, à savoir l'extraction par voie liquide-liquide modulée électrochimiquement (EMLLE) et l'extraction bar-micro en phase solide (bar- $\mu$ -SPE) afin de déterminer les composés pharmaceutiques metformine (MET), buformine (BUF), phénformine (PHEN) et propranolol (PROP). Dans la méthode EMLLE, un champ électrique a été appliqué pour extraire les composés pharmaceutiques ionisés à travers l'interface entre deux solutions électrolytiques non miscibles (ITIES). Des ITIES se forment lorsque deux solvants en vrac en phase aqueuse (chlorure de lithium) et en phase organique (I, 2-dichloroéthane), contenant l'électrolyte, sont mis en contact. Le potentiel de transfert pour chaque analyte a été analysé par voltamétrie. Le potentiel de transfert varie avec leur lipophilie; propranolol < phénformine < phényl biguanide < metformine. L'extraction des analytes a été réalisée en appliquant un potentiel fixe au système biphasique où l'aide d'une potentiostat pendant 15 minutes a donné des résultats médiocres. Une autre cellule de mesure et un potentiel interfacial obtenu par

polarisation chimique ont été mis en œuvre pour améliorer les performances d'extraction de cette méthode. Ainsi nous avons étudié la technique EMLLE basée sur l'application d'un potentiel interfacial due à la présence de différentes concentrations en ion tétraméthylammonium ( $\text{TMA}^+$ ) en tant qu'ion commun à chaque phase. Les conditions optimales d'extraction pour cette méthode sont les suivantes :  $[\text{TMA}^+]_o = 10 \text{ mM}$ ,  $[\text{TMA}^+]_w = 0,001 \text{ mM}$ ,  $V_{org} = 2 \text{ mL}$ ,  $pH_{\text{échantillon}} = 9$ , vitesse de rotation = 900 rpm, temps d'extraction = 600 s. Les paramètres optimisés pour la rétro-extraction sont les suivants :  $[\text{TMA}^+]_{\text{retour}} = 50 \text{ mM}$ ,  $V_{\text{final}} = 0,1 \text{ mL}$ ,  $pH_{\text{retour}} = 2$ . Les analytes ciblés ont été extraits à près de 100% et le facteur d'enrichissement obtenu jusqu'à environ 60 fois pour les biguanides. Dans le procédé bar- $\mu$ -SPE, (un adsorbant et une tige métallique ont été placés dans un sac à membrane en polypropylène). Parmi divers adsorbants étudiés, le graphène et une zéolite se sont révélés intéressants. Ainsi, les conditions d'extraction ont été optimisées pour ces deux adsorbants seuls et en mélange. Malgré les optimisations, l'extraction bas (5,03-39,2 %). Néanmoins, des facteurs d'enrichissement de 1,49 à 14,9 ont été obtenus. Les deux méthodes proposées ont été appliquées à la détermination des analytes dans l'urine. Dans l'ensemble, les méthodes nouvellement proposées sont simples et réduisent considérablement la consommation de solvants organiques.

## CHAPTER 1

### INTRODUCTION

Five steps are normally involved in an analytical procedure, which are; (i) sampling, (ii) sample preparation, (iii) separation, (iv) detection, and (v) data analysis. Although all these steps are connected to each other, it has been estimated that over 80 % of the analysis time is spent on sampling and sample preparation steps (Namera and Saito, 2013). If one of these steps is not performed properly, it would lead to error and inconsistent results (Pavlovic *et al*, 2007). Therefore, it is important to choose an appropriate sample preparation method for samples such as pharmaceutical drugs in biological fluids as it will influence the reliability and accuracy of analysis.

#### 1.1 Sample preparation

Samples from biological fluids such as urine and plasma contain complex matrix components, which are the main source of interference during analysis. These matrix components when analysed using high performance liquid chromatography (HPLC) could lead to loss of column efficiency and an increase in back-pressure due to system blockage caused by biological particles (Novakova and Vlckova, 2009). In addition to removing any interferences, the aim of sample preparation is also to preconcentrate analytes in a cleaner solution (Yamini *et al*, 2019). The preconcentration process happens when a sample is extracted from a large volume of sample solution into microliter volume of extracting solvent (Yamini *et al*, 2019). Characteristics of good sample preparation are simple, reproducible, not time-consuming, low solvent consumption, involve minimum steps and easy to automate (Abdel-Rahim *et al*, 2001). Various sample preparation methods have been introduced for analysis of drugs in

biological fluids such as protein precipitation, ultrafiltration, liquid-liquid extraction (LLE) and solid phase extraction (SPE).

The procedure for protein precipitation is, an internal standard is added with analytes to reduce/minimize the error of extraction and suitable organic solvent or precipitating agents is used to aid the precipitation of proteins. Common organic solvents used for protein precipitation are acetone, acetonitrile, and acetic anhydride. The supernatant produced is reconstituted with mobile phase before injecting into a chromatographic instrument to avoid poor peaks (Ali *et al.*, 2015). Even though protein precipitation is a simple method, unfortunately, it is ineffective to remove all endogenous substances as well as co-precipitation is possibly formed. This method lacks sensitivity and is time consuming due to the sample dilution and evaporation if needed (Mullet, 2007; Gabr *et al.*, 2010). Meanwhile, the most common extraction method used to isolate target analytes that is based on the phase transfer of analytes species from one liquid to another liquid phase is known as LLE or from liquid to solid phase and it is known as SPE.

#### **1.1.1 Liquid-liquid extraction (LLE)**

LLE is a classical method widely used in a variety of industries: chemical, pharmacy, food industry, oil refining, in nuclear industry as well as hydrometallurgical processes (Warade *et al.*, 2011). LLE leads to the mass transfer of a dissolved analyte from its solvent to another solvent (Zhang *et al.*, 2019). One phase is usually an aqueous phase and the second one is an organic solvent. There are some of the organic phase that is denser than the aqueous phase such as dichloroethane. Both solvents must be immiscible or partially immiscible with each other and will form two layers. (Dean, 2009). The relative solubility of analytes in two phases is the key to the separation.

Lipophilicity refers to the ability of a compound to dissolve in oil, lipids, or non-polar solvents such as 1-octanol or hexane. The lipophilicity can be defined as  $\log P_0$  value or known as a partition coefficient of un-ionized compounds between water and octanol (Vraka *et al.*, 2017; Hill *et al.*, 2010). LLE method is popular due to its simplicity. By choosing a suitable solvent, it can isolate targeted drugs from their endogenous components. The major drawbacks of LLE are consumption of a large volume of solvents, emulsion formation that leads to loss of analyte and low recovery, and time-consuming. In addition, LLE is not suitable with all drugs especially with polar drugs (Mcdowall *et al.*, 1986).

### **1.1.2 Solid phase extraction (SPE)**

SPE is a frequently used extraction technique for liquid samples. Unlike LLE, SPE use solid material or known as sorbent to isolate analyte of interest. The principle of SPE is based on the partition of analytes between liquid and adsorbent. The basic protocols of SPE consist of four steps; (i) conditioning of adsorbents, (ii) loading of sample, (iii) washing away undesired components, and (iv) elution of analytes (Andrade-Eiora *et al.*, 2016).

The SPE technique overcomes the drawbacks of LLE by using lower volumes of solvents, then generating less waste. It also produces cleaner extract. (Vasconcelos and Fernandes, 2017). Adsorbents in SPE can be prepared in several formats such as cartridge, disk, 96-well SPE plates and pipette tips (Zwer-Ferenc and Biziuk, 2006). During the extraction process, the analytes are adsorbed onto the sorbent in cartridge which can prevent any loss or change in analytes concentration, resulting in high recovery. The main benefit of SPE is that it can extract non-polar to very polar analytes (Andrade-Eiora *et al.*, 2016). However, there are some disadvantages of SPE. The

extraction involves multiple steps (i.e., conditioning, washing, loading, elution and evaporation) and it is time consuming. In SPE, it is important to choose appropriate adsorbent to obtain excellent retention and elution of analytes.

## **1.2 Solid phase microextraction**

Microextraction is a technique that uses small volumes ( $\mu\text{L}$  range) or amount of extraction medium (less than 100 mg), either liquid or solid. (Pawliszyn & Pedersen-Bjergaard, 2006). There are two categories in microextraction techniques which are, solvent microextraction and sorbent microextraction. Generally, solvent microextraction is known as liquid phase microextraction (LPME) and sorbent microextraction as solid phase micro extraction (SPME).

The SPME was introduced in 1990. The technique is based on the diffusion of analytes from sample to the adsorbent materials. In the first experiment, adsorption of analytes onto a solid coated optical fibre was used (Pawliszyn and Arthur, 1990). The first commercial SPME device was introduced in 1993 by Supelco (Pawliszyn, 2009). This method rapidly gained popularity with increasing number of publications. Even though at first, the technique was introduced in the environmental field for relatively volatile sample analysis, the applications are extended to non-volatile compounds. There are two steps in the SPME protocol. First is the partition of target analytes between the sample matrix to the coating. In the second step, the concentrated analytes are desorbed into the analytical instrument such as GC or HPLC. Table 1.1 shows the comparison between SPME and conventional extraction methods (LLE and SPE).

Table 1.1: Steps involved in LLE, SPE and SPME as sample preparation method (Alpendurada, 2000)

Method	General procedure
LLE	<ul style="list-style-type: none"> <li>- Addition of organic solvents</li> <li>- Agitation of solution</li> <li>- Separation of aqueous and organic phases</li> <li>- Evaporation of organic phase</li> <li>- Injection into analytical instrument</li> </ul>
SPE	<ul style="list-style-type: none"> <li>- Conditioning of cartridges/disk/column</li> <li>- Washing and loading sample</li> <li>- Elution of analytes using suitable solvent</li> <li>- Evaporation of organic phase</li> <li>- Injection into analytical instrument</li> </ul>
SPME	<ul style="list-style-type: none"> <li>- Extraction onto adsorbent</li> <li>- Desorption of analyte</li> </ul>

SPME has now become one of the commonly-used techniques in sample preparation. The benefits of SPME method are the reduction in extracting phases used, the analysis time is short, and it is also simple to carry out. In addition, it improves selectivity of extraction, facilitating automation, low-cost because of the low amount of solvent used, and can be coupled to most of analytical instruments such as GC, HPLC, AAS, CE, to name a few. Another advantage of the technique is that derivatizations can be carried out on the fibres.

Extraction can be performed either in the direct immersion (DI) or headspace (HS) modes. Unfortunately, both modes have their own limitations. Fibre is directly exposed to sample matrix in DI mode. Binding of interference substances from complex matrices such as food, sludge and biological samples onto the fibre has been encountered. HS-SPME is best applicable to volatile substances only. Due to these limitations, the hollow cellulose membrane protected SPME fiber was developed in 1996 and it can be immersed directly into complex samples. This was followed in 2004, by the use of polypropylene hollow fibre membrane protected SPME to analyse

triazines in milk and sludge samples (Pawliszyn and Zhang, 1993; Basheer and Lee, 2004). Several variations of the SPME technique have been developed such as microextraction in packed syringe (MEPS), stir bar sorptive extraction (SBSE), stir-cake sorptive extraction (SCSE), to name a few. Table 1.2 illustrates these related techniques. It also summarizes the benefits and drawbacks of each method.

Table 1.2: Techniques that are related to SPME method

Techniques	Description	Main features	References
Microextraction by packed sorbent (MEPS)	Sorbent is inserted into the barrel of syringe or between the syringe barrel. The injection needle is defined as a cartridge.	<p>Advantages</p> <ul style="list-style-type: none"> <li>- Automation</li> <li>- Extraction of wide range of analytes</li> <li>- Less time consuming</li> </ul> <p>Disadvantages</p> <ul style="list-style-type: none"> <li>- Irrepeatability</li> </ul>	Nováková and Vlčková, 2009
Stir bar sorptive extraction (SBSE)	PDMS as a polymeric phase is coated on magnetic stir bar. It promotes hydrophobic interaction with analytes. The analytes are desorbed using suitable organic solvents. The configuration is shown in Figure 1.1.	<p>Advantages</p> <ul style="list-style-type: none"> <li>- Eliminates use of solvents</li> <li>- Reduces labour sample preparation</li> <li>- Less time consuming</li> </ul> <p>Disadvantage</p> <ul style="list-style-type: none"> <li>- Limited analytes as most of the coating is nonpolar</li> <li>- High matrix effects</li> </ul>	Nogueira, 2015
Stir-cake sorptive extraction (SCSE)	Microporous materials (monolith) is placed inside a special holder. In the lower part of the cake holder, a mixture made from iron is coated with a glass protection layer (Figure 1.1).	<p>Advantages</p> <ul style="list-style-type: none"> <li>- The sorbent does not touch the bottom of the vessel</li> <li>- High recovery</li> <li>- Low detection limit</li> <li>- Easy to use</li> </ul> <p>Disadvantage</p> <ul style="list-style-type: none"> <li>- Possibility of high matrix effect</li> </ul>	Spietelun <i>et al.</i> , 2013

Table 1.2: Continued

Rotating disk sorbent extraction (RDSE)	PDMS as a stationary phase is deposited by sol-gel method on the Teflon disk. The bottom part is placed in a magnetic stirrer (Figure 1.1)	<p>Advantages</p> <ul style="list-style-type: none"> <li>- Improved enrichment factor due to strong stirring</li> <li>- Better recovery compared to SBSE</li> </ul> <p>Disadvantage</p> <ul style="list-style-type: none"> <li>- Possibility of high matrix effect</li> </ul>	Spietelun <i>et al.</i> , 2013
Stir rod sorptive extraction (SRSE)	Improved format of SBSE, RDSE and SCSE. It set up includes a metal rod, at one edge having magnet and the monolith polymer coating and shown in Figure 1.1.	<p>Advantages</p> <ul style="list-style-type: none"> <li>- Good extraction capacity</li> <li>- Easy to prepare and use</li> <li>- Device can be used for a long time</li> </ul> <p>Disadvantages</p> <ul style="list-style-type: none"> <li>- Strong matrix effects</li> <li>- More research necessary</li> </ul>	Plotka-Wasyłka <i>et al.</i> , 2015
Micro-solid phase extraction ( $\mu$ -SPE)	<p>Small amount (5-20 mg) of adsorbent is placed inside a small bag made up from porous membrane. The porous membrane bag is closed by heat-sealing the edges. It is as illustrated in Figure 1.1.</p> <p>The bag is conditioned before immersed in sample solution for extraction. Desorption of analytes was done by aid of ultrasonication with suitable <math>\mu</math>L of organic solvent.</p>	<p>Advantages</p> <ul style="list-style-type: none"> <li>- Protected from dirty matrixes</li> <li>- Cheap</li> <li>- EF is higher than SPME</li> <li>- The device is reusable</li> <li>- Flexible choice of sorbents</li> </ul> <p>Disadvantages</p> <ul style="list-style-type: none"> <li>- Long extraction time</li> <li>- High precision value (% RSD)</li> <li>- Possible to carry over analytes when re-use the bag</li> </ul>	Basheer <i>et al.</i> , 2006; Sajid, 2017

Table 1.2: Continued

Adsorptive $\mu$ - extraction (A $\mu$ E)	<p>Two geometrical configurations:</p> <p>i) Bar-adsorptive micro-extraction (BA<math>\mu</math>E)</p> <p>ii) Multi-spheres adsorptive micro-extraction (MSA<math>\mu</math>E)</p> <p>Generally, the sorbent is embedded physically on the substrate and placed in the sample solution. The solution is stirred using stir-bar or vortexed.</p>	<p>Advantages</p> <ul style="list-style-type: none"> <li>- For polar analytes</li> <li>- It is easy to prepare</li> <li>- Cheap</li> <li>- Selective as sorbent can be chosen depending on analyte of interest</li> </ul> <p>Disadvantages</p> <ul style="list-style-type: none"> <li>- Device's stability should be assessed in a case-by-case basis</li> </ul>	Neng <i>et al.</i> , 2010, Nogueira, 2012
Dispersive $\mu$ -SPE (D- $\mu$ -SPE)	An adsorbent is dispersed in the sample solution for extraction process by ultrasound-assisted or vortex-assisted. After the extraction, the adsorbent is recovered by centrifugation or filtration and external magnet (for magnetic adsorbent).	<p>Advantages</p> <ul style="list-style-type: none"> <li>- Simple</li> <li>- Increase extraction efficiency</li> <li>- Easy on-site reaction</li> </ul> <p>Disadvantages</p> <ul style="list-style-type: none"> <li>- Not feasible for automation</li> </ul>	Chisvert <i>et al.</i> , 2019 Khezeli and Daneshfar, 2017

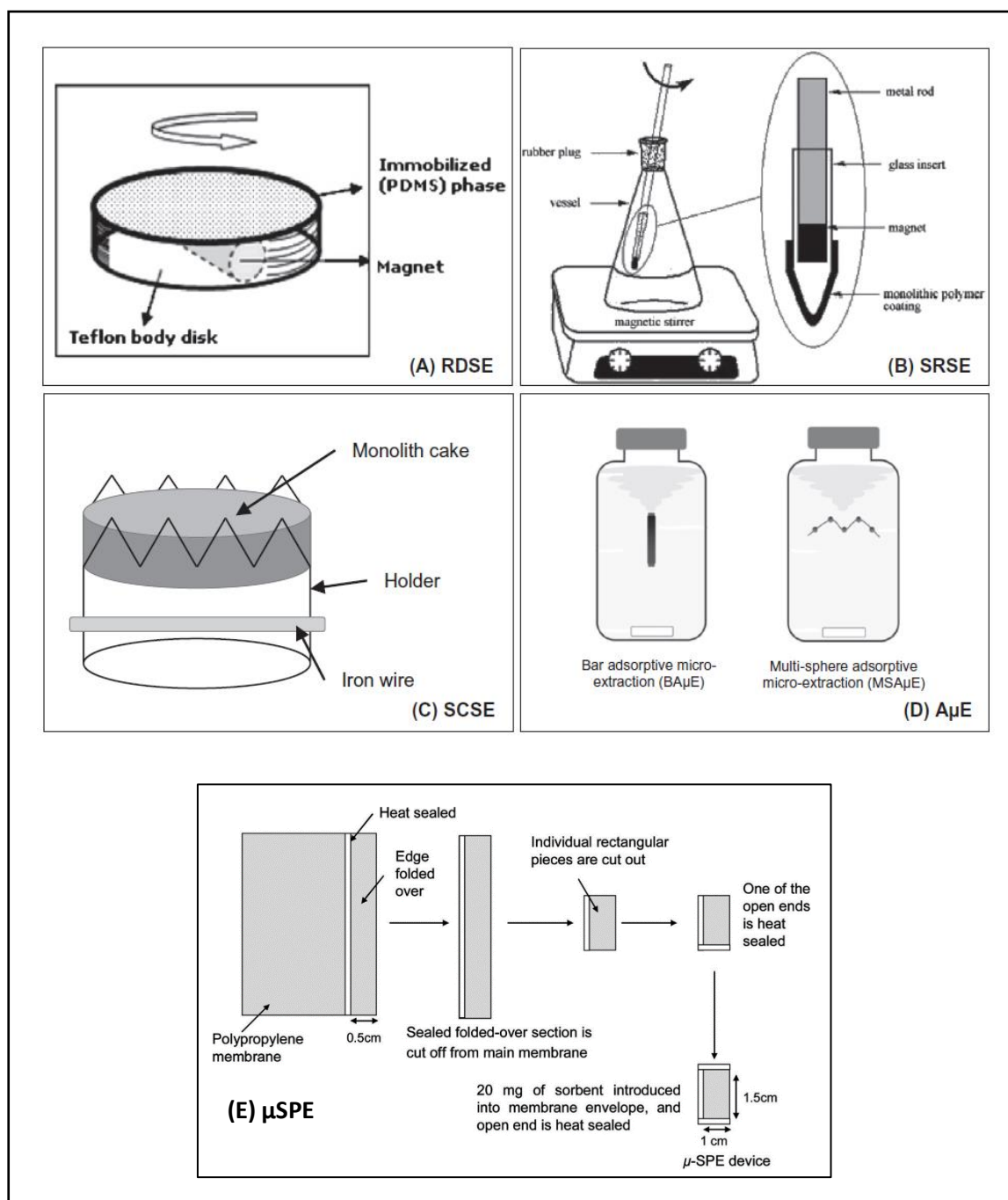


Figure 1.1: Configuration of adsorbent in RDSE, SRSE, SCSE, A $\mu$ E and  $\mu$ SPE method (Gilart *et al.*, 2014; Sajid, 2017)

### 1.2.1 Adsorbents

Variety types of solid materials are used as adsorbents in SPE as well as  $\mu$ -SPE. A good adsorbent is the one that can selectively extract the analyte of interest and able to achieve high enrichment factor. Several adsorbents are available such as the conventional adsorbent, ion imprinted materials, magnetic materials, core shell material, mesoporous materials, carbon nanotubes, graphene, TiO<sub>2</sub> nanotubes and arrays, bio sorbents, zeolite and metal organic framework.

Conventional commercialised adsorbents (Figure 1.2) can be categorised as normal phase, reverse phase, ion-exchange and polymer mixed-mode adsorbents (Krishann and Ibrahim, 1994) (Figure 1.2). Of these, C18 is the most popular. Extraction of the polar estrogen in ovarian cyst fluid samples was done by the slightly more polar C<sub>2</sub> because it shows more affinity towards C<sub>2</sub> compared to C<sub>8</sub>, C<sub>18</sub> or activated carbon, Haye-Sep A and Haye-Sep B (Kanimozhi *et al.*, 2011). Meanwhile, C<sub>18</sub> was employed to extract carbamazepine in surface water. C<sub>18</sub> was chosen because it has low polarity and carbamazepine is fairly hydrophobic (Teo *et al.*, 2016).

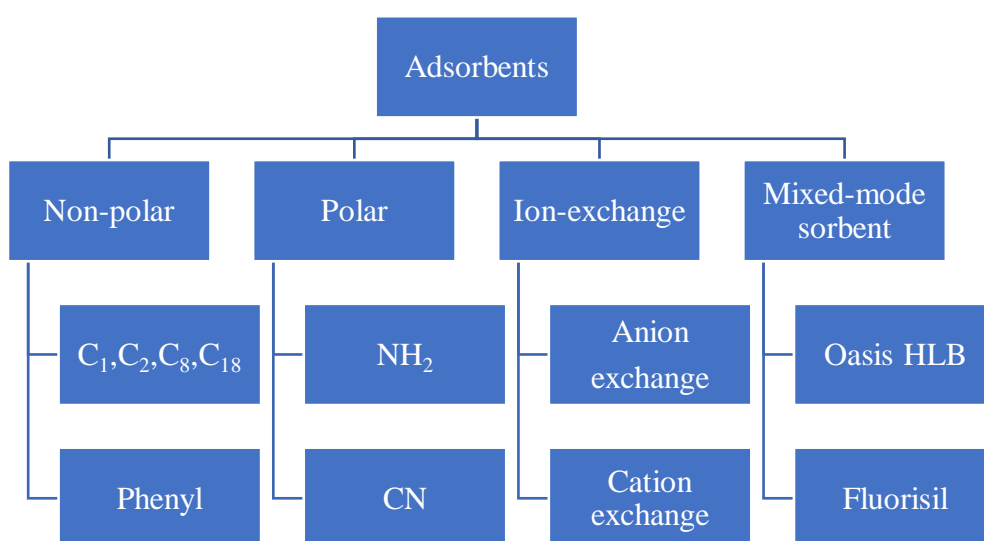


Figure 1.2: Summary on types of commercial adsorbents

Carbon nanotubes (CNT) is a rolled graphene sheet, and it was discovered in 1991 and became popular because of its high surface area, stability and mechanical strength (Iijima, 1991). CNTs can be classified as single-walled CNTs (SWCNTs) (one sheet) and multi-walled CNTs (MWCNTs) (more than one sheet). MWCNTs were used for determination of 16 polycyclic aromatic hydrocarbons (PAHs) in environmental water sample. It is effective compared to C<sub>2</sub>, C<sub>18</sub>, graphite fiber and granular carbon owing to the  $\pi$ - $\pi$  electrostatic interaction with aromatic rings of PAHs (Guo and Lee, 2011). The oxidised MWCNTs also exhibit high removal efficiency of metals such as manganese (96.8 %) from water (Ganesan *et al.*, 2013).

Recently, graphene has command considerable interest in sample preparation. The merits of graphene are the ultra-high surface area, double-sided surface area, chemical stability and excellent thermal stability. Graphene as an adsorbent in SPE for organochloride pesticide in water was reported (Han *et al.*, 2013). Graphene also was used to extract polar estrogen in water (Naing *et al.*, 2016). The product of graphite oxidation produces graphene oxide (GO). GO has more hydroxyl and carboxy groups compared to graphene, thus Co(II) and Ni(II) was pre-concentrated up to factor 250 by GO column in the SPE mode (Poujavid *et al.*, 2015). Simple SPME-GC-MS was developed to determine 16 PAHs in mainstream cigarette smoke (Wang *et al.*, 2015).

Metal-organic frameworks (MOFs) were increasingly used in SPE thanks to their unique properties such as the extremely high surface area, easy modification of surfaces and tunable pore size. MOFs consist of inorganic metal centres and organic linkers by coordinated bonds (Xiao *et al.*, 2016). The MOFs were used to remove the harmful dyes, methyl orange and methyl blue from contaminated water. The MOFs

used were based on iron terephthalate which is able to adsorb better than activated carbon (Haque *et al.*, 2011).

Zeolite is known as a group of open-framework aluminosilicates materials having well-defined microporous channels. The frameworks are constructed from tetrahedral consisting cations (Si/Al and oxygen atoms at the centre and corners, respectively). Due to the presence of Al, zeolites exhibit a negatively charged framework which is compensated by exchangeable cations that generate a system of pores and cavities of molecular dimensions (Li *et al.*, 2017). Zeolites as adsorbents have been broadly used in separation and environmental remediation. Invention of the first synthetic zeolite Linde Type L (LTL) was done in the 1960s (Gaona-Gomez., 2012). Zeolite LTL is a one-dimensional 12 membered-ring channel system. Zeolite LTL which have different sizes and shapes were investigated to extract the mycotoxin ochratoxin A (OTA) in coffee and cereal. The highest extraction efficiency was obtained by cylinder shaped LTL (Lee *et al.*, 2012). Meanwhile, online- SPE method using zeolite imidazole framework-8 (ZIF-8) was used to determine oxytetracycline (OTC), tetracycline (TC) and chlorotetracycline (CTC) in water and milk samples (Yang *et al.*, 2013).

### **1.3 Liquid phase micro-extraction (LPME)**

Liquid phase micro-extraction LPME techniques use minute amounts ( $\mu\text{L}$ ) of extracting solvent (water-immiscible). Several types of LPME techniques have been proposed such as single drop micro-extraction (SDME), hollow -fiber liquid-phase micro-extraction (HF-LPME), dispersive liquid-liquid micro-extraction (DLLME).

The SDME technique is based on a single drop of organic solvent hanging on the tip of micro-syringe needle into liquid sample either by direct immersion or head space mode. After the extraction, the drop is directly injected into analytical instruments (normally GC). Some disadvantages of SDME are low precision, reduction of extraction efficiency due to limited drop volume and low sensitivity, and mechanical stability of the drop is poor as it is easily dislodged (Farajzadeh *et al.* 2014; Kokosa, 2015; Pano-Farias *et al.*, 2017). Figure 1.3 illustrated SDME method.

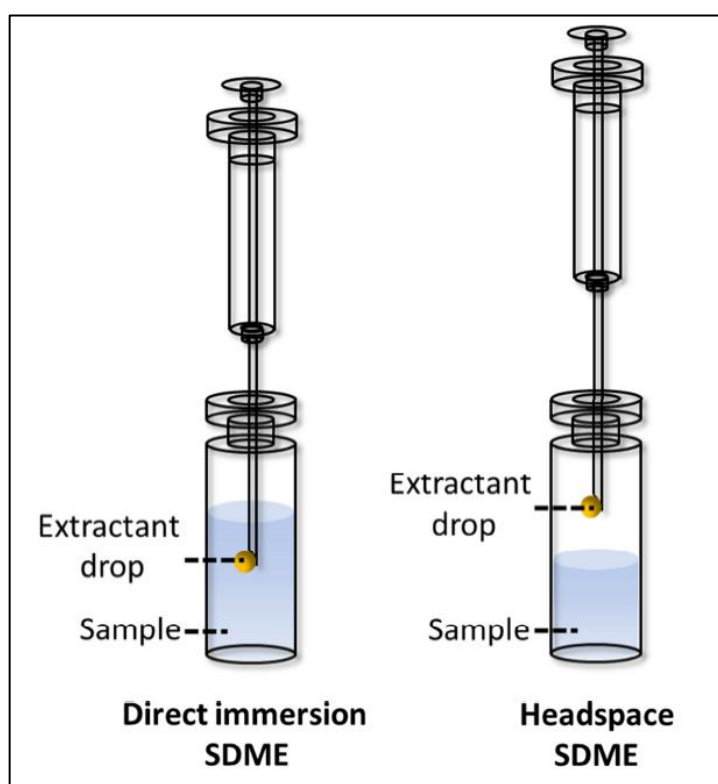


Figure 1.3: Illustration of SDME methods (Tang et al., 2018)

The HF-LPME method uses a hollow porous fibre (normally polypropylene) to trap the extraction solvent immersed in an aqueous solution (Figure 1.4). To extract analyte of interest, the empty U shape hollow fibre is immersed in an organic phase to fill the pores of the membrane and then, extraction solvent is introduced using micro-syringe into hollow fiber lumen. In the two phases HF-LPME, organic solvent is used to fill

the pores of the wall of the HF. Meanwhile, the three phases LPME can be described as an aqueous- organic – aqueous system (Esrafil *et al.*, 2018). The two phases HF-LPME method was developed for the determination of bisphenol A and metabolites of plasticizers (Fernandez *et al.*, 2017). Investigation on pharmacokinetics of echinacoside in Parkinson disease rat plasma also was reported where 1-octanol was chosen as the acceptor phase (Zhao *et al.*, 2013). Determination of anti-diabetic drugs in plasma and urine were done and good enrichment factor was obtained (Ben-Hander *et al.*, 2013; Ben-Hander *et al.*, 2015). This method has several advantages; high enrichment factor, cost-effectiveness, and high clean-up power. However, the disadvantages of this method are the need of expert personnel, long extraction time (up to 90 mins) and low precision (Carasek and Merib, 2015).

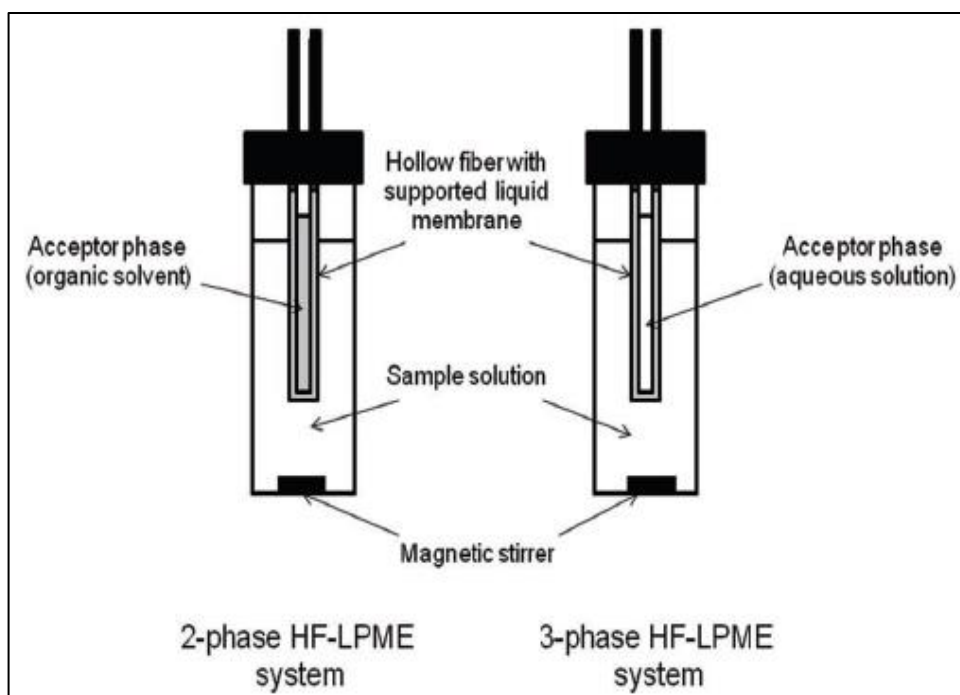


Figure 1.4: Illustration of two- and three-phases of HF-LPME method (Vičkačkaitė and Padarauskas, 2012)

For DLLME, a ternary solvent system, consists of sample solution (acceptor phase), disperser solvent and extraction solvent (donor phase). The dispersive solvent and acceptor phase mixture are rapidly injected into the sample solution that results in hydrophobic analytes enrichment in acceptor phase by aid of vortexing, shaking or sonication followed by centrifugation (Figure 1.5) (Jain and Singh, 2016). Application of this technique towards the determination of carvedilol was done and the enrichment factor obtained was 51 – 418 (Makaleh *et al.*, 2015). Ionic liquid-DLLME coupled with  $\mu$ -SPE technique was developed by Ge and Lee to extract antidepressant drugs from environmental samples. The proposed method has LOD of  $1 \mu\text{g L}^{-1}$  (Ge and Lee, 2013).

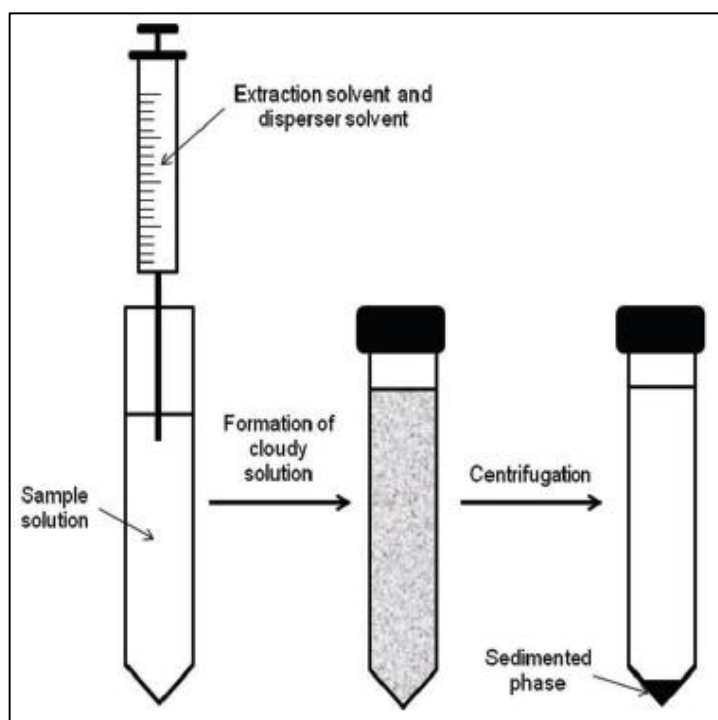


Figure 1.5: Illustration of DLLME method (Vičkačkaitė and Padarauskas, 2012)

Automated LPME was introduced to overcome risk of analyte loss during sample preparation. An automated instrument based on HF-LPME coupled with HPLC consists of an automated syringe pump, a platform lift, and a sampling loop along with an electronic board with an AVR microcontroller, was designed by Esrafilı that resulted in ease of operation (Esrafilı *et al.*, 2012).

More studies are performed to improve the efficiency, save time and overcome the downsides of the LPME technique. One of them is by applying auxiliary energy such as voltage to speed up the migration of analytes during the extraction

### **1.3.1 Electrified interface between two immiscible electrolyte solutions**

Liquid-liquid interface is formed by two immiscible solvents. When two bulk solvents are brought together, each containing an electrolyte, and that have low mutual miscibility, the interface that is formed between them is known as Interface between Two Immiscible Electrolyte Solution or ITIES.

Normally, the ITIES is made up of an aqueous solvent and an organic solvent. Common solvents used for the organic phase are nitrobenzene or dichloroethane. Lastly, to ensure the electrolyte and analyte is fully dissociated, the solvents should have high relative permittivity. Table 1.3 summarizes the permittivity value for common solvents. Lithium chloride is commonly used as an electrolyte in aqueous phase. Whereas, for organic phase, tetrabutylammonium tetraphenylborate ( $\text{TBA}^+\text{TPB}^-$ ) in nitrobenzene or bis(triphenylphosphoranylidene) tetrakis(4-chlorophenyl) borate ( $\text{BTPPA}^+\text{TPBCl}^-$ ) in dichloromethane were prepared (Vanysek, 1993).

Table 1.3: Relative permittivity,  $\epsilon$  of solvents at 25°C

Solvents	Relative permittivity, $\epsilon$
Water	78.58 <sup>a</sup>
Nitrobenzene	34.82 <sup>a</sup>
o-Nitrophenyl octyl ether	24.2 <sup>b</sup>
1,2 - dichloroethane	10.36 <sup>a</sup>
Trifluorotoluene	9.2 <sup>c</sup>

\*a (Vanysek, 1993)

\*b (Samec, 2004)

\*c (Olaya *et al.*, 2012)

According to early studies in 1970s, polarizability of ITIES behaves in a similar way as an electrode-solution interface (Koryta *et al.* 1977, Gavach *et al.*, 1968). Therefore, ion-transfer across ITIES can be studied by adopting the same electrochemical measurement (cyclic measurement, chronoamperometry, ac impedance spectroscopy) used for solid/liquid interface to ITIES.

### 1.3.2 Pseudo Nernst equation on ITIES

The general theory on charge transfer across ITIES can be explained based on thermodynamic equilibrium for ionic species. At equilibrium, the electrochemical potential of ions in each phase is as shown in Eq.1.1,

$$\tilde{\mu}_i^w = \tilde{\mu}_i^o \quad (1.1)$$

and electrochemical potential involves a chemical and electrical term,

$$\tilde{\mu}_i^w = \mu_i^w + z_i F \phi^w \quad (1.2)$$

$$\tilde{\mu}_i^o = \mu_i^o + z_i F \phi^o \quad (1.3)$$

Chemical potential can be described as Eqs. 1.4 and 1.5,

$$\mu_i^w = \mu_i^{0,w} + RT \ln a_i^w \quad (1.4)$$

$$\mu_i^o = \mu_i^{0,o} + RT \ln a_i^o \quad (1.5)$$

Where  $\mu_i^{0,o}$  is the standard chemical potential, R is universal gas constant, T is absolute temperature, z is the charge of the ion and F is the Faraday's constant and  $a_i$  is activity of ion in both phases.

When, the electrochemical potential is equal at equilibrium, the substitution of Eqs 1.2-1.5 into Eq 1.1, produces Eq 1.6,

$$\mu_i^{0,o} + RT \ln a_i^o + z_i F \phi^o = \mu_i^{0,w} + RT \ln a_i^w + z_i F \phi^w \quad (1.6)$$

The standard Gibbs energy of a species from water to dichloroethane is equal to the difference between standard Gibbs energy of solvation (organic),  $\mu_i^{0,o}$  and the standard Gibbs energy of hydration (water),  $\mu_i^{0,w}$  as shown in Eq 1.7,

$$\Delta G_t^{0,w \rightarrow o} = \mu_i^{0,o} - \mu_i^{0,w} \quad (1.7)$$

By rearranging Eqs. 1.6 and 1.7, the Galvanic potential difference between the two phases can obtained,  $\Delta_o^w \phi$ ,

$$\Delta_o^w \phi = \frac{\Delta G_t^{0,w \rightarrow o}}{z_i F} + \frac{RT}{z_i} \ln \left( \frac{a_i^o}{a_i^w} \right) \quad (1.8)$$

Where  $\Delta_o^w \phi = (\phi^w - \phi^o)$ , thus by rewriting Eq. 1.8,

$$\Delta_o^w \phi = \Delta_o^w \phi_i^o + \frac{RT}{z_i F} \ln \left( \frac{a_i^o}{a_i^w} \right) = \Delta_o^w \phi_i^{o'} + \frac{RT}{z_i F} \ln \left( \frac{c_i^o}{c_i^w} \right) \quad (1.9)$$

Where  $c_i$  is the concentration of ion in both phases,  $\Delta_o^w \phi_i^o$  is the standard transfer potential and  $\Delta_o^w \phi_i^{o'}$  is the formal transfer potential. The relationship in Eq. 1.9 is known as Nernst equation at liquid-liquid interface or called as Pseudo Nernst equation as its resemblance to classical Nernst equation for redox reaction at an electrode (Vallejo *et al.*, 2012).

### 1.3.3 Polarizable and non-polarizable liquid-liquid interfaces

The liquid-liquid interface is non-polarizable when common ion is dissolved in both the aqueous and organic phases. The partition of the salts between adjacent phases results in an interface polarization at a fixed potential. The fixed potential is determined by the standard transfer potential of different ionic species. Polarizable ITIES occurs when LiCl (hydrophilic salt) is dissolved in water and BTPPA<sup>+</sup>TPBCl<sup>-</sup> (hydrophobic salt) is dissolved in 1,2- DCE. When the concentration of LiCl is negligible in 1,2-DCE compared to BTPPA<sup>+</sup>TPBCl<sup>-</sup> and vice versa, the interface is polarizable. In this case, by using an external potential source (potentiostat), the interface of ITIES can be polarized without modifying the chemical composition of the adjacent phases. A potential window arises during interface polarization process depending on the capability of the ions to transfer based on their applied Galvanic potential difference (Peljo and Girault, 2012).

The important things to mention regarding Nernst equation relationship with the polarizability of ITIES are; 1)  $\Delta_o^w \phi$  will change if the concentration of salts in one phase is changed and 2) when  $\Delta_o^w \phi$  is applied using potentiostat, the distribution equilibrium of ions in both phases is manipulated (Velazquez-Manzanares, 2014).

### 1.3.4 Charge transfer at the ITIES

The principle of charge transfer in ITIES is divided into three groups; 1) simple ion transfer, 2) assisted ion transfer and 3) electron transfer.

#### 1.3.4(a) Ion transfer

Ion transfer in ITIES is a reversible reaction. The standard potential of ion can be determined using Eq. 1.9. Table 1.4 lists the standard ion-transfer potentials for different cations and anions across interface of 1,2 DCE and water.

Table 1.4: Standard ion-transfer potentials,  $\Delta^w_o\phi$  for different cations across interface of 1,2 DCE and water

Ion	$\Delta^w_o\phi$ , V
H <sup>+</sup>	0.549 <sup>a</sup>
Li <sup>+</sup>	0.591 <sup>a</sup>
Na <sup>+</sup>	0.591 <sup>a</sup>
K <sup>+</sup>	0.518 <sup>a</sup>
Rb <sup>+</sup>	0.435 <sup>a</sup>
Cs <sup>+</sup>	0.363 <sup>a</sup>
TMA <sup>+</sup>	0.160 <sup>a</sup>
TEA <sup>+</sup>	0.019 <sup>a</sup>
TPA <sup>+</sup>	-0.019 <sup>b</sup>
TBA <sup>+</sup>	-0.226 <sup>b</sup>
TPeA <sup>+</sup>	-0.360 <sup>b</sup>
ThEA <sup>+</sup>	-0.494 <sup>b</sup>
Ph <sub>4</sub> AS <sup>+</sup>	-0.364 <sup>b</sup>

\*a (Samec, 2004)

\*b (Volkov and Markin, 2004)

Abbreviations: H<sup>+</sup>: Hydrogen, Li<sup>+</sup>: Lithium, Na<sup>+</sup>: Sodium, K<sup>+</sup>: Potassium, Rb<sup>+</sup>: Rubidium, Cs<sup>+</sup>: Cesium, TMA<sup>+</sup>: Tetramethylammonium, TEA<sup>+</sup>: Tetraethylammonium, TPA<sup>+</sup>: Tetrapropylammonium, TBA<sup>+</sup>: Tetrabutylammonium, TPeA<sup>+</sup>: Tetrapentylammonium, ThEA<sup>+</sup>: Tetrahexylammonium, Ph<sub>4</sub>AS<sup>+</sup>: Tetraphenylarsonium

Table 1.5: Standard ion-transfer potentials,  $\Delta_o^w \phi$  for different anions across interface of 1,2 DCE and water

Ion	$\Delta_o^w \phi, \text{V}$
F <sup>-</sup>	-0.581 <sup>b</sup>
Cl <sup>-</sup>	-0.481 <sup>b</sup>
Br <sup>-</sup>	-0.446 <sup>a</sup>
I <sup>-</sup>	-0.342 <sup>a</sup>
ClO <sub>4</sub> <sup>-</sup>	-0.170 <sup>a</sup>
Picrate	-0.057 <sup>a</sup>

\*a (Samec, 2004)

\*b (Volkov and Markin, 2004)

Abbreviations: F<sup>-</sup>: Fluoride, Cl<sup>-</sup>: Chloride, Br<sup>-</sup>: Bromide, I<sup>-</sup>: Iodide, ClO<sub>4</sub><sup>-</sup>: Perchlorate,

### 1.3.4(b) Assisted ion-transfer

This type of transfer is due to the presence of an ionophore of hydrophobic ligand, L in the organic phase. The ligand can selectively combine with an ion in aqueous phase, M to form complex, M-L in organic phase (Senda *et al.*, 1991).



1:1 stoichiometry is assumed. The association constant of the reaction is,

$$K_a = \frac{a_{M-L}^o}{a_M^o a_L^o} \quad (1.11)$$

The Galvanic ion-transfer potential can be written as Eq. 1.12,

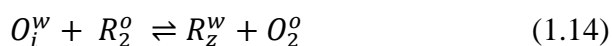
$$\Delta_o^w \phi = \Delta_o^w \phi_{M-L}^o + \frac{RT}{z_M} \ln \left( \frac{a_{M-L}^o}{a_M^w} \right) \quad (1.12)$$

With the apparent standard transfer potential given by Eq. 1.13,

$$\Delta_o^w \phi_{M-L}^o = \Delta_o^w \phi_M^o + \frac{RT}{z_M} \ln (K_{ML} a_L^o) \quad (1.13)$$

### 1.3.4(c) Electron transfer

Electron transfer (ET) reaction at ITIES is the transfer of electrons across interface. Two redox pairs, (O and R) are dissolved in organic and aqueous phase respectively and potential is applied to the system that leads to electron transfer (Quinn and Konturri, 2000).



For the above reaction, it expressed the Nernst equation for electron transfer across the ITIES,

$$\Delta_o^w \phi = \Delta_o^w \phi_{ET}^o + \frac{RT}{F} \ln \left( \frac{a_{O_2}^o a_{R_1}^w}{a_{O_1}^w a_{R_2}^o} \right) \quad (1.15)$$

The reaction depends on the relative reduction potential of the pairs in the system and it can occur spontaneously or can be controlled with a potentiostat.

### 1.3.5 Electrochemically modulated liquid-liquid extraction

LLE method is most suitable for hydrophobic analytes as they will transfer easily to the organic phase unlike hydrophilic ones that will remain in the aqueous sample. In the case of hydrophilic and ionic analytes, the extraction efficiency can be improved through: (i) pH change to make the analytes more soluble in the organic phase; or (ii) the dissolution of additives in the aqueous phase to form ion pairs and facilitate the phase transfer; or (iii) derivatization to reduce polarity of analytes.

Another approach to overcome main drawback of LLE method, consists of using an electric field as a driving force for the transfer of ionized analytes from the aqueous to the organic phase. In 1937, the work of electro-driven for sample preparative was

carried out by U-tube apparatus and followed by electrodialysis which transports ions through membranes under the influence of current (Tiselius, 1937; Davis, 1990; Aider *et al.*, 2008). After that, this electric field was put to use with liquid phase extraction.

Electrochemically modulated liquid-liquid extraction is based on the extraction of ions by applying the potential difference at ITIES and was introduced by Arrigan *et al.* in 2005. The ITIES is polarized by the application of a potential difference across the interface with a potentiostat. Hence, the driving force of the extraction is the electric potential. This method allows ion transfer at lower applied potentials (generally in the  $\pm 1$  V range). Variation of the interfacial potential difference modulates the ion partition on either side of the interface and this phenomenon has been harnessed to the investigation of redox catalysis or sensing among other applications (Scanlon *et al.*, 2018; Herzog, 2015). Other than that, application of ITIES was utilized on wide range of analytes as summarized in Table 1.6.

Table 1.6: Analytes of interest on ITIES applications

Type of analytes	Ionic analytes	References
Alkali metals	$\text{Li}^+$ , $\text{Na}^+$ , $\text{K}^+$ , $\text{Rb}^+$ , $\text{Cs}^+$	Stockmann <i>et al.</i> , 2012
Drugs	Propranolol	Collins <i>et al.</i> , 2009
Food additives	Aspartame, Acesulfame K	Herzog <i>et al.</i> , 2008
Dendrimers	Poly(propylenimine), Poly(amidoamine), Poly-L-Lysine,	Berduque <i>et al.</i> , 2007 Gonzalez-Fuentes <i>et al.</i> , 2010 Herzog <i>et al.</i> , 2012
Polyelectrolytes	Poly(diallyldialkylammonium) ions	Zhang <i>et al.</i> , 2011
Proteins	Haemoglobin, Insulin, hen-egg-white lysozyme	Herzog <i>et al.</i> , 2008 Scanlon <i>et al.</i> , 2010
Biological important species	DNA	Arrigan, 2008

An experimental set-up based on electrochemistry at ITIES was used for the extraction of ions (Berduque *et al.*, 2005; Berduque and Arrigan, 2006; Collins *et al.*, 2008). In their set-up, the analytes transfer potentials were determined by voltammetry. Then, the potentiostatic extraction process was performed to monitor current obtained over specific time. In these studies, the application of an interfacial potential between an aqueous solution containing the ions of interest flowing over a static hydrophobic phase, has caused the extraction of ions. Protonated drugs molecules (Propranolol and timolol) were demonstrated to be successfully extracted from artificial urine by applying appropriate positive potential (Collins *et al.*, 2008). In addition, selective ion-transfer (one from mixtures or co-extract ions in sample solution) is possible as each ion has its own transfer potential.

However, there are two main issues for sample preparation applications. First, electrochemistry at the ITIES is a process that is limited by the diffusion of species. As a consequence, the low surface area-to-volume ratio of the electrochemical cells used limited the extraction efficiency to 10 %, which is not acceptable for sample preparation applications (Berduque *et al.*, 2005; Berduque and Arrigan, 2006; Collins *et al.*, 2008). Mass transport can be improved by the design of hydrodynamic liquid-liquid cells for which limiting currents were achieved in agreement with Levich equation (Bard and Faulkner, 2001). The hydrodynamic cell was designed based on the rotating diffusion cell for LLE by Alberty and co-workers (Alberty *et al.*, 1974; Alberty *et al.*, 1976). Two cell designs were introduced; i) the liquid/liquid rotating disk electrode and ii) rotating paddle cell (Kralj and Dryfe, 2002; Kralj and Dryfe, 2003). It was observed that the mass transfer was induced by the rotation of paddle or disk in steady-state manner (Kralj and Dryfe, 2003).

The second limitation is the organic phase in which target ions are extracted into. Some organic solvents are not suitable for chromatography analysis, and thus aqueous samples are generally preferred. As for electro-membrane extraction, supported liquid membranes (SLM) were also used with two polarised water-oil interfaces. SLM such as Nafion membrane and Poly(vinylidene fluoride) (PVDF) were reported (Samec *et al.*, 2000; Ulmeanu *et al.*, 2002; Velicky *et al.*, 2012; Velicky *et al.*, 2014). Those membranes allowed the injection of an aqueous acceptor solution for the chromatographic analysis. Although a complex rotor was designed to improve the mass transport efficiently, this would be impractical for routine sample preparation prior to chromatographic analysis.

These previous researches inspired us to utilize electrochemistry as sample preparation method rather than detection. In addition, the advantages of ITIES-extraction are attractive. It requires a low volume of solvent and allows ions to transfer across interface at low applied potentials. Moreover, the set-up of the electrochemical extraction is simple and short time is required to provide efficient extraction (Pedersen-Bjerggaard and Rasmussen, 2008).

#### **1.4 Target analytes**

In the context of this thesis, target analytes refer to the compounds that are chosen for the studies. The chosen pharmaceutical compounds are; (i) biguanides, and (ii) beta-blocker drug. Background information on the targeted analytes are next to be discussed.

#### 1.4.1 Biguanides (Metformin, Buformin, Phenyl biguanide, Phenformin)

Diabetes is a group of metabolic disease. It is characterized by abnormalities at multiple organ sites which include defects in insulin secretion, insulin action, or both. Major classification of this disease falls into two groups, Type I and Type II. Type I (insulin dependent diabetes) diabetes is caused by an absolute insulin deficiency, and Type II (non-insulin dependent diabetes) is due to a combination of resistance to insulin and an inadequate compensatory insulin secretory response. Type II diabetes is also known as diabetes mellitus (American Diabetes Association, 2010). Biguanide compounds are nitrogen containing, known medication for diabetes treatment. Biguanide compounds in this study are shown in Table 1.7.

Table1.7: Chemical structure, pKa, log P<sub>0</sub> values for biguanide compounds

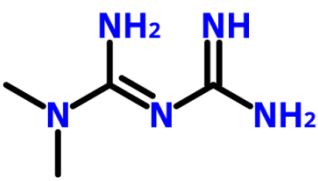
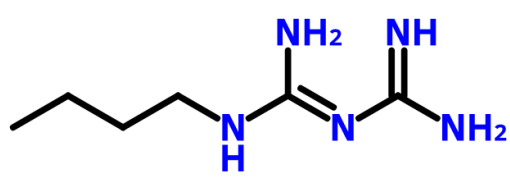
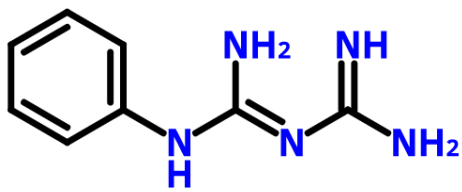
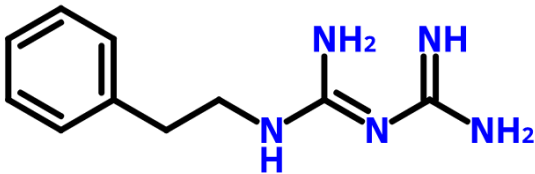
Biguanide compounds	Structure	Log P <sub>0</sub>	pKa
Metformin (MET)		-1.82 <sup>a</sup>	2.80, 11.5 <sup>b</sup>
Buformin (BUF)		-1.20 <sup>c</sup>	12.27 <sup>c</sup>
Phenyl bigunide (PHEBI)		-0.03 <sup>a</sup>	2.13, 10.8 <sup>d</sup>

Table 1.7. Continued

Phenformin (PHEN)	0.41 <sup>a</sup>	2.70, 11.8 <sup>e</sup>
		
<hr/> *a Calculated from ACD Software *b (Berduque, <i>et al.</i> , 2005) *c SciFinder *d (Langmaier <i>et al.</i> , 2016) *e (Florey, 1975)		

MET, BUF and PHEN are antihyperglycemic drugs prescribed orally in the WHO List of Essential Medicines (The International Pharmacopoeia, 2015). However, PHEN and BUF have been banned because of their high potential risk of developing lactic acidosis (Sorensen, 2012; Tucker *et al.*, 1981). Nevertheless, it is still available and legal in Italy, Greece, Portugal, Poland, Brazil Uruguay and Japan (Appleyard *et al.*, 2012).

MET (1, 1-dimethyl-biguanide) is first-line therapy used in the treatment of Type II diabetes. MET is a product from the synthesis reaction of N, N-dimethylguanidine. It is first reported in 1922 by Emil Werner and James Bell. For the first time in 1975, it was experimented for the treatment of diabetes. (Sterne, 1975). MET received the approval from FDA in 1995 even though it was available in Europe from the 1970s (Food and Drug Administration website, 1995). Apart from being used as medication for diabetes, MET also was used in the treatment of polycystic ovary disease and obesity (Nestler, 2007; Chen 2013; Kimmel and Inzucchi, 2005).

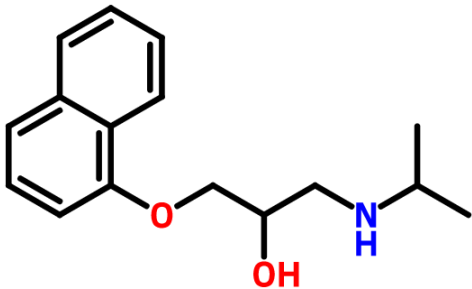
When taken orally, under physiological conditions, biguanides are protonated, thus will not be fully absorbed from gastro-intestinal tract. The bioavailability of MET is

from 40 to 60 % (Huttunen *et al.*, 2009). MET and BUF are not metabolized whereas 50 % of PHEN is metabolized in liver. While the rest are excreted in urine (Alshishani *et al.*, 2018).

#### 1.4.2 Beta -blocker drug (Propranolol)

1-isopropylamino-3-(1-naphthyloxy)-2-propanol or branded as PROP is one of cardiselective  $\beta$ -adrenergic receptor blocking agents. It is predominantly prescribed for cardiovascular disorders such as hypertension, angina pectoris, cardiac arrhythmias and myocardial infarction (Hardman *et al.*, 1996). Table 1.8 shows its chemical structure. Based on the structure, it has two enantiomers owing to the existence of a chiral carbon in the alkyl side chain, adjacent to a hydroxyl group (Singh *et al.*, 2004).

Table 1.8: Chemical structure, pKa, log P<sub>0</sub> values for PROP

Beta -blocker compounds	Structure	Log P <sub>0</sub>	pKa
Propranolol (PROP)		3.10 <sup>a</sup>	9.41 <sup>b</sup>

\*a Calculated from ACD Software

\*b (Szulga, 1998)

After oral administration, PROP is completely absorbed from gastro intestinal tract. PROP is basic and lipid soluble. Its bioavailability is between 15 to 23 % (Walle *et al.*, 1979). B-blocker drugs have a sedation effect and the usage has been abused in sports.

Hence, PROP is included in the list of forbidden substances by the International Olympic Committee (Casado *et al.*, 2016; Zhang *et al.*, 2009).

## 1.5 General problem statements

As discussed, sample preparation is one of the most vital part in chemical analysis, especially for the determination of medical drugs in biological samples. The analysis of biguanide compounds are complicated owing to their hydrophilicity properties particularly for MET. Derivatization of polar anti-diabetic drugs using desyl chloride, benzoin or anthraquinone-2-sulfonyl chloride have been reported (Ben-Hander *et al.*, 2013). Despite the enhancement of detection, there are some disadvantages of this method; it demands multi-extraction steps and produces unstable derivatives along with side products (Juan *et al.*, 2006; Ohta *et al.*, 1993; Ross, 1977).

It turns out to be more difficult and challenging to determine various nature of compounds simultaneously, for example, highly polar MET with non-polar PROP drug. The choice of these targeted drugs offers a span of hydrophilicity with log  $P$  (octanol-water partition coefficient) values ranging from -1.82 (MET) to 3.41 (PROP).

A novel sample preparation which can lead to significant enrichment is an important step of any analytical procedure. The simplification, low solvent and reagents consumption is highly recommended. Another important parameter is the separation step. Therefore, the compatibility between sample preparation and separation is the key to the success of the analytical method. An interesting application of electro-driven liquid-liquid extraction and mixed-adsorbent in porous membrane bar- $\mu$ -SPE are to be explored for simultaneous extraction of targeted analytes. Thus, this thesis is dedicated for those two techniques of microextractions.

It is proposed here to combine the droplet liquid-liquid extraction with the aid of electric field on the interface between two immiscible solutions to prepare samples before chromatographic analysis. A novel approach for liquid-liquid extraction using potentiostat and chemical polarisation (potentiostat-free) is chosen for the sample preparation of aqueous samples containing cationic analytes (drugs with various polarity). This instrument-free method is based on ion transfer modulated by the application of an interfacial potential controlled by the distribution of a common ion between the two phases.

The bar- $\mu$ -SPE method (an improvement of the original  $\mu$ -SPE) was chosen due to its numerous advantageous features such as simple to be implemented, rapid, significantly reducing the amounts of organic solvents used, in line with the green analytical chemistry aspiration. The  $\mu$ -SPE technique was first introduced by Basheer *et al.* in 2006 to overcome the shortcomings of the SPE technique. The benefits of using  $\mu$ -SPE are the lower consumption of solvents, low-cost, simple and it is easy to perform. The  $\mu$ -SPE device was prepared by placing a few milligrams of the adsorbent inside a heat-sealed porous membrane. A main weakness of the technique is the inefficient mixing of sample and the adsorbent as the device is just floating on top of the sample surface.

To address this problem, some groups have used magnetic adsorbents. Magnetic chitosan functionalized graphene oxide was used as stir bar during the extraction process (Naing *et al.*, 2016). In the same year, Basheer *et al.*, 2016 also made an improvement by placing a tiny stir bar along with adsorbent inside the  $\mu$ -SPE device. Another way to overcome this drawback is by putting a short metal bar in the slightly bigger bag which contains conventional  $\mu$ -SPE bag (Alshishani *et al.*, 2019). This was

necessary to overcome the leaking of seals when graphene was used as the adsorbent. All the modifications enable the device to be fully immersed in the sample solution, hence improving the extraction.

The adsorbents in the bar- $\mu$ -SPE method are protected by the membrane wall from macromolecules in the sample as only small analytes can diffuse to the surface of the adsorbent. It must also be highlighted that previous studies focussed on the extraction of a single class of compound using one adsorbent. Key to the success of the bar- $\mu$ -SPE extraction is the choice of adsorbents used. Due to the diverse polarities of the studied drugs, it was rationalised that the use of a mixture of adsorbents of contrasting surface properties (e.g., polar and non-polar) will be the way forward to achieve the objectives.

## **1.6 Objectives**

The main objectives of this thesis were:

1. To develop the electrochemically modulated liquid-liquid extraction for determination of metformin, phenyl biguanide, phenformin and propranolol based on potentiostatic method (Chapter 3)
2. To develop the sample preparation without potentiostatic method based on electrochemically modulated liquid-liquid extraction technique to determine metformin, phenyl biguanide, phenformin and propranolol in biological samples (Chapter 4)
3. To develop a new porous membrane bar- $\mu$ -SPE method with various adsorbents to determine metformin, buformin, phenformin and propranolol in biological samples (Chapter 5)

## **1.7 Scope of study**

Chapter 1 describes the basic concepts of the two techniques used in this study and their respective literature reviews. The potential transfer of target analytes determined by cyclic voltammetry and the extraction performed either by an external source (potentiostat) or imposing interfacial potential by common ions are discussed in chapters 3 & 4. Alternatively, the extraction of analytes will be done using a bar- $\mu$ -SPE device containing various commercially available adsorbent materials. These are discussed in Chapters 5. Quantitation of the extracted drugs for all techniques was done using HPLC-UV.

## CHAPTER 2

### GENERAL EXPERIMENTAL

#### 2.1 Experimental method I (Chapter 3 & 4)

##### 2.1.1 Chemicals & reagents

Lithium chloride (LiCl, 97%) as an aqueous phase, metformin hydrochloride (97%), phenyl biguanide hydrochloride (98%), phenformin hydrochloride (97%) and propranolol hydrochloride (99%), tetraethylammonium chloride (TEA 99.0%), tetrapropylammonium chloride (TPA 98.0%) were purchased from Sigma Aldrich. Tetramethylammonium chloride (TMA 99.0%) was purchased from Fluka BioChemika. All aqueous phase solutions were prepared in ultrapure water (18.2 MΩ Elga Water). pH adjustment of aqueous solution was done by using sodium hydroxide (97%) from BDH Prolabo and hydrochloric acid (37%) from Merck.

1,2-dichloroethane (1,2- DCE) as an organic phase, bis(triphenylphosphoranylidene) ammonium chloride (BTPPA<sup>+</sup>Cl<sup>-</sup>, 97%) and potassium tetrakis(4-chlorophenylborate) (K<sup>+</sup>TPBCl<sup>-</sup>, 98%) were purchased from Sigma Aldrich.

HPLC grade acetonitrile was from Sigma Aldrich. Buffer (pH 6.2) containing 20 mM of sodium phosphate monobasic monohydrate (Sigma Aldrich), and trimethylamine (Sigma Aldrich) was prepared in ultrapure water (18.2 MΩ.cm Elga Water). Ortho-phosphoric acid to adjust pH of buffer was purchased from BDH Prolabo.

## 2.1.2 Instrumentation

### 2.1.2(a) Voltammetry

Cyclic voltammetry was performed to investigate electrochemical properties of targeted compounds. Emstat3 potentiostat purchased from Palm Sens (Netherlands) which operated in four-electrode mode was used. Electrochemical cell was set up as shown in Figure 2.1. A custom-made borosilicate glass cell was used ( $A_{\text{interface}} = 1.10 \text{ cm}^2$ ) to host the biphasic system. Each phase in the cell contained one platinum (Pt) mesh counter electrode and one Ag/AgCl reference electrode. The interfacial potential difference was measured between the two reference electrodes and the current variation linked to charge transfer across liquid-liquid interface was recorded by counter electrodes. Three types of cells were investigated; 1) Static ITIES cell, 2) Rotating paddle in static ITIES cell, 3) Rotating disk electrode with polyethylene terephthalate, (PET) membrane supported ITIES as shown below.

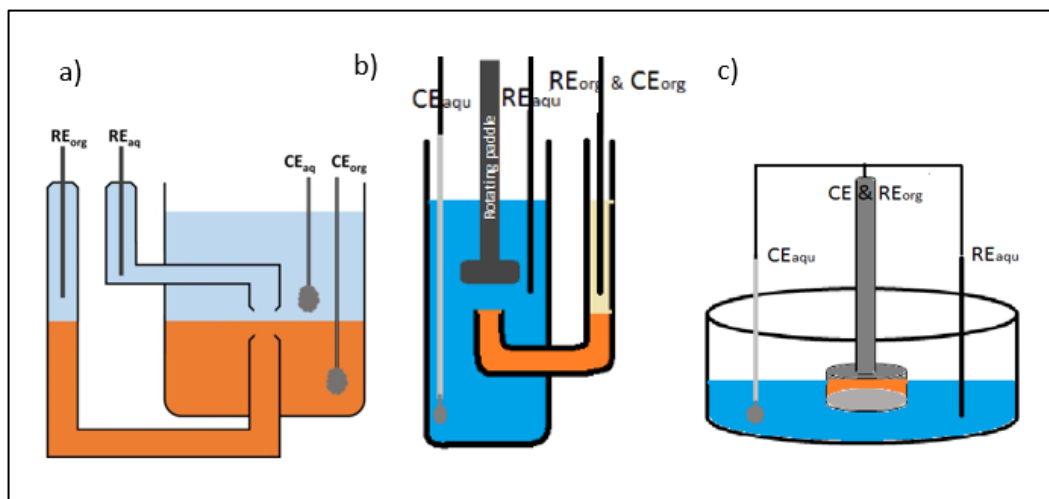


Figure 2.1: Custom made electrochemical cells a) Static ITIES cell b) Rotating paddle in ITIES cell c) Rotating disk electrode with PET membrane supported ITIES for ion transfer studies.  $RE_{\text{org}}$ : Reference electrode for the organic phase;  $RE_{\text{aq}}$ : Reference electrode for the aqueous phase;  $CE_{\text{aq}}$ : Counter electrode for the aqueous phase;  $CE_{\text{org}}$ : counter electrode for the organic phase

### **2.1.2(b) High Performance Liquid Chromatography – UV-vis detection**

Chromatographic experiments were conducted using an analytical column Agilent Zorbax TMS (C1) 5  $\mu\text{m}$ , 80 Å, 4.6 x 250 mm and protected by a guard column of Agilent Zorbax Reliance Cartridge Guard Column, 4.6 mm ID x 12.5 mm PPS Polymer Tubes. The mobile phase consisted of phosphate buffer (pH 6.2) with 20 mM sodium phosphate monobasic monohydrate: acetonitrile: trimethylamine (50:50:0.2). It was prepared daily, filtered using Nylon membrane filter (0.22  $\mu\text{m}$ ) from Agilent Technologies (Waldbronn, Germany) and degassed for 15 minutes just before its use. The device used was Shimadzu LC-20AD. The flow rate of the mobile phase under isocratic condition was 1.3 mL min<sup>-1</sup> at 37°C. Temperature remains constant with ultra-thermostat Colora Messtechnik GMBH. Injection volume was 20  $\mu\text{L}$ . The detection was performed at  $\lambda = 230$  nm using a Shimadzu SPD-20 A. Data recording was carried out using the LabSolutions software.

### **2.1.2(c) Small equipments**

pH of mobile phase and aqueous solution was adjusted using a pH meter (PHM 210, Radiometer Analytical). Vortexing and centrifuging step was performed using VTX-400 Labo-Moderne and Sorvall ST8 Centrifuge Thermo Scientific, respectively.

### **2.1.3 Cyclic voltammetry**

#### **2.1.3(a) Static ITIES cell**

The bottom half of the cell (Figure 2.1a) was filled with organic phase and 3.0 mL of aqueous phase was placed on the top of the cell in this set-up, taking care to ensure that no air bubbles were trapped at the interface. The formal transfer potential of TEA, = 0.049 V was used to calibrate the potential window (Abraham *et al*, 1976). TEA<sup>+</sup>

was added to the aqueous phase of the electrochemical cell at the end of a series of experiments for potential calibration purposes. Target analytes were added to aqueous phase. Scans were run at a scan rate of  $5 \text{ mV s}^{-1}$ . It was repeated three times. Voltammetry study of aqueous phase at pH 2 also was conducted.

Composition of the cell was as follows:

$\text{Ag}_{(s)} | \text{AgCl}_{(s)} | 10 \text{ mM LiCl}_{(aq)}, x \text{ mM analyte}_{(aq)} || 10 \text{ mM BTPPA}^+ \text{TPBCl}^-_{(org)} \text{ in } 1,2\text{-DCE} | \text{Saturated BTPPA}^+ \text{Cl}^- \text{ in } 10 \text{ mM LiCl in H}_2\text{O} | \text{Ag}_{(s)} | \text{AgCl}_{(s)}$

### **2.1.3(b) Rotating disk electrode with PET membrane supported ITIES**

A silver-silver chloride electrode was used as both reference and counter electrodes for the organic phase (Figure 2.1b). This was possible because the interfacial surface area was relatively small. A rotating paddle was installed in the aqueous phase to enhance the mass transfer of ions towards the interface. The organic phase volume was  $100 \mu\text{L}$ . After initial blank was recorded, required volume of metformin was added to aqueous phase. Then, rotating paddle was set to rotate at 150 rpm by connecting it to Controvit (Tacussel Electronique) system.

### **2.1.3(c) Rotating paddle in static ITIES cell**

The set up was illustrated in Figure 2.1c. A rotating cylinder, with its bottom limited by a filter, was filled with the organic phase and dipped in the aqueous phase. Three electrodes were operated in this cell. The  $\text{CE}_{org}$  at the same time as the  $\text{RE}_{org}$  was made of Ag/AgCl as for the previous set-up. The polyethylene terephthalate (PET) filter ( $0.45 \mu\text{m}$  pores) (Milipore) were sealed at the end of rotating disk using silicon sealant. The volume of the aqueous phase was typically  $20.0 \text{ mL}$ .  $100 \mu\text{L}$  of the organic phase were placed in hole on the rotating disk. Known volumes of target analytes were added

to aqueous phase. The rotating electrode was set to rotate at 100 rpm by connecting it to Controvit (Tacussel Electronique) system.

#### 2.1.4 Preparation of standard solution, aqueous and organic phase

An aqueous phase was prepared by dissolving the desired amounts (10 mM) of LiCl in deionized water. MET, PHEBI, PHEN and PROP stock solutions (10 mM) were prepared by dissolving the desired amounts in 10 mM LiCl solution and stored at 4°C. Working solutions were prepared from the stock solution by dilution with appropriate amounts of LiCl solution. For organic phase,  $\text{BTPPA}^+\text{TPBCl}^-$  was prepared by methathesis (Lee *et al*, 1997). The crystal product was dissolved in 1,2-DCE as described in Section 2.1.5.

#### 2.1.5 Preparation of organic salt ( $\text{BTPPA}^+\text{TPBCl}^-$ )

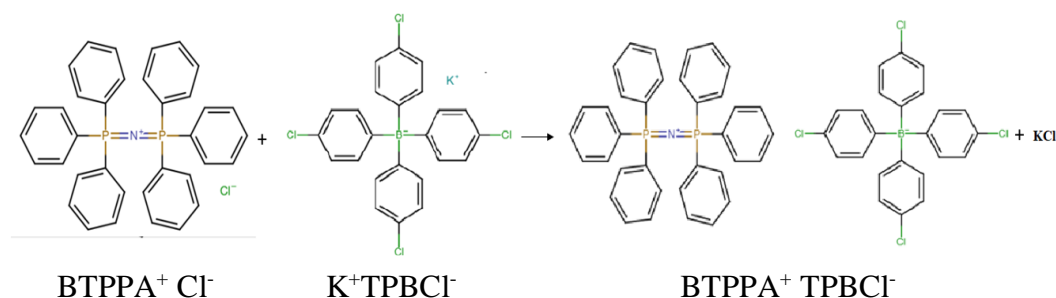


Figure 2.2: Metathesis reaction of  $\text{BTPPA}^+\text{TPBCl}^-$

1.25 g of  $\text{BTPPA}^+\text{Cl}^-$  and 1 g of  $\text{K}^+\text{TPBCl}^-$  were dissolved in 10 mL and 20 mL of 2:1 ratio of MeOH:  $\text{H}_2\text{O}$  solution, respectively. The  $\text{BTPPA}^+\text{Cl}^-$  solutions were added to  $\text{K}^+\text{TPBCl}^-$  solution dropwise while stirring, forming a white precipitate. The precipitate was kept for 2 h under stirring conditions. The solution was filtered using vacuum filter for ~30 mins to remove the solvent. 0.45 nm HVLP filter paper was used for filtration. It was dried overnight in dessicator. The product was collected and dissolved in acetone which was purchased from Prolabo. The beaker was covered by parafilm that had holes in it to allow acetone to evaporate and then stored in the fume

hood for 2 days covered with aluminium foil until complete evaporation of acetone (recrystallization). The crystals were rinsed and filtered with 1:1, acetone: H<sub>2</sub>O mixture. Lastly, the resulting crystals of BTPPA<sup>+</sup>TPBCl<sup>-</sup> were stored in fridge covered with aluminum foil to prevent degradation from light exposure.

## 2.2 Cyclic voltammetry studies

As discussed in 1.4.2, the ITIES can be polarized by applying electrical potential. Cyclic voltammetry study is applied to the ITIES. Normally, the study has been carried out using an electrochemical cell that is familiar with the name of ITIES cell (Figure 2.3).

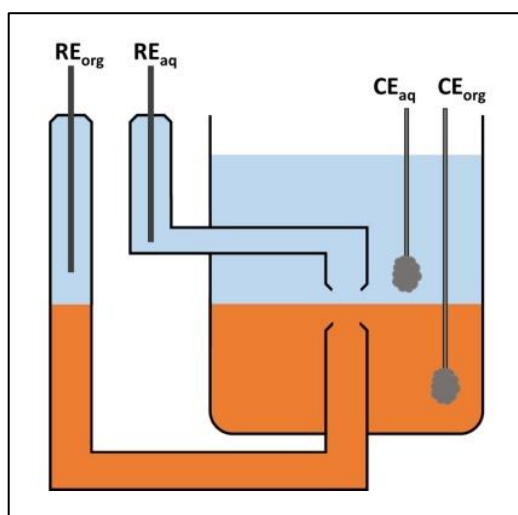


Figure 2.3: Custom made electrochemical cell or ITIES cell for ion transfer studies. RE<sub>org</sub>: Reference electrode for the organic phase; RE<sub>aq</sub>: Reference electrode for the aqueous phase; CE<sub>aq</sub>: Counter electrode for the aqueous phase; CE<sub>org</sub>: counter electrode for the organic phase

The ITIES cell has four electrode configurations. Two reference electrodes (Ag/AgCl) and two PT counter electrode are used and connected to a potentiostat. Each phase has its own reference and counter electrode. The ITIES is the working electrode. 10 mM LiCl as an electrolyte is dissolved in water and 10 mM BTPPA<sup>+</sup>TPBCl<sup>-</sup> is dissolved in

1,2- DCE. The voltammogram obtained for this ITIES system is depicted in Figure 2.4.

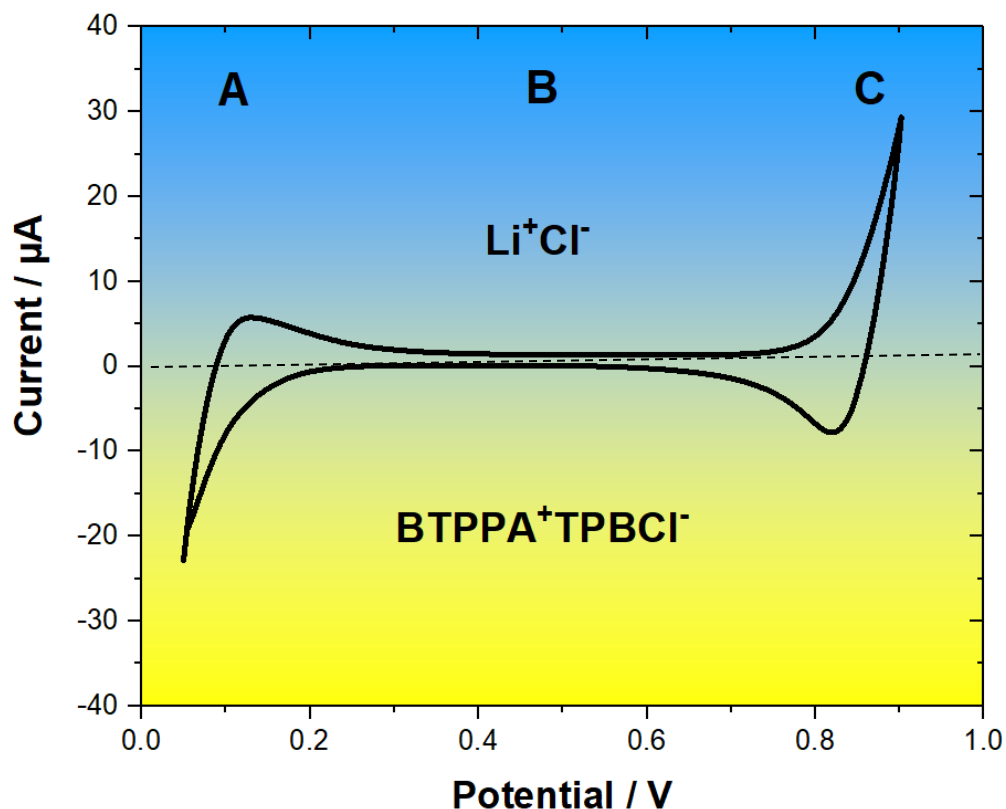


Figure 2.4: Voltammogram for blank solution. Aquoues phase: 10 mm LiCl, Organic phase: 10 mM BTPPA<sup>+</sup>TPBCl<sup>-</sup> in 1,2- DCE, Reference electrode: Ag/AgCl, Counter electrodes: Pt, Scan rate: 5 mV s<sup>-1</sup>. Blue region: Water, Yellow region: DCE

Figure 2.4 illustrates a cyclic voltammogram for typical supporting electrolytes present as a blank system. There are three regions in the voltammogram which are i) low potential region (A), ii) polarized region (B) and iii) high potential region (C). The most positive region is on the right side of the voltammogram. The potential window is limited by supporting electrolyte ions transfer (region A and C). The dash-line in the middle of the curve indicates the ITIES.

Starting at low potential region, ( $\sim 0.05$  V), the current is negative,  $\text{BTTPPA}^+$  is transferred from the organic to aqueous phase and/or  $\text{Cl}^-$  is transferred from the aqueous to organic phase. After the potential becomes more positive  $\sim 0.1$ -  $0.25$  V,  $\text{BTTPPA}^+$  and  $\text{Cl}^-$  will be back transferred to the organic phase and aqueous phase respectively. At C region, a positive current increase was observed at  $\sim 0.8$ -  $0.9$  V due to  $\text{Li}^+$  from the aqueous phase being transferred to the organic phase and/or  $\text{TPBCl}^-$  is transferred from the organic to aqueous phase. The back transfer occurs during a reverse sweep for  $\text{Li}^+$  and  $\text{TPBCl}^-$ . As the aqueous phase becomes less positive,  $\text{BTTPPA}^+$  is transferred from the organic to aqueous phase and/or  $\text{Cl}^-$  transferred from the aqueous to organic phase. Region B is the potential region or so-called 'ideal polarizable region'. The transfer of other chemical species or drugs ion such as metformin ion occurs here as shown in Figure 2.5 (Scanlon, 2009).

Figure 2.5 is the obtained voltammogram after the addition of target analytes into the biphasic system. A positive peak during forward sweep can be observed. The peak indicates that the cation is transferred from the aqueous to the organic phase. Meanwhile, on a reverse sweep, the negative peak results from the transfer of cation back into to the aqueous phase. The ion-transfer is a reversible reaction. The peak transfer of target analyte is the mid-peak potential (Eq. 2.1)

$$\Delta_o^w \phi^{1/2} = \frac{1}{2} ( \Delta_o^w \phi_{\text{Forward}} + \Delta_o^w \phi_{\text{Reverse}} ) \quad (2.1)$$

For the reversible reaction of ion transfer, the peak potential is independent of the scan rates and the peak to peak separation is  $59/z_i$  mV at  $25^\circ\text{C}$ .

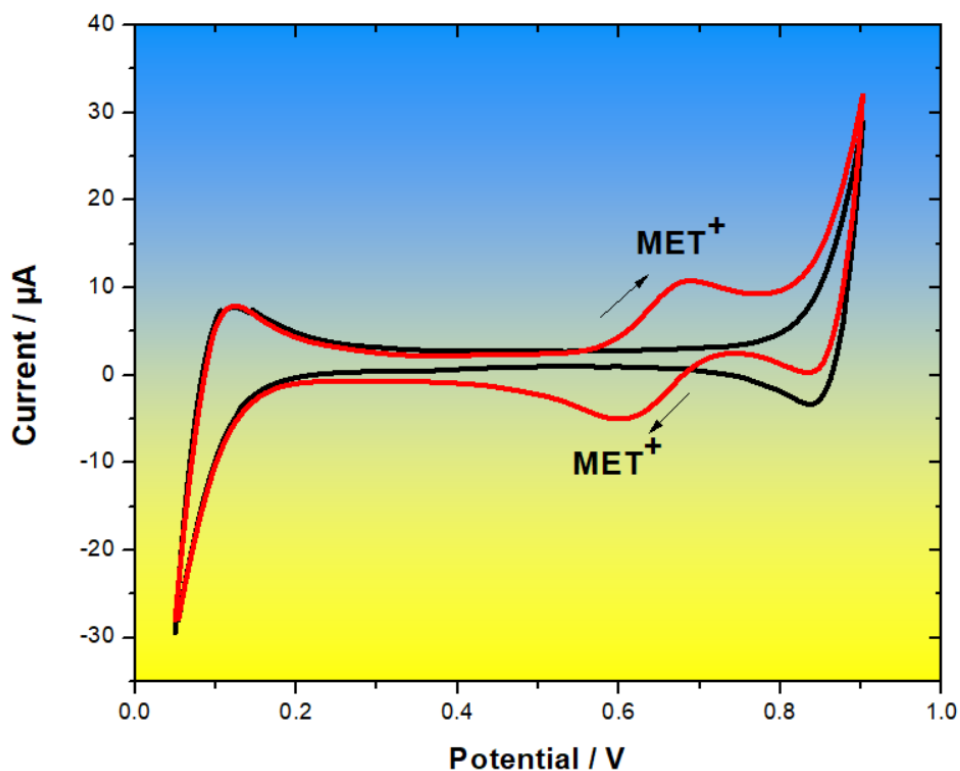


Figure 2.5: Voltammogram for blank solution containing MET. Aqueous phase: 10 mM LiCl, Organic phase: 10 mM BTTPA<sup>+</sup>TPBCl<sup>-</sup> in 1,2- DCE, Reference electrode: Ag/AgCl, Counter electrodes: Pt, Scan rate: 5mV s<sup>-1</sup>. Blue region: Water, Yellow region: DCE

The resulting current is associated with the direction of ion transfer at ITIES. Figure 2.6 illustrated the process of ion transfer across the interface. When the cation is transferred from the aqueous phase to an organic phase, and anion is transferred from the organic phase to the aqueous phase, the current is conventionally defined as positive. When the cation is transferred from the organic phase to aqueous phase and an anion is transferred from the aqueous to the organic phase, the current is conventionally defined as negative.

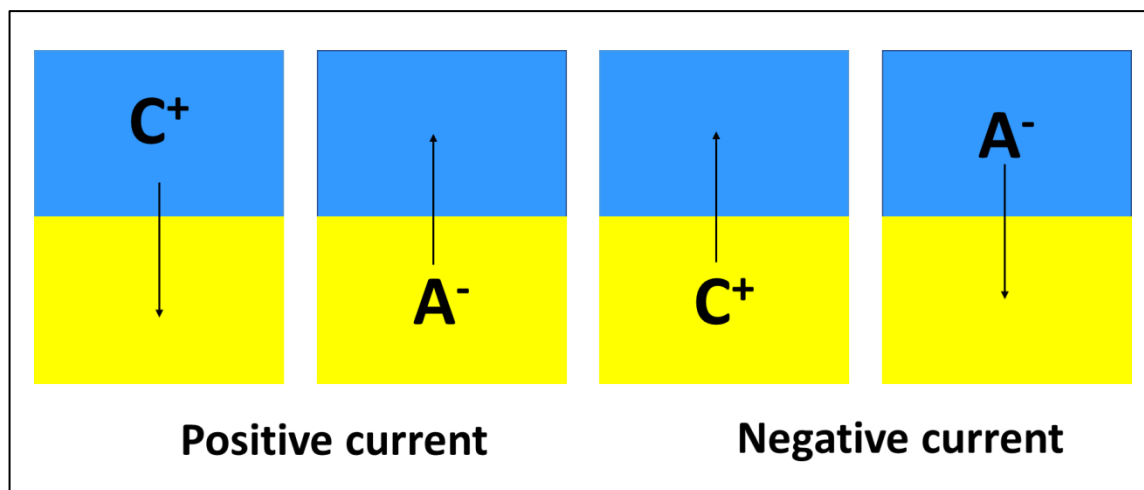


Figure 2.6: Direction of ion transfer.  $C^+$ : Cation,  $A^-$ : Anion

## 2.3 Experimental method II (Chapter 5)

### 2.3.1 Chemicals and reagents

Adsorbents used were graphene nanoplatelet (Sigma Aldrich, Steinheim, Germany), zeolite Linde Type L (LTL) (Tosoh Corporation, Japan), DSC-18 (Supelco, Bellefonte, PA, USA), silica particles (Merck, Darmstadt, Germany) and Si-CH, Si-NH<sub>2</sub>, and Si-CN from Isolute®. Buformin hydrochloride (95 %) was purchased from Wako Pure Chemicals Industries (Osaka, Japan). Metformin hydrochloride (97 %), phenformin hydrochloride (97 %) and propranolol hydrochloride (99 %), triethylamine, sodium monophosphate monobasic were purchased from Sigma Aldrich (Sigma Aldrich, Steinheim, Germany). Sodium chloride were purchased from Quality Reagent Chemicals (QReC, Auckland, New Zealand). HPLC grade tetrahydrofuran (THF) (>99.9 %), 2-propranol (IPA), dichloromethane (DCM) sodium hydroxide, ortho phosphoric acid were obtained from Merck (Darmstadt, Germany). Toluene and acetic acid (99.8 %) were purchased from HmbG Chemicals (Hamburg, Germany). Methanol (MeOH) and acetonitrile (ACN) HPLC grade were from Quality Reagent Chemicals (QReC, Auckland, New Zealand). Ultrapure water (resistivity, 18.2 MΩ cm<sup>-1</sup>) was produced from Milipore water (Molsheim, France) purification system and was used throughout. Polypropylene (PP) sheet membrane (Accurel 2E HF (R/P), 166 μm thickness, 0.2 μm pore size) was purchased from Membrana (Wuppertal, Germany).

### 2.3.2 Instrumentation

A HPLC system, Alliance model 2695 was obtained from Waters (Milford, MA, USA). The instrument was equipped with photodiode array detector (DAD model number 2998) that was set at 230 nm. Separation was done using ODS-3 Hypersil<sup>TM</sup> C18 column (4.6 x 250 mm, 5  $\mu$ m) and Agilent Zorbax TMS C1 column (5  $\mu$ m, 80 Å, 4.6 x 250 mm). The targeted compounds were separated by a mixture of acetonitrile: phosphate buffer (pH 6.2, containing 20 mM of sodium monophosphate monobasic): triethylamine (45:55:0.2, v/v). The mobile phase was filtered using Nylon membrane filter (0.22  $\mu$ m) from Agilent Technologies (Waldbronn, Germany). It was also freshly prepared and degassed for 15 mins before use. Isocratic elution at a flow rate of 1.3 mL min<sup>-1</sup> was used. Volume of injection was 20  $\mu$ L. The data were processed using licensed Empower V.2 software (Milford, MA, USA).

## CHAPTER 3

### ELECTROCHEMICALLY MODULATED LIQUID-LIQUID EXTRACTION BASED ON POTENTIOSTATIC METHOD

#### 3.1 Methodology

##### 3.1.1 Experimental strategy

First, determination of transfer potential was done by cyclic voltammetry using three types of ITIES cell as the protocol explained in Section 2.1.3. Then, extraction was performed by using 10 mM LiCl as the aqueous phase and 1,2- DCE containing  $\text{BTPPA}^+\text{TPBCl}^-$  in rotating paddle in static ITIES cell (Figure 2.1b). The yield of extraction was optimized by investigating; i) effect of back-extraction and ii) effect of waiting time after extraction.

##### 3.1.2 Sample preparation by applying potential using potentiostat

A rotating paddle in static ITIES cell was used. The preparation of the biphasic system is as mentioned in Section 2.1.3. The extraction was carried out using chronoamperometry technique. At Stage 1, potential of +0.80 V was applied to the system for 900 s. After that, the electrode was removed, and the organic phase was taken out. It was transferred to centrifuge tube. DI water was placed into the centrifuge tube for the purpose of back-extraction (Stage 2). The solution was vortexed and centrifuged for 90 s and 60 s, respectively. Finally, the aliquot of final aqueous phase was injected into HPLC (Stage 3). The diagram below summarizes the procedure.

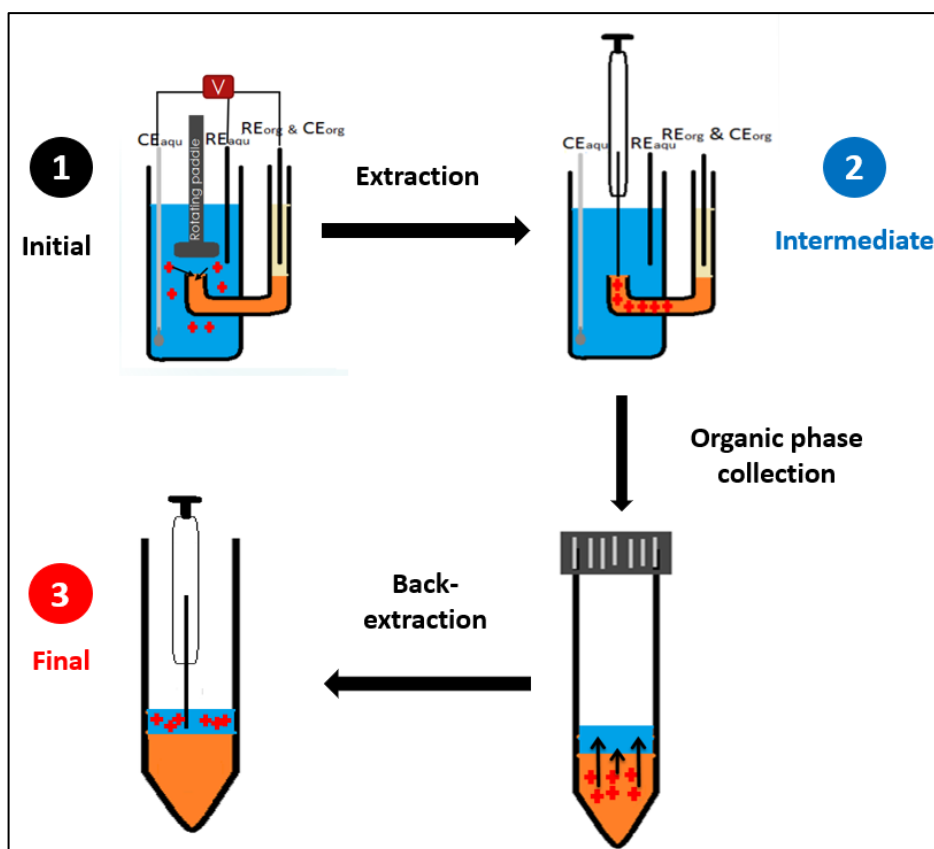


Figure 3.1: Experimental procedure of the electrochemically modulated liquid-liquid extraction. Target cations are extracted from the aqueous sample to organic phase before being back-extracted to a final aqueous phase. The numbers 1, 2 and 3 correspond to the initial, intermediate and final stages at which the aqueous phases are analysed by HPLC

## 3.2 Results and discussion

### 3.2.1 Optimization of HPLC method

The wide range of polarity of targeted drugs makes it challenging to find suitable reverse phase chromatographic conditions. Interference with solvent because of rapid elution of biguanide compounds especially MET on C18 column happened owing to their high polarity properties (Gabr *et al*, 2010). This problem can be solved by adding ion pair additives in the mobile phase such as sodium dodecyl sulphate or sodium heptane sulfonate (Yamamoto *et al*, 2002). The presence of optimum concentration of ion pair forming additive can reduce its polarity (Gabr, 2010).

A derivatization agent, p-nitrobenzoyl chloride was used to derivatize MET into less polar compound (Tache *et al*, 2001). According to recent study, C1 column gave good separation without using any derivatization agent or ion pair. This is due to the high polarity of C1 column compared to C18, C8, and pentafluoro phenyl (PFP) columns (Alshishani *et al*, 2016).

Different compositions mixtures of acetonitrile with phosphate buffer were investigated as the mobile phase on C1 column. The peak separation of the targeted drugs was good when the mobile phase consisted 40-60 % of acetonitrile. The retention time of MET, PHEBI, PHEN increased as acetonitrile composition increased. It is opposite with PROP as it is the most hydrophobic drug. Propranolol retention time decreased as acetonitrile composition increased. The optimum percentage was 50:50 of acetonitrile: 20 mM phosphate buffer (pH 6.2). As pH of buffer decreased, the retention time of analytes became shorter. 0.2 % (v/v) of triethylamine was added to reduce the peak tailing. Substituting acetonitrile to methanol gave overlapping peak for biguanide compounds. Methanol has polarity index value of 6.6 which is higher

than acetonitrile, 6.2 (Alshishani *et al*, 2016). This value indicates that methanol is more polar than acetonitrile. Therefore, the polarity of mobile phase became higher when methanol was used and caused the peak of hydrophilic biguanide compounds to be overlapped.

All analytes were eluted within 13 mins. The retention time of MET, PHEBI, PHEN and PROP were 3.9 mins, 5.3 mins, 6.2 mins and 11.1 mins, respectively as in Figure 3.2. Calibration curve (Figure 3.3) was established by plotting peak area versus concentration of each analyte. It was linear over the range of 0.8 – 16  $\mu\text{M}$ . Good correlation coefficient values ( $R^2$ ), 0.9991, 0.9994, 0.9998 and 0.9981 were obtained for MET, PHEBI, PHEN, and PROP, respectively.

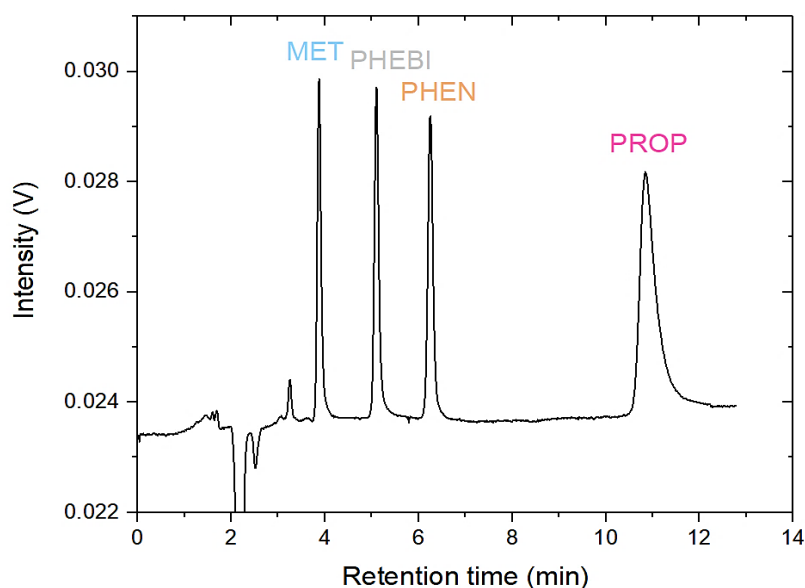


Figure 3.2: Chromatogram of MET, PHEBI, PHEN and PROP. Mobile phase: Phosphate buffer, 50: ACN, 50: triethylamine, 0.2. Column: Zorbax TMS (250 x 4.6 mm). Flow rate: 1.3 mL min<sup>-1</sup>. Injection volume: 20  $\mu\text{L}$ . Column temperature: 40 °C. Wavelength: 230 nm. Concentration of analytes: 16.4  $\mu\text{M}$

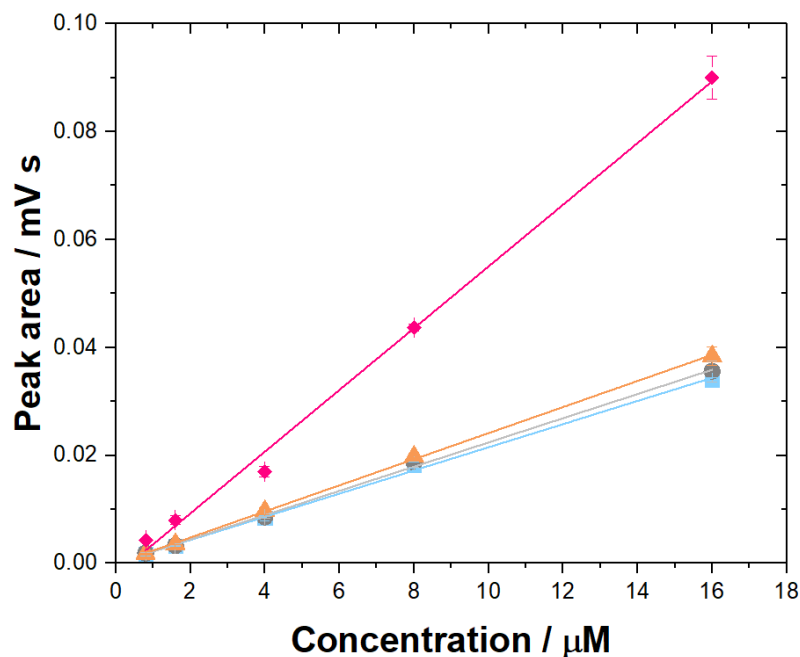


Figure 3.3: Calibration curves for MET, PHEBI, PHEN and PROP obtained by HPLC. Mobile phase: Phosphate buffer, 50: ACN, 50: triethylamine, 0.2. Column: Zorbax TMS (250 x 4.6 mm). Flow rate: 1.3 mL min<sup>-1</sup>. Injection volume: 20  $\mu\text{L}$ . Column temperature: 40 °C. Wavelength: 230 nm. Concentration of analytes: 0.8 -16  $\mu\text{M}$ . MET (blue squares), PHEBI (grey circles), PHEN (orange triangles) and PROP (pink diamond)

### 3.2.2 Cyclic voltammetry study of targeted compounds

The transfer of the mono-cationic form of metformin (MET), phenformin (PHEN), phenyl biguanide (PHEBI) and propranolol (PROP) was investigated by cyclic voltammetry at the ITIES as shown in Figure 3.4. For voltammetry study, static ITIES cell as shown in Figure 2.3 was used. The potential windows of the cyclic voltammogram were limited by  $\text{Li}^+$  and  $\text{TPBCl}^-$  transferring on the right side and by  $\text{Cl}^-$  and  $\text{BTPPA}^+$  on the left side. For each drug, a reversible ion transfer was observed, and the transfer potential was determined as the half-wave potential. For a reversible charge transfer, the classical conditions were fulfilled; 1) the peak potential independent of the scan rate, 2) Peak to peak separation is  $59/z_i$  mV at 25°C. The addition of positively charged analytes to the lithium chloride aqueous phase led to a

positive peak at forward sweep as a result of the analytes being transferred from aqueous phase to organic phase. The negative peak on the reverse sweep represents the back-transfer of analytes from organic to aqueous phase.

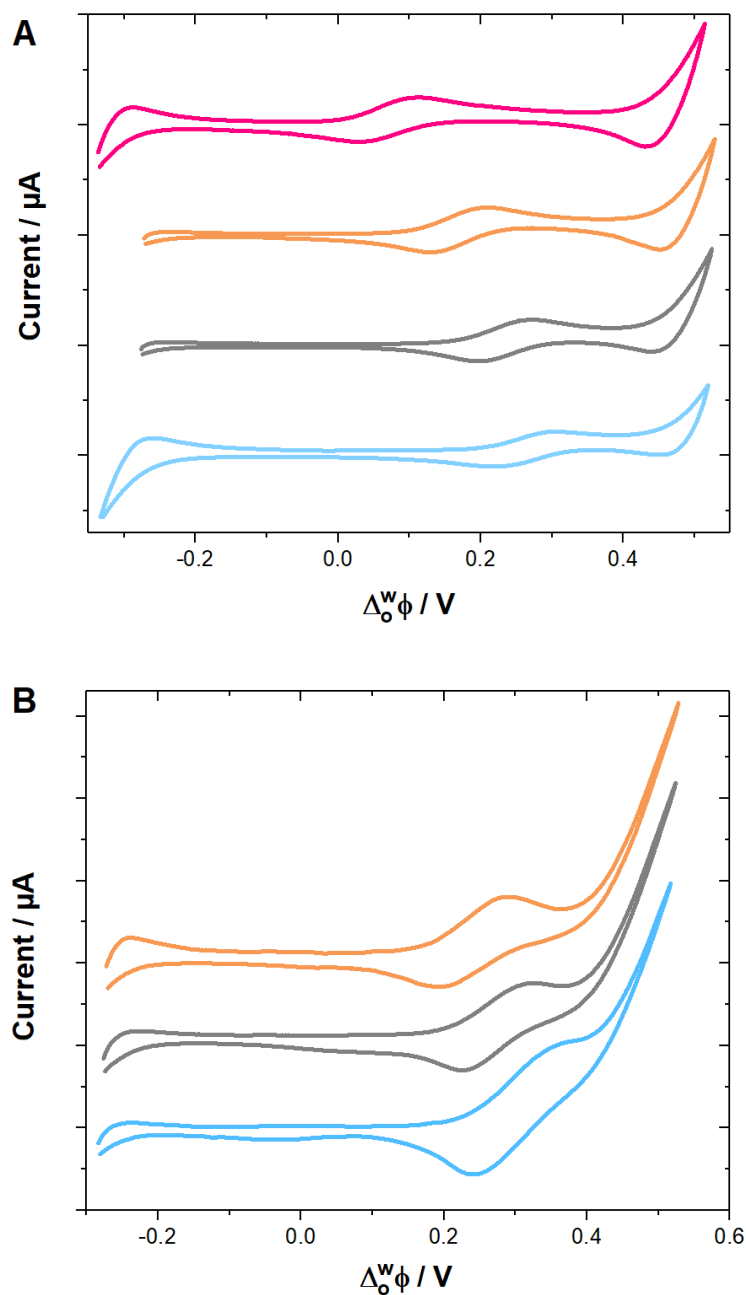


Figure 3.4: Cyclic voltammograms of 170  $\mu\text{M}$  MET (blue curve), PHEBI (grey curve), PHEN (orange curve) and PROP (pink curve) transferring across the ITIES. a) pH 6 b) pH 2. Experimental conditions: Aqueous phase: 10 mM LiCl. pH of aqueous phase: 6. Organic phase: 10 mM of BTPPA<sup>+</sup> TPBCl<sup>-</sup> in 1,2- DCE. Scan rate: 5 mV s<sup>-1</sup>. Cell: Static ITIES cell

TEA<sup>+</sup> and TPA<sup>+</sup> were added to the aqueous phase at the end of experiment as a reference. The purpose of adding them was to prove the experimental set up is adequate. TEA<sup>+</sup> transfer occurred at +0.377 V  $\pm$  0.005 which is lesser than MET, PHEBI, PHEN transfers as shown in Table 3.1 below. Figure 3.4 depicted a reversible ion transfer and the voltammogram was plotted in Galvanic scale. The formal Galvanic transfer potential was determined as the half-transfer potential. The formal Galvanic transfer potential can be calculated by using equation (3.1),

$$\Delta_o^w \phi_i^{1/2} - \Delta_o^w \phi_i' = \Delta_o^w \phi_{TEA^+/TPA^+}^{1/2} - \Delta_o^w \phi_{TEA^+/TPA^+}' \quad (3.1)$$

where  $\Delta_o^w \phi_i^{1/2}$  and  $\Delta_o^w \phi_{TEA^+/TPA^+}^{1/2}$  are the measured half-wave potentials of the ions and TEA<sup>+</sup>/TPA<sup>+</sup>, respectively. -0.090 V and +0.020 V is the standard ion transfer potential for TPA<sup>+</sup> and TEA<sup>+</sup>, respectively (Hung, 1980; Iwata *et al*, 2017). The formal Galvanic transfer potentials are (MET) +0.270 V, (PHEBI) +0.256 V, (PHEN) +0.186 V and (PROP) +0.116. All the values are listed in Table 3.1. The drug transfer potential followed the same trend when the pH of the aqueous phase was set at pH 2 as shown in Figure 3.4B.

Table 3.1: Transfer potential, pKa, and log P<sub>0</sub> for each drug

Targeted drugs	$\Delta_o^w \phi_i^{1/2}$ , V		$\Delta_o^w \phi_i'$ , V		$\Delta_o^w \phi_{TEA^+/TPA^+}^{1/2}$	pKa	Log P <sub>0</sub>
	pH 2	pH 6	pH 2	pH 6			
MET	+0.678	+0.630	+0.314	+ 0.270	+0.020	2.80, 11.5	-1.82
PHEBI	+0.610	+0.610	+0.268	+0.256	+0.020	2.13, 10.8	-0.03
PHEN	+0.566	+0.536	+0.234	+0.186	+0.020	2.70, 11.8	0.41
PROP	-	+0.507	-	+0.116	- 0.090	9.41	3.10

The transfer potential of the cations increased with their hydrophilic nature (Figure 3.5). Indeed, MET, with a  $\log P_o$  value of -1.82 (for the non-ionic form of MET), transfers at a potential of +0.678 V, which is higher than the potential of +0.566 V measured for PHEN ( $\log P_o = 0.41$ ), whereas PHEBI has an intermediate ( $\log P_o = -0.03$ ) and transfer potential is +0.610 V. PROP contains a naphthalene group, which makes it more hydrophobic than MET and a lower potential is needed to transfer from aqueous to organic phase.

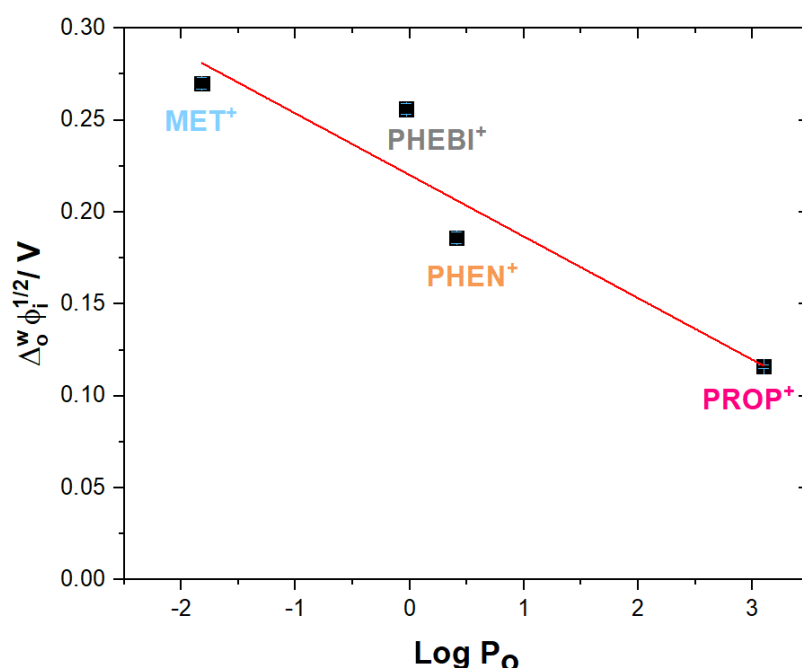


Figure 3.5: Graph of Galvanic transfer potential versus  $\log P_o$  for each drug

Effect of scan rate on cyclic voltammetry of MET was done during preliminary study (Figure 3.6). The peak current increased as the scan rate is increasing. The current increase is due to a diminution of the thickness of the diffusion layer. The diffusion layer grows much further from the interface when a slow scan rate is used. Consequently, the flux across the interface is smaller at slow scan rates than it is at high rates. As the current is proportional with flux, the current is lower at slow scan rates than at high rates. The linear relationship between the peak current and the

squares root of scan rate is the characteristic behaviour of linear-diffusion controlled electrochemical process. It can be explained by the Randles-Sevcik equation (3.2):

$$i_p = (2.69 \times 10^5) z_i^{3/2} A D^{1/2} C v^{1/2} \quad (3.2)$$

Where  $z_i$  is the net charge of the species,  $A$  is the area of interface ( $\text{cm}^2$ ),  $D$  is the diffusion coefficient of the species studied ( $\text{cm}^2 \text{s}^{-1}$ ),  $C$  is the concentration of the species ( $\text{mol cm}^{-3}$ ), and  $v$  is the scan rate ( $\text{V s}^{-1}$ ). The value of  $R^2$  obtained from the calibration curve in Figure 3.7 was 0.9961 which indicates that the relationship between peak current of MET and the squares root of scan rate is linear. This experiment explains that the diffusion in water is limiting the extraction flux and not the ion transfer kinetics. This led us to try to improve the mass transport of analyte in the aqueous phase.

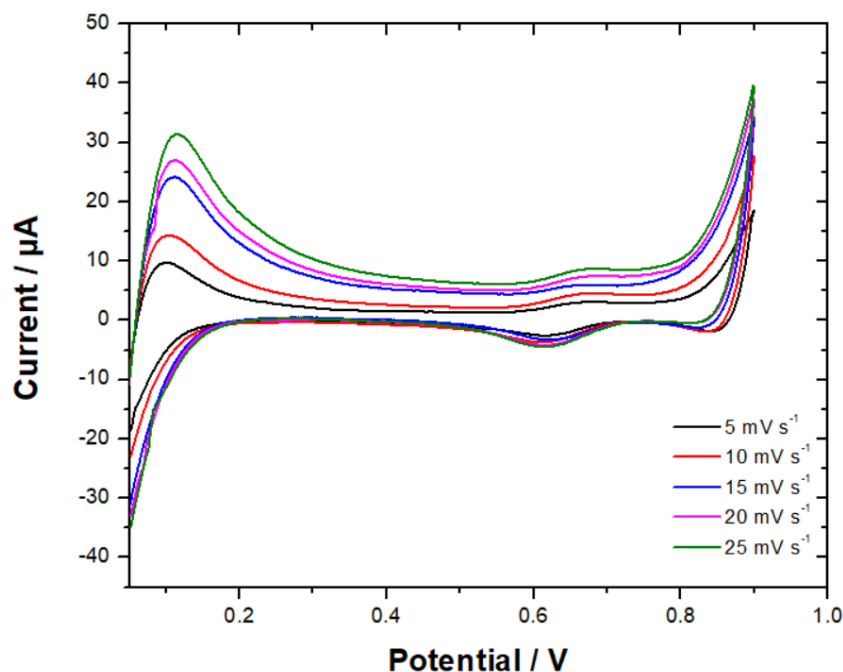


Figure 3.6: Effect of scan rate of on MET transfer. Experimental conditions: Aqueous phase: 10 mM LiCl. pH of aqueous phase: 6. Organic phase: 10 mM of BTPPA<sup>+</sup> TPBCL<sup>-</sup> in 1,2- DCE. Scan rate: 5 - 25  $\text{mV s}^{-1}$ . Cell: Static ITIES cell. [MET] :0.280 mM

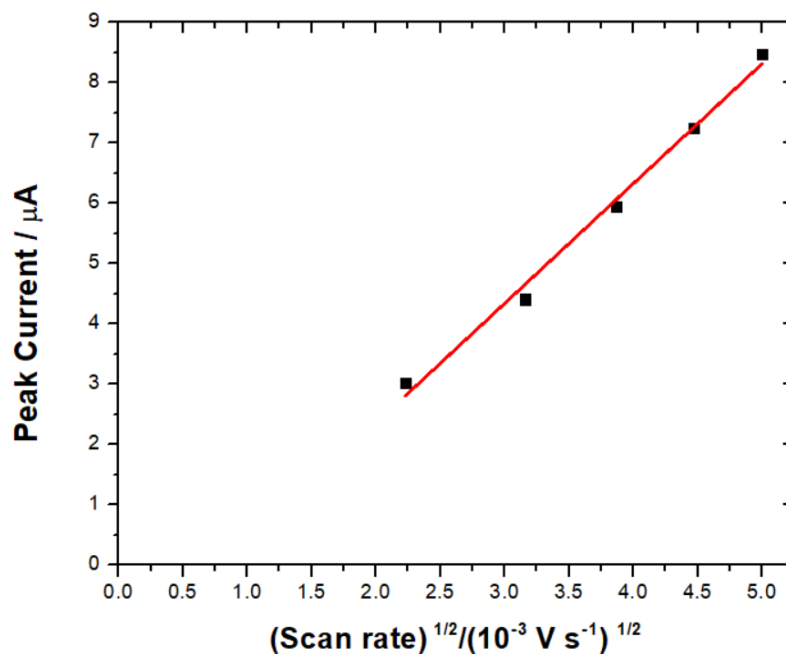


Figure 3.7: Peak current vs squares root of scan rate of MET. Experimental conditions: Aqueous phase: 10 mM LiCl. pH of aqueous phase: 6. Organic phase: 10 mM of BTPPA<sup>+</sup> TPBCl<sup>-</sup> in 1,2- DCE. Scan rate: 5 - 25 mV s<sup>-1</sup>. Cell: Static ITIES cell. [MET] :0.280 mM

### 3.2.3 Hydrodynamic cell

#### 3.2.3(a) Rotating paddle in membrane supported ITIES

Different types of cells were analysed in attempt to enhance mass transfer of analytes across interface. First, is rotating disk interface with polyethylene terephthalate, PET supported ITIES. PET membrane was used to stabilize the ITIES under stirring conditions. There are some advantages using PET membrane to modify interfaces: chemical stability, low tortuosity of the pores, availability with submicron pore diameters, a narrow pore size distribution, and the one-dimensional nature of the pore structure. PET membranes also do not swell on contact with many organic solvents (Kralj, 2002).

The voltammograms obtained (Figure 3.8) show that with the PET membranes the system suffers of a high electrical resistance. From the equation of Ohm's Law,  $I$  is inversely proportional to  $R$  at constant  $V$ . Supposedly, the voltammograms is sigmoidal shape due to enhancement of mass transfer. After the addition of MET with concentration range 0.099-0.392 mM, it can be seen that the highest current is approximately  $\sim 0.4 \mu\text{A}$  whereas without stirring in the classical cell values at least 10 times higher were obtained. Surface area of available interface is not the same, so the values were not strictly comparable. Nevertheless, the small values of current maybe attributed to a high electrical resistance in the system. Moreover, the transfer peak of MET cannot be defined as can be observed in Figure 3.8. The other problem occurred in this experiment is the organic solvent which is 1,2- DCE which passed through the membrane. This happens due to the density of 1,2- DCE ( $1.256 \text{ g mL}^{-1}$ ) and its low viscosity.

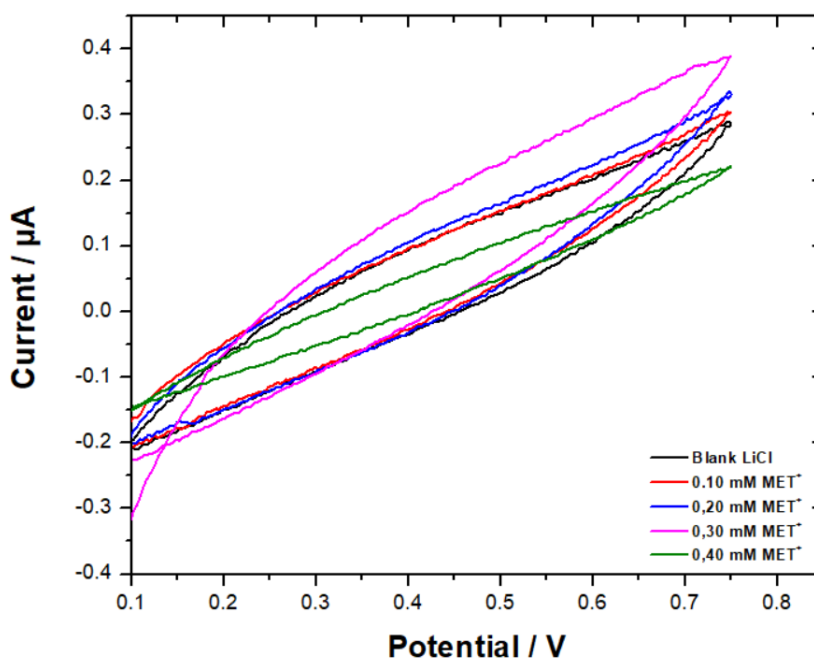


Figure 3.8: Effect of the concentration of MET. Experimental conditions: Aqueous phase: 10 mM LiCl. pH of aqueous phase: 6. Organic phase: 10 mM of BTPPA<sup>+</sup> TPBCL<sup>-</sup> in 1,2- DCE. Scan rate:  $5 \text{ mV s}^{-1}$ . Rotation speed: 100 rpm

The organic phase was changed from 1,2- DCE to nitrophenyl octyl ether, NPOE keeping the background salt the same. NPOE is comparable in density ( $1.04 \text{ g mL}^{-1}$ ) with the aqueous phase. NPOE is also widely used in liquid-liquid electrochemistry, electro-kinetic extraction of drugs, ion selective electrodes and both passive and electrochemically controlled drug transfer across supported liquid membranes (Velicky *et al.*, 2014). The most common ion used for observation of ion transfer process is tetraethylammonium ( $\text{TEA}^+$ ). Thus,  $\text{TEA}^+$  was used in this experiment to define the transfer peak. The voltammograms reported in Figure 3.9A revealed the same trend than those obtained in 1,2- DCE. The system suffered from high resistance and transfer peak of  $\text{TEA}^+$  cannot be observed.

Then, the effect of stirring rate was studied. At 100 rpm, the current was higher than at 200 rpm. The NPOE was also passing through the membrane at 200 rpm, and thus affecting the interface and also the transfer of ions. There was also no change in voltammogram when considering PROP that has low transfer potential as the target (Figure 3.9B). The efforts to improve the transfer across the interface by using a membrane supported interface and stirring with a paddle were ineffective.

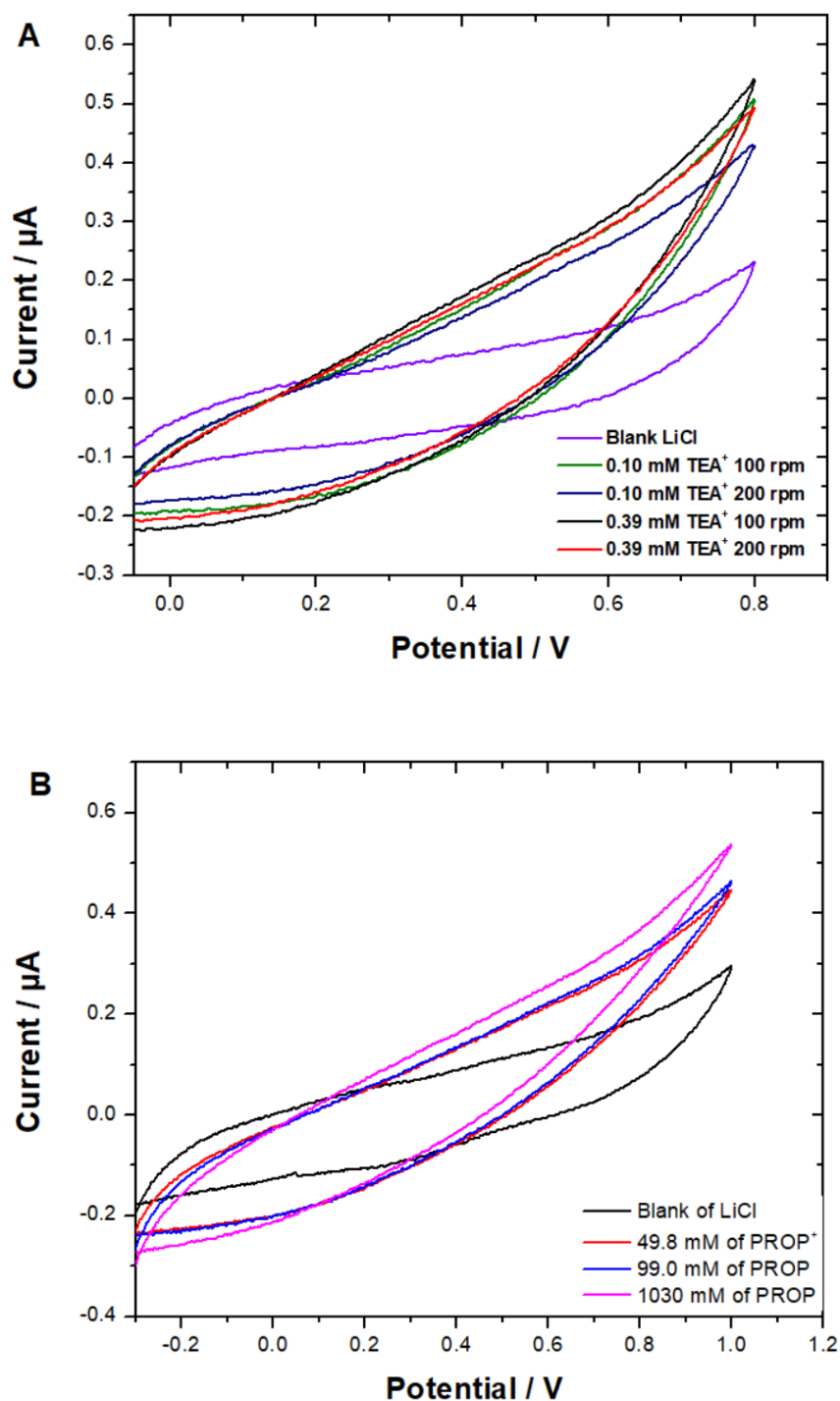


Figure 3.9: A) Effect of the concentration of TEA<sup>+</sup>. Rotation speed= 100 and 200 rpm. B) Effect of the concentration of PROP. Rotation speed= 100 rpm. Experimental conditions: Aqueous phase: 10 mM LiCl. pH of aqueous phase: 6. Organic phase: 10 mM of BTPPA<sup>+</sup> TPBCl<sup>-</sup> in NPOE. Scan rate: 5 mV s<sup>-1</sup>

### 3.2.3(b) Rotating paddle in static ITIES cell

A rotating paddle was installed in the aqueous phase to enhance the flux of the molecules transferred. In this hydrodynamic cell, voltammetric studies were operated with three electrodes. The aqueous phase contained one reference and one counter electrode. Meanwhile, the organic phase only had one electrode that acted as reference and counter electrode.

Figure 3.10A reports the electrochemistry of background electrolyte and transfer of TEA<sup>+</sup> under stirring conditions. The presence of a positive current at ~0.5 V indicates that TEA<sup>+</sup> is transferring from aqueous phase to organic phase in the forward sweep. The rotating paddle was used to induce convection (Figure 3.11) in the aqueous phase, causing the initial TEA<sup>+</sup> transfer from aqueous to the organic phase to occur under steady state conditions. Conversely, the TEA<sup>+</sup> returning to the aqueous phase during the backward sweep is transported across the ITIES solely by diffusion mainly because of no convection mechanism in the organic phase. Figure 3.10B shows that the voltammograms has the sigmoidal shape reflecting the convective-diffusion mode of mass transport. The transfer of TEA<sup>+</sup> is increasing as the rotation speed of the paddle is increased as demonstrated by the increase of the peak current.

The noise in voltammograms can be reduced by adjusting the height of the rotating paddle relative to ITIES of LiCl and 1,2- DCE. The noise was likely to be caused by i) vibration on the interface resulting from paddle with too fast rotation or ii) contact of rotating paddle with the interface. The highest rotation speed used was 150 rpm. The organic phase was sucked from its tube when 200 rpm rotation speed was applied. Furthermore, the optimum speed of rotation will preserve a steady convective flux of solute to and away from interface (Velicky *et al.*, 2012)

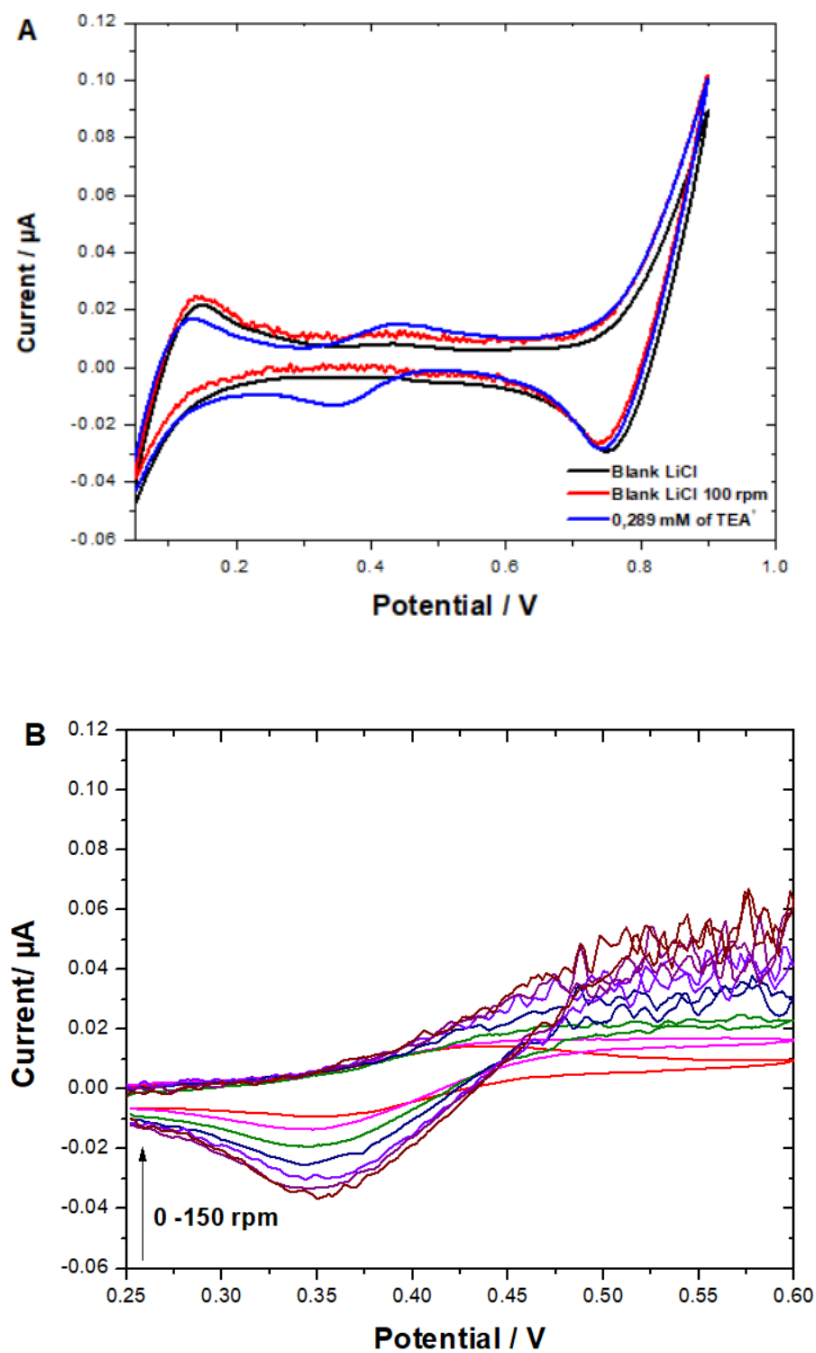


Figure 3.10: A) Effect of 0.029 mM  $\text{TEA}^+$  B) Effect of the rotation speed (25-150 rpm). Experimental conditions: Aqueous phase: 10 mM LiCl. pH of aqueous phase: 6. Organic phase: 10 mM of  $\text{BTTPPA}^+$   $\text{TPBCl}^-$  in 1,2- DCE. Scan rate:  $5 \text{ mV s}^{-1}$

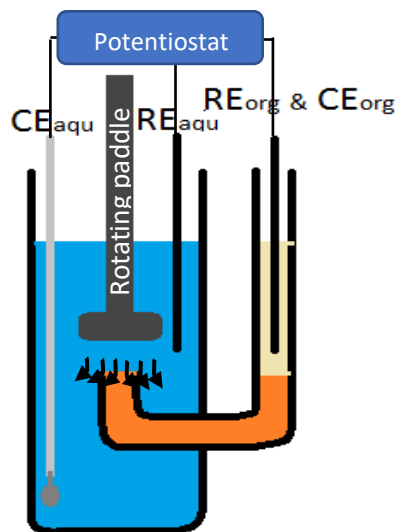


Figure 3.11: Schematic to illustrate the flow lines at interface

Figure 3.12 shows that the reciprocal limiting currents obtained experimentally during the forward sweep have a linear dependence on square root of rotation speed,  $\omega^{1/2}$ . The interfacial area can be calculated from the gradient of equation (3.3):

$$I_{lim} = 0.62 z F A D^{2/3} \nu^{-1/6} C_b \omega^{1/2} \quad (3.3)$$

Where  $z$  is the charge number of the transferring species,  $F$  is Faraday's constant,  $A$  is the total surfaces area,  $D$  is the diffusion coefficient of the active species,  $\nu$  is the kinematic viscosity of the moving solution,  $C_b$  is the bulk concentration of the transferring ion and  $\omega$  is the angular rotation frequency. The interfacial area calculated is  $5.61 \times 10^{-3} \text{ cm}^2$ . The interfacial area calculated is larger than geometric area of the cell ( $3.85 \times 10^{-3} \text{ cm}^2$ ) probably because of non-planarity of the surface.

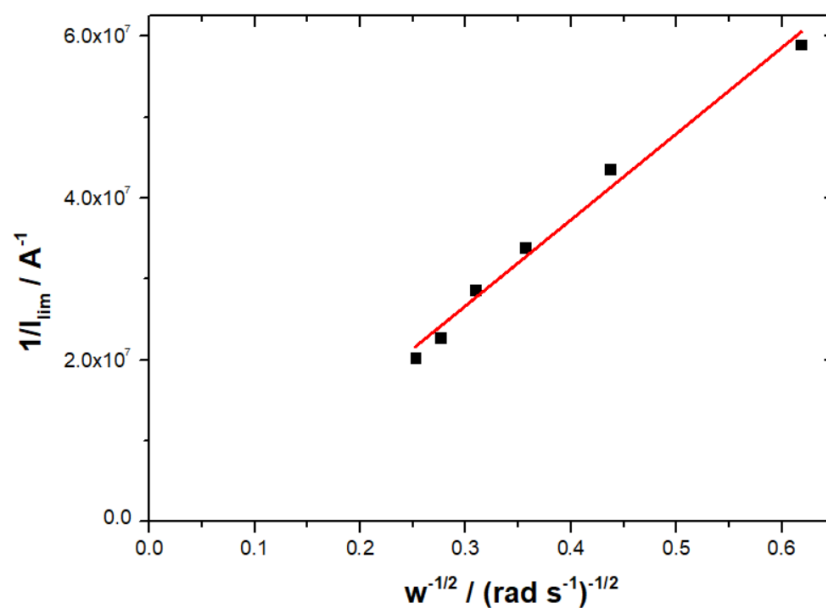


Figure 3.12: Calibration curve of  $1/I_{\text{lim}}$  versus the inverse squares root of the rotation speed at 0.55 V

Figure 3.13 shows that the rotating paddle in ITIES cell has the highest current density, followed by ITIES static cells and rotating disk cell with PET supported membrane. Whereas, Table 3.2 shows the current density for each electrochemical cell.

Table 3.2: Current density for each electrochemical cell

Electrochemical cell	Surface area of interface, $\text{cm}^2$	$I_{\text{max}}, \mu\text{A}$		$j, \mu\text{A cm}^{-2}$	
		LiCl	TEA+LiCl	LiCl	TEA+LiCl
ITIES cell	1.10	15.8	27.3	14.4	24.8
Rotating disk electrode with PET membrane	0.147	0.06	0.42	0.38	2.86
Rotating paddle in ITIES	$3.85 \times 10^{-3}$	0.090	0.100	23.4	26.3

\*  $I_{\text{max}}$ : These values are obtained at the maximum potential in voltammogram

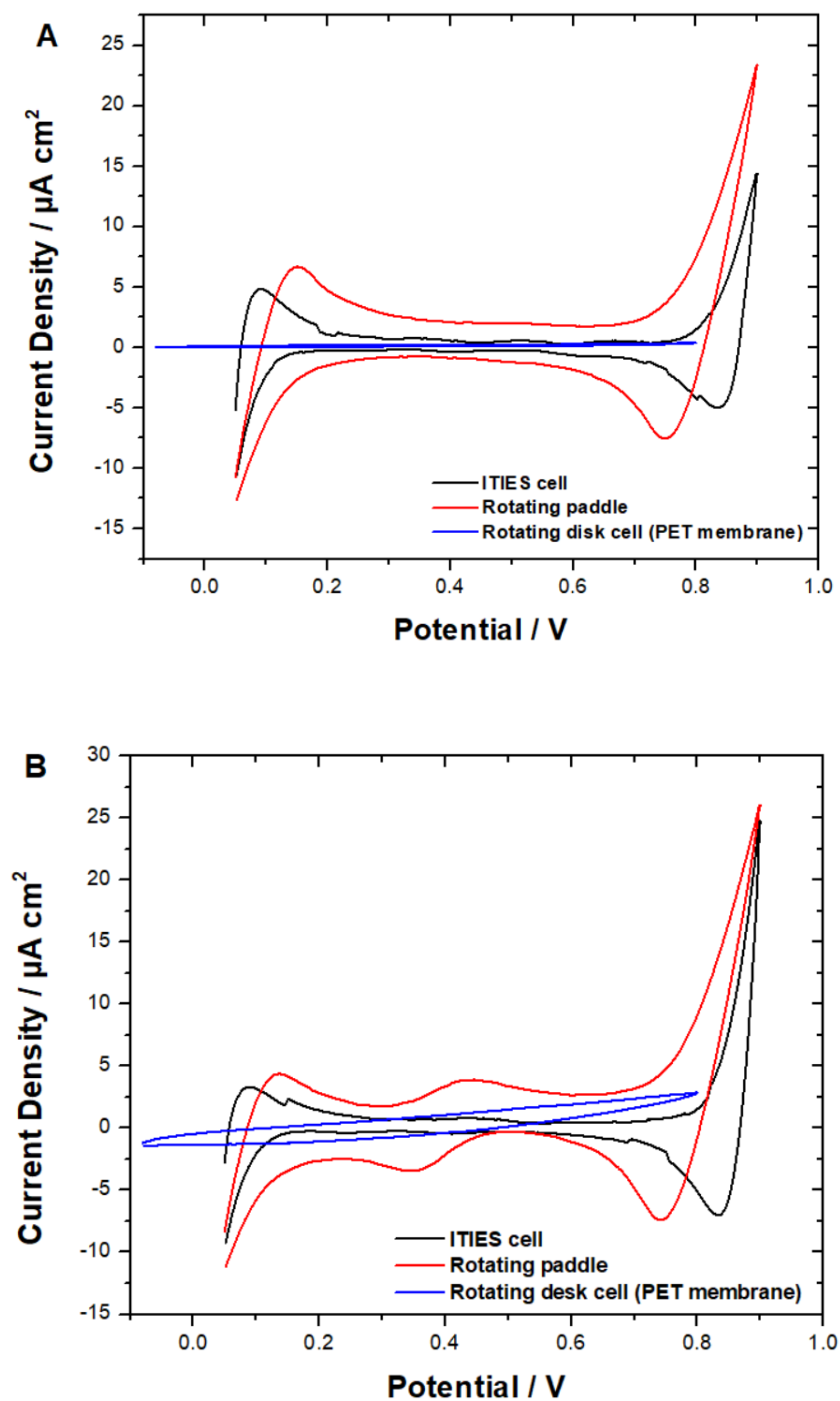


Figure 3.13: Effect of the type of cells on the current density. A) 10 mM LiCl B) TEA<sup>+</sup> in 10 mM LiCl. Experimental conditions: Aqueous phase: 10 mM LiCl. pH of aqueous phase: 6. Organic phase: 10 mM of BTPPA<sup>+</sup> TPBCl<sup>-</sup> in 1,2- DCE. Scan rate: 5 mV s<sup>-1</sup>

### **3.2.4 Electrochemical extraction as sample preparation**

From previous section 3.2.2, each of the ions were able to transfer across interface with their own transfer potential value as summarized in Table 1. To increase the mass transfer, a rotating paddle in ITIES was chosen to proceed with electro-driven extraction. By applying enough potential for certain time to the biphasic system, analytes can transfer from aqueous to organic phase. After that, the organic phase was collected and transferred into centrifuge tube for back-extraction to final aqueous phase. Lastly, the aliquot of final aqueous phase was quantified using HPLC.

#### **3.2.4(a) Potentiostatic drug extraction**

In this section, a constant extraction potential was applied using chronoamperometry techniques. Potential applied must be higher than any transfer potential of targeted drugs to ensure the analytes are fully transferred across interface. Thus, +0.80 V was selected using chronoamperometry set up as potential was applied for 15 mins to transfer drugs from aqueous to organic phase.

The current obtained in Figure 3.14 was close to zero value for blank extraction (without any drugs) at +0.8 V and +0.4 V. It can be concluded that the background electrolyte does not give any influence during extraction process, while the current in presence of drugs was significantly higher than with the blank solution. The current decreased with time during application of potential because of ions concentration depletion at vicinity of the interface due to ions transferring to the adjacent phase (Velazquez-Manzanarez, 2014).

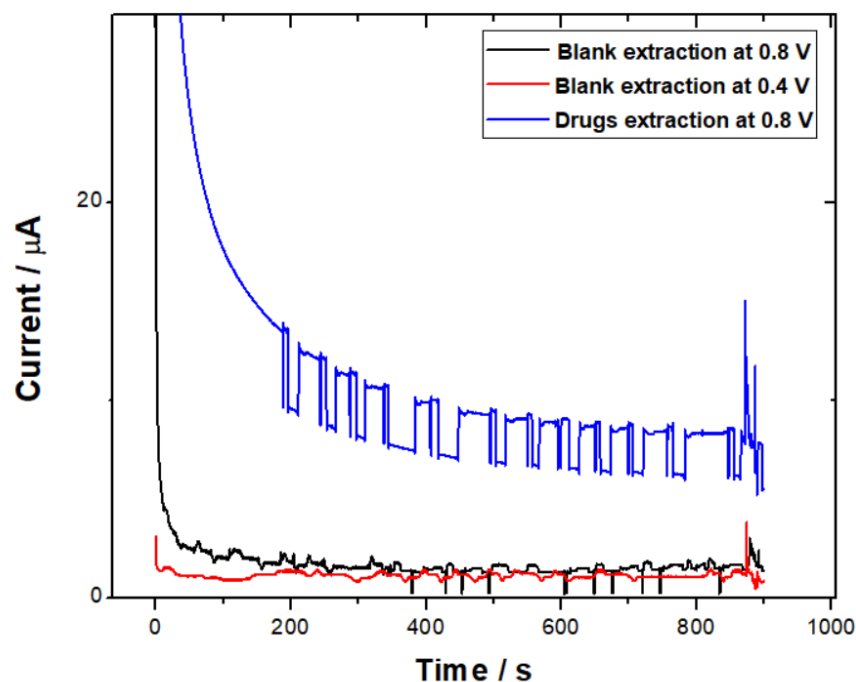


Figure 3.14: Chronoamperometry for different applied potential in the absence and in the presence of target analytes. Experimental conditions: Aqueous phase: 10 mM LiCl. Organic phase: 100  $\mu\text{L}$  of 10 mM of BTPPA<sup>+</sup> TPBCl<sup>-</sup> in 1,2- DCE. [Target analytes]: 0.164 mM. Scan rate: 5 mV s<sup>-1</sup>. Extraction time: 900 s. Rotation speed: 150 rpm. Cell: Rotating paddle in ITIES cell

Extraction for each drug individually and in mixture simultaneously were performed at constant potential (+0.80 V) for 900 s. Chronoamperometry of both cases were shown below (Figure 3.15). By integrating current versus time curve, we can calculate the total charge that was transferred up to 900 s at different potential applied.

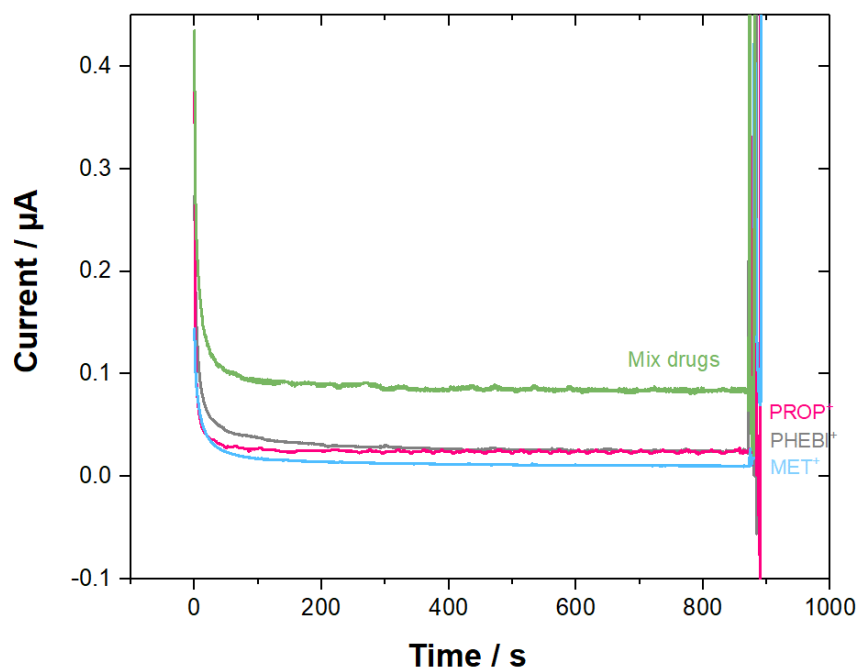


Figure 3.15: Chronoamperometry for potential driven extraction of analytes. Experimental conditions: Aqueous phase: 10 mM LiCl. Organic phase: 100  $\mu$ L of 10 mM of BTPPA<sup>+</sup> TPBCl<sup>-</sup> in 1,2- DCE. [Target analytes]: 0.164 mM. Scan rate: 5 mV s<sup>-1</sup>. Time extraction: 900 s. Rotation speed: 150 rpm. Cell: Rotating paddle in ITIES cell

From the calculation of the total charge at each point of potential applied, the graph of total charge versus potential, V can be plotted (Figure 3.16). Based on Figure 3.16B, we can conclude that no competition between analytes during extraction was observed. Indeed, the total individual charge transfers (obtained from the sum of individual drugs charge in Figure 3.16A) is very close to the charge transfer observed with mixed drugs.

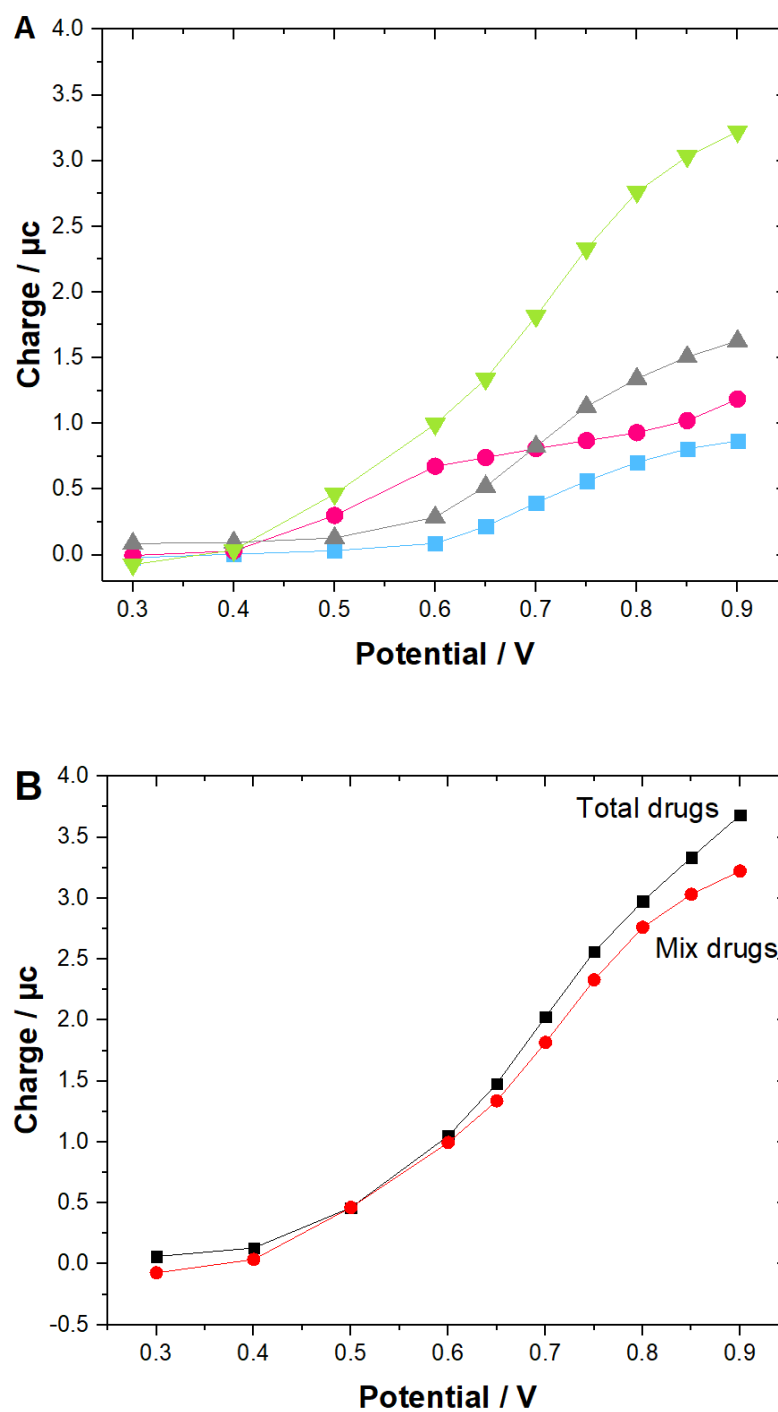


Figure 3.16: Graph of charge versus potential extraction of analytes, A) individually MET (blue curve), PHEBI (grey curve), PROP (pink curve) and mixed-drug (green curve). B) mixed-drugs simultaneously. Experimental conditions: Aqueous phase: 10 mM LiCl. Organic phase: 100  $\mu\text{L}$  of 10 mM of BTPPA<sup>+</sup> TPBCl<sup>-</sup> in 1,2- DCE. [Target analytes]: 0.164 mM. Scan rate: 5  $\text{mV s}^{-1}$ . Time extraction: 900 s. Rotation speed: 150 rpm. Cell: Rotating paddle in ITIES cell

### 3.2.4(b) Investigation on MET extraction performance

Extraction of MET was examined. There are two steps of preconcentration procedure as illustrated in Figure 3.1, which consisted of (i) extraction of analyte from aqueous phase to intermediate organic phase and (ii) back-extraction of analyte from intermediate organic phase to final aqueous phase. Number of total charges,  $Q$  was obtained during chronoamperometry. Thus, number of moles extracted to organic phase at Stage 2 can be calculated according to Faraday's Law constant,

$$Q = zNF \quad (3.4)$$

Where  $z$  is the charge transfer of analyte,  $N$  is the number of moles,  $F$  is Faraday constant in  $96\,485\text{ C mol}^{-1}$ .

Meanwhile, HPLC analysis at Stage 3 gave information on how many moles of drugs were extracted. The extraction efficiency can be calculated by comparing the initial number of moles with final number of moles.

By using this formula, the comparison between number of moles extracted during chronoamperometry and moles injected into HPLC can be done (Collins et al, 2008). Based on HPLC, the number of moles detected is only  $2.10 \times 10^{-10}$  moles whereas the number of moles transferred was  $1.33 \times 10^{-9}$  moles as depicted in Figure 3.17.

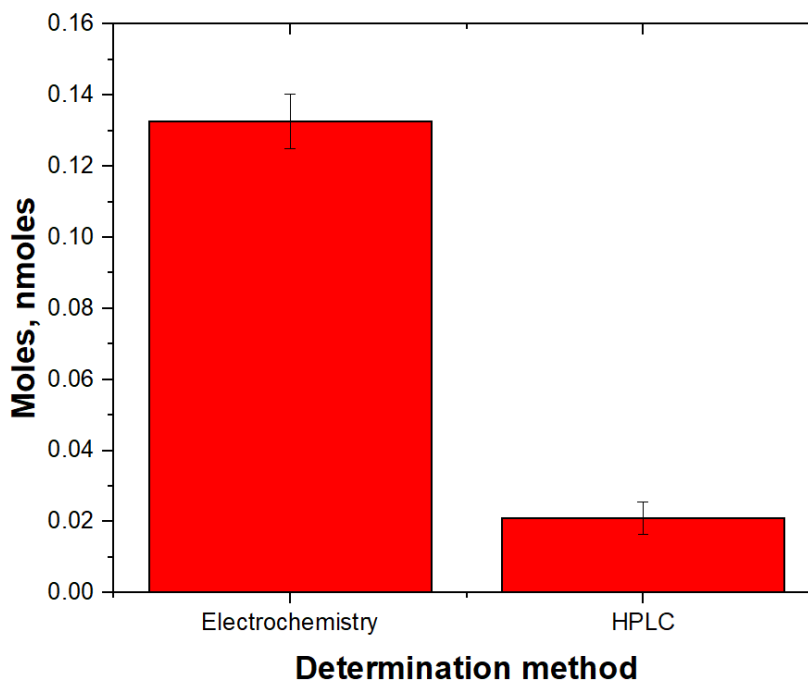


Figure 3.17: Comparison of faradaic and real extraction yield. Experimental conditions: Aqueous phase: 10 mM LiCl. Organic phase: 100 $\mu$ L of 10 mM of BTPPA<sup>+</sup>TPBCl<sup>-</sup> in 1,2- DCE. [MET] = 0.164 mM. Time of extraction: 900 s. Potential applied: + 0.8 V. Rotation speed: 150 rpm. Cell: Rotating paddle in ITIES cell

These results show a large discrepancy between the number of moles extracted and the number of moles actually detected. Indeed, 84.2 % of the moles of MET extracted are lost during the rest of the sample pre-treatment. There might be several reasons for this loss. The first reason could be that the MET is not fully back-extracted. Back-extraction using same organic phase containing drugs extracted was performed twice. The main purpose of this step is to confirm that all drugs extracted are not trapped inside the organic phase. As shown below in Figure 3.18, only 2.63 % moles of MET extracted was found during second back-extraction step. It proved that the back-extraction step did not contribute to the decrease of metformin extraction yield.

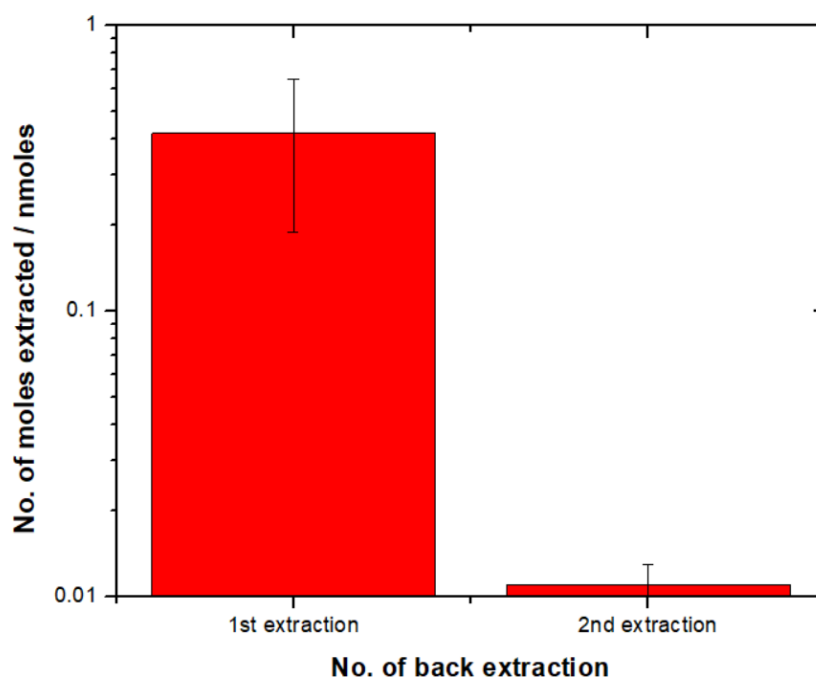


Figure 3.18: Graph of moles extracted against back-extraction step. Experimental conditions: Aqueous phase: 100  $\mu\text{L}$  of  $\text{H}_2\text{O}$ . Organic phase: 100  $\mu\text{L}$  of 10 mM of  $\text{BTTPA}^+ \text{TPBCl}^-$  in 1,2- DCE.  $[\text{MET}]$ : 0.164 mM. Vortex time: 90 s. Centrifuge time: 3 mins. Cell: Rotating paddle in ITIES cell

The second possibility is that MET back transferred spontaneously after the extraction potential was switched off and the electrochemical cell was left at open-circuit potential. In order to investigate this possibility, we varied the waiting time between the moment at which the extraction potential was switched off, and the organic phase collection was controlled. Figure 3.19 shows the number of moles detected by HPLC as a function of the waiting time. When the organic phase was collected as soon as the potential was switched off, 0.02 nmol were collected. If the waiting was 60 s or 300 s, the number of moles detected dropped to 0, demonstrating that the extracted MET transferred back spontaneously to the aqueous phase. Such results indicate the organic phase should be collected when the interfacial potential difference remained applied.

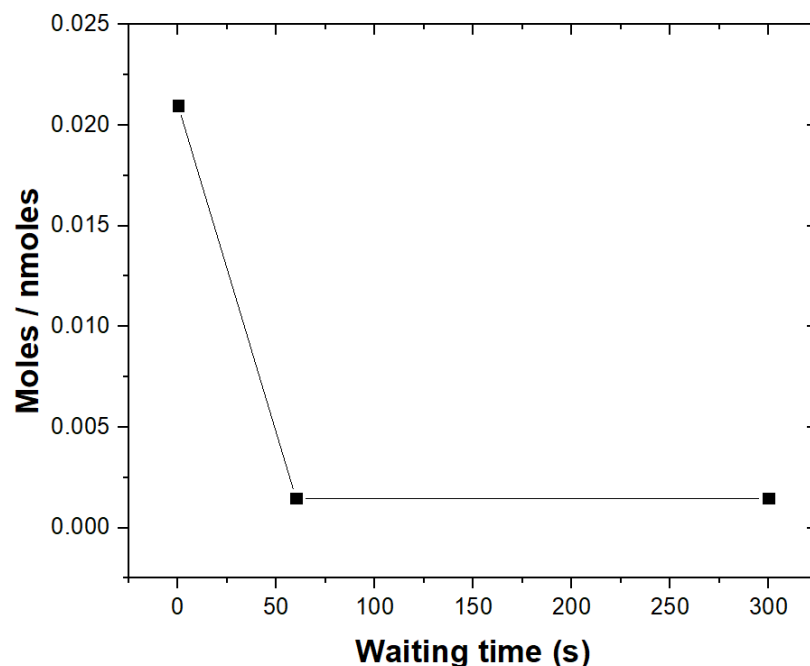


Figure 3.19: Graph of moles detected by HPLC against waiting time after extraction. Experimental conditions: Aqueous phase: 10 mM LiCl. Organic phase: 10 mM of BTPPA<sup>+</sup> TPBCl<sup>-</sup> in 1,2- DCE. [MET] = 0.164 mM Time extraction: 900 s. Potential applied: + 0.8 V. Rotation speed: 150 rpm. Cell: Rotating paddle in ITIES cell

### 3.3 Conclusion

This technique must be improved to achieve good extraction efficiency and good enrichment factor. As it is proven that the loss of analyte is not because of back-extraction step, different cell design must be investigated in future. Few important factors have to be noted in order to design different cell such as; 1) the biphasic system must be connected to potentiostat during sampling of organic phase, 2) the rotation should not disturb interface surface stability.

Another way is by introducing a new method, which uses concentration gradient of common ion between two phases to impose interfacial potential to extract the targeted compound.

## CHAPTER 4

### ELECTROCHEMICALLY MODULATED LIQUID-LIQUID EXTRACTION BASED ON POTENTIOSTATIC-FREE METHOD

#### 4.1 Methodology

##### 4.1.1 Cyclic voltammetry of rotating paddle in static ITIES cell

The set-up is as shown as in Section 2.1.2, Figure 2.1b. First, the organic phase was placed on bottom half of the cell. The aqueous phase was added slowly on top of the cell to ensure no air bubble presence in the interface. Analytes were added into aqueous phase. The CV was recorded in triplicates at  $5 \text{ mV s}^{-1}$  scan rate. Known amount of  $\text{TEA}^+$  was added to the aqueous phase at the end of a series of experiments for potential calibration purposes.

##### 4.1.2 Preparation of standard solution, aqueous and organic phase

An appropriate amount of analytes was dissolved in deionized water as a stock solution and stored at  $4^\circ\text{C}$ . An aqueous phase of  $\text{TMA}^+\text{Cl}^-$  was prepared by dissolving the desired amounts of compounds in deionized water. Working solutions were prepared from the stock solution by dilution of appropriate amounts in  $\text{TMA}^+\text{Cl}^-$  solution of targeted compound. An organic salt,  $\text{TMA}^+\text{TPBCl}^-$  was prepared by methathesis (Lee *et al*, 1997). The product was dissolved in 1,2- DCE as described in section 4.1.3.

#### 4.1.3 Preparation of organic salt (TMA<sup>+</sup>TPBCl<sup>-</sup>)

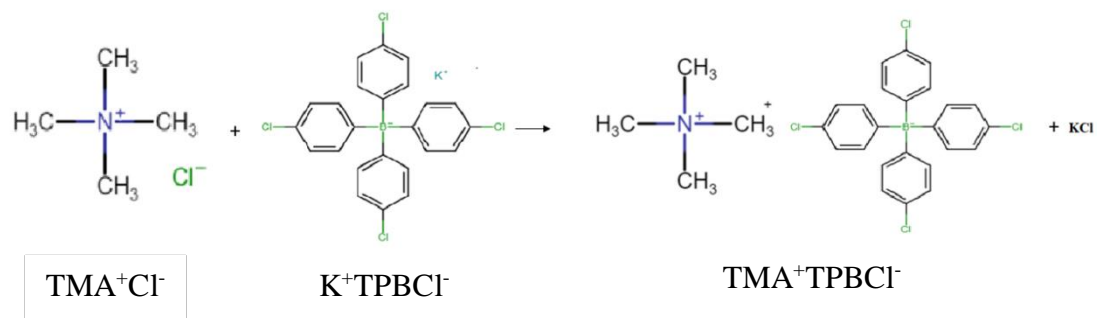


Figure 4.1: Metathesis reaction of TMA<sup>+</sup>TPBCl<sup>-</sup>

Equimolar amounts of TMA<sup>+</sup>Cl<sup>-</sup> and K<sup>+</sup>TPBCl<sup>-</sup> were weighted then dissolved in 10 mL and 20 mL mixture of H<sub>2</sub>O: MeOH in ratio 1:2, respectively as follows. The solution of TMA<sup>+</sup>Cl<sup>-</sup> was added dropwise into a vigorously stirring solution of K<sup>+</sup>TPBCl<sup>-</sup>. White precipitate was produced and left under stirring for 2 h. After that, the suspension was filtered under vacuum for about 30 minutes. The product was transferred to a dry beaker and placed in a desiccator overnight. Then, the product was dissolved in acetone and covered with aluminium foil with small holes to allow evaporation of acetone. Evaporation took place around 2 days to ensure complete evaporation. The resulting crystal was rinsed with acetone: H<sub>2</sub>O mixture, filtered under vacuum. The resulting TMA<sup>+</sup>TPBCl<sup>-</sup> was stored in refrigerator. The vessel was covered with aluminium foil to prevent from light exposure.

#### 4.1.4 Preparation of urine samples

Urine samples were obtained from voluntary healthy students of USM. In order to reduce the matrix effect of urine samples, simple and rapid pre-treatment has been used. A few sample pre-treatments were carried out; 1) Dilution with deionized water, 2) Protein precipitation by acetone. The samples spiked with standard mixture was

diluted, 1:4, 1:10, 1:20 with deionized water. For protein precipitation, acetone was added three times more than the volume of urine sample. Then, it was vortexed and centrifuged for 3 minutes. The supernatant was transferred for sample preparation.

#### **4.1.5 Sample preparation by interfacial potential difference by common ion**

Potential transfer of each analyte was determined using voltammetry. In this section, targeted drugs were extracted across interface by applying interfacial potential difference. The potential was imposed by introducing concentration gradient of common ion which is tetramethylammonium chloride ( $\text{TMA}^+$ ) between both phases. Thus,  $\text{TMA}^+\text{Cl}^-$  and  $\text{TMA}^+\text{TPBCl}^-$  salts were dissolved in the aqueous and the organic phase respectively to control the interfacial potential difference,  $\Delta_o^w \phi$ .

##### **4.1.5(a) Preconcentration procedure**

There are two steps of preconcentration procedure, which consisted of (i) extraction of analyte from aqueous phase to intermediate organic phase and (ii) back-extraction of analyte from intermediate organic phase to final aqueous phase. The extraction and back-extraction are controlled by the application of a chemical potential difference,  $\Delta_o^w \phi$ , favourable to the transfer of cations from one phase to another.

2 mL of 1,2- DCE containing 10 mM  $\text{TMA}^+\text{TPBCl}^-$  were placed on bottom of the 10 mL clear glass and 6 mL of 10 mM  $\text{TMA}^+\text{Cl}^-$  were placed on top of the organic phase. A known concentration of drugs mixture was pipetted into aqueous phase when the interface was formed well between biphasic system. The solution was stirred at 900 rpm for 10 minutes to ensure optimal mass transport and maximised ion transfer across interface. After 15 minutes, the intermediate organic phase was taken out using pipette and transferred into centrifuge tube. Then, 100  $\mu\text{L}$  of final aqueous phase (50 mM of

TMA<sup>+</sup>Cl<sup>-</sup> in deionized water, pH 2) was added. The biphasic system was vortexed at 25 Hz for 90 s and centrifuged for 60 s at 4000 rpm. Finally, the final aqueous phase was collected and injected into HPLC-UV to quantitate the analyte extracted.

#### **4.1.5(b) Yield of extraction, Y% and enrichment factor, EF**

Three aliquots from each sample treated by preconcentration procedure were injected into HPLC-UV: 1) initial aqueous phase as a control experiment; 2) aqueous sample after extraction and 3) final aqueous phase. The yield of extraction, Y%, can be calculated from the peak area obtained by the following equation:

$$\%_{Extraction} = \frac{A_1 - A_2}{A_1} \times 100 \quad (4.1)$$

where  $A_1$  and  $A_2$ , represent the area under the chromatographic peak at stages (1) and (2), respectively. Second parameter calculated from the chromatography experiments is the enrichment factor, EF according to equation (2):

$$EF = \frac{A_3}{A_1} \quad (4.2)$$

where  $A_3$ , represent the area under the chromatographic peak at Stage 3.

#### **4.1.6 Method validation**

Method validation parameters (i.e., linearity, limit of detection (LOD), limit of quantification (LOQ), precision, recovery) were tested after subjecting the working standard and spiked sample solutions to the potentiostatic extraction protocol using the optimized conditions.

Linearity was performed using seven concentration levels of targeted analytes. Calibration curves were established by plotting the peak area versus concentration of

each analyte. LOD and LOQ were calculated based on linear regression from plotted calibration curve:

$$\text{LOD} = 3 \sigma / S \quad (4.3)$$

Where  $\sigma$  = standard deviation of the response and S= slope of the calibration curve

While the LOQs were calculated by:

$$\text{LOQ} = 10 \sigma / S \quad (4.4)$$

Where  $\sigma$  = standard deviation of the response and S= slope of the calibration curve

Precision was demonstrated by determining intra-day and inter-day relative standard deviation of the analysis. The intraday was investigated by analysing six replicates of three concentration levels for all compounds. The interday was performed for five days.

Recovery test was studied by spiking urine samples in triplicates at three concentration levels for all compounds.

## 4.2 Results and Discussion

### 4.2.1 Sample preparation using interfacial potential

This section describes an alternative method for extraction of targeted analytes by potentiostatic-free electrochemistry. The extraction took place when certain potential was imposed by a difference in concentration of common ion, tetramethylammonium ( $\text{TMA}^+$ ) in the two phases.  $\text{TMA}^+$  is one of the simplest quaternary ammonium salts having molecular formula,  $\text{C}_4\text{H}_{12}\text{NCl}$ . Quaternary ammonium ions are among the most electrochemically stable organic cations (Mousavi *et al.*, 2016). It was chosen as it is mostly used as a model ion transfer in liquid-liquid electrochemistry studies (Poltorak *et al.*, 2017, Rahman and Doe, 1996).

General procedure involved is; 1) Determination of transfer potential of each drug, 2) Sample preparation of drugs using this method, 3) HPLC quantitation. For HPLC quantitation, similar parameters as in Section 3.1 were applied in this section.

#### 4.2.1(a) Ionic partition diagram of targeted compounds

Based on cyclic voltammetry experiments on Section 3.2.2, ionic partition diagrams were built in Figure 4.3-4.6 for each of the four targeted molecules (Reymond *et al.*, 1996; Gobry *et al.*, 2001). Such diagrams allow the prediction of the preferred phase of these compounds depending on the Galvanic potential difference applied at the liquid-liquid interface and the pH of the aqueous phase. Number of moles of ions, present in the solution is dependent on pH. Figure 4.2 shows the distribution of monocationic form of biguanide drugs. It can be said that the drugs at pH 9 are at least 97 % in their monoprotonated form.

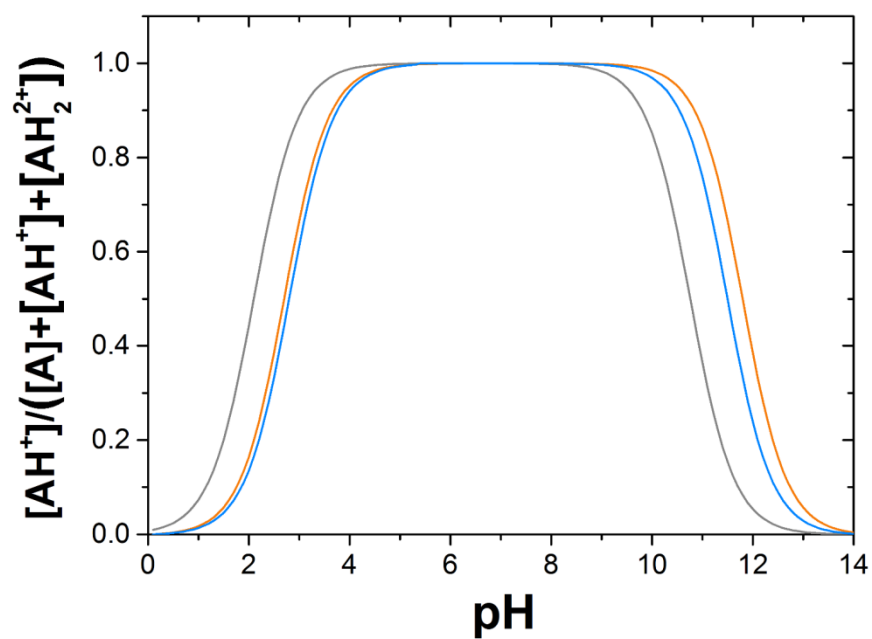


Figure 4.2: Distribution of the monocationic form ( $\text{AH}^+$ ) of MET (blue curve), PHEBI (gray curve) and PHEN (orange curve) as a function of pH

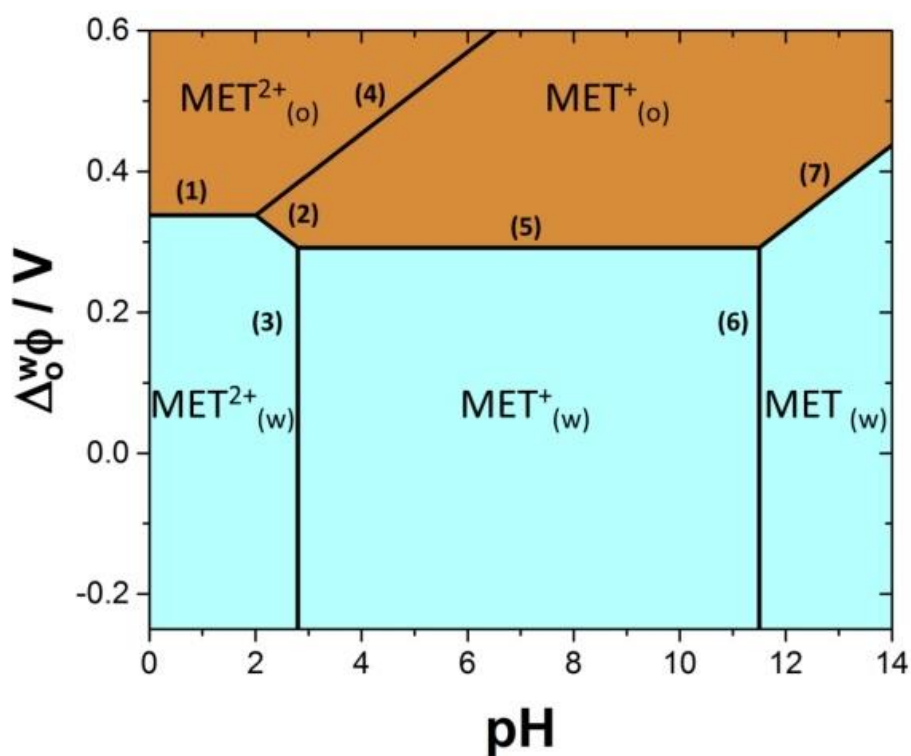


Figure 4.3: Ionic partition diagram for MET

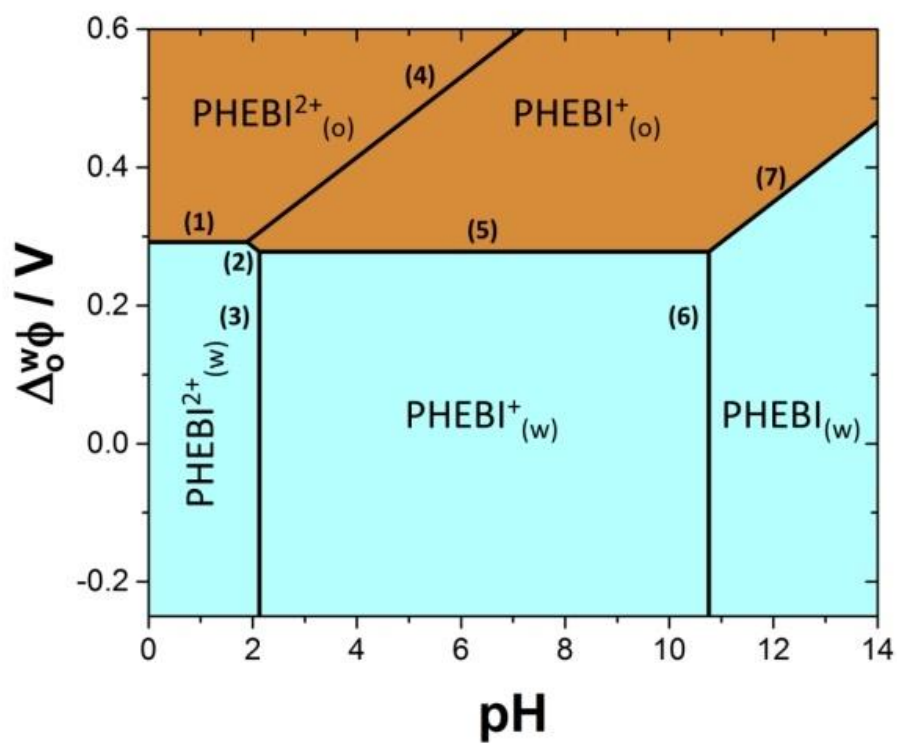


Figure 4.4: Ionic partition diagram for PHEBI

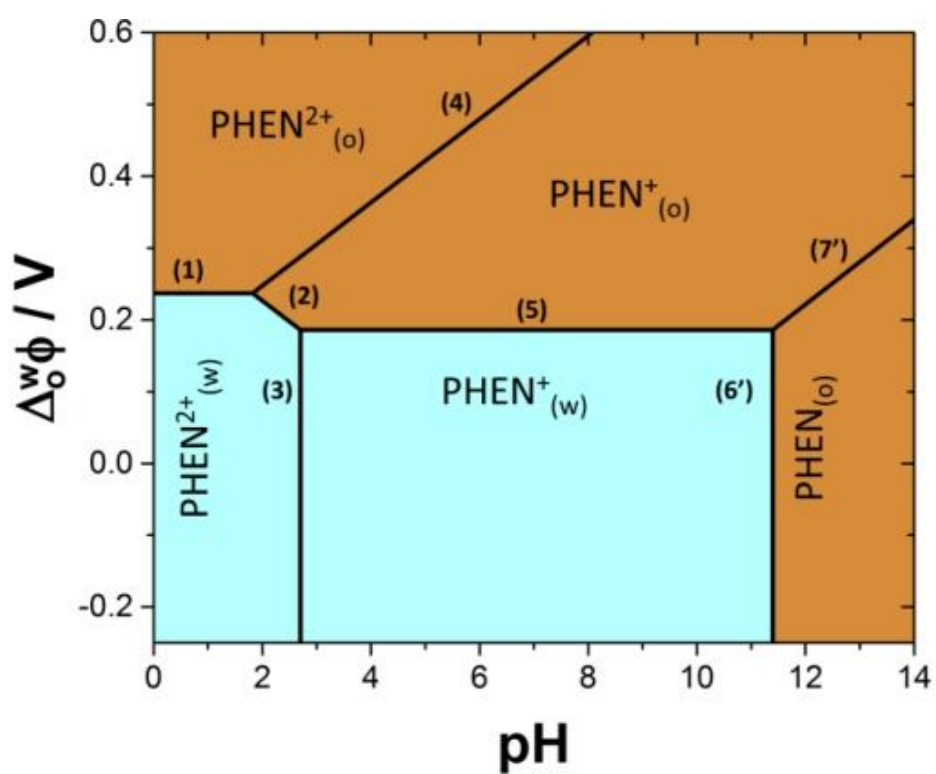


Figure 4.5: Ionic partition diagram for PHEN

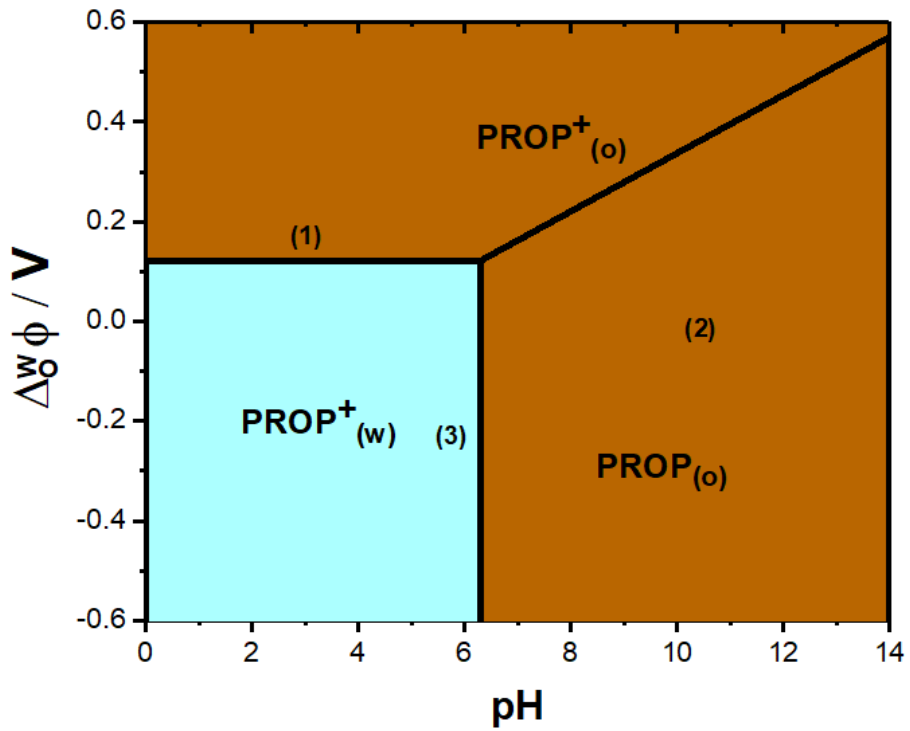


Figure 4.6: Ionic partition diagram for PROP

The difference between ionic partition diagrams of mono-cation and di-cationic are; 1) the number of forms of the same species involved and 2) the number of borderline presences in the diagram. In biphasic system, three species of PROP were present which are the neutral in organic phase and the charged species in both. Meanwhile, for di-cationic species of MET, PHEBI, PHEN are five different species with addition of doubly charged ions distributed over the two phases. Three boundary lines were determined for PROP as mono-cation. For di-cationic species, four supplementary boundary lines were introduced (Reymond *et al*, 1999).

At equilibrium, partition of ionized form of solute in dilute solution is described by Eq. 4.5 or known as Nernst equation (Gobry *et al*, 2001),

$$\Delta_o^w \phi = \Delta_o^w \phi_i^{1/2} + \frac{RT}{z_i F} \ln \left( \frac{a_i^o}{a_i^w} \right) = \Delta_o^w \phi_i^{1/2} + \frac{RT}{z_i F} \ln \left( \frac{c_i^o}{c_i^w} \right) \quad (4.5)$$

The ionic partition diagram boundary lines are described in Appendix 1. All points for boundary lines in ionic partition diagram were summarized in Tables 4.1 and 4.2. The completion of ionic partition diagram can help us to check appropriate Galvanic potential to be applied to transfer our analyte at certain pH. If we consider a sample with a pH between 6 and 8 (corresponding to the pH range of most real samples), the three compounds studied remain preferably in the aqueous phase at open circuit potential. For the four drugs to transfer to the organic phase, a Galvanic potential difference greater than +0.270 V is needed to favour their transfer to the organic phase.

Table 4.1: Equations of various boundary lines with coordinates of their end points a) MET b) PHEBI c) PHEN. The equations given correspond to the boundary lines shown in Figures 4.3-4.5. For all calculations, we have considered  $V_{org} = V_{aq}$

Line	Equation of the boundary line	Coordinates of the boundary lines and points					
		Analyte					
		MET		PHEBI		PHEN	
		1 <sup>st</sup> end point	2 <sup>nd</sup> end point	1 <sup>st</sup> end point	2 <sup>nd</sup> end point	1 <sup>st</sup> end point	2 <sup>nd</sup> end point
1	$\Delta_o^w \phi = \Delta_o^w \phi_{I^{2+}}^{0'}$	(0.00, 0.32)	(2.00, 0.32)	(0.00, 0.27)	(1.89, 0.27)	(0.00, 0.24)	(1.82, 0.24)
2		(2.00, 0.32)	(2.80, 0.27)	(1.89, 0.27)	(2.13, 0.26)	(1.82, 0.24)	(2.70, 0.19)
3	$pH = pK_{a1}^w$	(2.80, 0.27)	(2.80, -0.25)	(2.13, 0.26)	(2.13, -0.25)	(2.70, 0.19)	(2.70, -0.25)
4	$\Delta_o^w \phi = \frac{2\Delta_o^w \phi_{I^{2+}}^{0'} - \Delta_o^w \phi_{I^{+}}^{0'}}{RT \ln 10} (pH - pK_{a1}^w)$	(2.00, 0.32)	(6.90, 0.60)	(1.89, 0.27)	(7.50, 0.60)	(1.82, 0.24)	(8.05, 0.60)
5	$\Delta_o^w \phi = \Delta_o^w \phi_{I^{+}}^{0'}$	(2.80, 0.27)	(11.5, 0.27)	(2.13, 0.26)	(10.8, 0.26)	(2.70, 0.19)	(11.4, 0.19)
6	$pH = pK_{a2}^w$	(11.5, 0.27)	(11.5, -0.25)	(10.8, 0.26)	(10.8, -0.25)	--	--
6'	$pH = pK_{a2}^w - \log P_0$	--	--	--	--	(11.4, 0.19)	(11.4, -0.25)
7	$\Delta_o^w \phi = \Delta_o^w \phi_{I^{+}}^{0'} + \frac{RT \ln 10}{F} (pH - pK_{a2}^w)$	(11.5, 0.27)	(14.0, 0.42)	(10.8, 0.26)	(14.0, 0.44)	--	--
7'	$\Delta_o^w \phi = \Delta_o^w \phi_{I^{+}}^{0'} + \frac{RT \ln 10}{F} (\log P_0 - pK_{a2}^w) + \frac{RT \ln 10}{F} pH$	--	--	--	--	(11.4, 0.19)	(14.0, 0.34)

Equations (1-7) were calculated according to Reymond *et al*, 1999 and equations 6' and 7' were calculated according to Gobry *et al*, 2001.

Table 4.2: Equations of various boundary lines with coordinates of their end points for PROP. The equations given correspond to the boundary lines shown in Figures 4.6. For all calculations, we have considered  $V_{org} = V_{aq}$

Line	Equation of the boundary line	Coordinates of the boundary lines and points	
		Analyte	
		PROP	
		1 <sup>st</sup> end point	2 <sup>nd</sup> end point
1	$\Delta_o^w \phi = \Delta_o^w \phi_I'$	(0.00, 0.12)	(6.31, 0.12)
2	$\Delta_o^w \phi = \Delta_o^w \phi_{I^+}^{0'} + \frac{RT \ln 10}{F} (\log P_0 - pK_{a2}^w) + \frac{RT \ln 10}{F} pH$	(6.31, 0.12)	(6.31, -0.25)
3	$pH = pK_a^w - \log P_o$	(6.31, 0.12)	(14.0, -0.60)

Equations (1-3) were calculated according to Gobry *et al*, 2001.

#### 4.2.1(b) Preconcentration mechanism

TMA<sup>+</sup> was selected as the common ion in aqueous and organic phases to establish the interfacial potential difference,  $\Delta_o^w \phi$  according to pseudo-Nernst equation (Eq. 4.6).

$$\Delta_o^w \phi = \Delta_o^w \phi_{TMA^+}^{0'} + \frac{RT}{zF} \ln \frac{[TMA^+]_o}{[TMA^+]_w} \quad (4.6)$$

where  $\Delta_o^w \phi_{TMA^+}^{0'}$  is the formal transfer potential of TMA<sup>+</sup> between aqueous and 1,2-DCE (-0.182 V) (Wandlowski *et al*, 1990), and  $[TMA^+]_o$  and  $[TMA^+]_w$  are the TMA<sup>+</sup> concentration in the organic and in the water phases. The sample, containing the three targeted ions and TMA<sup>+</sup>, was placed in contact of the organic phase containing a known concentration of TMA<sup>+</sup>. The two solutions were stirred thoroughly for 600 s to maximise the area of contact between the two phases. The sample solution was analysed by chromatography before and after this extraction step. The organic phase was then collected and placed in contact with another aqueous solution to back-extract the three targeted ions for HPLC analysis. The protocol was illustrated in Figure 4.7.

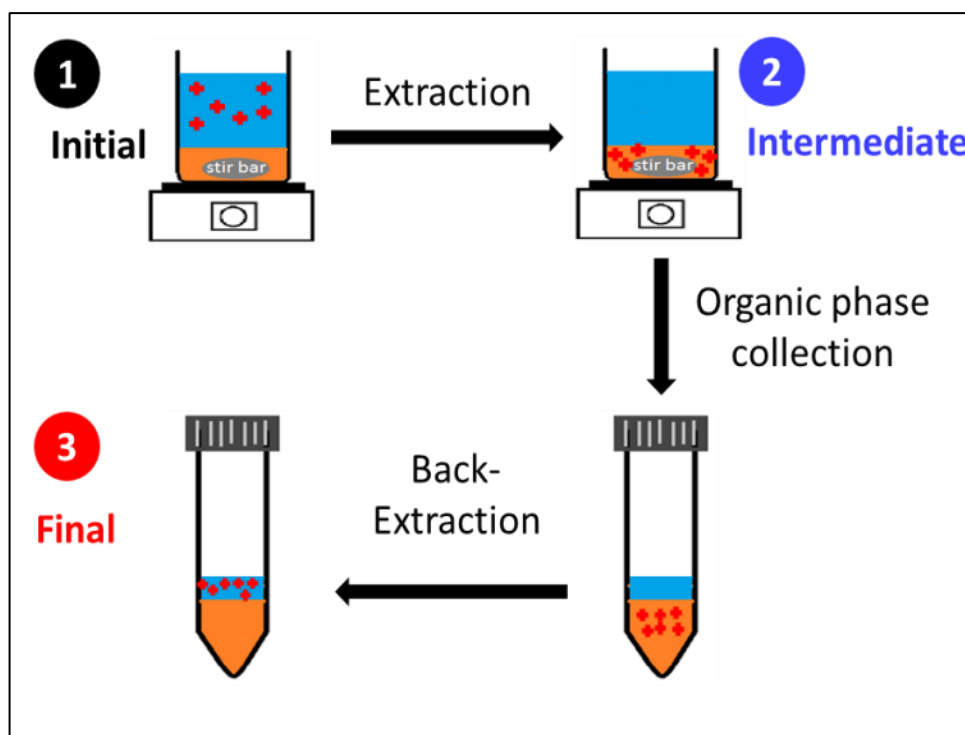


Figure 4.7: Experimental procedure of the electrochemically modulated liquid-liquid extraction. Target cations are extracted from the aqueous sample to organic phase before being back-extracted to a final aqueous phase. The numbers 1, 2 and 3 correspond to the initial, intermediate and final stages at which the aqueous phases are analysed by HPLC

Chromatograms before and after extraction are shown in Figure 4.8 for a given set of extraction parameters. The first sample analysed contained MET, PHEBI and PHEN (164  $\mu\text{M}$  each) and 1  $\mu\text{M}$  of  $\text{TMA}^+$ . The organic solution used for the extraction contained 10 mM of  $\text{TMA}^+\text{TPBCl}^-$ . Based on these  $\text{TMA}^+$  concentrations, the initial  $\Delta_o^w\phi$  was +0.392 V, which should be sufficient to extract 100 % of all three targeted ions, according to the ionic partition diagrams (Figure 4.3-4.6). However, the extraction is much lower than expected with 27 % for MET, 44 % for PHEBI and 76 % for PHEN. When the initial drug concentration is reduced down to 1.64  $\mu\text{M}$ , extraction efficiencies increased to 84.2 % for MET, 100 % for PHEBI and 100 % for PHEN although the same extraction conditions were used (Figure 4.8B).

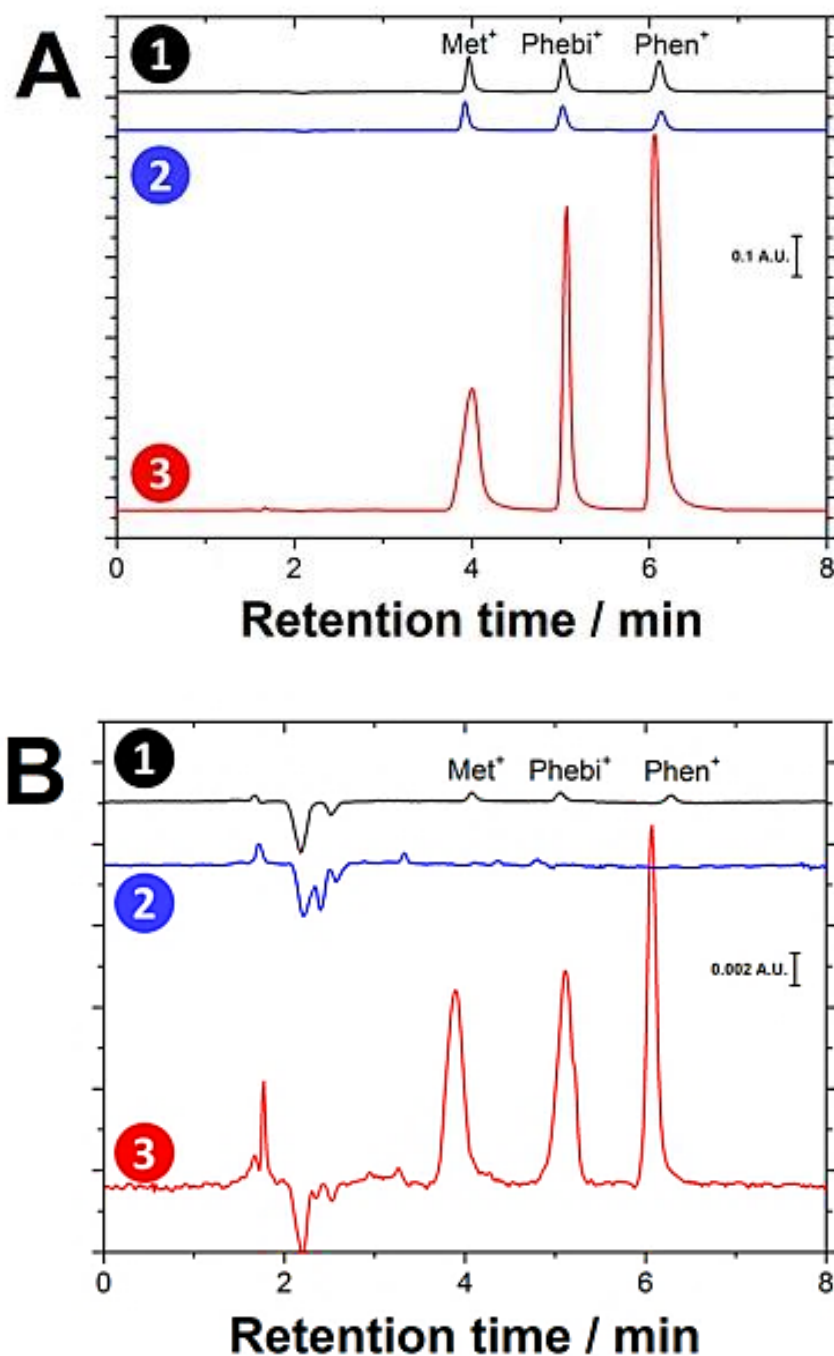


Figure 4.8: Chromatograms obtained for a sample containing MET, PHEBI and PHEN at (A) 164  $\mu\text{M}$  each and at (B) 1.64  $\mu\text{M}$  each before (1) and after (2) extraction, in the aqueous back-extraction phase (3). Extraction conditions were  $[\text{TMA}^+]_o = 10 \text{ mM}$ ,  $[\text{TMA}^+]_w = 0.001 \text{ mM}$ , pH 11,  $V_{\text{DCE}} = 2 \text{ mL}$ , Rotating speed = 900 rpm,  $t_{\text{ext}} = 15 \text{ min}$

This variation in the extraction efficiencies achieved is linked to the ion transfer mechanism. The electroneutrality has to be maintained. The extraction of one mole of cation from the sample must be compensated by the transfer of one mole of another

ion (either an anion from the sample to the organic phase or a cation from the organic phase to the sample). Due to its amphiphilic nature,  $\text{TMA}^+$  is able to compensate the electric charge of both the very hydrophobic  $\text{TPBCl}^+$  in the organic phase and the very hydrophilic  $\text{Cl}^-$  in the aqueous phase. During the transfer of cationic drugs, the lowest cost in terms of energy of the co-transfer is by the transfer of  $\text{TMA}^+$  from the organic phase to the sample. This equilibration of charge results in a variation of the interfacial potential difference, occurring as target ions are extracted. Eq. 4.6 cannot be used here as it describes the interfacial potential difference in the presence of a single common ion. However, in the case where many ions can partition on either side of the interface, they all contribute to the interfacial potential difference. We thus used instead the theory developed in the 1980s by Hung to calculate the Galvanic potential difference at equilibrium,  $\Delta_o^w \phi_{Eq}^{Ext}$  (Hung, 1980; Iwata *et al*, 2017). In brief, each ion is distributed between the sample and the organic phase, and for each of them we can define two functions, one for the aqueous phase,  $\zeta_i^w$ , and one for the organic phase,  $\zeta_i^o$ , (Eqs. 4.7 and 4.8).

$$\zeta_i^w = \frac{z_i C_i^{0,w}}{1 + re^{\left[\frac{z_i F}{RT}(\Delta_o^w \phi - \Delta_o^w \phi_i^0)\right]}} \quad (4.7)$$

$$\zeta_i^o = \frac{r z_i C_i^{0,o}}{1 + re^{\left[\frac{z_i F}{RT}(\Delta_o^w \phi - \Delta_o^w \phi_i^0)\right]}} \quad (4.8)$$

In these equations,  $r$  is the ratio of the organic to aqueous volumes. The total sum,  $\zeta_{total}$ , is be calculated as follows:

$$\zeta_{total} = \sum_i \zeta_i^w + \sum_i \zeta_i^o \quad (4.9)$$

As Eqs. 4.7 and 4.8 assumed equilibrium, extraction time (5-30 mins) and rotation speed (300-1200 rpm) were optimised (Figure 4.9). Variation extraction time did not give significant difference for percentage of extraction. 600 s was chosen as the optimum one for time of extraction. The percentage of extraction increased clearly especially for PHEN when the rotation speed increased from 300 rpm to 900 rpm. Small difference of percentage extraction can be seen between 900 rpm and 1200 rpm. It can be concluded that equilibrium was reached for an extraction time of 600 s and a rotation speed of 900 rpm.

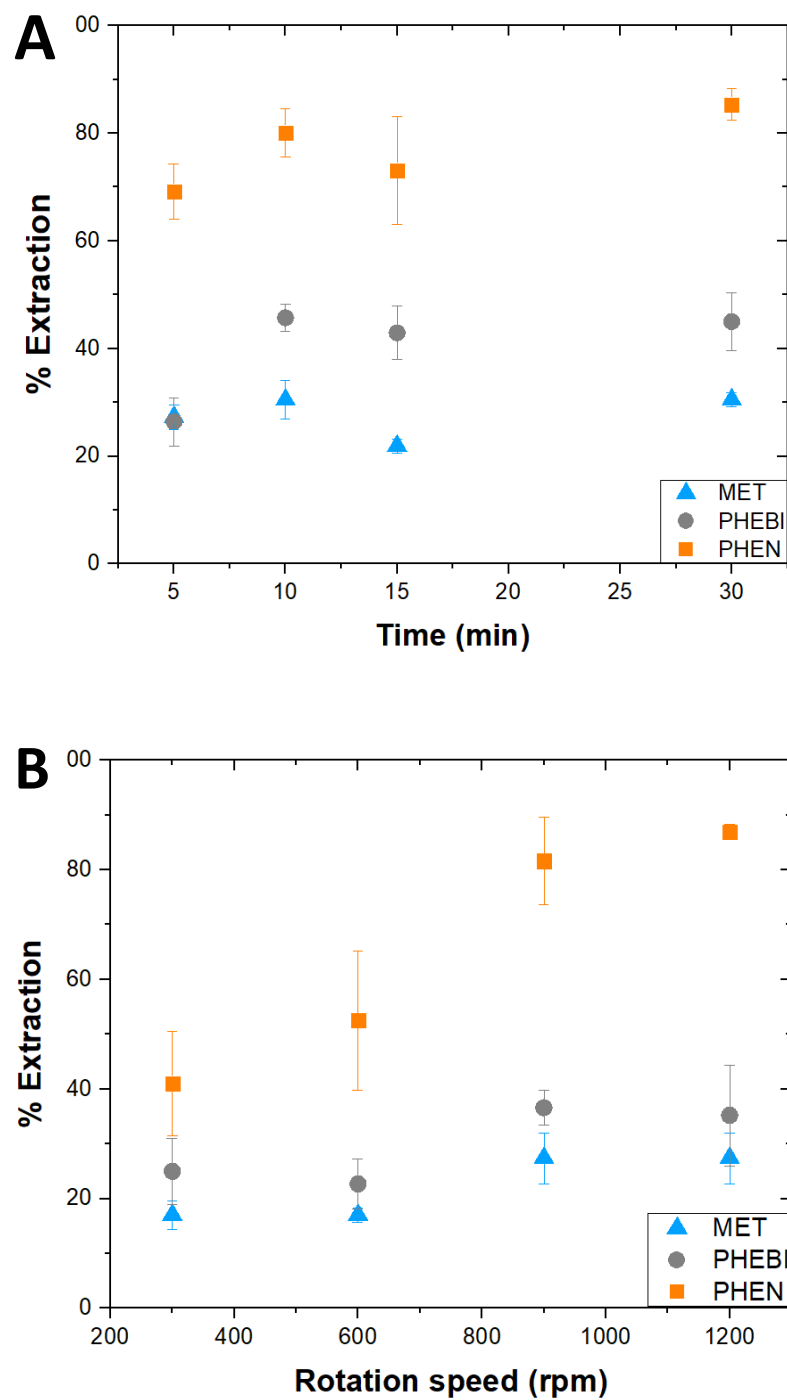


Figure 4.9: Extraction efficiency as a function of (A) time and (B) rotation speed. Other experimental parameters were:  $[TMA^+]_o = 10$  mM,  $[TMA^+]_w = 0.001$  mM, pH 11,  $V_{DCE} = 2$  mL

Figure 4.10A shows the variation of  $\zeta_{total}$  as a function of the interfacial potential difference. The Galvanic potential difference at equilibrium,  $\Delta_o^w \phi_{Eq}^{Ext}$ , is reached when  $\zeta_{total} = 0$ . The shift of  $\Delta_o^w \phi_{Eq}^{Ext}$  to higher values for the lower initial drug concentrations confirms the trend observed experimentally where extraction efficiencies were greater when the initial concentration decreased. Figure 4.10B also proved low initial concentration of analytes resulting in higher percentage of extraction. MET was extracted 100 % when the initial concentration starts at 8  $\mu\text{M}$  whereas for PHEBI and PHEN is at 16 and 40  $\mu\text{M}$ , respectively.

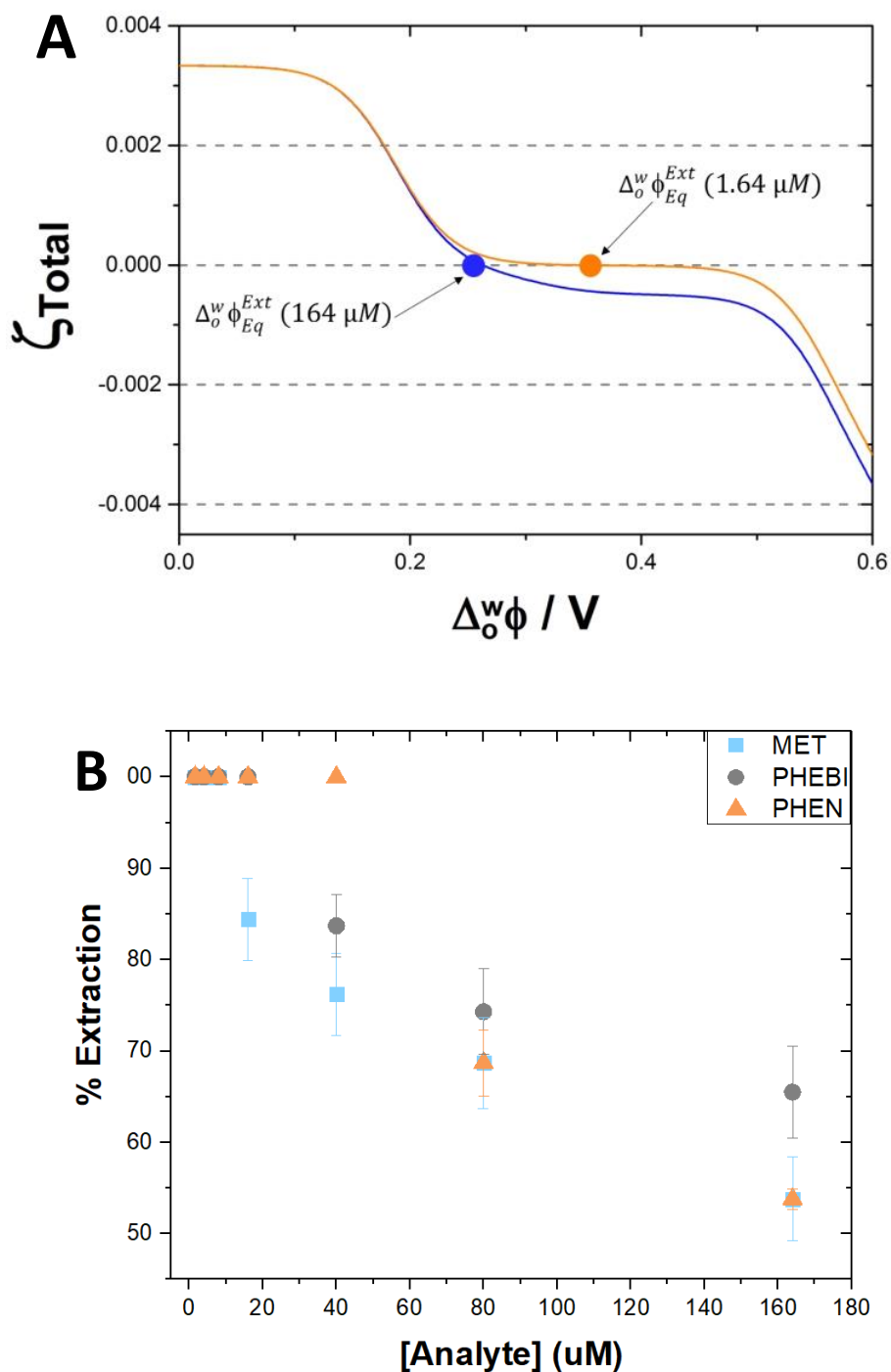


Figure 4.10: A) Dependence of  $\zeta_{total}$  as a function of the interfacial potential difference,  $\Delta_o^w \phi$ , for extraction conditions of Figure 4.8.  $[Analyte] = 164 \mu M$  for the blue curve and  $1.64 \mu M$  for the orange curve. B) Extraction efficiency as a function of initial concentration targeted analytes. Other experimental parameters were:  $[TMA^+]_o = 10 \text{ mM}$ ,  $[TMA^+]_w = 0.001 \text{ mM}$ , pH 9,  $V_{DCE} = 2 \text{ mL}$

#### 4.2.1(c) Parameters optimization

A variety of parameters (analyte concentration, common ion concentration in both sample and organic phase, volume of the organic phase, pH, rotation speed, and extraction time) were investigated to improve the extraction yield of the three drugs (Tables 4.3 and 4.4).

Table 4.3: Variation of conditions for the extraction step. Optimised parameters are in bold

Parameters	Values
Analyte concentration / $\mu\text{M}$	0.4; 0.5; 0.8; 1.64; 3.2; 4; 8; 16.4; 164
$[\text{TMA}^+]_{\text{org}}$ / mM	1, 5, <b>10</b>
$[\text{TMA}^+]_{\text{sample}}$ / mM	<b>0.001</b> ; 0.0001
$V_{\text{org}}$ / mL	0.3; 0.5; 1 ;1.5; <b>2</b>
$\text{pH}_{\text{sample}}$	6; 6.5; <b>9</b> ; 10; 11
Rotation speed / rpm	0, 300, 600, <b>900</b> , 1200
Extraction time / s	300, <b>600</b> , 900, 1800

Table 4.4: Variation of conditions for the back-extraction step. Optimised parameters are shown in bold

Parameters	Values
$V_{\text{BE}}$ / mL	<b>0.1</b> ; 0.2; 0.3; 0.4
$[\text{TMA}^+]_{\text{BE}}$ / mM	10; 20; <b>50</b>
$\text{pH}_{\text{BE}}$	1; <b>2</b> ; 6; 11

A series of three control experiments (Table 4.5) in the absence of chemical polarization were run to confirm that the ion extraction is due to the effect of the interfacial potential. Results are shown in Figure 4.11. For the first two control experiments, the initial aqueous phase was de-ionized water with 10  $\mu\text{M}$  of the three drugs. For control 1, pH was 6.5 and for control 2, pH was adjusted to 11 with NaOH solution. For these two control experiments, the organic phase was 1,2- DCE without added electrolyte. For the third control experiment, the organic phase contained 10 mM  $\text{BTTPA}^+\text{TPBCl}^-$ , which role was to check whether ion pairing between the drugs and  $\text{TPBCl}^-$  had a role in the extraction. For these three control experiments, the

enrichment factor ranged between 0.02 and 1.25 (all three drugs considered). These results confirmed that chemical polarization is responsible for the drug extraction. Therefore, the most influential parameters for the extraction efficiency are linked to the interfacial potential difference.

Table 4.5: Composition of the different phases for the control experiments 1-3

Control experiment	Initial aqueous solution	Organic phase	Final aqueous phase	Comments
1	DI water, pH 6.5	1,2-DCE	DI water, pH 6.5	Non-polarized interface
2	1 mM NaOH, pH 11	1,2-DCE	DI water, pH 6.5	Favours transfer of neutral species
3	DI water, pH 6.5	10 mM BTPPA <sup>+</sup> TPBCl <sup>-</sup>	DI water, pH 6.5	Ion-pair experiment

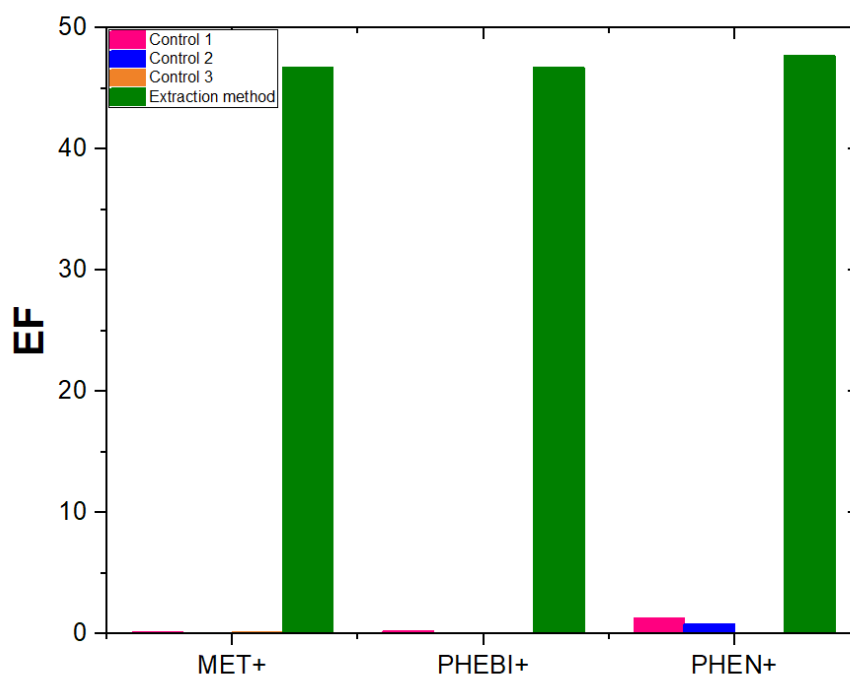


Figure 4.11: Enrichment factors for 10  $\mu$ M MET, PHEBI and PHEN achieved for control experiments 1-3 and the extraction method proposed here. Experimental conditions for control 1-3 are given in Table 4.5. Experimental conditions for the extraction method are the optimal conditions

Figure 4.12 below showed the extraction yield increased for biguanide compounds when the interfacial potential difference increased. This confirms the electrochemically modulated nature of the ion extraction.

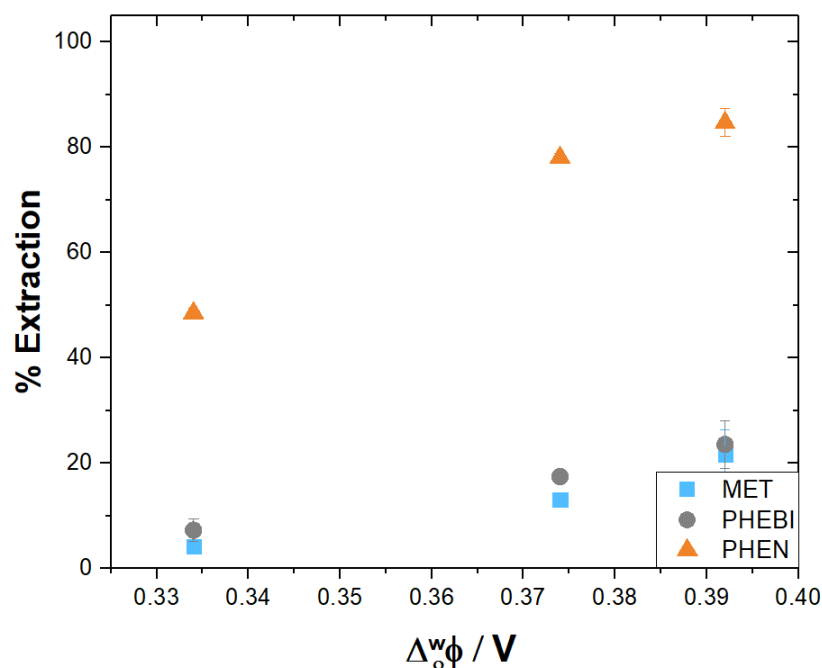


Figure 4.12: Extraction efficiency as a function of Galvanic transfer potential. Other experimental parameters were:  $[\text{TMA}^+]_o = 10 \text{ mM}$ ,  $[\text{TMA}^+]_w = 0.001 \text{ mM}$ , pH 11,  $V_{\text{DCE}} = 0.3 \text{ mL}$

Due to the poor solubility of the analytes in the organic phase, the volume of organic phase needs to be sufficiently large to increase the extraction yield. Thus, 2 mL of organic phase was chosen. Furthermore, by transferring analytes from large volume of sample solution to a  $\mu\text{L}$  volume of final phase can enhance the pre-concentration process. By maintaining the analytes in their monocationic form (i.e.  $4 < \text{pH} < 9$ , Figure 4.2), the extraction potential is at the lowest value, and is hence the easiest. For time of extraction and speed of rotation, 600 s and 900 rpm were considered the optimum ones (Figure 4.9).

The drugs extracted into the organic phase were then back-extracted to a final aqueous phase. The pH for the back-extraction phase was set at 2. In these acidic conditions, all three analytes were mainly di-cationic and, hence, transfer more easily to the aqueous phase. The interfacial potential was set at +0.119 V with  $[\text{TMA}^+]_{\text{back}} = 50$  mM, which is lower than the  $\Delta_o^w \phi^{1/2}$  of  $\text{MET}^{2+}$ ,  $\text{PHEBI}^{2+}$  and  $\text{PHEN}^{2+}$  (Figure 4.13A). A volume of aqueous phase for the back-extraction was selected at 0.1 mL. As can be seen in Figure 4.13B, the enrichment factor decreased as the volume is increased. Such a volume allowed to inject 20  $\mu\text{L}$  of solution to the HPLC after rinsing the injection loop with the excess sample volume. Hence, the optimised parameters for the extraction are the following:  $[\text{TMA}^+]_{\text{o}} = 10$  mM,  $[\text{TMA}^+]_{\text{w}} = 0.001$  mM,  $V_{\text{org}} = 2$  mL,  $\text{pH}_{\text{sample}} = 9$ , rotation speed = 900 rpm, extraction time = 600 s. The optimised parameters for back-extraction are:  $[\text{TMA}^+]_{\text{back}} = 50$  mM,  $V_{\text{final}} = 0.1$  mL,  $\text{pH}_{\text{back}} = 2$ .

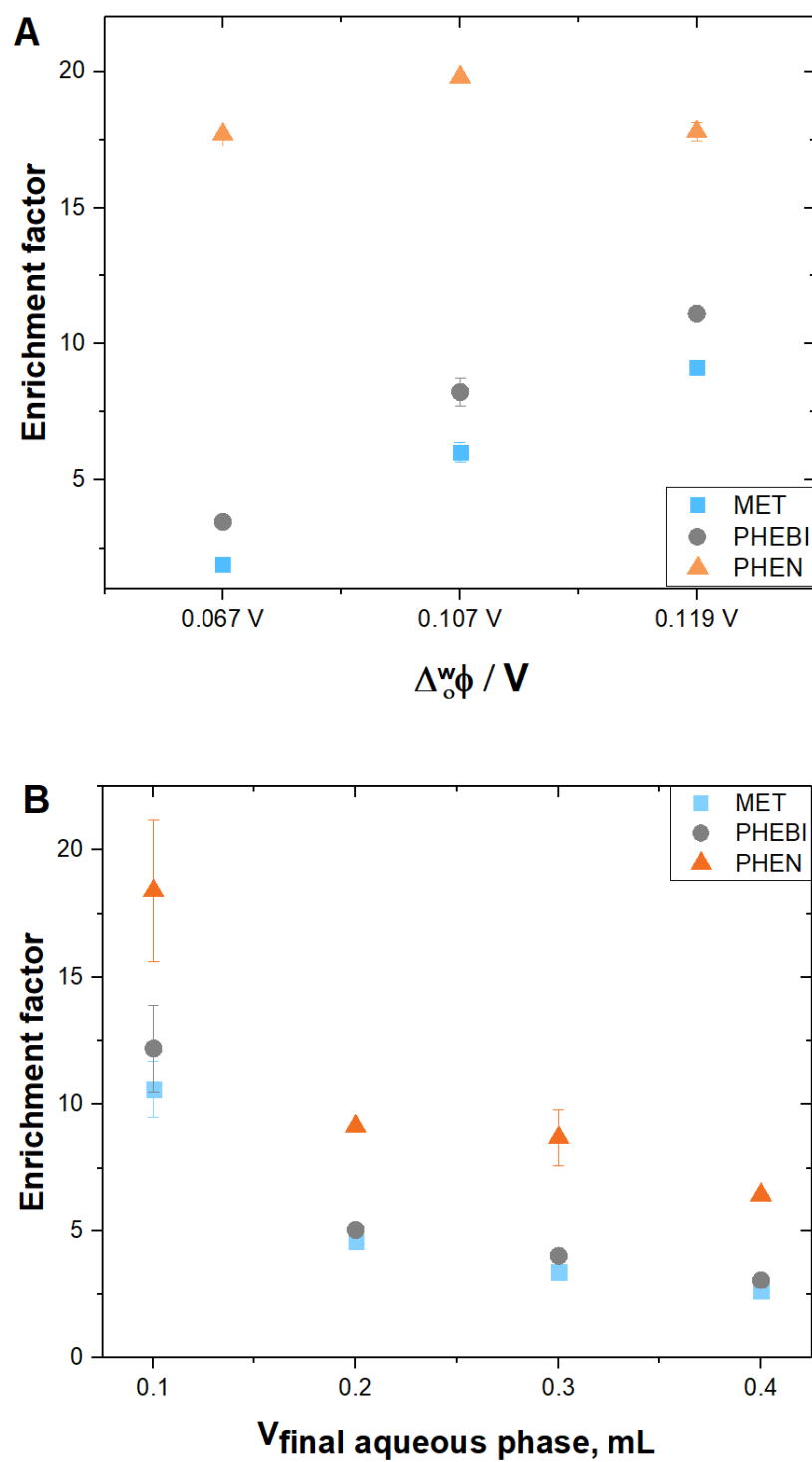


Figure 4.13: A) Enrichment factor as a function of Galvanic back-transfer potential. Other experimental parameters for back-extraction were:  $[TMA^+]_o = 10$  mM,  $[TMA^+]_{back} = 50$  mM, pH 2,  $V_{DCE} = 2$  mL. B) Enrichment factor vs final volume of aqueous phase

In the case of a 100 % extraction yield, the expected enrichment factor is the volume ratio between the initial sample and the back-extraction phase ( $EF_{\max} = 60$  in our study). We plotted the %<sub>Extraction</sub> as a function of the enrichment factor for the three analytes (Figure 4.14). The solid line symbolises the maximum enrichment factor expected if the back-extraction has reached 100 % efficiency. Data points above the straight line indicate that the extraction was more efficient than back-extraction. As the most hydrophobic, PHEN (orange squares) is easily extracted to the organic phase. Despite higher extraction, the enrichment factor barely reaches its expected value. On the contrary, there is a linear correlation between the %<sub>Extraction</sub> of MET (blue triangles) and its enrichment factor (slope = 1.655,  $R^2 = 0.869$ , for a theoretical slope of 1.667). Once MET is extracted to the organic phase, it easily transfers back to the final aqueous phase due to its hydrophilic nature.

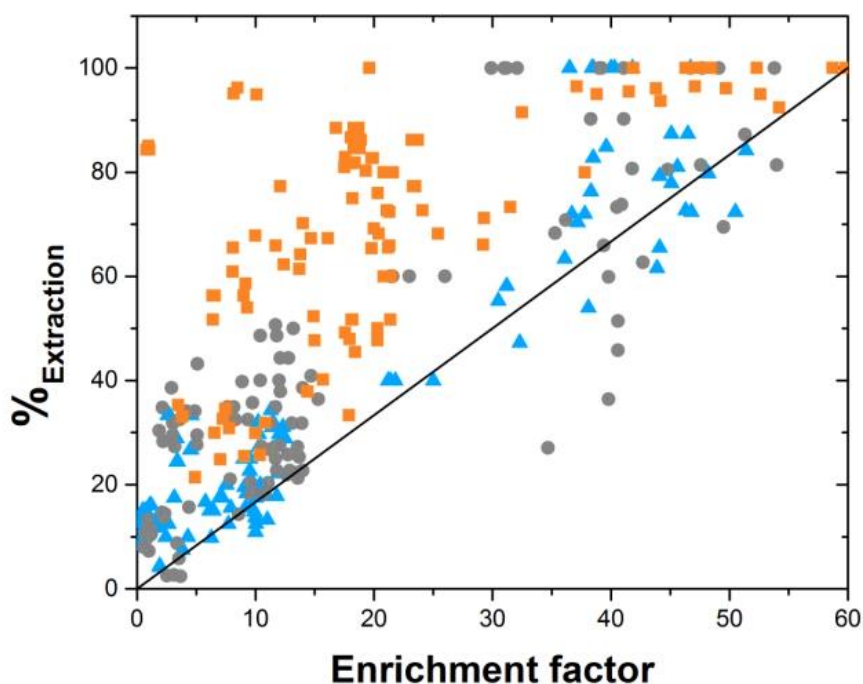


Figure 4.14: %<sub>Extraction</sub> as a function of the enrichment factor for MET, (blue triangles) PHEBI (grey circles) and PHEN (orange squares). The solid line represents the enrichment factor expected if back-extraction efficiency is 100 %

The extraction yield for each of the three drugs studied as a function the interfacial potential difference at equilibrium,  $\Delta_o^w \phi_{Eq}^{Ext}$  was plotted, (determined experimentally using the chromatograms recorded after extraction as described in below). To determine the interfacial potential difference at equilibrium,  $\Delta_o^w \phi_{Eq}^{Ext}$ , we need to know the ratio of concentration of an ion in each phase. The calculation was showed in Appendix 2.

The interfacial potential difference at equilibrium is given by the Nernst Eq. 4.10,

$$\Delta_o^w \phi_{Eq}^{Ext} = \Delta_o^w \phi_i^{0'} + \frac{RT}{zF} \ln \frac{C_{org}^i}{C_{aq}^i} \quad (4.10)$$

By combining Eqs. x, xiv (in Appendix 2) and 4.10 we obtain the following:

$$\Delta_o^w \phi_{Eq}^{Ext} = \Delta_o^w \phi_i^{0'} + \frac{RT}{zF} \ln \frac{n_{initial}^i V_{org}^i * Y}{n_{initial}^i V_{aq}^i (1-Y)} \quad (4.11)$$

$$\Delta_o^w \phi_{Eq}^{Ext} = \Delta_o^w \phi_i^{0'} + \frac{RT}{zF} \ln \frac{V_{org}^i * Y}{V_{aq}^i (1-Y)} \quad (4.12)$$

The extraction yield, Y, is obtained by calculating the ratio of the number of moles in the organic phase divided by the initial number of moles in the samples. According to calibration curve of analytes (Figure 3.3, Section 3.2.1), the number of moles is directly proportional to the peak area obtained by chromatography, so we can write Eq. 4.13:

$$Y = \frac{n_{initial}^i - n_{aq}^i}{n_{initial}^i} = \frac{A_1 - A_2}{A_1} \quad (4.13)$$

Combining Eqs. 4.12 and 4.13, we obtain the final expression that allowed us to calculate the interfacial potential difference at equilibrium used in Figure 4.15.

$$\Delta_o^w \phi_{Eq}^{Ext} = \Delta_o^w \phi_i^{0'} + \frac{RT}{zF} \ln \frac{V_{org}^i * (A_1 - A_2)}{V_{aq}^i * A_2} \quad (4.14)$$

Experimental results were shown as data points on Figure 4.15 and compared to the theoretical behaviour expected from the Nernst equation. Extraction yield increased with  $\Delta_o^w \phi_{Eq}^{Ext}$ , confirming that ion extraction can be modulated by controlling the interfacial potential.

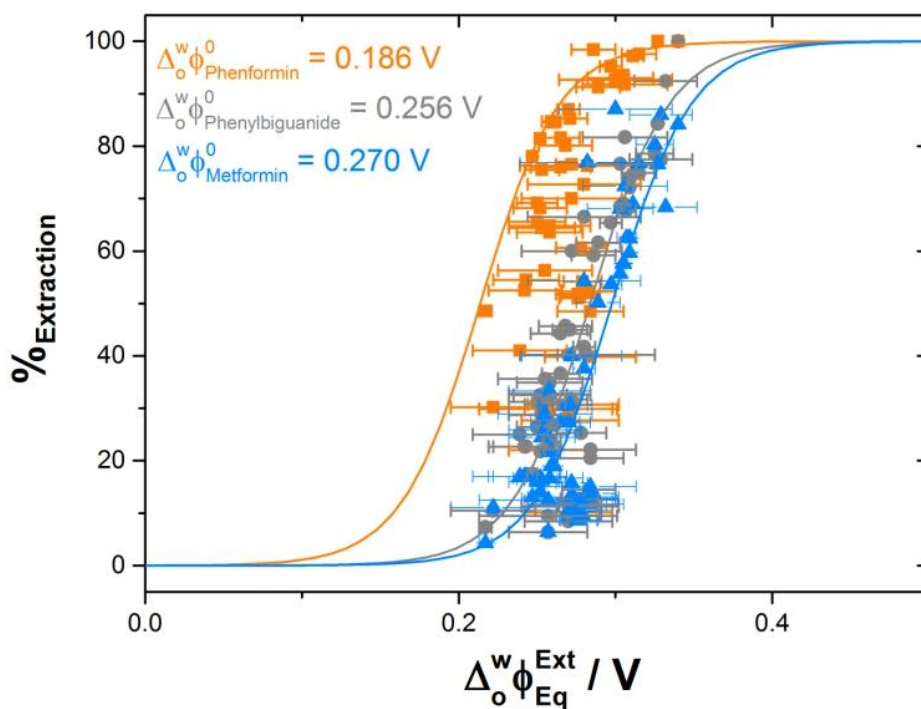


Figure 4.15: %Extraction yield of MET, (blue triangles) PHEBI (grey circles) and PHEN (orange squares) as a function of the interfacial potential difference at equilibrium  $\Delta_o^w \phi_{Eq}^{Ext}$ . These experimental points were obtained for a variety of parameters. Solid lines are the expected extraction yields for each of the drugs according to Nernst equation

One of the limitations of the method is the back-extraction of hydrophobic compounds, which could be improved by the use of a more hydrophobic common ion. In addition, adjusting the pH of the final solution to make sure that the analyte is under an ionic form would favour the back-extraction. As a control experiment, we have investigated the extraction of propranolol, a hydrophobic  $\beta$ -blocker, ( $\log P_0 = 3.1$ ,  $\Delta_o^w \phi_{Propranolol}^0 = 0.141$  V,  $pK_a = 9.41$ ). One has to bear in mind that the electrochemically modulated

is mainly interesting for very hydrophilic charged analytes. PROP used here as a reference compound does not justify by itself to develop such a method. The results showed in Figure 4.16 that in the extraction conditions studied, the extraction is relatively easy with efficiencies achieved ranging from 79 to 99 %, depending on  $\Delta_o \phi_{Eq}^{Ext}$ . However, the enrichment factor varied from 0.4 to 15.8 (while the maximum value expected is 60).

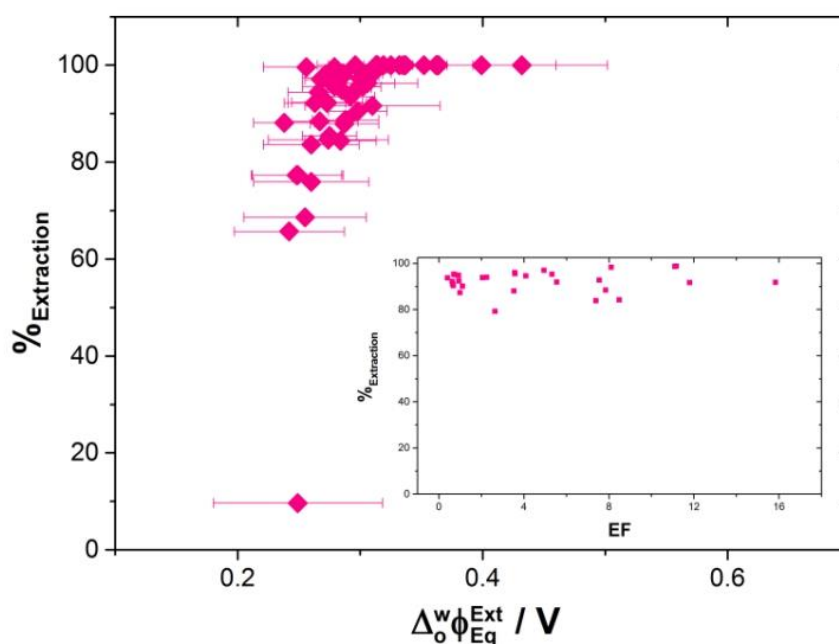


Figure 4.16: %<sub>Extraction</sub> vs  $\Delta_o \phi_{Eq}^{Ext}$  for the extraction of propranolol. %<sub>Extraction</sub> vs EF

#### 4.2.2 Method of validation

Using optimum conditions, samples were enriched for a series of seven initial concentrations ranging from 16 nM to 1.6  $\mu$ M. Figure 4.17 showed the chromatograms of extracted analytes obtained from injection of the final aqueous phase (i.e. after sample enrichment). Method validation parameters (linearity, limit of detection (LOD), limit of quantitation (LOQ), precision, recovery) were carried out. The calibration curve showed linear range with  $R^2$  values (0.9987 – 0.9999). Both LOD

and LOQ for MET are improved by a factor 50 whereas the improvement is lower for PHEBI (a factor 10) and PHEN (a factor 7), proving that the method is suitable for the sample enrichment of polar target analytes. Less polar analyte such as PROP is not suitable as the enrichment factor value is only 1.6. The interday and intraday assays showed an overall precision around 7 % (Table 4.6).

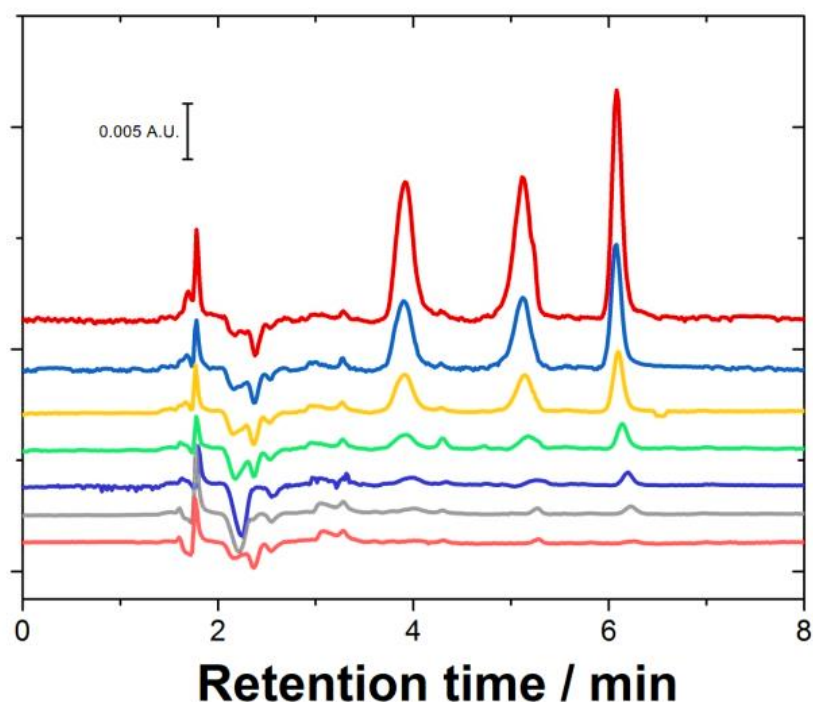


Figure 4.17: Chromatograms MET, PHEBI and PHEN after sample enrichment using the optimised conditions (shown in Tables 4.3 and 4.4). Concentrations ranged from 16 nM to 1.6  $\mu$ M

The analytical usefulness of the developed method was investigated by analysing urine samples. Urine samples from unknown donor were spiked with 1.6  $\mu$ M MET, PHEBI and PHEN. Three urine samples were pre-treated by diluting 1:4, 1:10 and 1:20 with deionized water to minimise the matrix effects and obtain clear interface between the two immiscible phases, according to published procedures (Charles *et al*, 1981; Ben-Hander *et al*, 2013; Ben-Hander *et al*, 2015; Karami *et al*, 2017; Santigosa *et al*, 2019). A fourth sample was pre-treated by protein precipitation in 1:3 acetone. The recovery

test was performed using the optimized extraction parameters. Recoveries in the range 80 – 115 % were obtained for MET (90.2-113.7 %), PHEBI (81.4-86.3 %) and PHEN (82.3-86.5 %) in urine pre-treated by dilution. It is clear visible from the chromatograms (Figure 4.18) that the targeted drugs could be determined selectively without interferences from matrix components of these samples. The enrichment factors were of 49.5 for MET, 59.5 for PHEBI and 58.0 for PHEN which are very close to the enrichment factors achieved for clean laboratory solutions. It has been reported that metformin hydrochloride is not fully metabolized in the human body. Approximately 70 % of the intake dose is extracted to urine unaltered and the rest in faeces (Scheurer *et al.*, 2012). Samples pre-treated by protein extraction gave recoveries which were not satisfactory for MET (151 %), PHEBI (74 %) and PHEN (45 %).

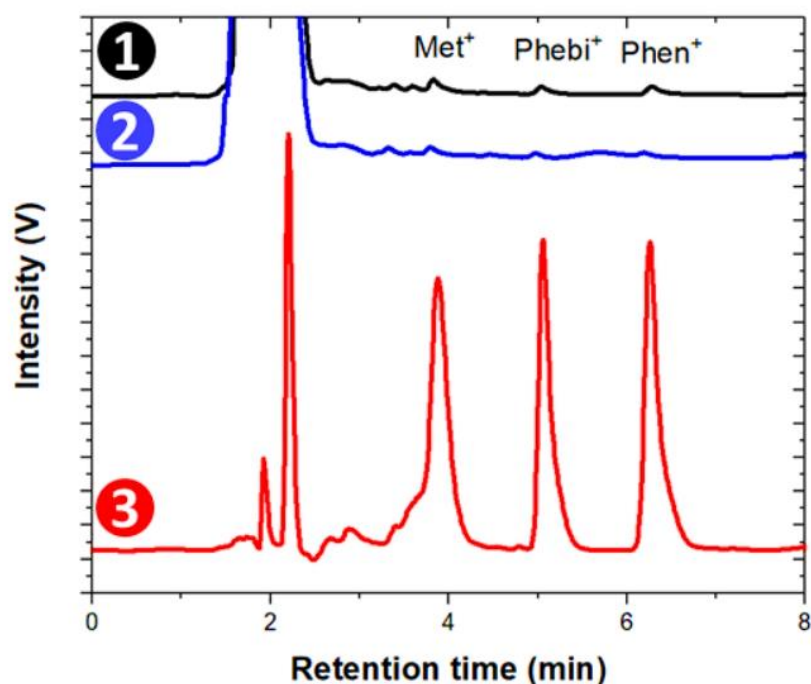


Figure 4.18: Chromatograms before (1) and after (2) extraction and after back-extraction (3).  $[TMA^+]_o = 10 \text{ mM}$ ,  $[TMA^+]_w = 0.001 \text{ mM}$ , pH 6,  $V_{DCE} = 2 \text{ mL}$ , Rotating speed = 600 rpm,  $t_{ext} = 15 \text{ min}$ . The chromatograms were obtained for sample pre-treated by dilution 1:4 in DI water

Table 4.6: Analytical parameters for the proposed method for MET, PHEBI and PHEN

Method development		Analytes		
		MET	PHEBI	PHEN
With sample enrichment	Sensitivity / $\text{mV s } \mu\text{M}^{-1}$	0.094	0.103	0.102
	$R^2$	0.9999	0.9987	0.9988
	Intercept / $\text{mV s}$	-0.0008	-0.0031	0.0002
	LOD / $\mu\text{M}$	0.017	0.068	0.066
	LOQ / $\mu\text{M}$	0.058	0.227	0.222
	Precision / %	6.84	6.79	6.89
Sample without enrichment	Sensitivity / $\text{mV s } \mu\text{M}^{-1}$	0.0022	0.0022	0.0024
	$R^2$	0.9991	0.9994	0.9998
	Intercept / $\text{mV s}$	4.577E-5	2.156E-5	3.648E-5
	LOD / $\mu\text{M}$	0.903	0.727	0.438
	LOQ / $\mu\text{M}$	3.001	2.422	1.459

### 4.3 Comparison to previously reported analytical methods

The analytical characteristics of the proposed method were compared with the previous reported methods for analysis of biguanide compounds. The two-step extraction is achieved in 16.5 minutes, which remains faster than most existing extraction methods that often include a lengthy evaporation time. This faster analysis does not compromise the analytical performance as the LOD and LOQ achieved are in the same order of magnitude as published methods. Existing electro-driven extraction methods rely on the application of a potential with an external power source with potential ranging from a few volts up to several tens of thousands of volts. In the method reported here, the extraction potential is applied through the partition of a common ion, i.e. the interface is polarized chemically. This instrument-free approach is the major difference with the existing electro-driven extraction methods reported in the literature. This method demonstrated that chemical polarization of the interface favours the extraction of hydrophilic drugs compared to non-polarized extraction

methods. To the best of our knowledge, this is the first report on the use of chemical polarization of the interface method for sample preparation of biguanide compounds in urine.

Table 4.7: Comparison of the analytical performances of published extraction procedures with the method reported here

Sample preparation and determination	Biguanides	Time of extraction (min)	Extraction organic solvents	LOD ( $\mu\text{g L}^{-1}$ )	LOQ ( $\mu\text{g L}^{-1}$ )	Refs
IP VALLE – HPLC UV	MET	10	150 $\mu\text{L}$ IP/1-octanol	1.4	4.1	Alshishani <i>et al.</i> , 2016
HF- LPME – HPLC UV	MET	30	Diethyl ether + PFBC as derivatizing agent	0.36	3.0	Ben-Hander <i>et al.</i> , 2013
Protein Precipitation – HPLC UV	MET	10 + evaporation time	2 mL ACN	-	30	Porta <i>et al.</i> , 2008
LLE – LC MS MS	MET GLM PIO	19 + evaporation time	3 mL DCM: Amyl alcohol	-	10 2.5 2.5	Sengupta <i>et al.</i> , 2009
LLE – HPLC UV	MET	7.5 + evaporation time	3 mL of butanol and hexane (50:50)	7.8 (plasma) 1600 (urine)	-	Gabr <i>et al.</i> , 2010
SPE- Fluorimetry	PHEN	10 + SPE time	1.5 MeOH	3	-	Shi <i>et al.</i> , 2016
SPE - CE	MET PHEN	SPE time	MeOH + 3% HOAc	12 6	- -	Lai and Feng, 2006
SALLE -HPLC PDA	MET BUF PHEN	8	0.2 mL ACN	<b>Plasma</b> Met: 4.2 Buf: 3.8 Phen: 5.6 <b>Urine</b> Met: 1.3 Buf: 0.8 Phen: 1.5	<b>Plasma</b> Met: 13 Buf: 12 Phen:17 <b>Urine</b> Met: 3.8 Buf: 2.3 Phen: 4.5	Alshishani <i>et al.</i> , 2018

Table 4.7: Continued

				<b>Lake water</b> Met: 0.8 Buf: 0.3 Phen: 0.5	<b>Lake water</b> Met: 2.3 Buf: 0.83 Phen: 1.6	
IP SPE- IP HPLC UV	MET	NA	1 mL MeOH	3	5	AbuRuz <i>et al.</i> , 2003
EMLLE – HPLC UV	MET PHEBI PHEN	16.5	2 mL DCE containing TMA <sup>+</sup> TPBCl <sup>-</sup>	2.2 12 13.5	7.5 40.2 45.6	This work

Abbreviations: MET: Metformin, PHEBI: Phenyl biguanide, PHEN: Phenformin, BUF: Buformin, GLM: Glimepiride, PIP: Pioglitazone, EMLLE: Electrochemically modulated liquid-liquid extraction, SALLE: Salting out assisted liquid-liquid extraction, PDA: Photodiode array, LLE: Liquid-liquid extraction, IP: Ion pair, SPE: Solid phase extraction, MeOH: Methanol, HOAc: Acetic acid, VALLE: Vortex assisted liquid- liquid extraction, CE: Capillary electrophoresis, HF: Hollow fiber, LPME: Liquid phase micro extraction, PFBC: Pentafluorobenzoyl chloride

#### 4.4 Conclusion

Aqueous samples containing cationic drugs were prepared by electrochemically modulated liquid-liquid extraction. This two-step method (a first extraction to an intermediate organic phase before a back extraction to an aqueous final phase) is based on 1) applied potential from potentiostat 2) the control of interfacial potential difference between two immiscible solutions by the distribution of a common ion. The first technique unfortunately failed to achieve good extraction yield mainly due to the cell design. Cell that can give continuous supplied potential to the system should be designed in future. A full extraction yield was achieved for all four drugs, including metformin using the second technique of sample preparation. As the most hydrophilic one, it is the most difficult one to extract and commercially available methods have proven to be unsuccessful in many cases. The improved analytical performances achieved in terms of sensitivity, limits of detection and quantitation, and precision are a promise of the application of this method to a wider range of hydrophilic analytes and natural samples.

## CHAPTER 5

### GRAPHENE AND ZEOLITE AS ADSORBENTS IN BAR-MICRO-SOLID PHASE EXTRACTION FOR THE HPLC DETERMINATION OF SELECTED PHARMACEUTICAL COMPOUNDS

#### 5.1 Methodology

##### 5.1.1 Preparation of standard solutions

Metformin (MET), buformin (BUF), phenformin (PHEN), and propranolol (PROP) stock solutions (500 mg L<sup>-1</sup>) were prepared by dissolving the weighed amounts in water. It was stored in the refrigerator at 4 °C. Working solutions were prepared from the stock solution by dilution with appropriate volume of water.

##### 5.1.2 Urine samples

Human urine samples were obtained from volunteers of healthy postgraduate students from the School of Chemical Sciences, USM in February 2019. Urine samples were spiked with the desired concentration of the targeted analytes and diluted with water (1:4, v/v). The urines samples were stored in a refrigerator at 4 °C and were used within 2 days.

##### 5.1.3 Preparation of bar-micro-solid phase extraction (bar-μ-SPE)

The bar-μ-SPE extraction device was made according to the earlier report (Alshishani *et al.*, 2019) with slight modification as shown in Figure 5.1. First, the polypropylene (PP) membrane was cut (2.4 x 1.8 cm), folded into half and heat-sealed from two sides. After that, the adsorbent (20 mg) was placed through the open edge. Next, a piece of

metal rod (diameter, 1 mm; length, 1.1 cm) was also introduced and the open edge was heat-sealed completely. The tiny metal rod functioned as a magnetic bar itself.

Finally, the PP membrane bag was folded into half and heat-sealed again. The size of the prepared bag was 1.5 cm x 0.4 cm. This PP membrane bag is coined as bar- $\mu$ -SPE device. The device was immersed in acetonitrile and sonicated for 5 mins before use.

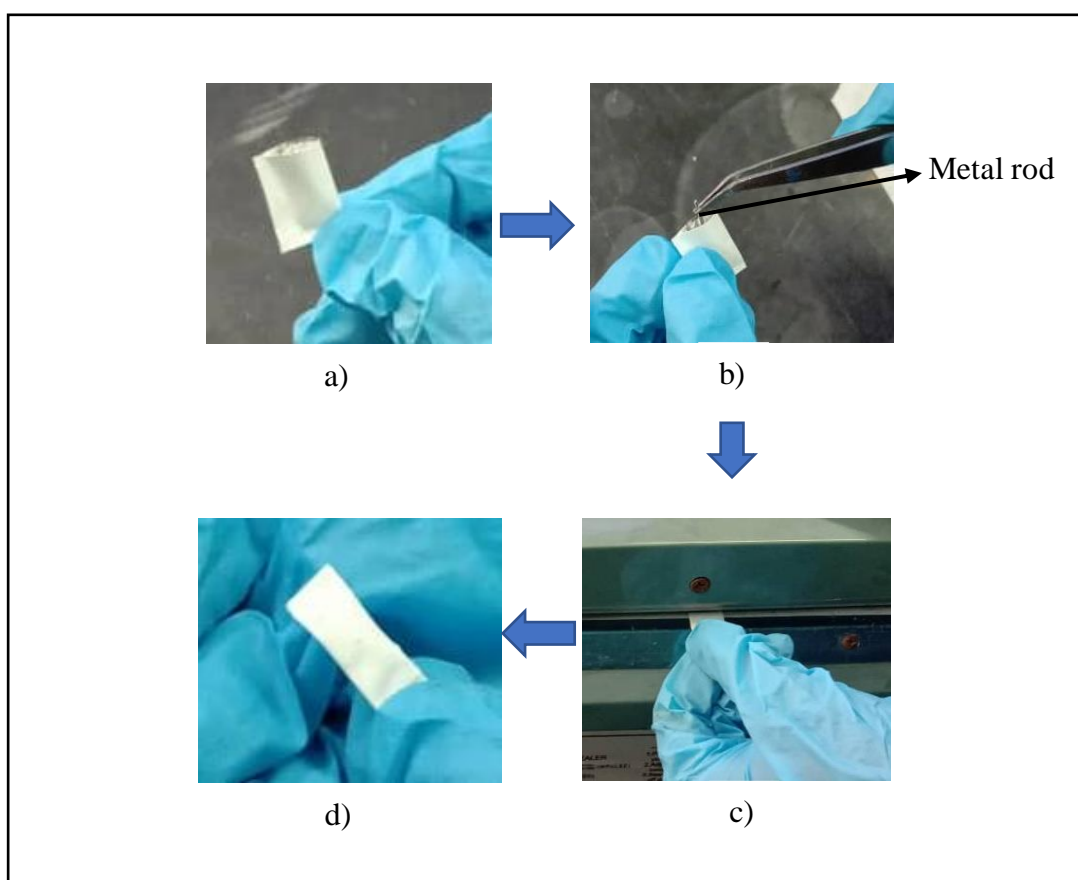


Figure 5.1: Preparation of bar- $\mu$ -SPE. a) Preparation of PP bag b) Insertion of metal rod in PP bag c) heat-sealed of edges d) completed device

#### **5.1.4 Bar- $\mu$ -SPE procedure**

The bar- $\mu$ -SPE device was cleaned by soaking in acetonitrile for 5 mins and left for 2 mins. The device was then immersed in 20 mL sample solution which was stirred (800 rpm) for 60 mins for the extraction process. Next, the device was removed from the sample solution, washed with water and dried with lint-free tissue paper. The device was put into a centrifuge tube that contained acetonitrile as back-extraction solvent. The desorption process was done by sonicating the device for 30 mins. Finally, 20  $\mu$ L of the extract was directly injected into the HPLC unit. This entire procedure is illustrated in Figure 5.2.

Optimization parameters of the chosen adsorbents were examined. These included the type of conditioning solvent, the effect of pH of sample solution, amount of adsorbent, volume of sample solution, rotating speed, time of extraction, and ionic strength of solution, desorption solvent, time of desorption and volume of desorption solvent.

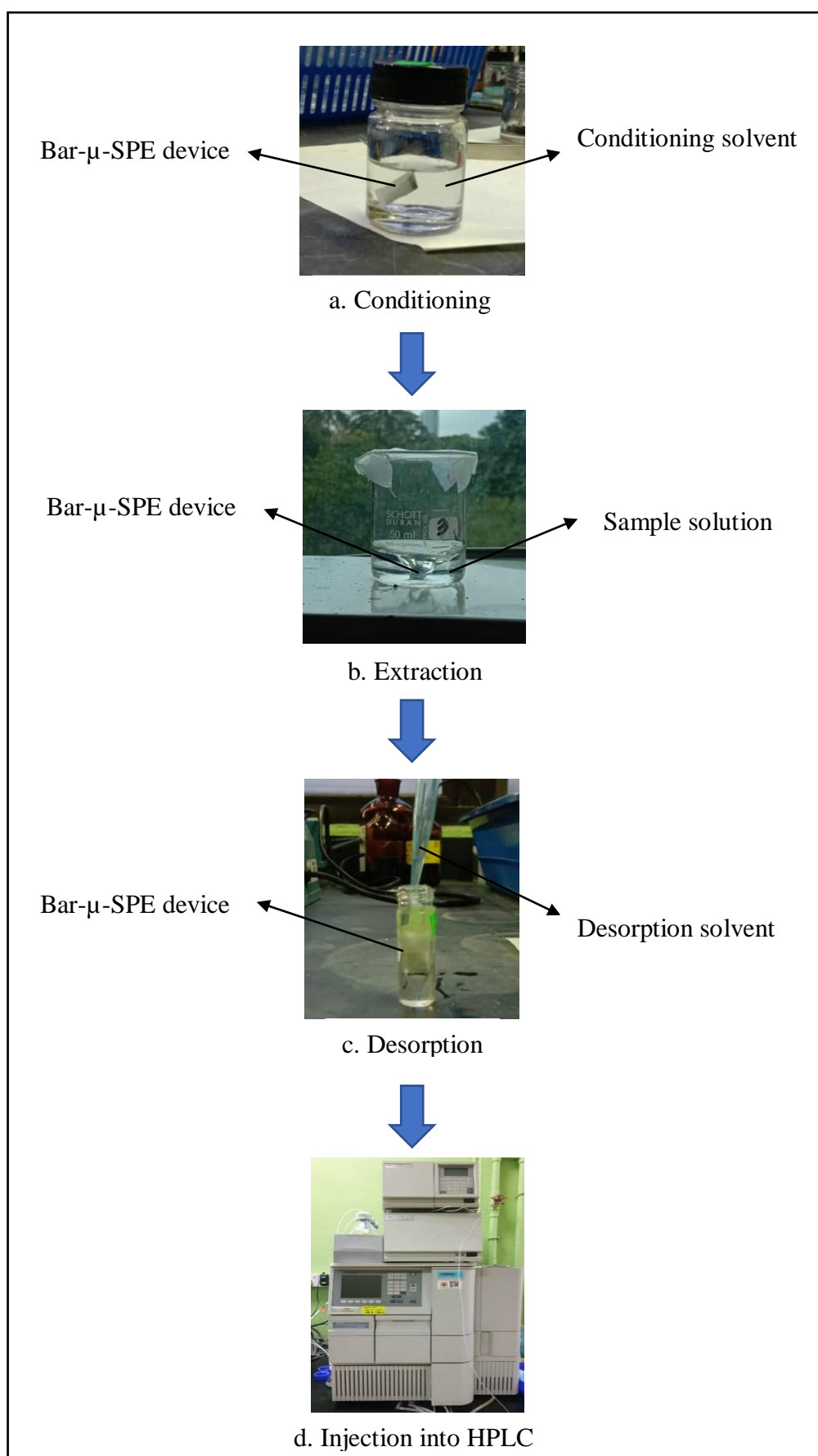


Figure 5.2: Protocol of extraction and desorption steps

### 5.1.5 Method validation of bar- $\mu$ -SPE- HPLC method

Method validation parameters (i.e., linearity, limit of detection (LOD), limit of quantification (LOQ), precision, recovery) were tested after subjecting the working standard and spiked sample solutions to the bar- $\mu$ -SPE protocol using the optimized conditions and HPLC separation. Linearity was performed using seven concentration levels (17-2000  $\mu\text{g L}^{-1}$ ) of targeted analytes. Calibration curves were established by plotting the peak area versus concentration of each analyte. LOD and LOQ were calculated based on linear regression from the calibration curve plots:

$$\text{LOD} = 3 \sigma / S \quad (5.1)$$

Where  $\sigma$  = standard deviation of the response and S = slope of the calibration curve

While the LOQs were calculated by:

$$\text{LOQ} = 10 \sigma / S \quad (5.2)$$

Precision was demonstrated by determining the intra-day and inter-day relative standard deviation (RSD) of the analysis using working solutions. The intraday RSD was investigated by analysing six replicates of three concentration levels (600, 750, and 950  $\mu\text{g L}^{-1}$ ) for all compounds. The interday determination was performed for five days.

Recovery test was studied by spiking the standard mixtures to urine samples in triplicates at three concentration levels (600, 750, and 950  $\mu\text{g L}^{-1}$ ) for all compounds.

### 5.1.6 Extraction efficiency (EE %), enrichment factor (EF)

Percentage of extraction and enrichment factor was used to choose the optimum value.

EF was obtained from the ratio of final peak area to that of the initial.

Whereas, the EE % was calculated from the peak area obtained from HPLC. The equation is as shown below:

$$EE \% = \frac{P_{final} - P_{initial}}{P_{initial}} \times 100 \quad (5.3)$$

Whereby,  $P_{initial}$  is original peak area (standard) and  $P_{final}$  is the peak area after desorption.

## 5.2 Results and discussion

### 5.2.1 Optimization of HPLC method

Separation of biguanides on reversed-phase columns is challenging because of their polar nature especially for MET, as well as the diverse polarities of the drugs. When initially separated on the C18 column, MET was eluted together with the solvent. This was not surprising as there was poor retention of MET on the non-polar C18 column. A common strategy to overcome the rapid elution, is to add ion-pairing reagents such as hexanesulphonate, heptanesulphonate and octanesulphonate to the mobile phase. When the hydrophobicity of the ion-pair reagent increased, the retention time of the analyte increased (Georgita *et al.*, 2010). The high polarity of the analytes also can be reduced by derivatization (Tache *et al.*, 2001). However, in these studies, the C18 column was replaced with a slightly more polar column such as C1. The use of C1 column gives satisfactory separation even without the use of ion-pairing reagents. The slightly more polar C1 column compared to the C18 resulted in more favourable interaction on the stationary phase, hence the longer retention (Alshishani *et al.*, 2016).

A simple buffered acetonitrile containing triethylamine was found appropriate for the separation of all analytes with wide range polarities based on their log  $P_o$  values (refer to Tables 1.7 and 1.8 in Chapter 1). Phosphate buffer containing 20 mM sodium monophosphate monobasic (pH 6.2) was found to be a promising component of the mobile phase together with acetonitrile (ACN). To improve the separations, small amounts of triethylamine was added to the mobile phase to reduce the peak tailing. Several compositions of the mobile phase were tested, and the optimum composition was 45:55:0.2 (phosphate buffer: ACN: triethylamine).

All analytes were separated and eluted within 13 mins (Figure 5.3). The order of elution is in accordance with their lipophilicity. Based on its structure, BUF has higher retention time than MET as it contains N-butyl group (Tahara *et al.*, 2006). This HPLC conditions will be used in all HPLC analysis.

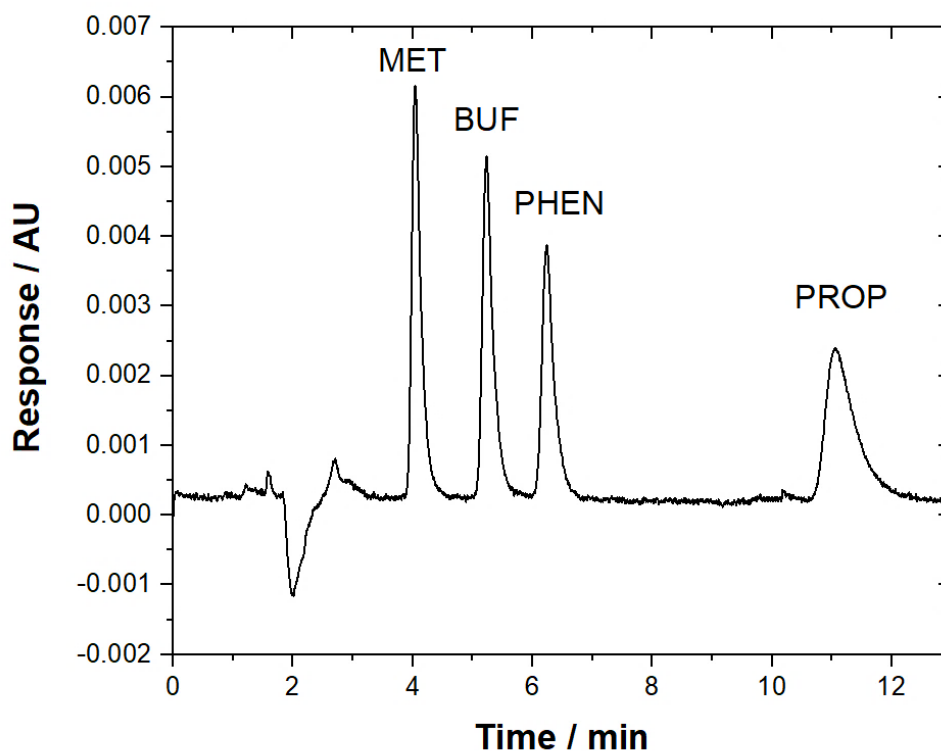


Figure 5.3: Chromatogram for the separation of analytes. HPLC conditions: mobile phase, 20 mM phosphate buffer (pH 6.2): ACN: trimethylamine (45:55:0.2, v/v) Column: Zorbax TMS (250 x 4.6 mm). Flow rate, 1.3 mL min<sup>-1</sup>: Injection volume, 20  $\mu$ L. Wavelength: 230 nm. Concentration of analytes: 1 mg L<sup>-1</sup>

### 5.2.2 Type of adsorbents

The success of the bar- $\mu$ -SPE lies on the choice of adsorbent. Retention of an analyte by an adsorbent is mainly by weak interactions such as hydrogen bonding,  $\pi$ - $\pi$  interactions, electrostatic interaction and Van der Waals interaction. This facilitates the desorption and the possible regeneration of the adsorbent for repeated use. Thus, several commercial adsorbents (Si-CH, Si-CN, Si-NH<sub>2</sub>, Si, zeolite, C18 and graphene) were tested by placing 20 mg adsorbents into the device.

Regarding the choice of adsorbents, it can be categorized into: (i) Polar adsorbent (Si-CH, Si-CN, Si-NH<sub>2</sub>, Si, zeolite) and (ii) Non-polar adsorbent (C18 and graphene). Different polarities of adsorbents were chosen as the targeted analytes have wide range polarities. Initially, this adsorbent was tested one at a time. In these studies, the extraction using 1 ppm of the drugs mixture was tested. The concentration of the drugs that remained in the solution was analysed using HPLC. Results are shown in Figure 5.4. The highest extraction among the adsorbents tested was obtained when using zeolite and graphene as adsorbents. With the exception of graphene, the other adsorbents were easy to handle due to their favourable particle size. The use of graphene requires special introduction into the bag. This was done by using a modified filter funnel fitted with a tip at the end. In addition, the sticking of the graphene to the wall of the PP bag caused difficulty in the heat-sealing process. During introduction of graphene into the PP bag, the tip was wrapped with paper (membrane's cover) to prevent any graphene sticking to the wall of membrane. For the other adsorbents, this was not necessary. The PP bag was folded into half to obtain constant rotation. The rest of the studies were focused using zeolite and graphene. Important parameters that affect the extraction processes were systematically investigated.

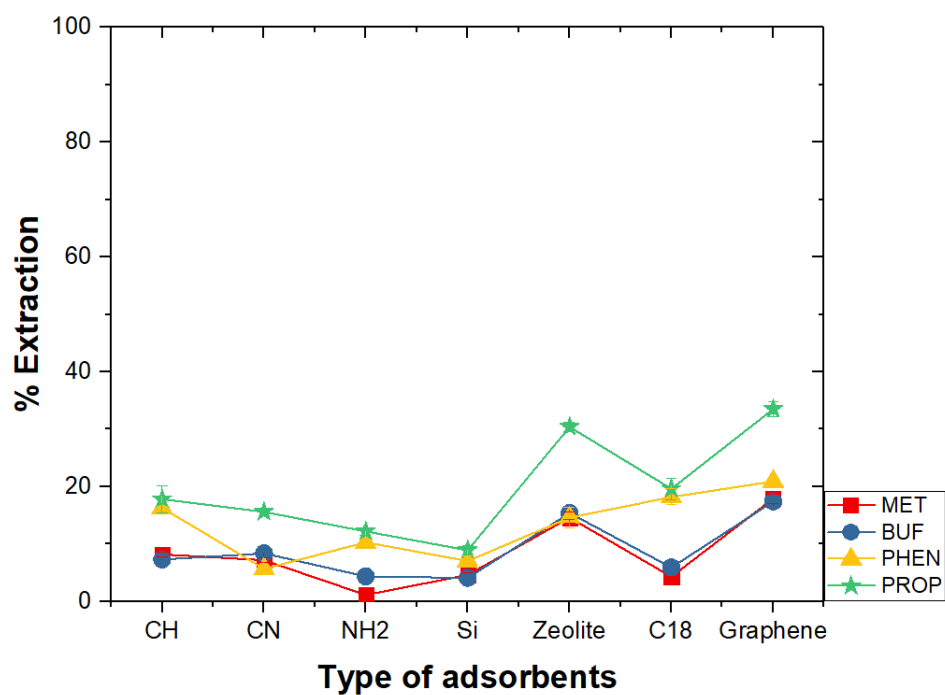


Figure 5.4: Effect of type of adsorbents on extraction. Experimental conditions: Conditioning solvent: ACN,  $V_{\text{solution}}$ : 20 mL,  $\text{pH}_{\text{solution}}$ : 6, amount of adsorbent: 20 mg, time of extraction: 60 mins, rotation speed: 800 rpm

### **5.2.2(a) Optimization of extraction parameters**

#### **5.2.2.(a)(i) Pre-conditioning solvent**

Before the device is used for extraction, it must be immersed in an organic solvent to activate the membrane for better analyte diffusion. It also helps to condition the adsorbent and to clean it from any contaminants. Thus, several commonly used pre-conditioning solvents such as 3 % acetic acid, MeOH, ACN and THF were tested. Before that, the device was soaked in the conditioning solvents for 5 mins. After that, it was removed and was left for 2 mins. The device was next placed into a standard solution of the drug mixture (1 ppm). It was left stirred for 60 mins. The device was removed, and the sample solution was analysed using HPLC. Results when graphene and zeolite were used are shown in Figure 5.5.

As illustrated in Figure 5.5, after extraction, the highest extraction was obtained when ACN was used. Thus, the best preconditioning solvent was ACN for both adsorbents. ACN is a mid-polar solvent and the most common solvent used for conditioning adsorbent in SPE (Alshishani *et al.*, 2019). Therefore, ACN was used for further assays.

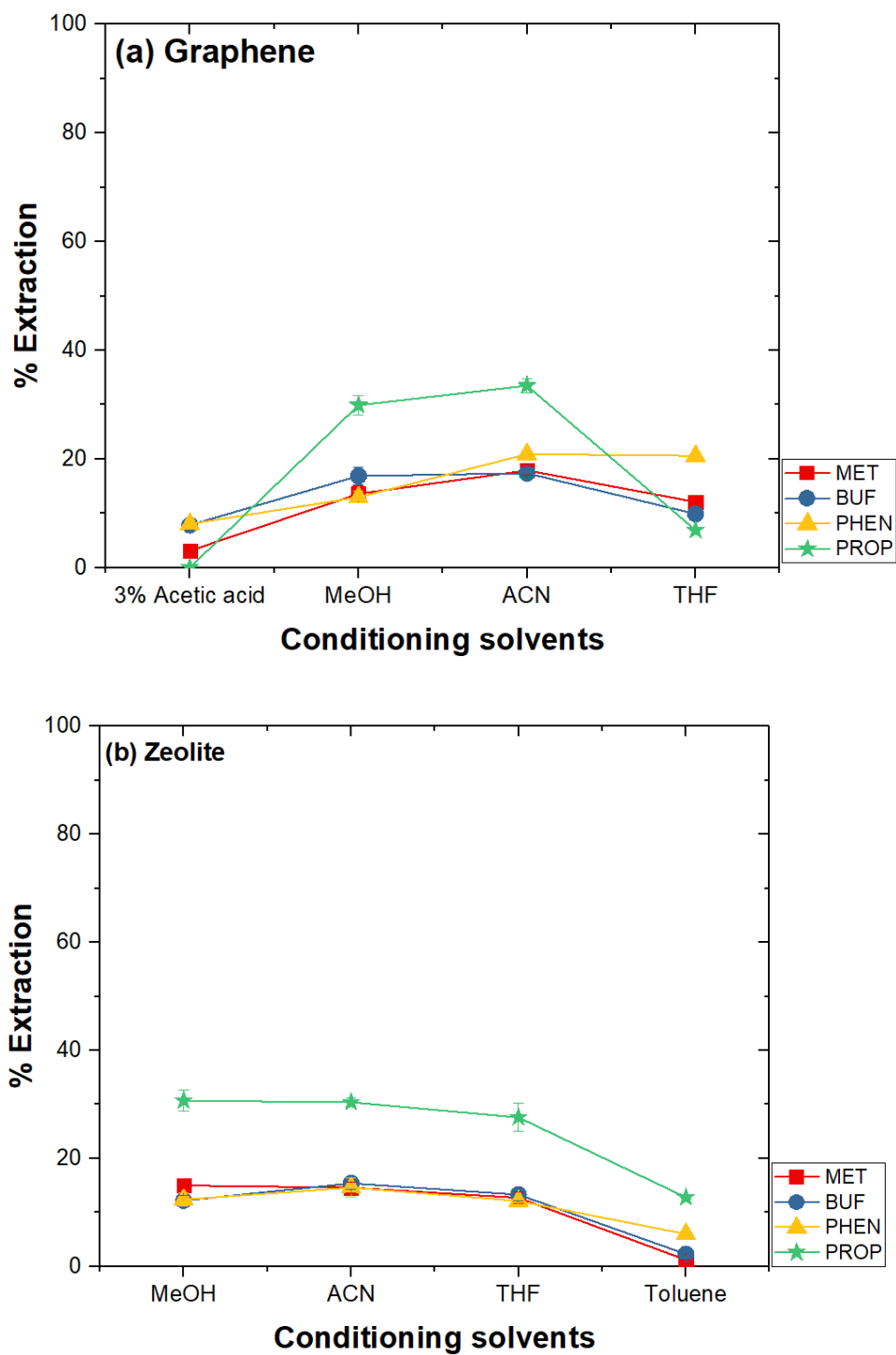


Figure 5.5: Effect of conditioning solvents on the extraction of drugs. Experimental conditions:  $V_{\text{solution}}$ : 20 mL,  $\text{pH}_{\text{solution}}$ : 6, amount of adsorbent: 20 mg, time of extraction: 60 mins, rotation speed: 800 rpm

### 5.2.2(a)(ii) Effect of pH

The pH of the sample solution greatly affects the extraction especially for amines and other ionisable compounds. Thus, the effect of solution pH on the extraction of the drugs was studied. The pH of sample solution was varied from pH 3 until 10. The form of analytes in solution changed when the pH was changed. From Figure 5.6a, it was found the percentage extraction did not increase significantly, indicating that the percentage of extraction did not change until pH 9 for all analytes except for PROP. The favourable extraction under basic condition can be explained by the favourable adsorption of the neutral form of the drugs. Meanwhile at lower pH, the amine group will be protonated. This phenomenon leads to the low extraction efficiency of biguanide compounds since the membrane is hydrophobic in nature.

Based on Figure 5.6b, it can be seen that the percentage of extraction of targeted compounds generally decreased with the increase in pH. This showed that the extraction efficiency was reduced. Therefore, the highest extraction efficiency for biguanide compounds occurred at pH 3. This is because, when in acidic media, the drugs were protonated and will become positively charged. Therefore, it promotes the adsorption of the analytes on zeolite, since the negative charges on zeolite are more predominant. This also has been observed in an earlier study (Lee *et al.*, 2012). Hence, pH 10 was used for graphene and pH 3 for zeolite as the best pH of sample solution.

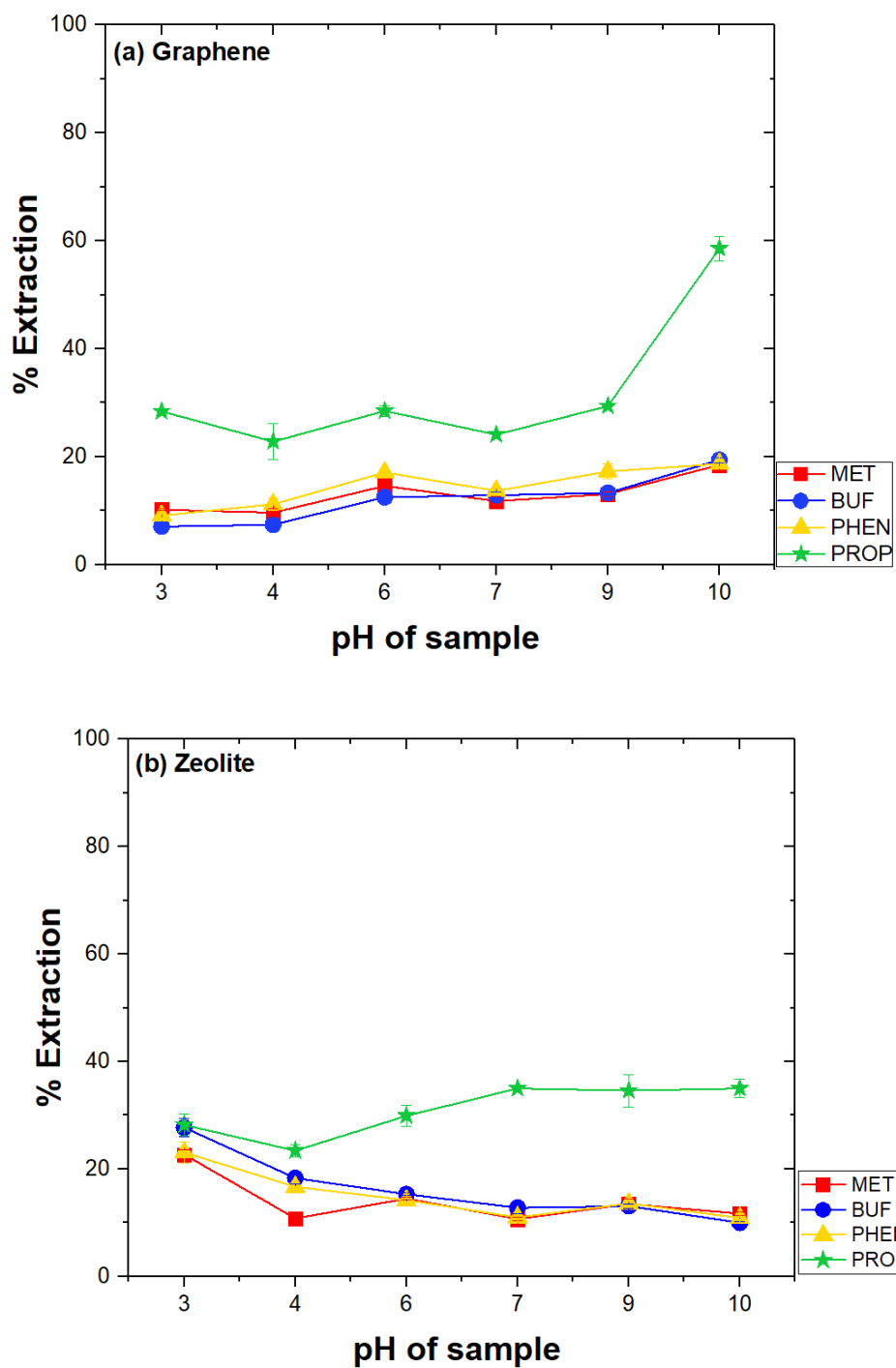


Figure 5.6: Effect of pH solution on the extraction of drugs. Experimental conditions: Conditioning solvent: ACN,  $V_{\text{solution}}$ : 20 mL, amount of adsorbent: 20 mg, time of extraction: 60 mins, rotation speed: 800 rpm

### 5.2.2(a)(iii) Amount of adsorbent

The effect of different masses (10, 20, and 25 mg) of adsorbents on the extraction of the drugs was studied and results are shown in Figure 5.7. Figure 5.7 showed that the best results were obtained when 10 mg of graphene and 25 mg of zeolite were used. The smaller mass of graphene was suitable due to its large surface area ( $750 \text{ m}^2 \text{ g}^{-1}$ ) compared to zeolite ( $290 \text{ m}^2 \text{ g}^{-1}$ ).

This indicates high loading capacity of graphene as it has a large surface area ( $750 \text{ m}^2 \text{ g}^{-1}$ ). Extraction that occurred was mainly due to; i)  $\pi$ - $\pi$  interaction between the analytes and the graphene layers, ii) van-der-Waals interaction. It can be seen from the graph that PROP has the highest percentage of extraction owing to the presence of aromatic rings, which lead to its binding on graphene. The lowest extraction efficiency obtained was when 25 mg of graphene was used. Graphene is difficult to disperse in all solvents due its strong van-der-Waals interaction. Therefore, it can hamper sorption of analyte (Sitko *et al.*, 2013). Moreover, in order to use graphene more than 20 mg, a bigger bag of PP sheet must be used. Unlike graphene, the results of zeolite showed that the extraction efficiency increased as the amount of adsorbent increased. This is because zeolite has  $290 \text{ m}^2 \text{ g}^{-1}$  of surface area which is twice lower than graphene.

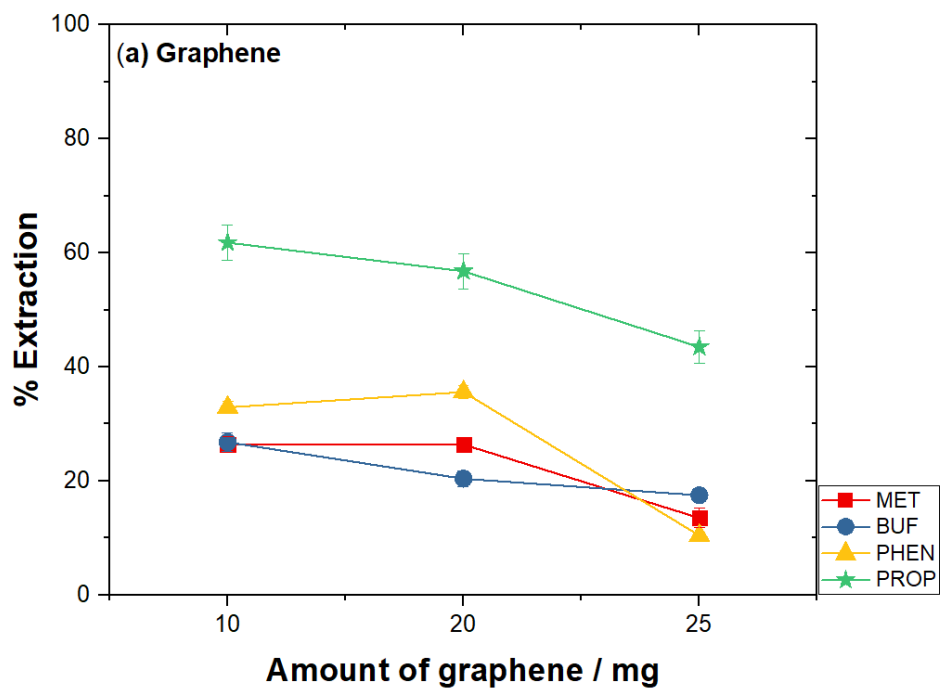


Figure 5.7: Effect of amount of adsorbent on the extraction of drug. Experimental conditions: Conditioning solvent: ACN,  $V_{\text{solution}}$ : 20 mL, pH solution: pH 10 (Graphene) and pH 3 (Zeolite), time of extraction: 60 mins, rotation speed: 800 rpm

#### **5.2.2(a)(iv) Volume of sample solution**

The effect of different volumes of sample solution (10, 20, 30 and 40 mL) on the extraction using the two adsorbents is shown in Figure 5.8. For both adsorbents a smaller sample volume is preferred.

The percentage extraction for both adsorbents reduced with the increase of volume in sample. This could have happened because longer time was needed when large volume was used. Volume of sample solution more than 10 mL will result in higher time of extraction. It is time-consuming for extraction step, as 60 mins of extraction time was used. Hence, 10 mL sample volume was used for subsequent experiment.

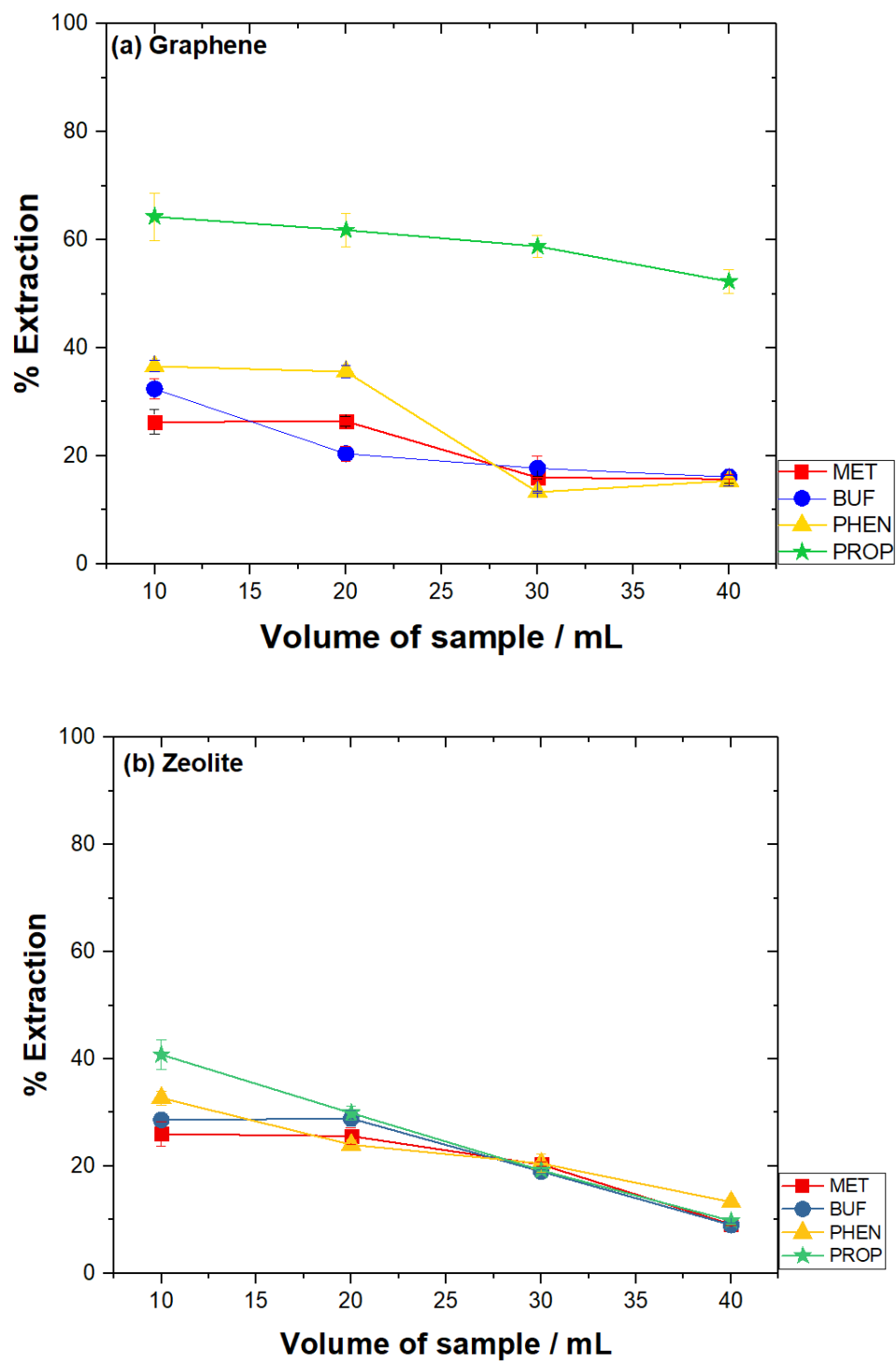


Figure 5.8: Effect of volume of solution on the extraction of drugs. Experimental conditions: Conditioning solvent: ACN, pH solution: pH 10 (Graphene) and pH 3 (Zeolite), amount of adsorbent: 10 mg (Graphene) and 25 mg (Zeolite), time of extraction: 60 mins, rotation speed: 800 rpm

### **5.2.2(a)(v) Stirring rate**

Stirring of the solution can enhance the mass transfer of analytes toward the adsorbent materials. In this work, the bar-device acted as a magnetic bar itself. The effect of different stirring rates (600, 800, 1000 and 1200 rpm) of the drugs mixture was evaluated on the extraction. Results are shown in Figure 5.9.

The trend of extraction obtained was similar for both adsorbents under the experimental conditions. 800 rpm was found to be the best stirring rate for both adsorbents. The percentage of extraction decreased when the rotation speed was greater than 800 rpm. This is due to the formation of bubbles under higher stirring rates.

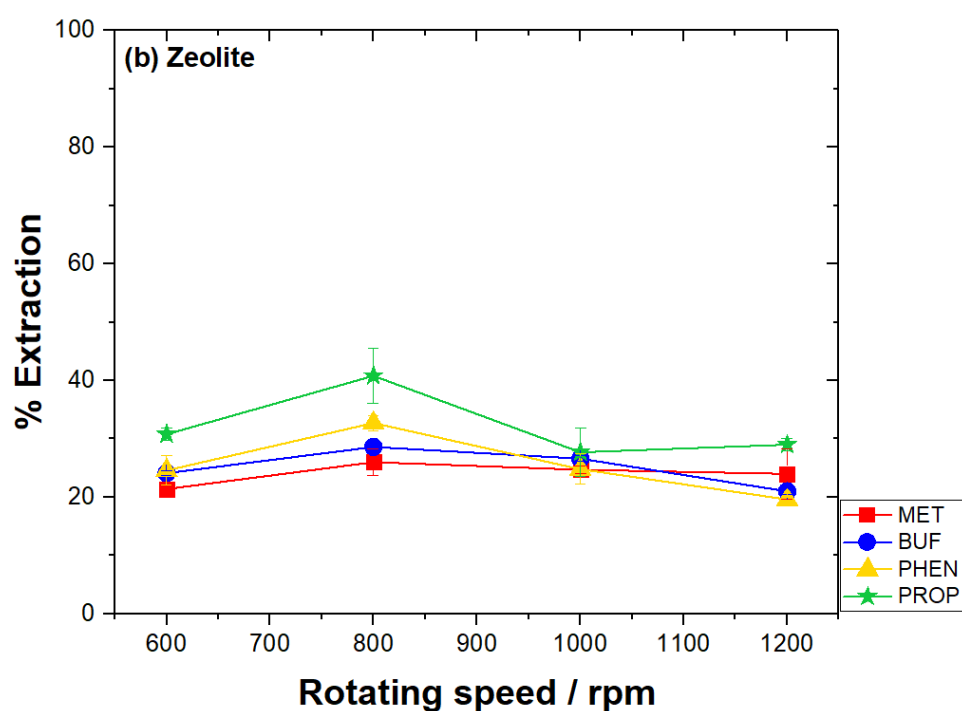
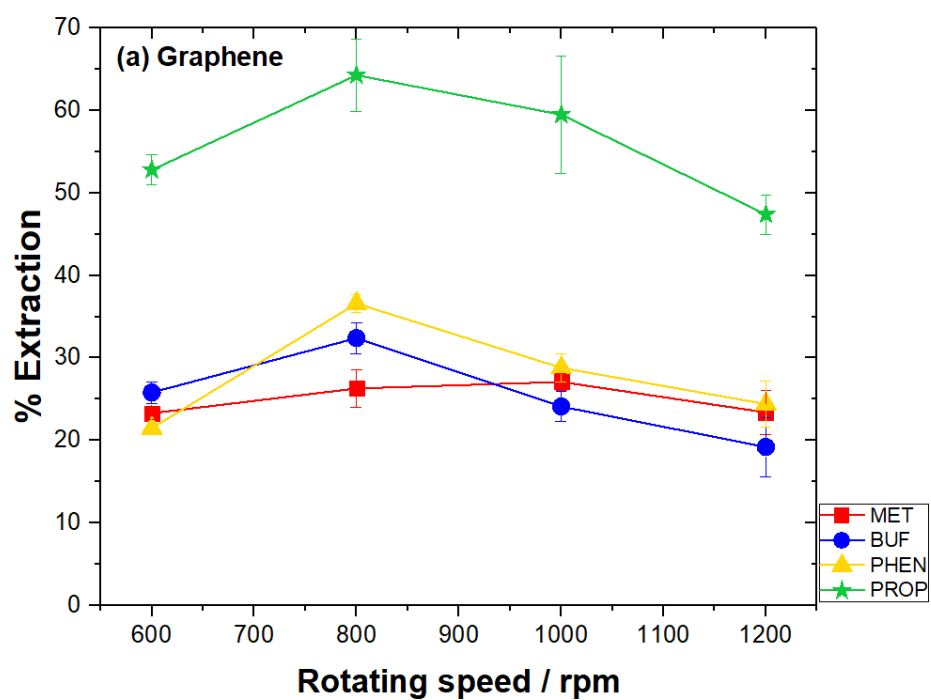


Figure 5.9: Effect of rotation speed on the extraction of drugs. Experimental conditions: Conditioning solvent: ACN,  $V_{\text{solution}}$ : 10 mL, pH solution: pH 10 (Graphene) and pH 3 (Zeolite), amount of adsorbent: 10 mg (Graphene) and 25 mg (Zeolite), time of extraction: 60 mins

### **5.2.2(a)(vi) Time of extraction**

It is important to examine the time of extraction because it determines the time required for the compounds to migrate from solution towards the adsorbent. The effect of time of extraction (30, 60, 90, 120 and 240 mins) of the drugs mixture was evaluated on the extraction capability. Results are shown in Figure 5.10.

As expected, percentage of extraction increased with time of extraction for graphene (Figure 5.10a). However, the percentage of extraction remained almost constant from 90 to 120 mins. On the other hand, for zeolite, the percentage of extraction for PROP decreased after 120 mins probably due to back-desorption (Figure 5.10b). It can be concluded that mass-transfer is a time dependent process. For subsequent experiments, 90 mins and 120 mins were chosen for graphene and zeolite, respectively.

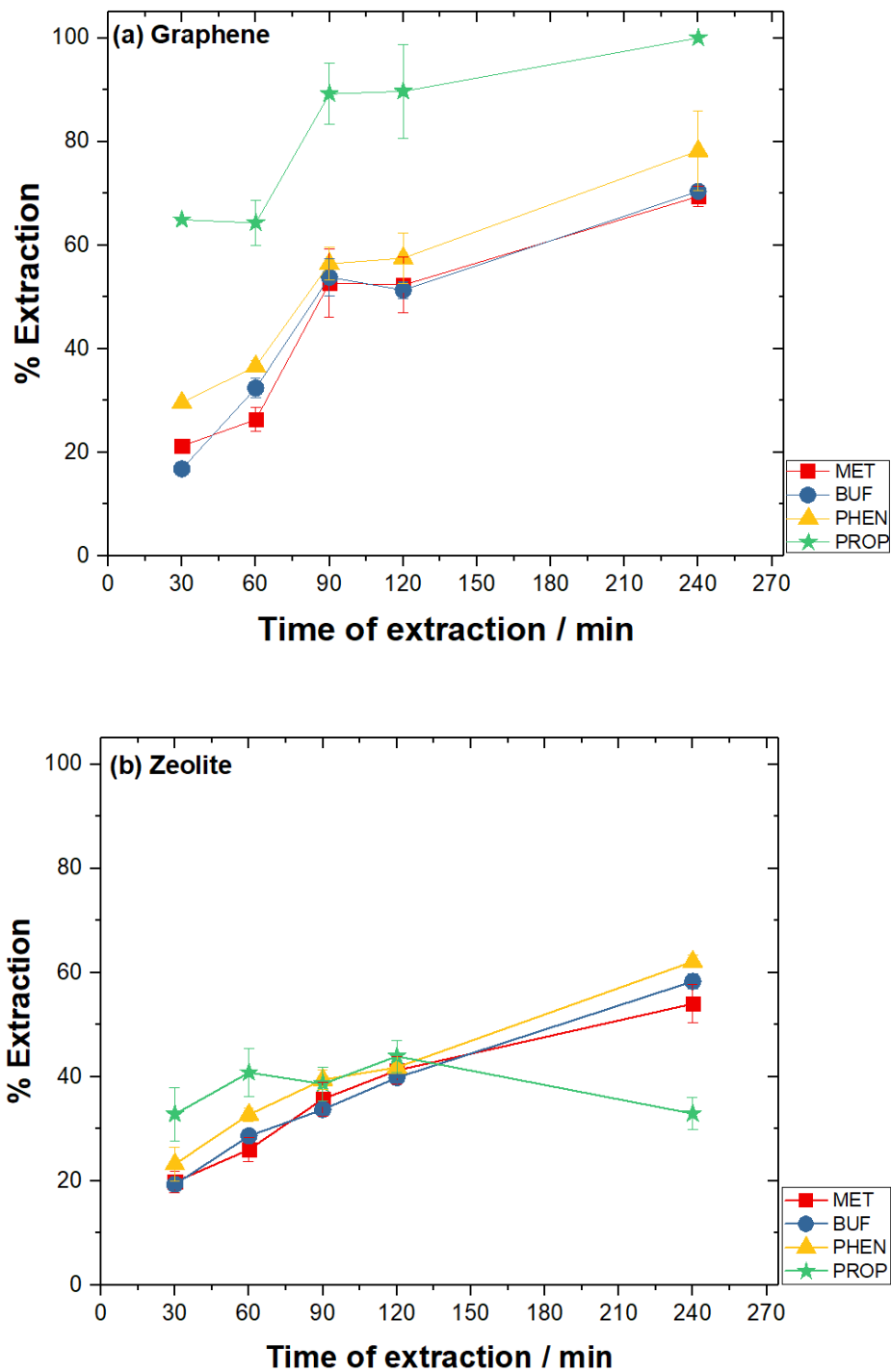


Figure 5.10: Effect of time of extraction on the extraction of drugs. Experimental conditions: Conditioning solvent: ACN,  $V_{\text{solution}}$ : 10 mL, pH solution: pH 10 (Graphene) and pH 3 (Zeolite), amount of adsorbent: 10 mg (Graphene) and 25 mg (Zeolite), rotating speed: 800 rpm

### 5.2.2(a)(vii) Ionic strength

The influence of ionic strength was evaluated by the addition of sodium chloride, NaCl (0, 2, 5, 10 %) to 10 mL sample solution during the extraction process. In brief, addition of salt results in decreasing the solubility of analytes in the sample solution and promotes their migration to adsorbent or so-called 'salting-out' effect (Sequeiros *et al.*, 2011). Results are shown in Figure 5.11.

Figure 5.11a shows that the percentage of extraction decreased with the addition of NaCl during extraction using graphene. Whereas, Figure 5.11b depicted that as the salt was progressively added, the peak also increased for biguanide compounds. It was reported that the addition of salt increases the viscosity of sample solution which restricts the migration of analytes (Lee *et al.*, 2012). In contrast, the percentage of extraction for PROP increased as the percentage of NaCl increased during extraction using zeolite. The effect of salt addition is only effective for PROP since it is more hydrophobic than the other compounds. Thus, for both adsorbents, further assays were continued without the addition of salt.

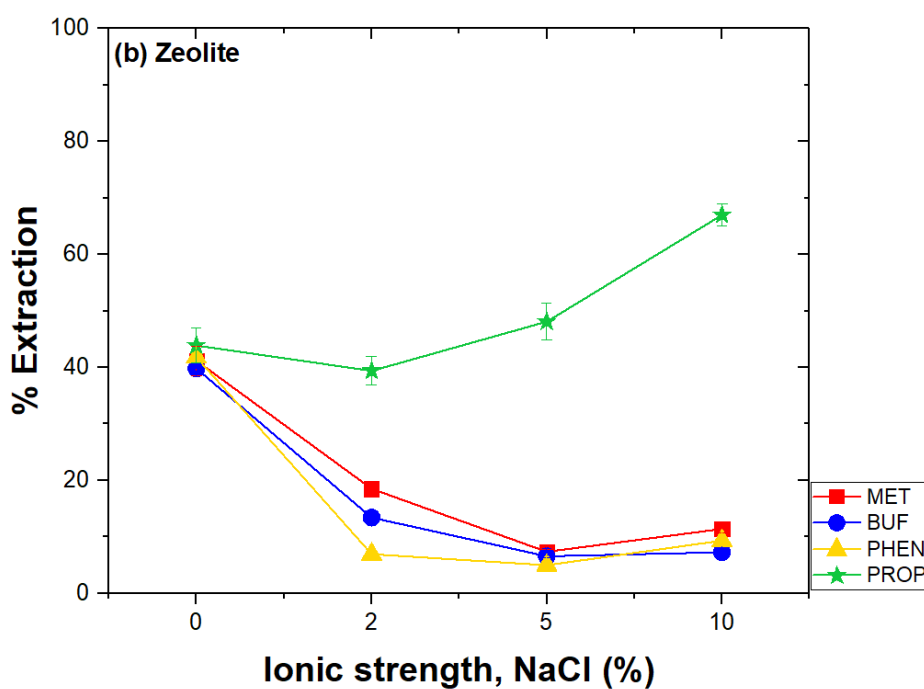
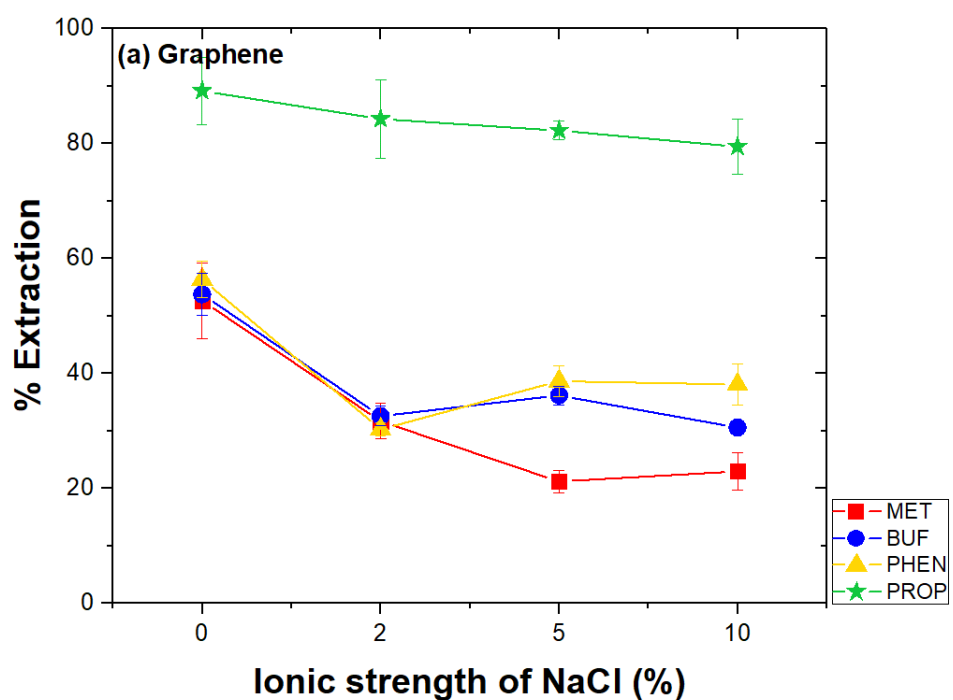


Figure 5.11: Effect of ionic strength, NaCl on the extraction of drugs. Experimental conditions: Conditioning solvent: ACN,  $V_{\text{solution}}$ : 10 mL, pH solution: pH 10 (Graphene) and pH 3 (Zeolite), amount of adsorbent: 10 mg (Graphene) and 25 mg (Zeolite), time of extraction: 90 mins (Graphene) and 120 mins (Zeolite), rotating speed: 800 rpm

### **5.2.2(b) Optimization of desorption parameters**

#### **5.2.2(b)(i) Type of solvents for back-extraction**

After extraction of analytes, analytes were desorbed with the aid of ultrasonication after adding a suitable organic solvent. The organic solvent must be able to disrupt the interaction between analyte and adsorbent. A high peak area indicates better desorption of the analyte.

From Figure 5.12a, the highest peak area was obtained when IPA was used for graphene adsorbent. IPA, being the most non-polar solvent compared to others was found to be the best desorption solvent for graphene. To further enhance the desorption process, ion-pair reagent (0.1 M sodium heptanesulphonate) was added to the IPA. To help in the dissolution of the ion-pair reagent, 0.1 M of sodium heptanesulphonate was dissolved in IPA water mixture (4:1, v/v). Significant increase of peak area for MET and BUF was observed. ACN was found to be the best desorption solvent for zeolite (Figure 5.12b) and significant increase for MET, BUF and PHEN was found when 0.1 M of sodium heptanesulphonate was added to ACN-water mixture. Highest enrichment factor for graphene (non-polar adsorbent) is BUF (polar analytes) and for zeolite (polar adsorbent) is PROP (non-polar analyte). The opposite properties between adsorbent and analyte resulted in weak interaction. Hence, it is easier to disrupt the interaction and back-extract them into desorption solvent.

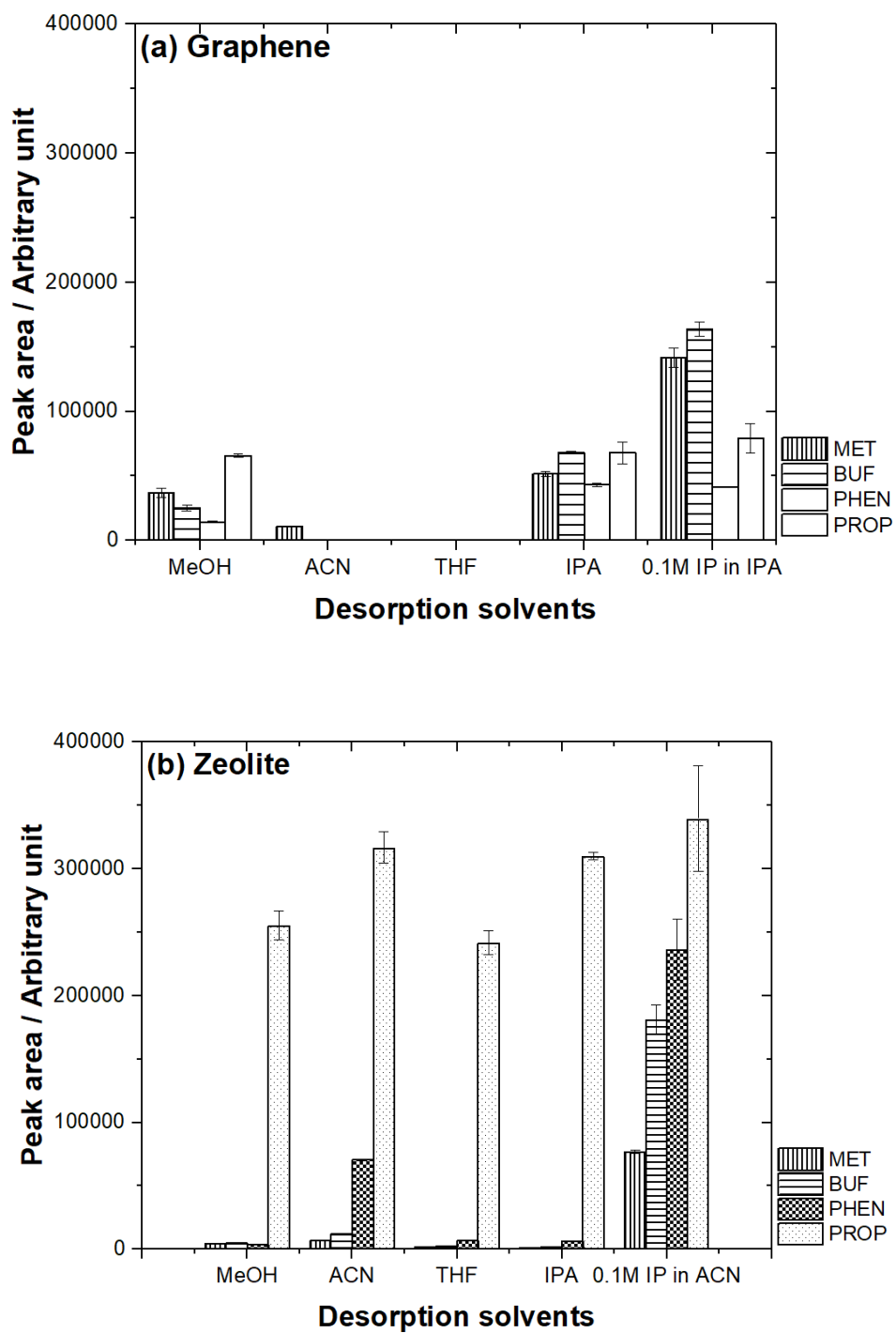


Figure 5.12: Effect on desorption solvents. Experimental conditions;  $V_{\text{desorption solvent}}$ : 0.6 mL, sonication time: 30 mins. Ion-pair reagent (IP): Sodium heptanesulphonate

### **5.2.2(b)(ii) Time of desorption**

The analytes were desorbed ultrasonically in their own suitable solvent. Different sonication durations were tested (15, 30, 45, 60 mins) as shown in Figure 5.13.

Generally, the peak area after desorption increased when the desorption time increased from 15 to 30 mins which then continued to reduce until 60 mins for both adsorbents. After 30 mins, the temperature of ultrasonic may result in the evaporation of analyte or the analytes degrade under ultrasonic mode for longer time (Sajid, 2019). The other possible reason why the peak area dropped is probably because analytes are being re-adsorbed by the adsorbent material (Kanimozhi *et al.*, 2011). The highest peak area after desorption was obtained when 30 mins of desorption time was used for both adsorbents.

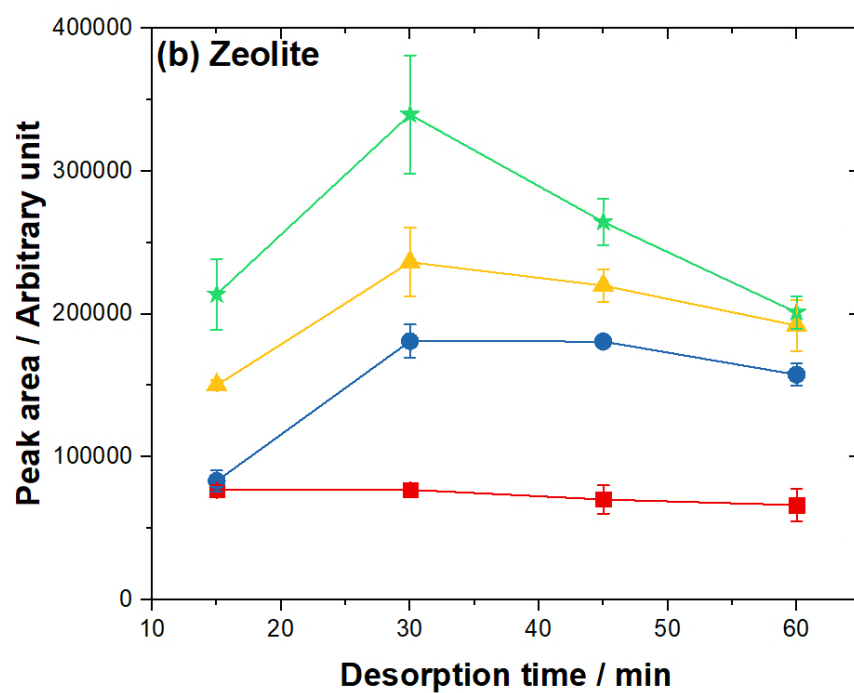
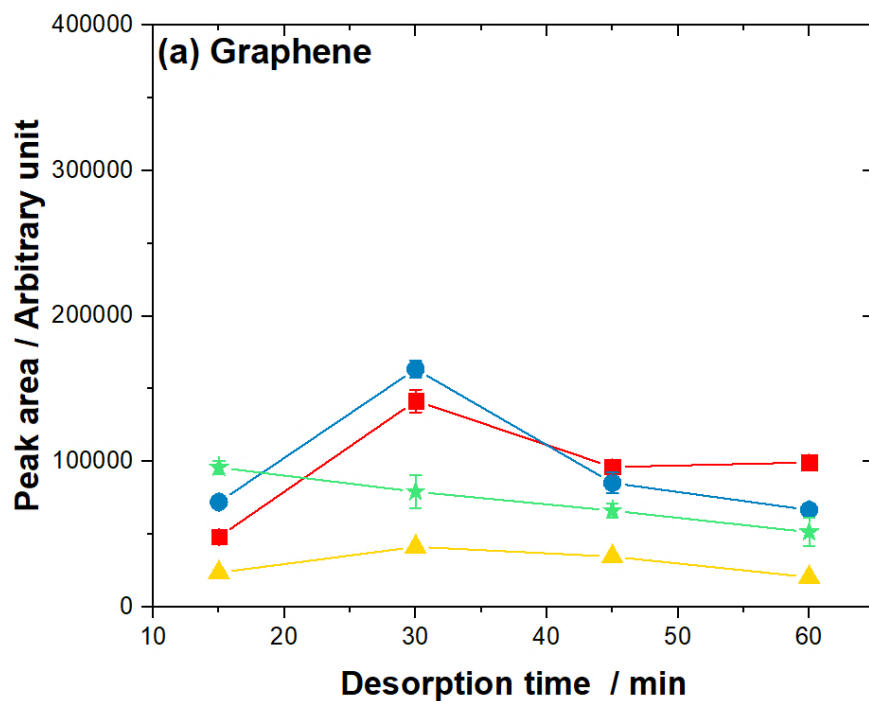


Figure 5.13: Effect on time of desorption. Experimental conditions;  $V_{\text{desorption solvent}}$ : 0.6 mL, Desorption solvents: 0.1 M IP in IPA, 0.1 M IP in ACN. Ion-pair reagent (IP): Sodium heptanesulphonate. MET (red squares), BUF (blue circles), PHEN (yellow triangles), PROP (green stars)

### **5.2.2(b)(iii) Volume of desorption solvent**

The effect of different volumes of desorption solvent (0.6, 0.8 and 1.0 mL) was examined. Results are shown in Figure 5.14.

From Figure 5.14, the highest peak area was found when 0.6 mL of desorption solvents was used for both adsorbents. Smaller volume of desorption solvent is desirable to increase the EF. In addition, volume of desorption solvent to be used must be able to immerse the bar-device completely to ensure effective desorption. The higher the volume, the lower is the peak area obtained after desorption due to dilution factor. The reason behind decreasing peak area value is, the mass transfer increases as the volume increases but not the concentration.

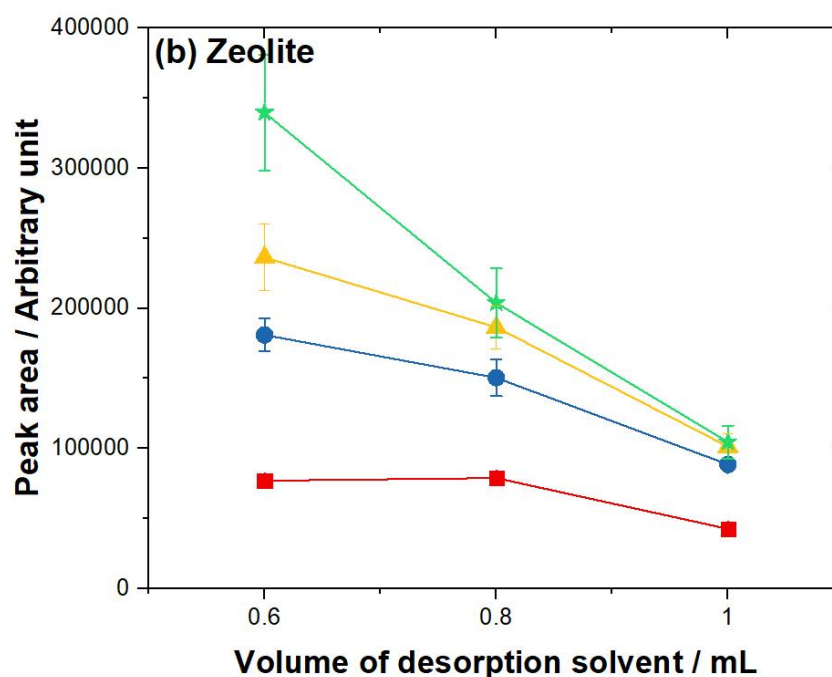
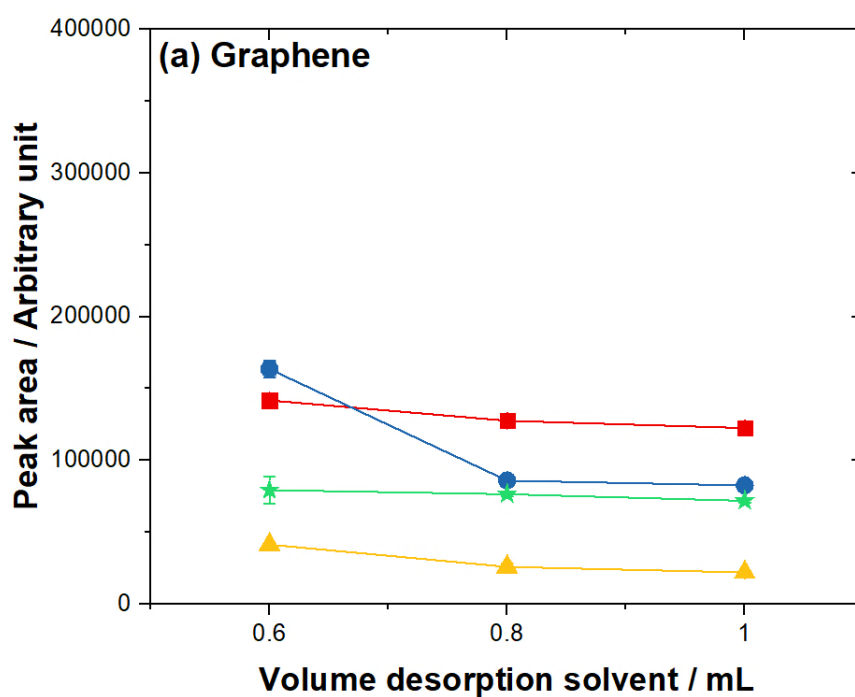


Figure 5.14: Effect on desorption solvents volume. Experimental conditions;  $V_{\text{desorption solvent}}$ : 0.6 mL, desorption solvents: 0.1 M IP in IPA, 0.1 M IP in ACN, sonication time: 30 mins. Ion-pair reagent (IP): Sodium heptanesulphonate. MET (red squares), BUF (blue circles), PHEN (yellow triangles), PROP (green stars)

### 5.2.2(c) Adopted conditions

The adopted extraction and desorption conditions are listed in Table 5.1. These conditions were used in the remaining studies. The EE % can be calculated by Eq 5.3 in Section 5.1.6. EE % for each analyte using graphene were; MET (13.9 %), BUF (15.3 %), PHEN (5.03 %) and PROP (9.13 %). Whereas, for zeolite were; MET (7.57 %), BUF (17.0 %), PHEN (28.8 %) and PROP (39.2 %). Based on peak area obtained after desorption, the EF can be calculated. The EF for graphene were; 4.42, 4.76, 1.49 and 1.71 for MET, BUF, PHEN, and PROP respectively. For zeolite were; 3.07, 7.12, 11.5 and 14.9 for MET, BUF, PHEN, and PROP respectively. The EF were typical of SPE.

Table 5.1: Summary of the adopted conditions of bar- $\mu$ -SPE-HPLC method using graphene and zeolite as adsorbent

Conditions	Graphene	Zeolite
Conditioning solvent	ACN	ACN
pH of sample solution	10	3
Volume of sample solution, mL	10	10
Amount of adsorbent, mg	10	25
Rotating speed, rpm	800	800
Time of extraction, min	90	120
Ionic strength, % NaCl	0	0
Solvent for desorption	0.1 M IP in IPA	0.1 M IP in ACN
Time of desorption, min	30	30
Volume of desorption solvent, mL	0.6	0.6

### 5.2.2(c)(i) Linearity, LOD, LOQ and recovery

Method validation parameters; linearity, LOD, LOQ and recovery were tested after subjecting the working standards and spiked sample solutions to the bar- $\mu$ -SPE procedure under the optimized conditions.

As listed in Tables 5.2 and 5.3, the proposed method using graphene as adsorbent shows wide range of linear ranges with  $R^2$  ranging from 0.9870 – 0.9971. LOD and LOQ obtained were in the range (126-269  $\mu\text{g L}^{-1}$ ) and (420-896  $\mu\text{g L}^{-1}$ ), respectively. For zeolite (Figure 5.3), the calibration curve was plotted from 30 to 1000  $\mu\text{g L}^{-1}$ . It was well correlated,  $R^2 > 0.9924$ . The calculated LOD ranged from 62.2 – 126  $\mu\text{g L}^{-1}$  and LOQ ranged from 207-422  $\mu\text{g L}^{-1}$ . The calibration curves plotted are shown in Appendix 3.

Recovery studies were first conducted using the original urine (undiluted) that was spiked with drugs mixture (950  $\mu\text{g L}^{-1}$ ). Generally, the recoveries were less satisfactory (61-117 %). To improve the recovery, the urine samples were diluted 1:4 (v/v) with water and this was used for the rest of the studies. Table 5.4 lists all recoveries obtained. All recoveries data were satisfactory except for BUF when zeolite was used.

Table 5.2: Analytical parameters for the bar-uSPE-HPLC method using graphene as adsorbent

Parameter	Analytes			
	MET	BUF	PHEN	PROP
<b>Linearity range, <math>\mu\text{g L}^{-1}</math></b>	250-2000	250-2000	250-2000	250-2000
<b><math>R^2</math></b>	0.9971	0.9889	0.9870	0.9942
<b>LOD, <math>\mu\text{g L}^{-1}</math></b>	126	248	269	178
<b>LOQ, <math>\mu\text{g L}^{-1}</math></b>	420	825	896	594

Table 5.3: Analytical parameters for the bar-uSPE-HPLC method using zeolite as adsorbent

Parameter	Analytes			
	MET	BUF	PHEN	PROP
<b>Linearity range, <math>\mu\text{g L}^{-1}</math></b>	30-1000	30-1000	30-1000	30-1000
<b><math>R^2</math></b>	0.9958	0.9959	0.9981	0.9924
<b>LOD / <math>\mu\text{g L}^{-1}</math></b>	93.3	92.7	62.2	126
<b>LOQ / <math>\mu\text{g L}^{-1}</math></b>	311	309	207	422

Table 5.4: Recovery for urine that was spiked with 950  $\mu\text{g L}^{-1}$  of drugs mixture (n = 6)

Adsorbent	Recovery (%)			
	MET	BUF	PHEN	PROP
Graphene	96.4 $\pm$ 6.22	92.3 $\pm$ 2.44	96.6 $\pm$ 2.40	99.6 $\pm$ 11.2
Zeolite	107 $\pm$ 9.20	76.8 $\pm$ 5.27	90.9 $\pm$ 5.10	76.8 $\pm$ 6.67

### 5.2.3 Mixed-adsorbent

In this section, experiments were continued by using mixtures of graphene and zeolite as adsorbent. The reason to use mixtures of adsorbents is to enhance the EE % for drugs that are not well extracted when a single adsorbent was used, such as for PHEN and PROP when graphene was used and MET when zeolite was used for extraction.

Investigation on the mixed-adsorbent was based on the optimized conditions of the individual adsorbent. As listed in Table 5.1, most of the optimized parameters are similar except for pH of the sample, amount of adsorbent and type of desorption solvent. 120 mins was chosen for time of extraction.

#### 5.2.3(a) Optimization parameters of mixed-adsorbent

##### 5.2.3(a)(i) Composition on mixed-adsorbent

Adsorbent containing different compositions of zeolite and graphene were studied. The optimum amount for zeolite and graphene is 25 and 10 mg, respectively. Thus, the total amount of mixed-adsorbent used was 35 mg. Different ratio compositions of zeolite: graphene (w:w) mixtures were studied, i.e., 1:1, 3:7 and 7:3. The mixed-adsorbent was prepared by placing zeolite first and followed by graphene into the extraction device. Results are shown in Figure 5.15.

The different compositions of mixed-adsorbent did not have significant difference in percentage of extraction for all analytes except MET. This was because increasing the amount of zeolite influences more adsorption of MET. It can be observed, by mixing the adsorbents, PROP was fully extracted (100%). Therefore, 7:3 ratio of zeolite:graphene with total amount of 35 mg was used for further investigations.

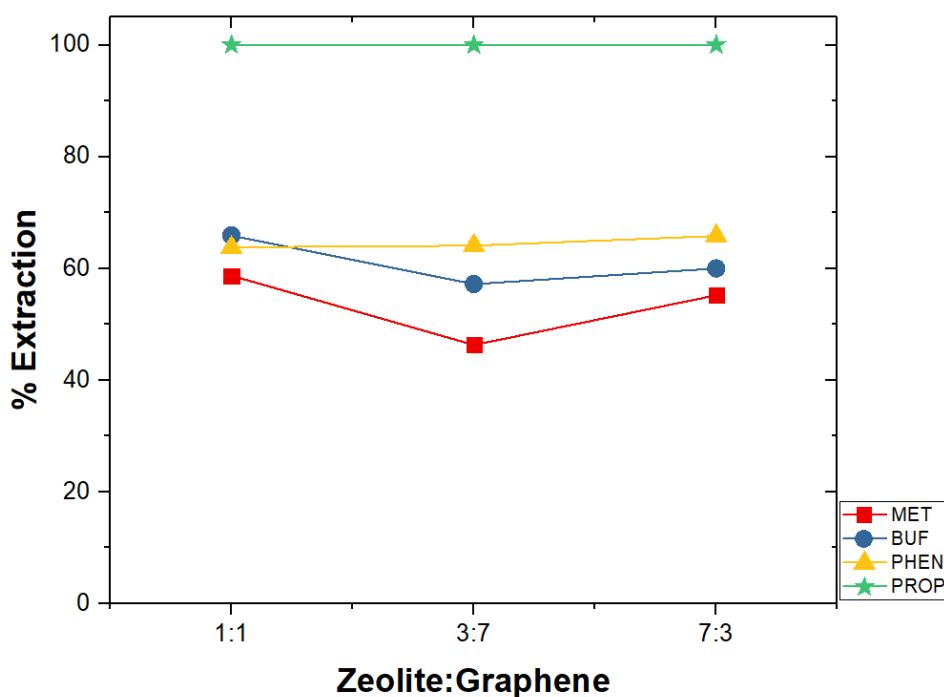


Figure 5.15: % extraction vs % zeolite:graphene ratio. Experimental conditions: Conditioning solvent: ACN, pH of solution: 6, time of extraction: 120 mins, rotation speed: 800 rpm

### 5.2.3(a)(ii) Effect of pH

The influence of pH (3, 6 and 10) was studied and depicted in Figure 5.16. As discussed in Section 5.2.2(a)(ii), each adsorbent has its own optimum pH value; pH 3 for zeolite and pH 10 for graphene. However, when mixed together, the highest extraction occurred at pH 6 (Figure 5.16).

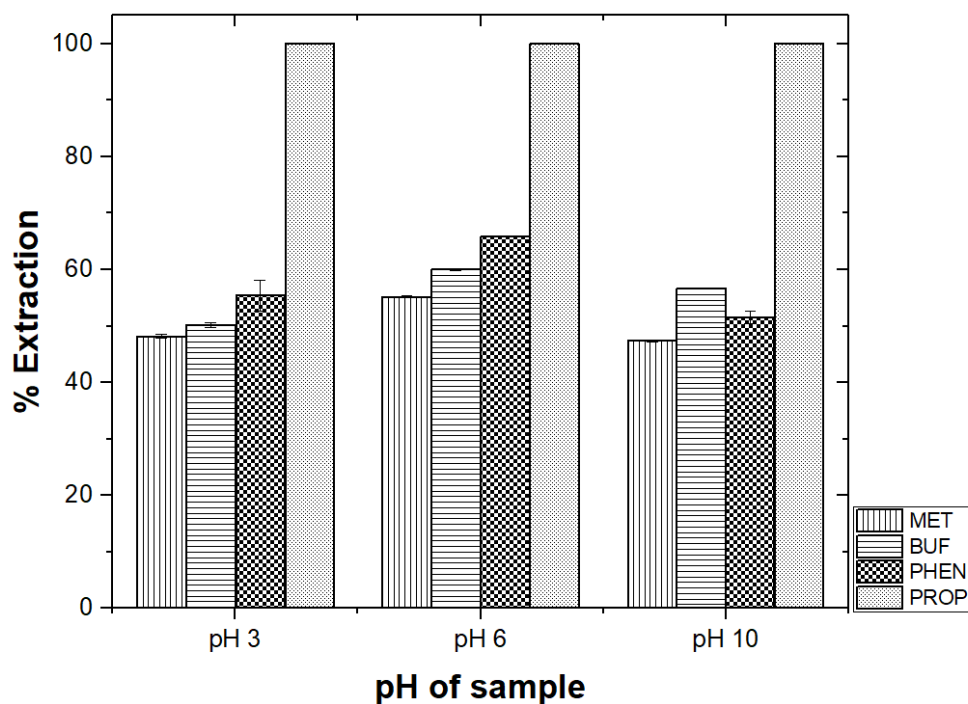


Figure 5.16: Effect of pH on extraction of drugs. Experimental conditions: Conditioning solvent: ACN,  $V_{\text{solution}}$ : 10 mL, Zeolite: Graphene: 7:3, time of extraction: 120 mins, rotation speed: 800 rpm

### 5.2.3(a)(iii) Desorption solvents

Investigation on mixture of IPA and ACN containing 0.1 M IP as the desorption solvent for mixed-adsorbent was performed. Results are shown in Figure 5.17. The optimal was found to be 7:3 of ACN:IPA ratio. It is as expected, because the optimum amount of mixed-adsorbent is 7:3 of zeolite:graphene, hence, ACN:IPA having the same ratio was the most appropriate desorption solvent for zeolite.

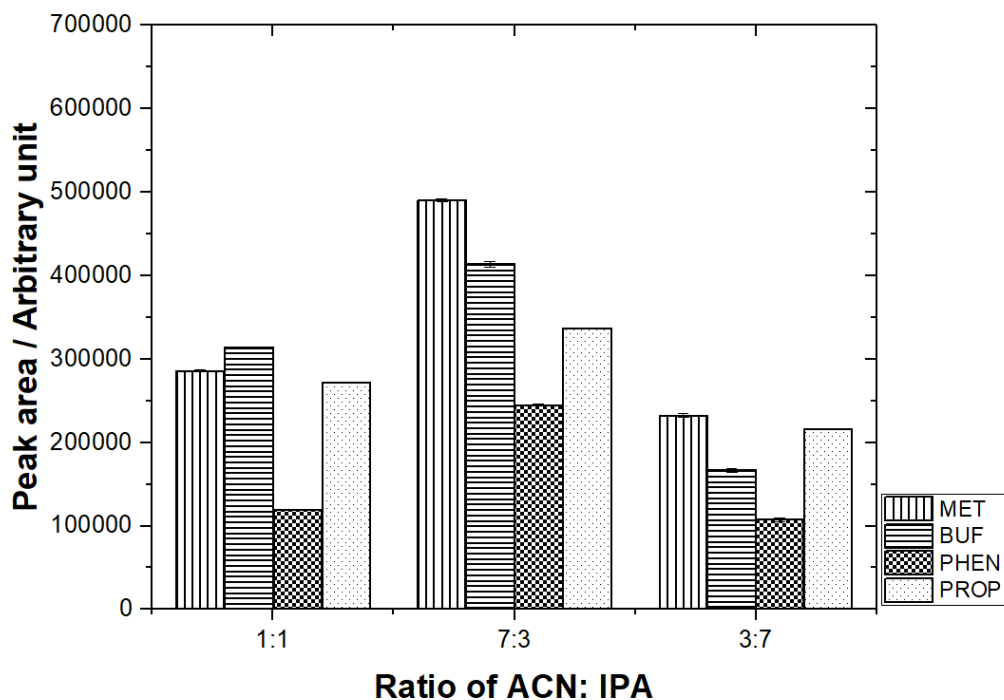


Figure 5.17: Effect of desorption solvent on mixed-adsorbent. Experimental conditions:  $V_{\text{Desorption solvent}}$ : 0.60 mL, sonication time: 30 mins

### 5.2.3(b) Final adopted conditions

The final adopted extraction and desorption conditions are listed in Table 5.5. These conditions were used in the remaining studies.

Table 5.5: Summary of the final adopted conditions of bar- $\mu$ -SPE-HPLC method using mixed-adsorbent

Conditions	Mixed-adsorbent
Composition ratio (Zeolite: Graphene)	7: 3
Conditioning solvent	ACN
pH of sample solution	6
Volume of sample solution, mL	10
Rotating speed, rpm	800
Time of extraction, min	120
Ionic strength, % NaCl	0
Solvent for desorption	7: 3 (ACN: IPA)
Time of desorption, min	30
Volume of desorption solvent, mL	0.6

### 5.2.3(c) Method validation

Method validation was performed by spiking drug-free urine samples (blank analysis was done before use). Linearity was studied using seven concentrations of standard mixtures ( $17 - 1000 \mu\text{g L}^{-1}$ ). Calibration curve was established by plotting peak area versus concentration of each targeted compounds. The calibration curve was linear over the concentration range. All the analytes were found to be well-correlated ( $R^2 > 0.99$ ) as shown in Table 5.6. The obtained LOD values were in the range  $33.7 - 107 \mu\text{g L}^{-1}$ . Compared to the individual adsorbent, LOD of MET obtained was significantly lower as the EF is higher.

Table 5.6: Analytical parameters for the bar-uSPE-HPLC method using mixed-adsorbent

Method development	Analytes			
	MET	BUF	PHEN	PROP
Linearity range, $\mu\text{g L}^{-1}$	17-1000	17-1000	30-1000	50-1000
$R^2$	0.9993	0.9960	0.9937	0.9942
LOD, $\mu\text{g L}^{-1}$	33.7	82.5	107	106
LOQ, $\mu\text{g L}^{-1}$	112	275	357	355

Precision was measured using three different concentration levels (600, 750 and  $950 \mu\text{g L}^{-1}$ ) for all compounds. It was expressed using RSD values. Good repeatability for the intra-day and inter-day were obtained ( $\% \text{RSD} < 9.12$ ) as listed in Tables 5.7 and 5.8. The recovery test was done by spiking three concentrations of standard mixtures into urine sample (600, 750, and  $950 \mu\text{g L}^{-1}$ ). Good recoveries were obtained for all targeted analytes as shown in Table 5.9. Figure 5.18 shows the chromatogram of urine sample that has been subjected to the bar- $\mu$ -SPE method.

Table 5.7: Intraday precision of the method using mixed-adsorbent (n=6)

Spiked concentration ( $\mu\text{g L}^{-1}$ )	% RSD			
	MET	BUF	PHEN	PROP
950	4.99	6.27	5.73	5.87
750	5.16	8.28	8.62	6.90
600	6.66	6.91	7.35	8.40

Table 5.8: Interday precision of the method using mixed-adsorbent (n=6)

Spiked concentration ( $\mu\text{g L}^{-1}$ )	% RSD			
	MET	BUF	PHEN	PROP
950	6.50	7.23	7.41	7.67
750	8.02	8.87	9.01	7.80
600	8.28	8.62	8.55	9.12

Table 5.9: Recovery of urine sample for using mixed-adsorbent (n=6)

Spiked concentration ( $\mu\text{g L}^{-1}$ )	% Recovery			
	MET	BUF	PHEN	PROP
950	$80.9 \pm 4.57$	$81.2 \pm 1.76$	$116 \pm 8.95$	$97.8 \pm 7.06$
750	$75.1 \pm 6.92$	$72.8 \pm 8.53$	$114 \pm 13.5$	$116 \pm 16.7$
600	$85.4 \pm 8.98$	$84.6 \pm 10.2$	$109 \pm 15.2$	$97.0 \pm 8.58$

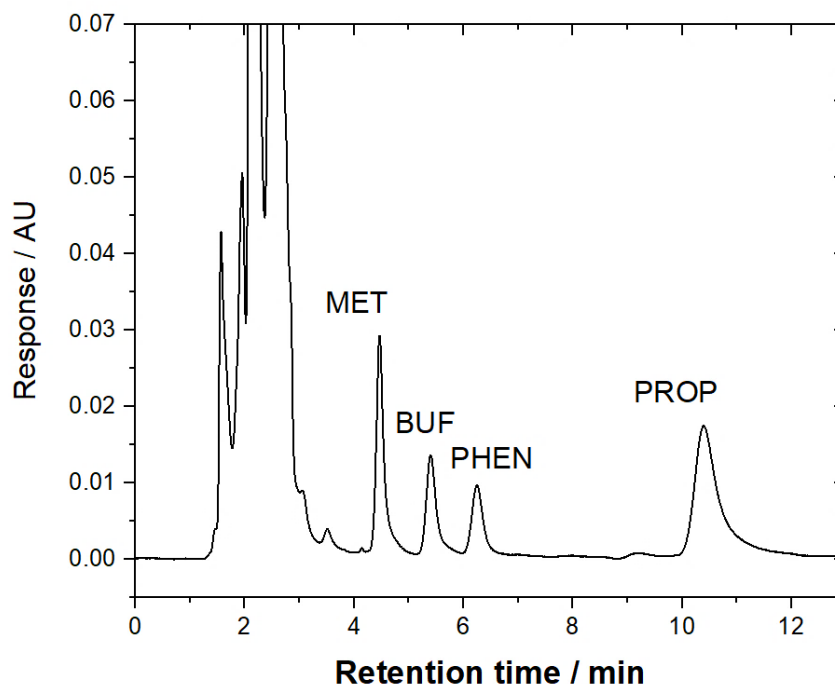


Figure 5.18: Typical chromatogram of urine sample that were spiked with the drug ( $950 \mu\text{g L}^{-1}$ ) using the bar- $\mu$ -SPE-HPLC method

#### 5.2.4 Comparison of performance between individual and mixed-adsorbent

Comparison on EE % using the adsorbents studied is shown in Figure 5.19. By mixing both adsorbents, the EE % only increased for MET. The highest EE % was obtained for BUF, PHEN and PROP when zeolite was used. Overall, the mixed-adsorbent gave better EE % compared to graphene. Figure 5.20 compares the EF between the different adsorbents studied. The highest EF were obtained for polar compounds (MET and BUF) when mixed-adsorbent were used. Meanwhile, zeolite gave the highest EF for PHEN and PROP. This is because hydrophobicity properties of the compound make it easier to desorb than polar compounds. In general, the EF obtained were typical of adsorbent based on SPE.

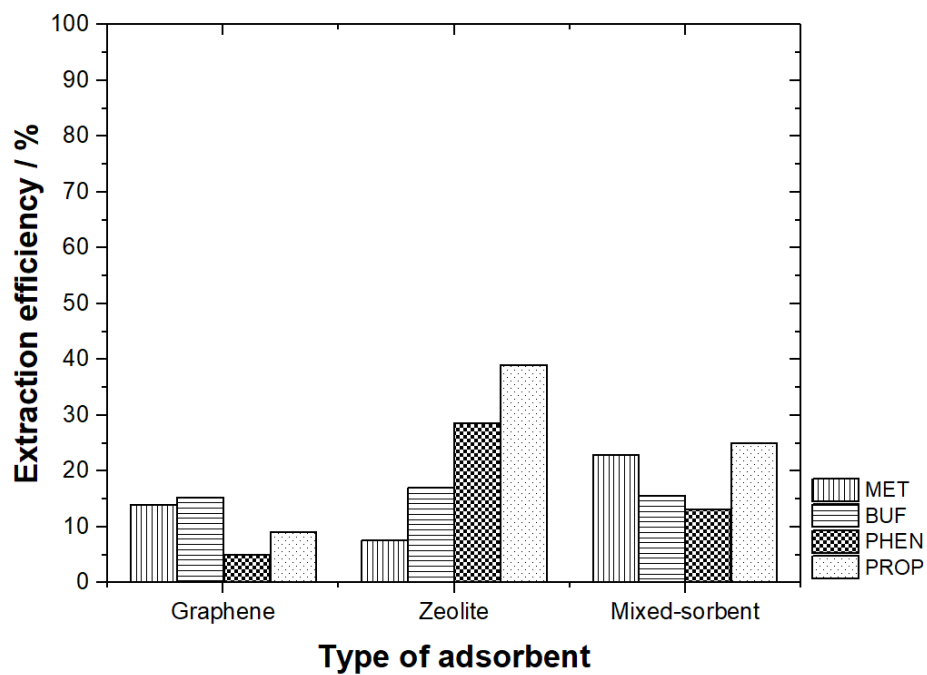


Figure 5.19: EE % for different type of adsorbents studied

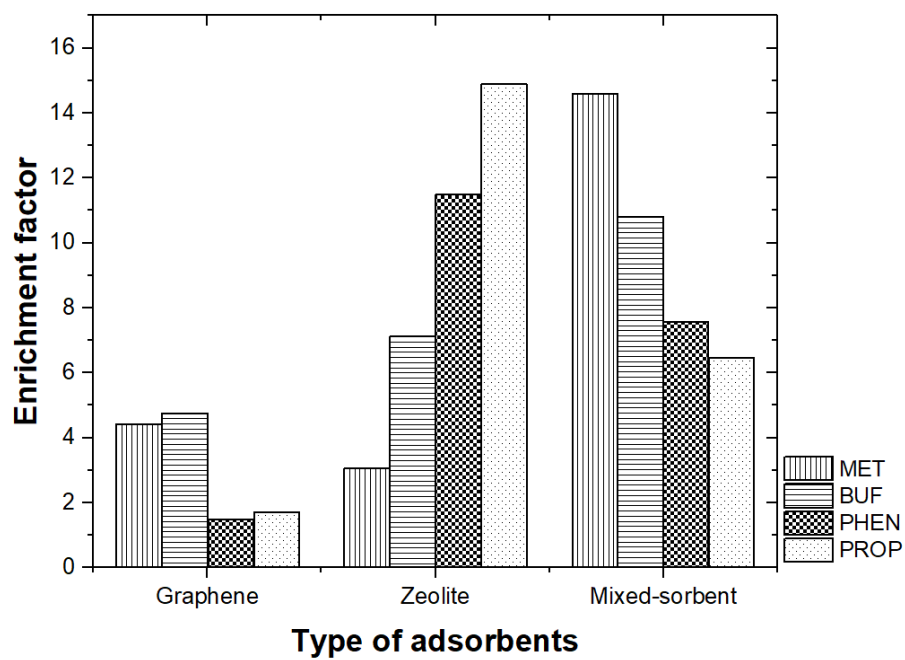


Figure 5.20: EF for different types of adsorbents studied

### 5.2.5 Comparison with previously reported analytical methods

The analytical characteristics of the proposed bar- $\mu$ -SPE- HPLC method was compared to some previously reported methods as shown in Table 5.10. A direct comparison between the methods is not possible since different drugs were studied. It can be seen that SPE is the most common sample preparation method used. The proposed method is simple, unlike conventional SPE method and does not require lengthy evaporation step (Partani *et al.*, 2009; Aburuz *et al.*, 2003; Magiera *et al.*, 2014). The major strength of the work lies in the fact that compounds with diverse polarity, especially drugs, can potentially be simultaneously extracted. It must be highlighted that current methods for the analysis of these compounds require different extraction and separation conditions, thus making the analysis very lengthy and more expensive (Lai *et al.*, 2006). Unfortunately, the sensitivity of the method is rather disappointing.

Table 5.10: Comparison of previously determination method for MET, BUF, PHEN and PROP with this work

Sample preparation and determination	Sample	Analytes	Type of adsorbent	Extraction organic solvents	LOD ( $\mu\text{g L}^{-1}$ )	LOQ ( $\mu\text{g L}^{-1}$ )	Ref
SPE- HPLC-MS		MET	PCX + clean-up by 50 mg PSA	2 mL 0.5 M NaOH/MeOH (40/60)	Capsule - 3.0 Tablets-2.0 Oral liquids – 2.0 Honeyed pills - 2.5		Wu et al., 2012
MISPE-PE-HPLC	Plasma	MET	MIP	MeOH + 3% TFA	50		Feng et al., 2004
IP SPE- IP LC	Plasma	MET	Oasis HLB	1 mL of MeOH	3	5	Aburuz et al., 2003
SPE- Non-aqueous CE	Plasma	MET PHEN	C18	2 mL of MEOH + 3% acetic acid	12 6		Lai et al., 2006
IP SPE-HPLC MS	Plasma	MET	Strata X	5 % acetic acid + ACN		2.49	Shah et al., 2018
Bar-u-SPE - HPLC UV	Urine	MET BUF PHEN PROP	Graphene + Zeolite	0.6 mL of 0.1 M sodium heptane sulphonate in ACN+IPA	33.7 82.5 107	112 275 357	This works
SPE- LC ESI/ MS MS		PROP 4-HYD PROP	Oasis HLB	MeOH	0.05 0.10	0.20 0.20	Partani et al, 2009
MIP SBSE-HPLC UV	Urine	PROP	Graphene oxide	0.1 mL of MeOH+ NaOH	0.37	1.0	Fan et al, 2016
SPE-UHPLC UV	Urine	PROP	Phenyl SPE cartridge	5 mL of MeOH	19	59	Magiera et al., 2014

Table 5.10: Continued

Bar-u-SPE - HPLC UV	Urine	PROP	Graphene + Zeolite	0.1 M sodium heptane sulphonate in ACN+IPA	126	422	This works
------------------------	-------	------	-----------------------	--	-----	-----	------------

Abbreviations: MISPE: Molecularly imprinted solid phase extraction, MIP: Molecularly imprinted polymer, TFA: trifluoroacetic acid, IP SPE: Ion pair solid phase extraction, IP LC: Ion pair liquid chromatography, MIP SBSE: Molecularly imprinted polymer stir-bar sorptive extraction, UHPLC: Ultra high-performance liquid chromatography, ESI: Electrospray ionization, MS: Mass spectromet

### 5.3 Conclusions

The use of a slightly polar C1 HPLC column was able to overcome the inconvenience of working with IP reagent when C18 column was used. Baseline separation of the peaks was obtained in about 11 min. A new bar- $\mu$ -SPE technique with mixed adsorbent (graphene and zeolite) for the extraction of polar and non- polar compounds has been developed. The use of a single PP bag was found to be satisfactory, in contrast to an earlier work that requires two bags to trap the adsorbents. The extracts are compatible with HPLC, thus can be directly analysed. However, the sensitivity of the method is not as good as the other reported methods.

## CHAPTER 6

### GENERAL CONCLUSIONS AND SUGGESTIONS FOR FUTURE STUDIES

#### 6.1 Conclusion

Biguanide compounds especially metformin have high hydrophilicity which makes it difficult to extract from aqueous samples. Sample preparation of these high polar compounds using LLE does give good results. In addition, the determination of compounds with broad range lipophilicities in a complex matrix such as urine is challenging. Hence, this thesis focusses on new sample preparation methods for the determination of such compounds. The antidiabetic (MET, BUF, PHEBI, PHEN) and beta-blocker drugs (PROP) were used as model compounds.

The EMLLE technique is based on the mass transfer of analytes of interest by application of potential difference across ITIES. ITIES is formed when an aqueous phase and organic phase which both contain suitable electrolyte are brought into contact. Generally, the application of an electric field is well-known for detection rather than sample preparation. Therefore, in our work, the EMLLE method was developed as a sample preparation technique that was subsequently analysed with HPLC-UV. Based on Pseudo-Nernst equation, the application of electric field can be done either with a potentiostat or by the manipulation of concentration of a common ion in both phases.

The transfer of targeted analytes across interface is influenced by the potential applied. Each ion has its own transfer potential. Thus, it is important to investigate the optimum potential that results in transfer of analytes from aqueous to organic phase. Cyclic voltammetry using a static ITIES cell was performed to investigate analytes potential

transfer. MET has the highest potential transfer followed by PHEBI, PHEN and PROP. MET is a polar drug which has a great solubility in water, it requires more energy to transfer MET from aqueous to organic phase than PROP (a less polar drug). Furthermore, the trend of potential transfer followed their lipophilicity. It can be concluded from CV studies that all analytes were able to transfer across the interface. Another information obtained from voltammetry studies was the mass transfer in static ITIES cell is limited by diffusion. For the sample preparation approach, a rotating paddle was adapted in a static ITIES cell to overcome the limitation. The mass transfer across interface then occurred in steady-state by convection mode.

Fixed potential was applied to biphasic system with the aid of potentiostat for 15 mins to extract cationic drugs. Consecutively, the drugs were quantified using HPLC-UV. Comparison of the number of moles extracted with number of actual moles detected showed 84.2 % loss of analytes. Based on this investigation, the collection must be done under the influence of potential applied to prevent extracted drugs being back-transferred spontaneously. Hence, designation of a different cell has to be done.

A gradient of tetramethylammonium ion concentrations in both phases was able to create potential in biphasic system without potentiostat. The use of 0.001 mM TMA<sup>+</sup> in aqueous and 10 mM TMA<sup>+</sup> in DCE allows imposing the potential needed to fully extract cationic drugs across the interface. This method consists of two major steps: extraction and back-extraction. Back-extraction must be done in order to pre-concentrate and protect the HPLC column. The key in this method is the electroneutrality of the system. By employing optimum conditions, cationic drugs were almost 100 % extracted and almost ~60 times enriched for biguanide drugs. In

contrast with PROP, it is well-extracted, but it was poorly back-extracted owing to its polarity. In addition, this method can be applied to urine sample.

The second sample preparation approach was the development of the bar- $\mu$ -SPE. Among several adsorbents that were studied, promising results were obtained using graphene and zeolite. Graphene was studied due to its ultra-high surface area, while the zeolite has the potential to act as molecular sieve to trap the targeted analytes.

Optimization of extraction parameters was done for each adsorbent. To desorb the analytes, ion-pair reagent (sodium heptanesulphonate) must be used to help in polar analytes desorption. Highest EF was obtained with graphene for BUF and with zeolite for PROP. It indicates that by having opposite polarity of compound and adsorbent during desorption process, it is easiest to disrupt their interaction with the adsorbent. The adopted condition was applied to urine as biological matrix and resulted in good recovery value.

To increase their extraction capability, mixture of graphene and zeolite was used as adsorbents in the PP bag. The use of adsorbent mixtures, after the optimisations, improves the extraction of MET but not the others. The extraction is also enhanced compared to that of graphene.

The EF for all adsorbents is in the range 1.49 – 14.9 which is typical for solid adsorbent. Unfortunately, the LOD for this method is not as good when compared to other reported methods. This work showed that graphene and zeolite are able to extract compounds with diverse polarity simultaneously.

Between the two sample preparation approaches, the EMLLE is superior with the LOD is significantly lower than the one obtained with bar- $\mu$ -SPE method. It also has shorter

time of analysis and does not require any IP reagent. Moreover, the selectivity can be tuned depending on the applied potential transfer.

## 6.2 Suggestions for future studies

1. Chapter 3: The extraction can be improved using potentiostat by designing a new ITIES cell. Important features of the cell are that the biphasic system must be connected to potentiostat during collection of organic phases after the extraction. The rotating paddle and ITIES must of appropriate distance to prevent disrupting surface of ITIES.

2. Chapter 4: Improving the sensitivity of EMLLE with potentiostatic-free method by enhancement of the EF can be done by using larger initial volume of aqueous phase and smaller volume ( $<100\ \mu\text{L}$ ) of organic phase. To overcome the limitation of poor back-extraction of PROP, different common ions that have lower transfer potential than  $\text{TMA}^+$  can be tested.

3. Chapter 5: As bar- $\mu$ -SPE method has low sensitivity, large volume of sample solution (40-100 mL) but small volume of desorption solvents can be tested. Manipulation of sample volume: desorption volume is a straightforward approach to improve the preconcentration of the analyte. Improving the permeability of analytes through PP membrane can be achieved by using new membrane materials and modification on PP membrane to reduce the hydrophobicity and selectively penetrate the analyte of interest.

4. Chapter 5: The idea of using mixed adsorbent deserves further investigations. Nanocarbons, metal organic frameworks, in their pristine forms as well as when functionalised with functional groups will not only result in adsorbents of high

surface areas and porosity, but polarity that favour the extraction of the target analytes.

5. Hydrophilic interaction chromatography (HILIC) has been used for the separation of polar analytes (Wu *et al.*, 2012; Liu and Coleman, 2009). HILIC column use environmentally-friendly water miscible mobile phases without the need of ion-pairing reagents and derivatizations that are necessary on RPLC methods (Alshishani *et al.*, 2019). Thus, HILIC method is worth to be investigated.

6. The fully validated method can be tested on other real samples such as plasma, wastewater and environmental waters.

## REFERENCES

- Abdel-Rehim, M. Anderson, M., Portelius, E., Norsten-Hoog, C., Blomber, L. G., (2001) 'Determination of ropivacaine and its metabolites in human plasma using solid phase microextraction and GC-NPD / GC-MS', *Journal of Microcolumn Separations*, 13(8), pp. 313–321. doi: 10.1002/mcs.10012.
- Abraham, M. H., Danil de Namor, A. F., (1974) 'Solubility of electrolytes in 1,2-dichloroethane and 1,1-dichloroethane, and derived from free energies of transfer', *Journal of Chemical Society, Faraday Transactions 1*, 72, pp 952-96
- AbuRuz, S., Millership, J. and McElnay, J. (2003) 'Determination of metformin in plasma using a new ion pair solid phase extraction technique and ion pair liquid chromatography', *Journal of Chromatography B: Analytical Technologies in the Biomedical and Life Sciences*. doi: 10.1016/j.jchromb.2003.09.043.
- Aider, M., de Halleux, D. and Bazinet, L. (2008) 'Potential of continuous electrophoresis without and with porous membranes (CEPM) in the bio-food industry: review', *Trends in Food Science and Technology*, 19(7), pp. 351–362. doi: 10.1016/j.tifs.2007.12.008.
- Albery, W. J., Burke, J. F., Leffler, E. B., Hadgraf, J., (1976) 'Interfacial Transfer Studied with a Rotating Diffusion Cell', *Journal of Chemical Society Faraday Transactions 1*, 72, 1618–1626
- Albery, W. J., Couper, A. M., Hadgraft, J., Ryan, C., (1974), *Journal of Chemical Society Faraday Transactions 1*, 70, 1124
- Ali, I. Hussain, I., Sanagi, M. M., Wan Ibrahim, W. A., Aboul-Enein, H. Y., (2015) 'Analyses of biguanides and related compounds in biological and environmental samples by HPLC', *Journal of Liquid Chromatography and Related Technologies*, 38(3), pp. 303–321. doi: 10.1080/10826076.2014.940803.
- Alpendurada, M. D. F., (2000) 'Solid-phase microextraction: a promising technique for sample preparation in environmental analysis', *Journal of Chromatography A*, 889, 3-14
- Alshishani, A., Makahleh, A., Yap, H. F., Gubartallah, E. A., Salhimi, S. M., Saad, B., (2016) 'Ion-pair vortex assisted liquid-liquid microextraction with back extraction coupled with high performance liquid chromatography-UV for the determination of metformin in plasma', *Talanta*. Elsevier, 161, 398–404. doi: 10.1016/j.talanta.2016.08.067.
- Alshishani, A., Salhimi, S. M. and Saad, B. (2018) 'Salting-out assisted liquid-liquid extraction coupled with hydrophilic interaction chromatography for the determination of biguanides in biological and environmental samples', *Journal of Chromatography B: Analytical Technologies in the Biomedical and Life Sciences*. Elsevier, 1073(December 2017), pp. 51–59. doi: 10.1016/j.jchromb.2017.12.013.

Alshishani, A. Saaid, M., Basheer, C., Saad, B., (2019) 'High performance liquid chromatographic determination of triclosan, triclocarban and methyl-triclosan in wastewater using mini-bar micro-solid phase extraction', *Microchemical Journal*, 147, pp. 339–348. doi: 10.1016/j.microc.2019.03.044.

Andrade-Eiroa, A. Canle, M., Leroy-Cancellieri, V., Cerda, V., (2016) 'Solid-phase extraction of organic compounds: A critical review (Part I)', *TrAC - Trends in Analytical Chemistry*. Elsevier B.V., 80, pp. 641–654. doi: 10.1016/j.trac.2015.08.015.

Appleyard, M. V. C. L., Murray, K. E., Coates, P. J., Wullschleger, S., Bray, S. E., Kernohan, N. M., Thompson, A. M. (2012). Phenformin as prophylaxis and therapy in breast cancer xenografts. *British Journal of Cancer*, 106(6), 1117–11

Arrigan, D.W.M (2008) 'Bioanalytical Detection Based on Electrochemistry at Interfaces between Immiscible Liquids', *Analytical Letter*, 41, 3233–3252

Bard, A. J., Faulkner, L. R., (2001) 'Electrochemical Methods: Fundamentals and Applications, 2<sup>nd</sup> Edition, New York: Wiley

Basheer, C., Ali Alnedhary, A., Rao, B. S. M., Valliyaveetil, S., & Lee, H. K. (2006). Development and application of porous membrane-protected carbon nanotube micro-solid-phase extraction combined with gas chromatography/mass spectrometry. *Analytical Chemistry*, 78(8), 2853–2858.

Basheer, C., Lee, H.K. (2004) Hollow fiber membrane-protected solid-phase micro-extraction of triazine herbicides in bovine milk and sewage sludge samples, *J. Chromatogr. A*, 1047, 189-194, <http://dx.doi.org/10.1016/j.chroma.2004.06.130>

Ben-Hander, G. M. *et al.* (2013) 'Hollow fiber liquid phase microextraction with in situ derivatization for the determination of trace amounts of metformin hydrochloride (anti-diabetic drug) in biological fluids', *Journal of Chromatography B: Analytical Technologies in the Biomedical and Life Sciences*. doi: 10.1016/j.jchromb.2013.10.007.

Ben-Hander, G. M., Makahleh A., Saad, B., Saleh, M. I., Cheng, K. W., (2015) 'Sequential hollow-fiber liquid phase microextraction for the determination of rosiglitazone and metformin hydrochloride (anti-diabetic drugs) in biological fluids', *Talanta*. doi: 10.1016/j.talanta.2014.08.037.

Berduque, A., Sherburn, A., Ghita, M., Dryfe, R. A. W., Arrigan, D. M. W., (2005) 'Electrochemically modulated liquid-liquid extraction of ions', *Analytical Chemistry*, 77(22), pp. 7310–7318. doi: 10.1021/ac051029u.

Berduque, A. *et al.* (2007) 'Electrochemistry of Non-Redox-Active Poly (propylenimine) and Poly (amidoamine) Dendrimers at Liquid - Liquid Interfaces', (28), pp. 7356–7364.

Berduque, A. and Arrigan, D. W. M. (2006) 'Selectivity in the coextraction of cation and anion by electrochemically modulated liquid-liquid extraction', *Analytical Chemistry*, 78(8), pp. 2717–2725. doi: 10.1021/ac0521192.

Carasek, E., Morés, L. and Merib, J. (2018) 'Trends in Environmental Analytical Chemistry Basic principles , recent trends and future directions of microextraction techniques for the analysis of aqueous environmental samples', *Biochemical Pharmacology*. Elsevier Inc., 19, p. e00060. doi: 10.1016/j.teac.2018.e00060.

Casado, N. Morante-Zarcero, S., Perez-Quintanilla, D., Sierra, I., . (2016) 'Application of a hybrid ordered mesoporous silica as sorbent for solid-phase multi-residue extraction of veterinary drugs in meat by ultra-high-performance liquid chromatography coupled to ion-trap tandem mass spectrometry', *Journal of Chromatography A*. Elsevier B.V., 1459, pp. 24–37. doi: 10.1016/j.chroma.2016.06.077.

Charles, B. G., Jacobsen, N. W. and Ravenscroft, P. J. (1981) 'Rapid liquid-chromatographic determination of metformin in plasma and urine', *Clinical Chemistry*.

Chen, Ch. (2013) Effects of Adjunctive Metformin on Metabolic Traits in Nondiabetic Clozapine-treated Patients with Schizophrenia and the Effect of Metformin Discontinuation on Body Weight: A 24-week, Randomized, Double-blind, Placebo-Controlled Study. *Journal of Clinical Psychiatry*. 74, 424–330. doi: 10.4088/JCP.12m08186.

Chisvert, A., Cárdenas, S. and Lucena, R. (2019) 'Dispersive micro-solid phase extraction', *TrAC - Trends in Analytical Chemistry*, 112, pp. 226–233. doi: 10.1016/j.trac.2018.12.005.

Collins, C. J. and Arrigan, D. W. M. (2009) 'Ion-transfer voltammetric determination of the  $\beta$ -blocker propranolol in a physiological matrix at silicon membrane-based liquid|liquid microinterface arrays', *Analytical Chemistry*, 81(6), pp. 2344–2349. doi: 10.1021/ac802644g.

Collins, C. J., Berduque, A. and Arrigan, D. W. M. (2008) 'Electrochemically modulated liquid-liquid extraction of ionized drugs under physiological conditions', *Analytical Chemistry*, 80(21), pp. 8102–8108. doi: 10.1021/ac800646b.

Davis, T. A. (1990) in: M.C. Potter (Ed.), *Handbook of Industrial Membrane Technology*, Noyes Publications, NJ, p. 482

Dean, J. R. (2009) *Extraction Techniques in Analytical Sciences (Dean 2010).pdf*.

'Diagnosis and classification of diabetes mellitus' (2010) *Diabetes Care*. doi: 10.2337/dc10-S062.

De Fátima Alpendurada, M. (2000) 'Solid-phase microextraction: A promising technique for sample preparation in environmental analysis', *Journal of Chromatography A*, 889(1–2), pp. 3–14. doi: 10.1016/S0021-9673(00)00453-2.

Esfarili, A., Yamini, Y., Ghambarian, M., & Ebrahimpour, B. (2012). Automated preconcentration and analysis of organic compounds by on-line hollow fiber liquid-phase microextraction–high performance liquid chromatography. *Journal of Chromatography A*, 1262, 27–33. doi: 10.1016/j.chroma.2012.09.003

Esrafil, A. Baharfar, M., Tajik, M., Yamini, Y., Ghambarian, M. (2018) Two-phase hollow fiber liquid-phase microextraction, *TrAC - Trends in Analytical Chemistry*, 108, pp. 314–322. doi: 10.1016/j.trac.2018.09.015.

Fan, W., HE, M., You, L., Zhu, X., Chen, B., Hu, B. (2016) ‘Water-compatible graphene oxide/molecularly imprinted polymer coated stir bar sorptive extraction of propranolol from urine samples followed by high performance liquid chromatography-ultraviolet detection’, *Journal of Chromatography A*. Elsevier B.V., 1443, pp. 1–9. doi: 10.1016/j.chroma.2016.03.017.

Farajzadeh, M., Nouri, N., (2014) Derivatization and microextraction methods for determination of organic compounds by gas chromatography, *Trends in Analytical Chemistry*, 55, 14-23. doi: 10.1016/j.trac.2013.11.006

Feng, S. Y., Lai, E. P. C., Dabek-Zlotorzynska, E., Sadeghi, S., (2004) ‘Molecularly imprinted solid-phase extraction for the screening of antihyperglycemic biguanides’, *Journal of Chromatography A*, 1027(1–2), pp. 155–160. doi: 10.1016/j.chroma.2003.11.042.

Fernandez, M. A. M., Andre, L. C., Cardeal, Z. L. (2017) Hollow fibre liquid-phase microextraction-gas chromatography-mass spectrometry method to analyze bisphenol A and other plasticizer metabolites. *Journal of Chromatography A*, 1481, 31-36

Food and Drug Administration website. (1995). No Title. Retrieved from April 1, 2016,

Gabr, R. Q., Padwal, R. S. and Brocks, D. R. (2010) ‘Determination of Metformin in Human Plasma and Urine by High- Performance Liquid Chromatography Using Small Sample Volume and Conventional Octadecyl Silane Column’, 13(4), pp. 486–494.

Ganesan, P., Kamaraj, R., Sozhan, G., Vasuvedan, S., (2013) Oxidised multiwalled carbon nanotubes as adsorbent for the removal of manganese from aqueous solution, *Environmental Science and Pollution Research*, 20, 987-996. doi 10.1007/s11356-012-0928-7

Gaona-Gómez, A. and Cheng, C. H. (2012) ‘Modification of zeolite L (LTL) morphology using diols, (OH)  $2(\text{CH}_2)_{2n+2}\text{O}$  ( $n = 0, 1, \text{ and } 2$ )’, *Microporous and Mesoporous Materials*, 153, pp. 227–235. doi: 10.1016/j.micromeso.2011.12.056.

Gavach, C., Mlodnicka, T., Guastalla. J., (1968), *Proceedings of the academy of Sciences*. 266, 1196 (1968). 18.

Ge, D., & Lee, H. K. (2013). Ionic liquid based dispersive liquid–liquid microextraction coupled with micro-solid phase extraction of antidepressant drugs from environmental water samples. *Journal of Chromatography A*, 1317, 217–222. doi: 10.1016/j.chroma.2013.04.014

Georgiță, C., Sora, I., Albu, F., Monciu, C. M., (2010) ‘comparison of a lc/ms method with a lc/uv method for the determination of metformin in plasma samples’, *Farmacia*, 58(2).

Gilart, N. *et al.* (2014) ‘New coatings for stir-bar sorptive extraction of polar emerging

organic contaminants', *TrAC - Trends in Analytical Chemistry*, 54, pp. 11–23. doi: 10.1016/j.trac.2013.10.010.

Gobry, V. *et al.* (2001) 'Generalization of ionic partition diagrams to lipophilic compounds and to biphasic systems with variable phase volume ratios', *Journal of the American Chemical Society*, 123(43), pp. 10684–10690. doi: 10.1021/ja015914f.

González-Fuentes, M. A. *et al.* (2010) 'Electrochemically driven transfer of carboxyl-terminated PAMAM dendrimers at the water/dichloroethane interface', *Electrochemistry Communications*. Elsevier B.V., 12(1), pp. 137–139. doi: 10.1016/j.elecom.2009.11.007.

Guo, L., Lee, H. K. (2011) Development of multiwalled carbon nanotubes based micro- solid-phase extraction for the determination of trace levels of sixteen polycyclic aromatic hydrocarbons in environmental water samples, *Journal of Chromatography A*, 1218, 9321–9327, <http://dx.doi.org/10.1016/j.chroma.2011.10.066>.

Han, Q. *et al.* (2013) 'Graphene as an efficient sorbent for the SPE of organochlorine pesticides in water samples coupled with GC-MS', *Journal of Separation Science*, 36(21–22), pp. 3586–3591. doi: 10.1002/jssc.201300373.

Haque, E., Jun, J. W., & Jhung, S. H. (2011). *Adsorptive removal of methyl orange and methylene blue from aqueous solution with a metal-organic framework material, iron terephthalate (MOF-235)*. *Journal of Hazardous Materials*, 185(1), 507–511. doi: 10.1016/j.jhazmat.2010.09.035

Hardman, J. G., Limbird, L.E., Gilman, A.G., (1996) Goodman & Gilman's—The Pharmacological Basis of Therapeutics, 9th ed., McGraw-Hill, New York

Herzog, G., Flynn, Shane., Johnson, C., Arrigan, D. M. W., . (2012) 'Electroanalytical behavior of poly-L-lysine dendrigrafts at the interface between two immiscible electrolyte solutions', *Analytical Chemistry*. doi: 10.1021/ac300856w.

Herzog, G. (2015) 'Recent developments in electrochemistry at the interface between two immiscible electrolyte solutions for ion sensing', *Analyst*. Royal Society of Chemistry, 140(12), pp. 3888–3896. doi: 10.1039/c5an00601e.

Herzog, G., Kam, V. and Arrigan, D. W. M. (2008) 'Electrochemical behaviour of haemoglobin at the liquid/liquid interface', *Electrochimica Acta*. 53, pp. 7204–7209. doi: 10.1016/j.electacta.2008.04.072.

Hill, A. P. and Young, R. J. (2010) 'Getting physical in drug discovery: A contemporary perspective on solubility and hydrophobicity', *Drug Discovery Today*. Elsevier Ltd, 15(15–16), pp. 648–655. doi: 10.1016/j.drudis.2010.05.016.

Hung, L. Q. *J. Electroanal. Chem.* 1980, 115, 159–174.

Huttunen, K. M. *et al.* (2009) 'Determination of metformin and its prodrugs in human and rat blood by hydrophilic interaction liquid chromatography', *Journal of Pharmaceutical and Biomedical Analysis Journal of Pharmaceutical and Biomedical*, 50, pp. 469–474. doi: 10.1016/j.jpba.2009.04.033.

Ijima, S., (1991) Helical microtubules of graphitic carbon, *Nature*, 354, pp. 56-58

IWATA, T., NAGATANI, H. and OSAKAI, T. (2017) 'Determination of the Electrostatic Potential of Oil-in-Water Emulsion Droplets by Combined Use of Two Membrane Potential-Sensitive Dyes', *Analytical Sciences*, 33(7), pp. 813–819. doi: 10.2116/analsci.33.813.

Jain, R., & Singh, R. (2016). Applications of dispersive liquid-liquid microextraction in forensic toxicology. *TrAC Trends in Analytical Chemistry*, 75, 227–237

Juan, J. J., Fang, F., Ming, M., Xing, Z. Z., (2006) 'Study on a new precolumn derivatization method in the determination of metformin hydrochloride', *Journal of Chromatographic Sciences*, 44, pp 193-199

Karami, M. *et al.* (2017) 'On-chip pulsed electromembrane extraction as a new concept for analysis of biological fluids in a small device', *Journal of Chromatography A*. Elsevier B.V., 1527, pp. 1–9. doi: 10.1016/j.chroma.2017.10.049.

Kanimozhi, S., Basheer, C., Narasimhan, K., Liu, L., Koh, S., Xue, F., Choolani, M., Lee, H. K., (2011) 'Application of porous membrane protected micro-solid-phase-extraction combined with gas chromatography-mass spectrometry for the determination of estrogens in ovarian cyst fluid samples', *Analytica Chimica Acta*. Elsevier B.V., 687(1), pp. 56–60. doi: 10.1016/j.aca.2010.12.007.

Kataoka, H., Lord, H. L. and Pawliszyn, J. (2000) 'Applications of solid - phase microextraction in food analysis', *Journal of Chromatography A*, 880, pp. 35–62. doi: 10.1016/S0021-9673(00)00309-5.

Khezeli, T. and Daneshfar, A. (2017) 'Development of dispersive micro-solid phase extraction based on micro and nano sorbents', *TrAC - Trends in Analytical Chemistry*. Elsevier Ltd, 89, pp. 99–118. doi: 10.1016/j.trac.2017.01.004.

Kimmel, B. and Inzucchi, S. E. (2005) 'Oral Agents for Type 2 Diabetes: An Update', *@bullet clinical diabetes*, 23(64).

Kokosa, J. M., (2015) Recent trends in using single-drop microextraction and related techniques in green analytical methods, *Trends in Analytical Chemistry*, 71, pp. 194-204

Koryta, J. (1983) 'Electrochemical polarization phenomena at the interface of two immiscible electrolyte solutions. II Progress since 1978', *Electrochimica Acta*, 29(4), pp. 445–452.

Koryta, J., Březina, M., Vanýsek. P. (1977) *Journal of Electroanalytical Chemistry*. 75, 211

Kralj, B. and Dryfe, R. A. W. (2002) 'Hydrodynamic voltammetry at the liquid/liquid interface: The rotating diffusion cell', *Journal of Physical Chemistry B*, 106(26), pp. 6732–6739. doi: 10.1021/jp025683e.

Kralj, B. and Dryfe, R. A. W. (2003) 'Hydrodynamic voltammetry at the liquid|liquid interface: Facilitated ion transfer and the rotating diffusion cell', *Journal of*

*Electroanalytical Chemistry*, 560(2), pp. 127–133. doi: 10.1016/j.jelechem.2003.07.024.

Kralj, B. and Dryfe, R. A. W. (2003) ‘The rotating paddle cell’, *Electrochemistry Communications*, 5(4), pp. 325–328. doi: 10.1016/S1388-2481(03)00056-0.

Krishnan, T. R. and Ibrahim, I. (1994) ‘Solid-phase extraction technique for the analysis of biological samples’, *Journal of Pharmaceutical and Biomedical Analysis*. doi: 10.1016/0731-7085(94)90001-9.

Lai, E. P. C. and Feng, S. Y. (2006) ‘Solid phase extraction-Non-aqueous capillary electrophoresis for determination of metformin, phenformin and glyburide in human plasma’, *Journal of Chromatography B: Analytical Technologies in the Biomedical and Life Sciences*, 843(1), pp. 94–99. doi: 10.1016/j.jchromb.2006.05.030.

Langmaier, J. Pizl, M., Samec, Z., Zalis, S., (2016) ‘Extreme Basicity of Biguanide Drugs in Aqueous Solutions: Ion Transfer Voltammetry and DFT Calculations’, *Journal of Physical Chemistry A*. doi: 10.1021/acs.jpca.6b04786.

Lee, H. J., Beattie, P. D., Seddon, B. J., Osborne, M. D., Girault, H. H., (1997) Amperometric ion sensors based on laser-patterned composite polymer membranes, *Journal of Electroanalytical Chemistry*, 440(1–2), 73–82. doi: 10.1016/s0022-0728(97)80042-3.

Lee, T. P., Saad, B., Ng, E. P., Salleh, B., (2012) ‘Zeolite Linde Type L as micro-solid phase extraction sorbent for the high performance liquid chromatography determination of ochratoxin A in coffee and cereal’, *Journal of Chromatography A*. Elsevier B.V., 1237, pp. 46–54. doi: 10.1016/j.chroma.2012.03.031.

Li, Y., Li, L. and Yu, J. (2017) ‘Applications of Zeolites in Sustainable Chemistry’, *Chem*, 3(6), pp. 928–949. doi: 10.1016/j.chempr.2017.10.009.

Liu, A. and Coleman, S. P. (2009) ‘Determination of metformin in human plasma using hydrophilic interaction liquid chromatography-tandem mass spectrometry’, *Journal of Chromatography B: Analytical Technologies in the Biomedical and Life Sciences*. doi: 10.1016/j.jchromb.2009.09.020.

Magiera, S., Hejniak, J. and Baranowski, J. (2014) ‘Comparison of different sorbent materials for solid-phase extraction of selected drugs in human urine analyzed by UHPLC-UV’, *Journal of Chromatography B: Analytical Technologies in the Biomedical and Life Sciences*. Elsevier B.V., 958, pp. 22–28. doi: 10.1016/j.jchromb.2014.03.014.

Makahleh, A., Yap, H. F. and Saad, B. (2015) ‘Vortex-assisted liquid-liquid-liquid microextraction (VALLLME) technique: A new microextraction approach for direct liquid chromatography and capillary electrophoresis analysis’, *Talanta*. Elsevier, 143, pp. 394–401. doi: 10.1016/j.talanta.2015.05.011.

Mcdowall, R. D., Pearce, J. C. and Murkitt, G. S. (1986) ‘Liquid-solid sample preparation in drug analysis’, *Journal of Pharmaceutical & Biomedical Analysis*, 4(1), pp. 3–21.

Mousavi, M. P. S., Kashefolgheta, S., Stein, A., Buhiman, P., (2016) 'Electrochemical stability of quaternary ammonium cations: An experimental and computational study', *Journal of The electrochemical Society*, 163 (2), pp 74-80. doi:10.1149/2.0671602jes

Mullett, W. M. (2007) 'Determination of drugs in biological fluids by direct injection of samples for liquid-chromatographic analysis', *Journal of Biochemical and Biophysical Methods*. doi: 10.1016/j.jbbm.2006.10.001.

Naing, N. N., Li, S. F. Y. and Lee, H. K. (2016) 'Evaluation of graphene-based sorbent in the determination of polar environmental contaminants in water by micro-solid phase extraction-high performance liquid chromatography', *Journal of Chromatography A*. Elsevier B.V., 1427, pp. 29–36. doi: 10.1016/j.chroma.2015.12.012.

Naing, N. N., Yau Li, S. F. and Lee, H. K. (2016) 'Magnetic micro-solid-phase-extraction of polycyclic aromatic hydrocarbons in water', *Journal of Chromatography A*. Elsevier B.V., 1440, pp. 23–30. doi: 10.1016/j.chroma.2016.02.046.

Namera, A. and Saito, T. (2013) 'Advances in monolithic materials for sample preparation in drug and pharmaceutical analysis', *TrAC - Trends in Analytical Chemistry*, 45, pp. 182–196. doi: 10.1016/j.trac.2012.10.017.

Neng, N. R., Silva, A. R. M. and Nogueira, J. M. F. (2010) 'Adsorptive micro-extraction techniques-Novel analytical tools for trace levels of polar solutes in aqueous media', *Journal of Chromatography A*. Elsevier B.V., 1217(47), pp. 7303–7310. doi: 10.1016/j.chroma.2010.09.048.

Nestler, J. E. (2008). Metformin for the Treatment of the Polycystic Ovary Syndrome. *The New England Journal of Medicine*, 358, 47–54. doi: 10.1056/NEJMct0707092.

Nogueira, J. M. F. (2012) 'Novel sorption-based methodologies for static microextraction analysis: A review on SBSE and related techniques', *Analytica Chimica Acta*. Elsevier B.V., 757, pp. 1–10. doi: 10.1016/j.aca.2012.10.033.

Nogueira, J. M. F. (2015) 'Stir-bar sorptive extraction: 15 years making sample preparation more environment-friendly', *TrAC - Trends in Analytical Chemistry*. Elsevier B.V., 71, pp. 214–223. doi: 10.1016/j.trac.2015.05.002.

Nováková, L. and Vlčková, H. (2009) 'A review of current trends and advances in modern bio-analytical methods: Chromatography and sample preparation', *Analytica Chimica Acta*. doi: 10.1016/j.aca.2009.10.004.

Ohta, M., Iwasaki, M., Kai, M., Ohkura, Y., (1993) 'Determination of a biguanide, metformin, by high-performance liquid chromatography with precolumn fluorescence detector', *Analytical Sciences*, 9, pp 217-220

Olaya, A. J., Ge, P. and Girault, H. H. (2012) 'Ion transfer across the water|trifluorotoluene interface', *Electrochemistry Communications*, 19(1), pp. 101–104. doi: 10.1016/j.elecom.2012.03.010.

Pano-Farias, N. S., Ceballos-Magana, S. G., Muniz-Valencia, R., Jurado, J. M., Alcazar, A., Aguayo-Villarreal, I. A., (2017) 'Direct immersion single drop micro-

extraction method for multi-class pesticides analysis in mango using GC–MS', *Food Chemistry*. Elsevier Ltd, 237, pp. 30–38. doi: 10.1016/j.foodchem.2017.05.030.

Partani, P., Modhave, Y., Gurule, S., Khuroo, A., Monif, T., (2009) 'Simultaneous determination of propranolol and 4-hydroxy propranolol in human plasma by solid phase extraction and liquid chromatography/electrospray tandem mass spectrometry', *Journal of Pharmaceutical and Biomedical Analysis*, 50, 966-976

Pavlović, D. M., Babic, S., Horvat, A. J. M., Kastelan-Macan, M., (2007) 'Sample preparation in analysis of pharmaceuticals', *TrAC - Trends in Analytical Chemistry*, 26(11), pp. 1062–1075. doi: 10.1016/j.trac.2007.09.010.

Pawliszyn, J., (2009) Handbook of SPME, *Chemical Industry Press*, Beijing

Pawliszyn, J., Arthur, C. L., (1990). Solid phase microextraction with thermal desorption using fused silica optical fibre. *Analytical Chemistry*, 62 (19), 2145-2148

Pawliszyn, J., & Pedersen-Bjergaard, S. (2006). Analytical Microextraction: Current Status and Future Trends. *Journal of Chromatographic Science*, 44(6), 291–307.

Pawliszyn, J., Zhang, Zhouyan., (1993). Headspace solid-phase microextraction. *Analytical Chemistry*, 65, 1843-1852

Pedersen-Bjergaard, S. and Rasmussen, K. E. (2008) 'Electrical potential can drive liquid-liquid extraction for sample preparation in chromatography', *TrAC - Trends in Analytical Chemistry*, 27(10), pp. 934–941. doi: 10.1016/j.trac.2008.08.005.

Peljo, P. and Girault, H. H. (no date) 'Liquid/Liquid Interfaces, Electrochemistry at'. doi: 10.1002/9780470027318.a5306.pub2.

Plotka-Wasyłka, J., Szczepanska, N., de la Guardia, M., & Namiesnik, J. (2015). Miniaturized solid-phase extraction techniques. *TrAC - Trends in Analytical Chemistry*, 73, 19–38.

Poltorak, L., Sudhölter, E. J. R., de Smet, L. C. P. M., (2017) 'Effect of charge of quaternary ammonium cations on lipophilicity and electroanalytical parameters: Task for ion transfer voltammetry', *Journal of Electroanalytical Chemistry*, 796, pp 66-74, doi: 10.1016/j.jelechem.2017.04.051

Porta, V., Schramm, S. G., Kano, E. K., Koono, E. E., Armando, Y. P., Fukuda, K., Serra, C. H. D. R. S., (2008) 'HPLC-UV determination of metformin in human plasma for application in pharmacokinetics and bioequivalence studies', *Journal of Pharmaceutical and Biomedical Analysis*. doi: 10.1016/j.jpba.2007.10.007.

Poujavid, M. R., rabieh, M., Yousefi, S. R., Jamali, M. R., Rezaee, M., Hosseini, M. H., Sehat, A. A. (2015) Study on column SPE with synthesized graphene oxide and FAAS for determination of trace amount of Co(II) and Ni(II) ions in real samples, *Materials Science and Engineering C*, 47, 114-122

Profiles of drugs substances, excipients and related methodology, Klaus Florey, Academic Press, 1975, Volume 4325

- Quinn, B., Kontturi, K., (2000) 'Aspects of electron transfer at ITIES', *Journal of Electroanalytical Chemistry*, 483, 124-134
- Rahman, M. A., Doe, H., (1997) 'Ion transfer of tetraalkylammonium cations at an interface between frozen aqueous solution and 1,2-dichloroethane', *Journal of Electroanalytical Chemistry*, 424, pp 159-164
- Reymond, F., Steyaert, G., Carrupt, P-A., Testa, B., Girault, H., (1996) 'Ionic partition diagrams: A potential-pH representation', *Journal of the American Chemical Society*, 118(47), pp. 11951–11957. doi: 10.1021/ja962187t.
- Ross, M. S. F., (1977) 'Determination of metformin in biological fluids by derivatization followed by high-performance liquid chromatography', *Journal of Chromatography*, 133, pp 408-411
- Santigosa, E., MasPOCH, S. and Ramos Payán, M. (2019) 'Liquid phase microextraction integrated into a microchip device for the extraction of fluoroquinolones from urine samples', *Microchemical Journal*. Elsevier, 145(October 2018), pp. 280–286. doi: 10.1016/j.microc.2018.10.051.
- Samec, Z., (2004) Electrochemistry at the interface between two immiscible electrolyte solutions, *Pure Applied Chemistry*, 76 (12), 2147-2180
- Samec, Z., Trojánek, A., Langmaier, J., Samcová, E. (2000) *Journal of Electroanalytical Chemistry*. 481
- Sajid, M. (2017) 'Porous membrane protected micro-solid-phase extraction: A review of features, advancements and applications', *Analytica Chimica Acta*. Elsevier Ltd, 965, pp. 36–53. doi: 10.1016/j.aca.2017.02.023.
- Sanchez Vallejo, L. J., Ovejero, J. M., Fernandez, R. A., Dassie, S. A., (2012) 'Simple Ion Transfer at Liquid|Liquid Interfaces', *International Journal of Electrochemistry*, 2012, pp. 1–34. doi: 10.1155/2012/462197.
- Scanlon, M., Electrochemical processes of bio-analytical importance at micro- and nano-liquid | liquid interfaces, Phd Thesis, Tyndall National Institute, University College Cork, 2009
- Scanlon, M. D., Smirnov, E., Stockmann, T. J., Peljo, P., (2018) 'Gold Nanofilms at Liquid-Liquid Interfaces: An Emerging Platform for Redox Electrocatalysis, Nanoplasmonic Sensors, and Electrovariable Optics', *Chemical Reviews*, 118(7), pp. 3722–3751. doi: 10.1021/acs.chemrev.7b00595.
- Scanlon, M. D., Strutwolf, J. and Arrigan, D. W. M. (2010) 'Voltammetric behaviour of biological macromolecules at arrays of aqueous|organogel micro-interfaces', *Physical Chemistry Chemical Physics*, 12(34), pp. 10040–10047. doi: 10.1039/c003323e.
- Scheurer, M., Sacher, F., Brauch, H-J., (2012) 'Occurrence and fate of the antidiabetic drug metformin and its metabolite guanilurea in the environment and during drinking water treatment', *Water Research*, 46(15), pp. 4790–4802. doi: 10.1016/j.watres.2012.06.019.

Senda, M., Kakiuchi, T. and Osakais, T. (1991) Electrochemistry at the interface between two immiscible electrolyte solutions, *Electrochimica Acta*, 36(2), pp. 253–262.

Sengupta, P., Bhaumik, U., Ghosh, A., Sarkar, A. K., Chatterjee, B., Bose, A., Pal, T. K., (2009) 'LC–MS–MS Development and Validation for Simultaneous Quantitation of Metformin, Glimepiride and Pioglitazone in Human Plasma and Its Application to a Bioequivalence Study', *Chromatographia*, 69(11–12), pp. 1243–1250. doi: 10.1365/s10337-009-1056-5.

Sequeiros, R. C. P., Neng, N. R., Portugal, F. C. M., Pinto, M. L., Pires, J., Nogueira, J. M. F., (2011) 'Development and application of stir bar sorptive extraction with polyurethane foams for the determination of testosterone and methenolone in urine matrices', *Journal of Chromatographic Sciences*, 49, 297–302

Shah, P. A. and Shrivastav, P. S. (2018) 'Ion-pair solid phase extraction for the simultaneous separation and quantitation of metformin and canagliflozin in human plasma by LC-MS/MS', *Microchemical Journal*. Elsevier, 143(May), pp. 181–189. doi: 10.1016/j.microc.2018.08.005.

Shi, L., Xie, J., Du, L., (2016) 'Determination of phenformin hydrochloride employing a sensitive fluorescent probe', *Spectrochimica Acta Part A: Molecular and Biomolecular Spectroscopy*, 162, 98–104

Singh, A. K., Kedor-Hackmann, E. R. M., Santoro, M. I. R. M., (2004) 'Enantiomeric separation and quantitative determination of propranolol enantiomers in pharmaceutical preparations by chiral liquid chromatography', *Revista Brasileira de Ciências Farmacêuticas Brazilian Journal of Pharmaceutical Sciences*, 40(3).

Sitko, R., Zawisza, B., Malicka, E. (2013) 'Graphene as a new sorbent in analytical chemistry', *TrAC Trends in Analytical Chemistry*, 5, pp. 33–43. doi: 10.1016/j.trac.2013.05.011

Sørensen, L. K. (2012). Determination of metformin and other biguanides in forensic whole blood samples by hydrophilic interaction liquid chromatography-electrospray tandem mass spectrometry. *Biomedical Chromatography*, 26(1), 1–5.

Spietelun, A., Marcinkowski, L., Guardia, M. D. L., Namiesnik, J., (2013) 'Recent developments and future trends in solid phase microextraction techniques towards green analytical chemistry', *Journal of Chromatography A*, 1321, pp. 1–13. doi: 10.1016/j.chroma.2013.10.030.

Sterne, J. (1957). Du nouveau dans les antidiabétiques. La NN diméthylamine guanyle guanide (N.N.D.G.). *Maroc Med.* (36), 1295–1296

Stockmann, T. J., Montgomery, A. M. and Ding, Z. (2012) 'Determination of alkali metal ion transfers at liquid|liquid interfaces stabilized by a micropipette', *Journal of Electroanalytical Chemistry*. Elsevier B.V., 684, pp. 6–12. doi: 10.1016/j.jelechem.2012.08.013.

Szulgá, J., Introduction to random chaos, 1st Edition, Chapman & Hall, London, UK, 1998

Tache, F., David, V., Farca, A., Medvedovici, A., (2001) 'HPLC-DAD determination of Metformin in human plasma using derivatization with p-nitrobenzoyl chloride in a biphasic system', *Microchemical Journal*. doi: 10.1016/S0026-265X(00)00170-3.

Tahara, K., Yonemoto, A., Yoshiyama, Y., Nakamura, T., Aizawa, M., Fujita, Y., Nishikawa, T. (2006) 'Determination of antihyperglycemic biguanides in serum and urine using a ion-pair solid-phase extraction technique followed by HPLC-UV on a pentafluorophenylpropyl column and on an octadecyl column', *Biomedical Chromatography*, 20, 1200-1205. doi: 10.1002/bmc.685

Tang, S., Qi, T., Ansah, P. D., Fouemina, J. C. N., Shen, W., B, C., Lee, H. K., (2018) *Single-drop microextraction, TrAC - Trends in Analytical Chemistry*. Elsevier B.V. doi: 10.1016/j.trac.2018.09.016.

Teo, H. L., Wong, L., Liu, Q., Teo, T. L., Lee, T. K., Lee, H. K (2016) Simple and accurate measurement of carbamazepine in surface water by use of porous membrane-protected micro-solid-phase extraction coupled with isotope dilution mass spectrometry, *Analytical Chimica Acta*, 912, 49-57, <http://dx.doi.org/10.1016/j.aca.2016.01.028>.

The International Pharmacopoeia, 19th WHO Model List of Essential Medicines, (2015), pp. 1–43, [http://dx.doi.org/10.1016/S1473-3099\(14\)70780-7](http://dx.doi.org/10.1016/S1473-3099(14)70780-7) [Http://www.who.int/medicines/publications/essentialmedicines/en..](http://www.who.int/medicines/publications/essentialmedicines/en..)

Tiselius, A., (1973) *Transaction of Faraday Society*, 33, 524–531.

Tucker, G. *et al.* (1981) 'Metformin kinetics in healthy subjects and in patients with diabetes mellitus.', *British Journal of Clinical Pharmacology*. doi: 10.1111/j.1365-2125.1981.tb01206.x.

Ulmeanu, S. M., Jensen, H., Samec, Z., Bouchard, G., Carrupt, P. A., Girault, H. H. (2002) (*Journal of Electroanalytical Chemistry*, 530 (1–2), 10–15

Vallejo, L. S., Ovejero, J., Fernandez, R., Dassie, S. A., (2012) 'Simple ion transfer at liquid|liquid interfaces', *International Journal of Electrochemistry*, pp 1-34

Vanýsek, P. (1993) 'Analytical applications of electrified interfaces between two immiscible solutions', *Trends in Analytical Chemistry*. doi: 10.1016/0165-9936(93)87026-T.

Vasconcelos, I. and Fernandes, C. (2017) 'Magnetic solid phase extraction for determination of drugs in biological matrices', *TrAC - Trends in Analytical Chemistry*. Elsevier Ltd, 89, pp. 41–52. doi: 10.1016/j.trac.2016.11.011.

Velázquez-Manzanares, M. (2014) 'Fundamentals and Applications in Electrochemistry of Liquid-liquid Interfaces', *Procedia Chemistry*. Elsevier Ltd., 12, pp. 100–107. doi: 10.1016/j.proche.2014.12.047.

Velický, M., Tam, K. Y. and Dryfe, R. A. W. (2012) 'Hydrodynamic voltammetry at the liquid-liquid interface: Application to the transfer of ionised drug molecules', *Journal of Electroanalytical Chemistry*, 683, pp. 94–102. doi: 10.1016/j.jelechem.2012.07.037.

Velický, M., Tam, K. Y. and Dryfe, R. A. W. (2012) 'Permeation of a fully ionized species across a polarized supported liquid membrane', *Analytical Chemistry*, 84(5), pp. 2541–2547. doi: 10.1021/ac300016n.

Velický, M., Tam, K. Y. and Dryfe, R. A. W. (2014) 'Mechanism of ion transfer in supported liquid membrane systems: Electrochemical control over membrane distribution', *Analytical Chemistry*, 86(1), pp. 435–442. doi: 10.1021/ac402328w.

Vičkačkaitė, V. and Padarauskas, A. (2012) 'Ionic liquids in microextraction techniques', *Central European Journal of Chemistry*, 10(3), pp. 652–674. doi: 10.2478/s11532-012-0023-4.

Volkov, A. G. and Markin, V. S. (2004) *Chapter 4 Electric properties of oil/water interfaces*, *Interface Science and Technology*. Elsevier Masson SAS. doi: 10.1016/S1573-4285(04)80006-1.

Vraka, C., Nics, L., Wagner, K-H., Hacker, M., Wadsak, W., Mitterhauser, M., (2017) 'LogP, a yesterday's value?', *Nuclear Medicine and Biology*. Elsevier Inc., 50, pp. 1–10. doi: 10.1016/j.nucmedbio.2017.03.003.

Walle, T., Walle, U. K., Olanoff, L.S., (1985). Quantitative account of propranolol metabolism in urine of normal man, *Drug Metabolism and Disposition*. 13, 204–209

Wandlowski, T., Mareček, V., Samec, Z., (1990) 'Galvani potential scales for water-nitrobenzene and water-1,2-dichloroethane interfaces', *Electrochimica Acta*, 35(7), pp 1173-1175

Wang, X., Wang, Yuan., Qin, Y., Ding, L., Chen, Y., Xie, Fuwei., (2015). Sensitive and selective determination of polycyclic aromatic hydrocarbons in mainstream cigarette smoke using a graphene-coated solid-phase microextraction fibre prior to GC/MS. *Talanta*. 140, 102-108. doi: 10.1016/j.talanta.2015.03.030

Warade, A., Gaikwad, R., Sapkal, R., Sapkal, V., 2011. Simulation of multistage countercurrent liquid-liquid extraction, *Leonardo Journal of Sciences*, pp 79-94

Wu, X., Zhu, B., Lu, L., Huang, W., Pang, D. (2012) 'Optimization of a solid phase extraction and hydrophilic interaction liquid chromatography-tandem mass spectrometry method for the determination of metformin in dietary supplements and herbal medicines', *Food Chemistry*. doi: 10.1016/j.foodchem.2012.01.005.

Wu, X., Hong, H., Liu, X., Guan, W., Meng, L., Ye, Y., Ma, Y. (2013) 'Graphene-dispersive solid-phase extraction of phthalate acid esters from environmental water', *Science of the Total Environment*. Elsevier B.V., 444, pp. 224–230. doi: 10.1016/j.scitotenv.2012.11.060.

Xiao, J, Wang, J., Fan, H., Zhou, Q., Liu, X., (2016) 'Recent advances of adsorbents in solid phase extraction for environmental samples', *International Journal of Environmental Analytical Chemistry*. Taylor & Francis, 96(5), pp. 407–435. doi: 10.1080/03067319.2016.1150459.

Yamamoto, T., Kusama, M., Matsuno, K., Sugiyama, E., Yamada, Y., Iga, T., (2002) 'A new method for determination of buformin in plasma and urine by ion-paired

reversed-phase HPLC with ultraviolet detection', *Biomedical Chromatography*, 16(7), pp. 453–454. doi: 10.1002/bmc.182.

Yamini, Y., Rezazadeh, M. and Seidi, S. (2019) 'Liquid-phase microextraction – The different principles and configurations', *TrAC - Trends in Analytical Chemistry*. Elsevier Ltd, 112, pp. 264–272. doi: 10.1016/j.trac.2018.06.010.

Yang, X-Q., Yang C-X., Yan, X-P., (2013). Zeolite imidazolate framework-8 as sorbent for on-line solid-phase extraction coupled with high-performance liquid chromatography for the determination of tetracyclines in water and milk samples. *Journal of Chromatography A*, 1304, 28–33

Zhang, J., Ding, L., Wen, A., Wu, F., Sun, L., Yang, L., (2009) 'An HPLC-ESI-MS method for the determination of propranolol in human plasma and its application to pharmacokinetic studies', *Asian Journal of Pharmaceutical Sciences*, 4(3), pp. 169–177.

Zhang, J. Wang, Y., Stevens, G. W., Fei, W., (2019) 'A state-of-the-art review on single drop study in liquid–liquid extraction: Experiments and simulations', *Chinese Journal of Chemical Engineering*. doi: 10.1016/j.cjche.2019.03.025.

Zhang, L., Kitazumi, Y. and Kakiuchi, T. (2011) 'Potential-dependent adsorption and transfer of poly(diallyldialkylammonium) ions at the nitrobenzene|water interface', *Langmuir*, 27(21), pp. 13037–13042. doi: 10.1021/la2028077.

Zhou, J., Zeng, P., Sun, J. B., Wang, F. Q., & Zhang, Q. (2013). Application of two-phase hollow fiber liquid phase microextraction coupled with high-performance liquid chromatography for the study of the echinacoside pharmacokinetics in Parkinson's disease rat plasma. *Journal of Pharmaceutical and Biomedical Analysis*, 81-82, 27–33. doi: 10.1016/j.jpba.2013.03.020

Żwir-Ferenc, A. and Biziuk, M. (2006) 'Mechanism of Solid Phase Extraction Process', *Department of Analytical Chemistry, Chemical Faculty, Gdańsk university of Technology*, 15(Solid Phase Extraction Technique – Trends, Opportunities and Applications), pp. 677–69.

## APPENDICES

### 1. Ionic partition diagram

**Line 1.** It corresponds to the equi-concentration of ion in both phases. The Nernst equation became simplified into Eq (i) because the term of  $(\frac{c_i^o}{c_i^w})$  is zero in Nernst equation (Reymond et al, 1999).

$$\Delta_o^w \phi = \Delta_o^w \phi \quad (\text{based on value of Galvani potential transfer at pH 2}) \quad (\text{i})$$

**Line 2.** Connection between line 1, 3 and 4

**Line 3.** (Acid-base equilibria define the boundaries between two ions that have different charge. When the concentration of ionised form in aqueous phase is equal to the neutral form, thus, acid-base equilibria became (Reymond et al, 1999).

$$\text{pH} = \text{p}K_{a1}^w \quad (\text{ii})$$

**Line 4.** It is related to the equilibria that are given by Eq (iii),

$$\Delta_o^w \phi = 2\Delta_o^w \phi'_{I2+} - \Delta_o^w \phi'_{I2+} + \frac{RT \ln 10}{F} (\text{pH} - \text{p}K_{a1}^w) \quad (\text{iii})$$

**Line 5, 6, 7** were still determined by Eq (i), (ii) and (iii), respectively.

**Line 5.**  $\Delta_o^w \phi = \Delta_o^w \phi'_{I+}$  (based on value of Galvani potential transfer at pH 6)

**Line 6.**  $\text{pH} = \text{p}K_{a2}^w$  for MET and PHEBI

$$\text{pH} = \text{p}K_{a2}^w - \log P_o \text{ for PHEN} \quad (\text{iv})$$

**Line 7.**  $\Delta_o^w \phi = \Delta_o^w \phi'_{I+} + \frac{RT \ln 10}{F} (\text{pH} - \text{p}K_{a2}^w)$  for MET and PHEBI

$$\Delta_o^w \phi = \Delta_o^w \phi'_{I+} + \frac{RT \ln 10}{F} (\log P_o - \text{p}K_{a2}^w) + \frac{RT \ln 10}{F} \text{pH} \text{ for PHEN} \quad (\text{v})$$

For ionic partition diagram boundary lines for monocation:

**Line 1.**  $\Delta_o^w \phi = \Delta_o^w \phi'_i$

**Line 2.**  $\Delta_o^w \phi = \Delta_o^w \phi'_{I^+} + \frac{RT \ln 10}{F} (\log P_o - pK_{a2}^w) + \frac{RT \ln 10}{F} pH$

**Line 3.**  $pH = pK_a^w - \log P_o$

## 2. Interfacial potential at equilibrium

To determine the interfacial potential difference at equilibrium,  $\Delta_o^w \phi_{Eq}^{Ext}$ , we need to know the ratio of concentration of an ion in each phase. We used the following calculation to do so.

The mass balance of the ion  $i$ , can be written as Eq. (vi):

$$n_{initial}^i = n_{aq}^i + n_{org}^i \quad (vi)$$

The yield of the extraction is defined by Eq. (vii):

$$Y = \frac{n_{org}^i}{n_{initial}^i} \quad (vii)$$

The number of moles of ions, present in the solution is dependent on pH.

Combining Eqs. 4.12 and 4.13, we can express the concentration of species  $i$  in the aqueous phase,  $C_{aq}^i$ , can be written as Eqs (viii-x)

$$Y = \frac{n_{initial}^i - n_{aq}^i}{n_{initial}^i} \quad (viii)$$

$$n_{aq}^i = n_{initial}^i (1 - Y) \quad (ix)$$

$$C_{aq}^i = n_{initial}^i V_{aq}^i (1 - Y) \quad (x)$$

Similarly, for the concentration of species  $i$  in the organic phase,  $C_{org}^i$ , can be written as follows (Eqs. xi-xiv):

$$n_{org}^i = n_{initial}^i - n_{aq}^i \quad (xi)$$

$$n_{org}^i = n_{initial}^i - n_{initial}^i(1 - Y) \quad (xii)$$

$$n_{org}^i = n_{initial}^i * Y \quad (xiii)$$

$$C_{org}^i = n_{initial}^i V_{org}^i * Y \quad (xiv)$$

### 3. Calibration curves for graphene and zeolite

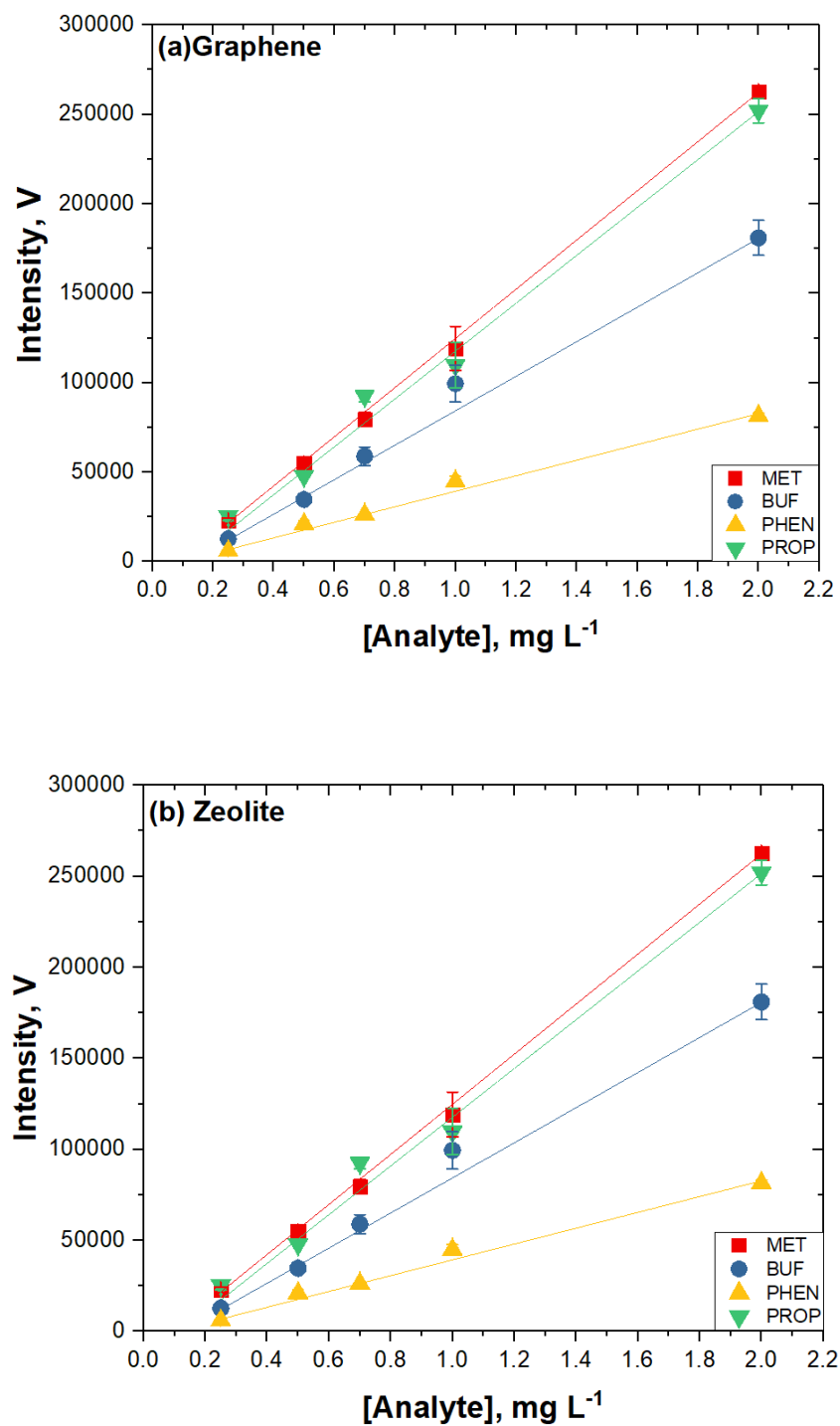


Figure i. Calibration curves plotted for (a) graphene and (b) zeolite.

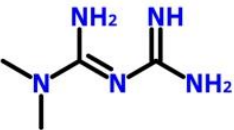
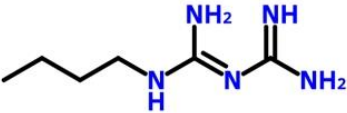
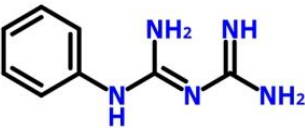
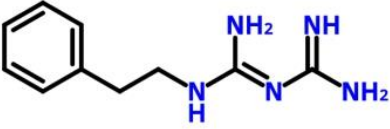
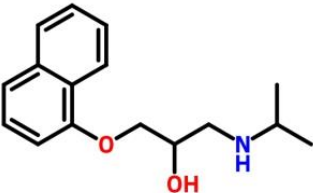
## LIST OF PUBLICATION

Jajuli, M. N., Hussin, M. H., Saad, B., Rahim, A. A., Hebrant, M., Herzog, G., (2019)  
'Electrochemically modulated liquid-liquid extraction for sample enrichment'.  
*Analytical Chemistry*, 91 (11), 7466-7473

## 1. INTRODUCTION

Une méthode d'analyse comporte normalement cinq étapes, soit i) l'échantillonnage, ii) la préparation des échantillons, iii) la séparation, iv) la détection et v) l'analyse des données. Bien que toutes ces étapes soient reliées entre elles, on estime que plus de 80 % du temps d'analyse est consacré à l'échantillonnage et à la préparation des échantillons (Namera et Saito, 2013). Si l'une de ces étapes n'est pas exécutée correctement, il en résultera des erreurs et des résultats incohérents (Pavlovic et al, 2007). Par conséquent, il est important de choisir une méthode de préparation d'échantillons appropriée pour les composés tels que les médicaments pharmaceutiques dans les fluides biologiques. Les composés pharmaceutiques choisis (Tableau 1.1) sont : (i) les biguanides et (ii) le Propranolol. La metformine, la buformine et la phénformine sont des antihyperglycémiants prescrits par voie orale dans la Liste OMS des médicaments essentiels (The International Pharmacopoeia, 2015). 1-isopropylamino-3-(1-naphthoxy)-2-propanol-1 appelé propranolol est l'un des agents  $\beta$ bloquants des récepteurs  $\beta$ -adrénergiques (Hardman et al., 1996).

Tableau 1.1: Structure chimique, pKa, log P<sub>0</sub> pour les composés pharmaceutiques

Biguanide composés	La structure	Log P <sub>0</sub>	pKa
Metformine (MET)		-1.82 <sup>a</sup>	2.80, 11.5 <sup>b</sup>
Buformin (BUF)		-1.20 <sup>c</sup>	12.27 <sup>c</sup>
Phényl bigunide (PHEBI)		-0.03 <sup>a</sup>	2.13, 10.8 <sup>d</sup>
Phénformine (PHEN)		0.41 <sup>a</sup>	2.70, 11.8 <sup>e</sup>
Propranolol (PROP)		3.10 <sup>a</sup>	9.41 <sup>f</sup>

a Calculé à l'aide du logiciel ACD Labs, b (Berduque, *et al.*, 2005) ; c SciFinder ; d (Langmaier *et al.*, 2016) ; e (Florey, 1975) ; f (Szulga, 1998)

L'analyse des composés biguanides est compliquée en raison de leurs propriétés hydrophiles, en particulier pour la MET. Il s'avère plus difficile de déterminer simultanément la nature et la concentration de divers composés, par exemple, la MET hautement polaire lorsqu'un médicament PROP moins polaire doit aussi être déterminé. Le choix de ces médicaments ciblés offre une plage d'hydrophobie avec des valeurs log P (coefficient de partage octanol-eau) allant de -1,82 (MET) à 3,41 (PROP). La compatibilité entre la préparation des échantillons et la séparation est la clé du succès de la méthode analytique. En cas de succès, ce type d'analyse constituerait une application intéressante de

l'extraction liquide-liquide électromodulée ou de la bar- $\mu$ -SPE (microextraction sur phase solide) avec un l'adsorbant mixte. Ainsi, cette thèse est consacrée à ces deux techniques d'extraction. Il est proposé ici de combiner l'extraction liquide-liquide des gouttelettes de phase organique à l'aide d'un champ électrique à l'interface entre deux solutions non miscibles pour préparer les échantillons avant analyse chromatographique. Une nouvelle approche pour l'extraction liquide-liquide dans laquelle le potentiel est imposé par un potentiostat ou obtenu par polarisation chimique (sans potentiostat) est choisie pour la préparation d'échantillons aqueux contenant des analytes cationiques (médicaments à polarité variable). La méthode sans instrument, par polarisation chimique est basée sur le transfert d'ions modulé par l'application d'un potentiel interfacial contrôlé par la distribution d'un ion commun entre les deux phases. La méthode bar- $\mu$ -SPE (c'est une amélioration de la  $\mu$ -SPE originale introduite par Basheer et al. en 2006) a été choisie en raison de ses nombreuses caractéristiques avantageuses telles que la simplicité de mise en œuvre, la rapidité, la réduction significative des quantités de solvants organiques utilisés, en accord avec les principes de la chimie analytique verte. Le dispositif  $\mu$ -SPE a été préparé en plaçant quelques milligrammes de l'adsorbant dans une membrane poreuse thermosoudée. Les adsorbants de la méthode bar- $\mu$ -SPE sont protégés des macromolécules éventuellement présentes dans la matrice de l'échantillon par la membrane car seuls de petits analytes peuvent diffuser. Il faut également souligner que les études antérieures se sont concentrées sur l'extraction d'une seule classe de composés à l'aide d'un adsorbant. La clé du succès de l'extraction de la barre- $\mu$ -SPE est le choix des adsorbants utilisés. En raison de la diversité des polarités des médicaments étudiés ici, il a été imaginé que l'utilisation d'un mélange d'adsorbants aux propriétés de surface contrastées (p. ex. polaires et non polaires) serait la voie à suivre pour atteindre les objectifs.

Les principaux objectifs de cette thèse étaient :

1. Développer l'extraction liquide-liquide modulée électrochimiquement à l'aide d'un potentiostat pour la détermination de la metformine, du phényl biguanide, de la phénformine et du propranolol (Chapitre 3).
2. Développer la préparation d'échantillons basée sur la technique d'extraction liquide-liquide modulée électrochimiquement sans potentiostat pour déterminer la metformine, le phényl biguanide, la phénformine et le propranolol dans les échantillons biologiques (Chapitre 4).
3. Mettre au point une nouvelle méthode à membrane poreuse en bar- $\mu$ -SPE avec divers adsorbants pour déterminer la metformine, la buformine, la phénformine et le propranolol dans des échantillons biologiques (Chapitre 5).

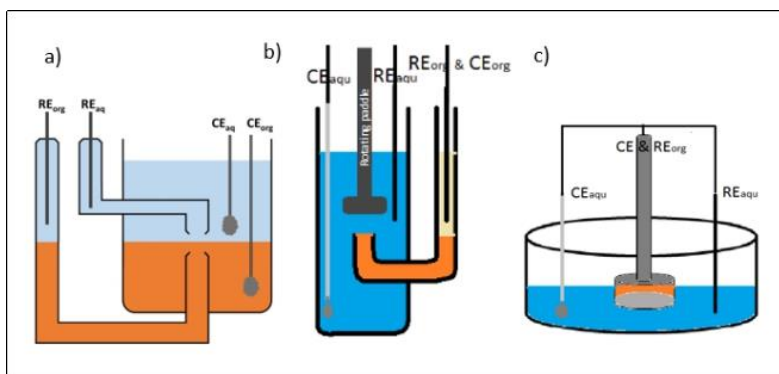
## **2. EXPÉRIMENTAL GÉNÉRAL**

### **2.1 Méthode expérimentale (Chapitres 3 et 4)**

#### **2.1.1 Instrumentation**

##### **2.1.1 a) Voltampérométrie**

Une étude par voltampérométrie cyclique a été effectuée pour décrire les propriétés électrochimiques des composés ciblés. Le potentiostat Emstat3 (Palm Sens - Pays-Bas) qui fonctionnait en mode quatre électrodes a été utilisé. La cellule électrochimique a été mise en place comme le montre la graphique 2.1. Une cellule en verre borosilicaté sur mesure (Ainterface = 1,10 cm<sup>2</sup>) a été utilisée pour accueillir le système biphasique. Chaque phase de la cellule contenait une contre-électrode en platine (Pt) et une électrode de référence Ag/AgCl. La différence de potentiel interfaciale a été mesurée entre les deux électrodes de référence et la variation de courant liée au transfert de charge à travers l'interface liquide-liquide a été enregistrée par des contre électrodes. Trois types de cellules ont été étudiés : 1) cellule statique ITIES, 2) palette rotative dans la cellule statique ITIES, 3) électrode à disque rotatif avec polyéthylène téréphtalate, (PET) membrane supportée ITIES comme indiqué ci-dessous.



Graphique 2.1: Cellules électrochimiques sur mesure a) Cellule ITIES statique b) Palette rotative dans la cellule ITIES c) Electrode à disque rotatif avec membrane PET supportée ITIES pour études de transfert d'ions. REorg : Électrode de référence pour la phase organique ; REaq : Électrode de référence pour la phase aqueuse ; CEaq : Contre électrode pour la phase aqueuse ; CEorg : Contre électrode pour la phase organique.

### 2.1.2(b) Chromatographie liquide à haute performance - Détection UV-vis

Les expériences chromatographiques ont été réalisées à l'aide d'une colonne Agilent Zorbax TMS (C1) 5  $\mu\text{m}$ , 80  $\text{\AA}$ , 4,6 x 250 mm. La phase mobile consistait en un tampon phosphate (pH 6,2) avec 20 mM de phosphate monobasique de sodium monohydraté : acétonitrile : triméthylamine (50:50:0,2). Le dispositif utilisé était Shimadzu LC-20AD. Le débit de la phase mobile en condition isocratique était de 1,3  $\text{mL min}^{-1}$  à 37°C. La température est contrôlée avec le thermostat Colora Messtechnik GMBH. Le volume d'injection était de 20  $\mu\text{L}$ . La détection a été effectuée à  $\lambda = 230 \text{ nm}$  à l'aide d'un SPD-20 A de Shimadzu.

## 2.2 Méthode expérimentale II (Chapitre 5)

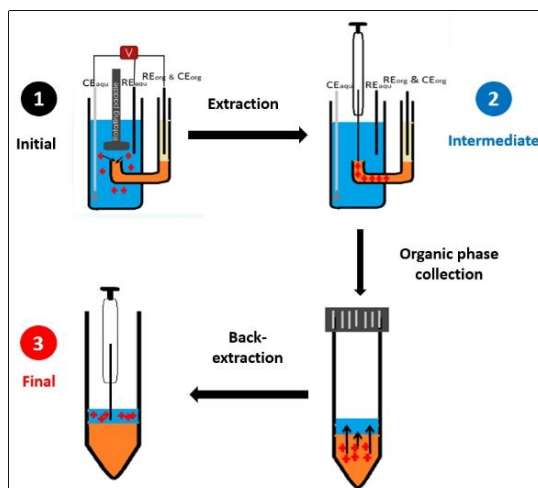
### 2.3.1 Instrumentation

Un système CLHP, modèle Alliance 2695, a été obtenu de Waters (Milford, MA, USA). L'instrument était équipé d'un détecteur à réseau de photodiodes (modèle DAD numéro 2998) réglé à 230 nm. La séparation a été effectuée à l'aide de la colonne ODS-3 Hypersil<sup>TM</sup> C18 (4,6 x 250 mm, 5  $\mu\text{m}$ ) et de la colonne Agilent Zorbax TMS C1 (5  $\mu\text{m}$ , 80  $\text{\AA}$ , 4,6 x 250 mm). Les composés ciblés ont été séparés par un mélange d'acétonitrile : tampon phosphate (pH 6,2, contenant 20 mM de monophosphate de sodium monobasique) : triéthylamine (45:55:0,2, v/v). L'élution isocratique à un débit de 1,3  $\text{mL min}^{-1}$  a été utilisée. Le volume d'injection était de 20  $\mu\text{L}$ .

## 3. EXTRACTION LIQUIDE-LIQUIDE ÉLECTROCHIMIQUEMENT MODULÉE BASÉE SUR LA MÉTHODE POTENTIOSTATIQUE

### 3.1 Stratégie expérimentale

Premièrement, la détermination du potentiel de transfert a été effectuée par voltampérométrie cyclique à l'aide de trois types de cellules ITIES (Graphique 2.1). Ensuite, l'extraction a été réalisée en utilisant 10 mM LiCl comme phase aqueuse et du 1,2- DCE contenant du  $\text{BTPPA}^+\text{TPBCl}^-$  dans cellule ITIES équipée de la palette rotative (Graphique 3.1). Le rendement de l'extraction a été optimisé en étudiant : i) l'effet de la rétro-extraction et ii) l'effet du temps d'attente après extraction.

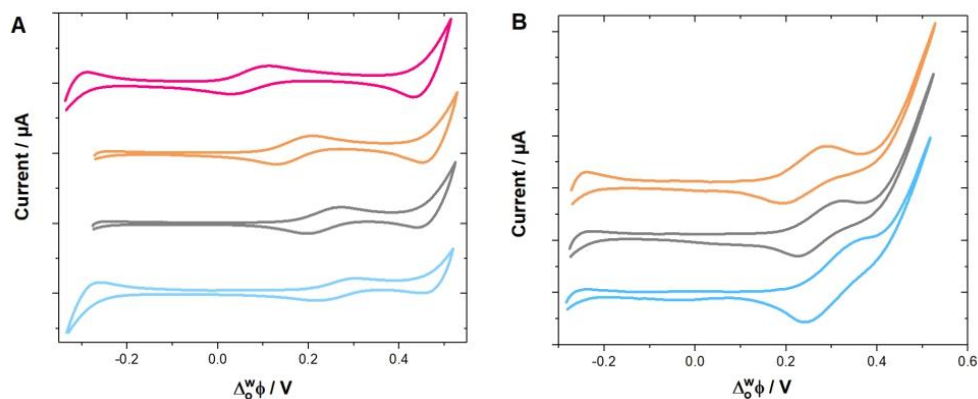


Graphique 3.1: Procédé expérimental d'extraction liquide-liquide à modulation électrochimique. Les cations cibles sont extraits de l'échantillon aqueux vers la phase organique avant d'être ré-extraits vers une phase aqueuse finale. Les chiffres 1, 2 et 3 correspondent aux étapes initiales, intermédiaires et finales auxquelles les phases aqueuses sont analysées par CLHP.

### 3.2 Résultats et discussion

#### 3.2.1 Étude de voltampérométrie cyclique des composés ciblés

La graphique 3.2 montre un transfert d'ions réversible et le voltammogramme a été tracé à l'échelle des potentiels galvaniques. L'ajout d'analytes chargés positivement à la phase aqueuse de chlorure de lithium a entraîné un pic positif lors du balayage vers l'avant en raison du transfert des analytes de la phase aqueuse à la phase organique. Le pic négatif sur le balayage inverse représente le rétro-transfert des analytes de la phase organique à la phase aqueuse. Le potentiel de transfert du médicament a suivi la même tendance lorsque le pH de la phase aqueuse a été fixé à pH 2, comme le montre la graphique 3.4B. Le potentiel de transfert des cations augmente avec leur nature hydrophile. Toutes les valeurs sont indiquées dans le tableau 3.1.



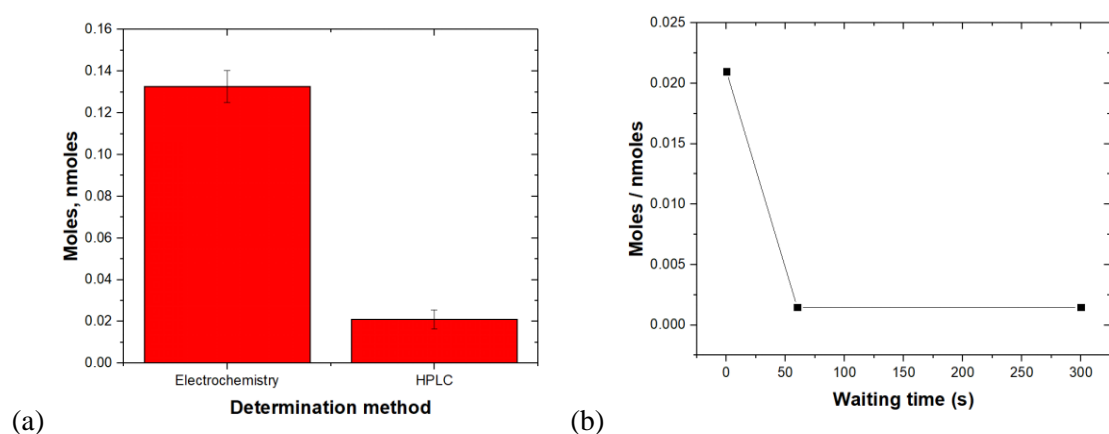
Graphique 3.2: Voltammogrammes cycliques de 170  $\mu\text{M}$  MET (courbe bleue), PHEBI (courbe grise), PHEN (courbe orange) et PROP (courbe rose). a) pH 6 b) pH 2. Conditions expérimentales : Phase aqueuse : 10 mM LiCl. pH de la phase aqueuse: 6. Phase organique: 10 mM de BTTPA<sup>+</sup> TPBCl<sup>-</sup> en 1,2-DCE. Fréquence de balayage : 5  $\text{mV s}^{-1}$ . Cellule : Cellule ITIES statique

#### 3.2.2 Extraction électrochimique comme préparation des échantillons

La procédure de préconcentration comporte deux étapes, comme l'illustre la graphique 3.1, consiste à (i) extraire l'analyte d'une phase aqueuse à une phase organique intermédiaire et (ii) extraire l'analyte de la phase organique intermédiaire à la phase aqueuse finale. Nombre de charges totales,  $Q$  a été obtenu pendant la chronoampérométrie. Ainsi, le nombre de moles extraites en phase organique au stade 2 peut être calculé selon la constante de la loi de Faraday,

$$Q = zNF \quad (3.1)$$

Où  $z$  est le transfert de charge de l'analyte,  $N$  est le nombre de moles,  $F$  est la constante de Faraday dans  $96\,485\text{ C mol}^{-1}$ . Pendant ce temps, l'analyse CLHP à l'étape 3 a donné des informations sur le nombre de moles extraites. L'efficacité d'extraction peut être calculée en comparant le nombre initial de moles avec le nombre final de moles. En utilisant cette formule, la comparaison entre le nombre de moles extraites calculé sur la base de la chronoampérométrie et le nombre de moles injectées dans la CLHP peut être faite (Collins et al, 2008). D'après la CLHP, le nombre de mole transféré n'est que de  $2,10 \times 10^{-10}$  mole, alors que le nombre de mole transférés était de  $1,33 \times 10^{-9}$  mol sur la base de la chronoampérométrie, comme le montre la graphique 3.3a. La graphique 3.3b montre le nombre de mole transféré mesuré par CLHP en fonction du temps d'attente après fin d'application du potentiel pour prélever la phase organique. Lorsque la phase organique a été collectée dès que le potentiel a été coupé, 0,02 nmol ont été collectés. Si l'attente était de 60 s ou 300 s, le nombre de moles détectées tombait à 0, ce qui démontre que le MET extrait revenait spontanément dans la phase aqueuse. De tels résultats indiquent que la phase organique doit être collectée lorsque la différence de potentiel interfacial reste appliquée.



Graphique 3.3: (a) Graphique des grains de beauté extraits par rapport à l'étape de rétro-extraction. (b) Graphique des grains de beauté détectés par CLHP par rapport au temps d'attente après extraction.

**Conclusion :** Cette technique doit être améliorée pour obtenir une bonne efficacité d'extraction et un bon facteur d'enrichissement. Comme il est prouvé que la perte de rendement de l'extraction de l'analyte n'est pas due à l'étape de rétro-extraction, il faudra à l'avenir étudier d'autres types de cellules. Une autre façon est d'introduire une nouvelle méthode, qui utilise le gradient de concentration d'un ion commun entre deux phases pour imposer un potentiel interfacial pour extraire le composé visé.

## 4. EXTRACTION LIQUIDE-LIQUIDE À MODULATION ÉLECTROCHIMIQUE BASÉE SUR LA MÉTHODE SANS POTENTIOSTATIQUE

### 4.1 Stratégie expérimentale

Le transfert de chaque analyte a été déterminé par voltampérométrie. Dans cette section, les médicaments ciblés ont été extraits à travers l'interface en imposant la différence de potentiel interfaciale grâce à un gradient de concentration d'ion commun, ici le tétraméthylammonium ( $\text{TMA}^+$ ) entre les deux phases. Ainsi, les sels  $\text{TMA}^+\text{Cl}^-$  et  $\text{TMA}^+\text{TPBCl}^-$  ont été dissous respectivement dans la phase aqueuse et la phase organique pour contrôler la différence de potentiel interfacial,  $\Delta\phi_o^w$ .

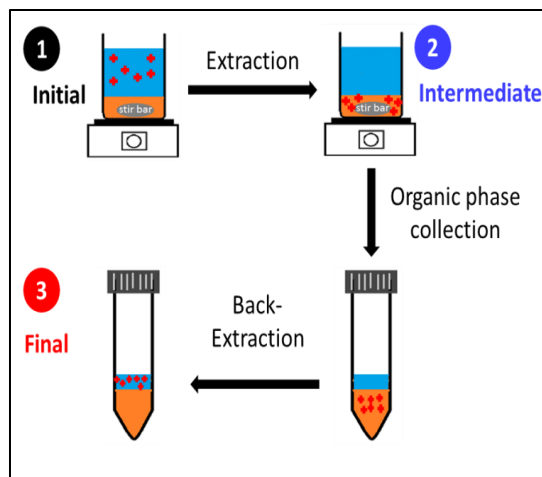
### 4.2 Résultats et discussion

#### 4.2.1 Mécanisme de préconcentration

Le  $\text{TMA}^+$  a été choisi comme ion commun dans les phases aqueuse et organique pour établir la différence de potentiel interfacial,  $\Delta\phi_o^w$  selon l'équation pseudo-Nernst (Eq. 4.1).

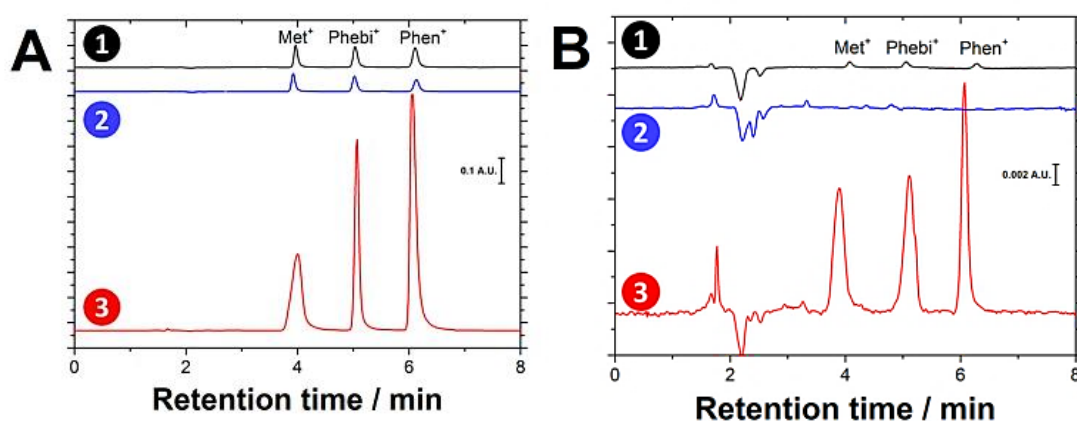
$$\Delta_o^w \phi = \Delta_o^w \phi_{TMA^+}^{0'} + \frac{RT}{zF} \ln \frac{[TMA^+]_o}{[TMA^+]_w} \quad (4.1)$$

$\Delta_o^w \phi_{TMA^+}^{0'}$  est le potentiel de transfert formel du  $TMA^+$  entre le 1,2-DCE (-0,182 V) et l'eau (Wandlowski et al, 1990), et  $[TMA^+]_o$  et  $[TMA^+]_w$  sont les concentrations de  $TMA^+$  dans les phases organique et aqueuse. Le protocole est illustré à la graphique 4.2.



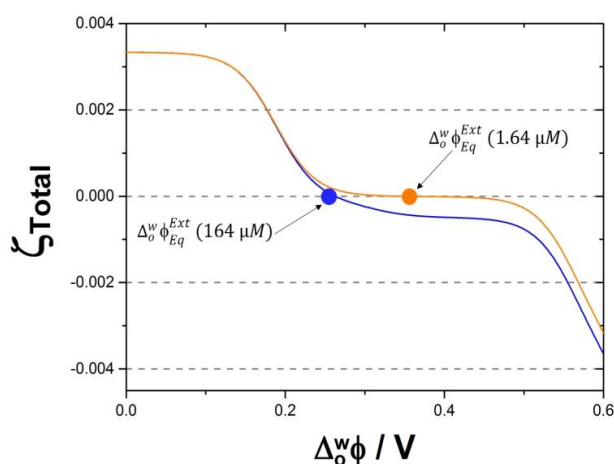
Graphique 4.2: Procédure d'extraction liquide-liquide à modulation électrochimique par gradient de concentration d'ion commun. Les cations cibles sont extraits de l'échantillon aqueux vers la phase organique avant d'être ré-extraits vers une phase aqueuse finale. Les chiffres 1, 2 et 3 correspondent aux étapes initiales, intermédiaires et finales auxquelles les phases aqueuses sont analysées par CLHP.

Les chromatogrammes avant et après l'extraction sont présentés à la graphique 4.3 pour un ensemble donné de paramètres d'extraction. Le premier échantillon analysé contenait du MET, du PHEBI et du PHEN (164  $\mu$ M chacun) et 1  $\mu$ M de  $TMA^+$ . La solution organique utilisée pour l'extraction contenait 10 mM de  $TMA^+TPBCl^-$ . Sur la base de ces concentrations de  $TMA^+$ , la valeur initiale de  $\Delta_o^w \phi$  était de +0,392 V, ce qui devrait être suffisant pour extraire 100 % des trois ions cibles, sur une base thermodynamique. Toutefois, l'extraction est beaucoup plus faible que prévu : 27 % pour le MET, 44 % pour le PHEBI et 76 % pour le PHEN (Figure 4.3A). Lorsque la concentration initiale du médicament est réduite à 1,64  $\mu$ M, l'efficacité d'extraction augmente à 84,2 % pour le MET, 100 % pour le PHEBI et 100 % pour le PHEN, bien que les mêmes conditions d'extraction aient été utilisées (figure 4.3B).



Graphique 4.3 Chromatogrammes obtenus pour un échantillon contenant MET, PHEBI et PHEN à (A) 164  $\mu$ M chacun et à (B) 1,64  $\mu$ M chacun avant (1) et après (2) extraction, en phase aqueuse de contre-extraction (3). Les conditions d'extraction étaient les suivantes :  $[TMA^+]_o = 10$  mM,  $[TMA^+]_w = 0,001$  mM, pH 11,  $V_{DCE} = 2$  mL, vitesse de rotation = 900 rpm, temps = 15 min

Cette variation de l'efficacité d'extraction est liée au mécanisme de transfert d'ions qui doit respecter le principe d'électroneutralité. L'extraction d'une mole de cation de l'échantillon doit être compensée par le transfert d'une mole d'un autre ion (soit un anion de l'échantillon à la phase organique ou un cation de la phase organique à l'échantillon). Lors du transfert de médicaments cationiques, le coût énergétique le plus faible en termes de co-transfert est le transfert de  $\text{TMA}^+$  de la phase organique à l'échantillon. Cet équilibre de charge entraîne une variation de la différence de potentiel interfaciale, qui se produit au fur et à mesure que les ions cibles sont extraits. Le potentiel interfacial ne peut pas être calculé comme s'il y avait en présence d'un seul ion commun. Tous les ions susceptibles de transférer contribuent à la différence de potentiel interfacial. Nous avons donc utilisé la théorie développée dans les années 80 par Hung pour calculer la différence de potentiel galvanique à l'équilibre,  $\Delta_o^w \phi_{Eq}^{Ext}$  (Hung, 1980; Iwata et al., 2017). La graphique 4.4 montre la variation de  $\zeta_{total}$  en fonction de la différence de potentiel interfacial. La différence de potentiel galvanique à l'équilibre,  $\Delta_o^w \phi_{Eq}^{Ext}$ , est atteinte lorsque  $\zeta_{total} = 0$ . Le décalage de  $\Delta_o^w \phi_{Eq}^{Ext}$  en fonction des concentrations initiales du médicament est visible sur la figure 4.4. La plus grande valeur à faible 1.64  $\mu\text{M}$  qu'à 164  $\mu\text{M}$  confirme la tendance observée expérimentalement où l'efficacité d'extraction était plus grande lorsque la concentration initiale diminuait.



Graphique 4.4: Dépendance à l'égard du  $\zeta_{total}$  en fonction de la différence de potentiel interfacial,  $\Delta_o^w \phi$ , pour les conditions d'extraction de la figure 4.3.

#### 4.2.2 Optimisation des paramètres

Divers paramètres (concentration de l'analyte, concentration d'ions communs à l'échantillon et à la phase organique, volume de la phase organique, pH, vitesse de rotation et temps d'extraction) ont été étudiés pour améliorer le rendement d'extraction des trois médicaments. Les paramètres optimisés de l'extraction sont les suivants:  $[\text{TMA}^+]_o = 10 \text{ mM}$ ,  $[\text{TMA}^+]_w = 0,001 \text{ mM}$ ,  $V_{org} = 2 \text{ mL}$ ,  $\text{pH}_{sample} = 9$ , vitesse de rotation = 900 tr/min, temps d'extraction = 600 s. Les paramètres optimisés pour la contre-extraction sont :  $[\text{TMA}^+]_{des} = 50 \text{ mM}$ ,  $V_{final} = 0.1 \text{ mL}$ ,  $\text{pH}_{des} = 2$ .

#### 4.2.3 Méthode de validation

Dans des conditions optimales, la courbe d'étalonnage montre une plage linéaire avec des valeurs  $R^2$  comprises entre 0,9987 et 0,9999. La LD et la LQ pour MET sont améliorées d'un facteur 50, tandis que l'amélioration est plus faible pour PHEBI (facteur 10) et PHEN (facteur 7), ce qui prouve que la méthode est appropriée pour l'enrichissement des échantillons d'analytes cibles polaires. Un analyte moins polaire tel que PROP ne convient pas car la valeur du facteur d'enrichissement n'est que de 1,6. Les essais interjournaliers et intrajournaliers ont montré une précision globale d'environ 7 % (Tableau 4.1).

Tableau 4.1: Paramètres analytiques de la méthode proposée pour MET, PHEBI et PHEN

Développement de méthodes		Analytes		
		MET	PHEBI	PHEN
Avec enrichissement d'échantillon	Sensibilité / $\text{mV s } \mu\text{M}^{-1}$	0.094	0.103	0.102
	$R^2$	0.9999	0.9987	0.9988
	Interception / $\text{mV s}$	-0.0008	-0.0031	0.0002
	LOD / $\mu\text{M}$	0.017	0.068	0.066
	LOQ / $\mu\text{M}$	0.058	0.227	0.222
	Précision / %	6.84	6.79	6.89
Échantillon sans enrichissement	Sensibilité / $\text{mV s } \mu\text{M}^{-1}$	0.0022	0.0022	0.0024
	$R^2$	0.9991	0.9994	0.9998
	Interception / $\text{mV s}$	4.577E-5	2.156E-5	3.648E-5
	LOD / $\mu\text{M}$	0.903	0.727	0.438
	LOQ / $\mu\text{M}$	3.001	2.422	1.459

L'utilité analytique de la méthode mise au point a été étudiée en analysant des échantillons d'urine. Les chromatogrammes montrent clairement que les médicaments ciblés ont pu être déterminés de façon sélective sans interférence avec les composants matriciels de ces échantillons. Les facteurs d'enrichissement étaient de 49,5 pour le MET, 59,5 pour le PHEBI et 58,0 pour le PHEN, ce qui est très proche des facteurs d'enrichissement obtenus pour les solutions aqueuses de laboratoire.

**Conclusion :** Un rendement d'extraction intéressant a été obtenu pour les quatre médicaments, notamment pour la MET, la plus hydrophile, la plus difficile à extraire pour laquelle les méthodes disponibles sur le marché se sont avérées infructueuses dans la plupart des cas. L'amélioration des performances analytiques obtenues en termes de sensibilité, de limites de détection et de quantification, et de précision est une promesse de l'application de cette méthode à une plus large gamme d'analytes hydrophiles et d'échantillons naturels.

## 5. LE GRAPHÈNE ET LA ZÉOLITE COMME ADSORBANTS DANS LA MICROEXTRACTION EN PHASE SOLIDE POUR LA DÉTERMINATION HPLC DE COMPOSÉS PHARMACEUTIQUES SÉLECTIONNÉS

### 5.1 Méthodologie

Le dispositif d'extraction à bar- $\mu$ -SPE a été réalisé selon la littérature (Alshishani et al., 2019) avec de légères modifications. Tout d'abord, la membrane en polypropylène (PP) a été coupée (2,4 x 1,8 cm), pliée en deux et thermosoudée des deux côtés. Ensuite, l'adsorbant (20 mg) a été placé par le bord ouvert. Ensuite, un morceau de tige métallique (diamètre 1 mm ; longueur 1,1 cm) a également été introduit et le bord ouvert a été complètement thermosoudé. La tige métallique minuscule a fonctionné comme une barre magnétique elle-même. Enfin, le sachet à membrane en PP a été plié en deux et thermosoudé à nouveau. La taille du sac préparé était de 1,5 cm x 0,4 cm. Ce sachet à membrane en PP est estampé en tant qu'appareil bar- $\mu$ -SPE. L'appareil a été immergé dans de l'acétonitrile et soniqué pendant 5 minutes avant son utilisation. Le dispositif bar- $\mu$ -SPE a été nettoyé par trempage dans de l'acétonitrile pendant 5 minutes et laissé en place pendant 2 minutes. L'appareil a ensuite été immergé dans une solution d'échantillon de 20 mL qui a été agitée (800 tr/min) pendant 60 minutes pour le processus d'extraction. Ensuite, l'appareil a été retiré de la solution d'échantillon, lavé à l'eau et séché avec du papier de soie non pelucheux. L'appareil a été placé dans un tube de centrifugation contenant de l'acétonitrile comme solvant de contre-extraction. Le processus de désorption s'est fait par sonication de l'appareil pendant 30 minutes. Enfin, 20  $\mu\text{L}$  de l'extrait ont été injectés directement dans l'unité CLHP.

## 5.2 Résultats et discussion

### 5.2.2 Type d'adsorbants

Le succès de la bar- $\mu$ -SPE repose sur le choix de l'adsorbant. Ainsi, plusieurs adsorbants commerciaux (Si-CH<sub>3</sub>, Si-CN, Si-NH<sub>2</sub>, SiO<sub>2</sub>, zéolite, Si-C<sub>18</sub> et graphène) ont été testés en plaçant 20 mg de ces adsorbants de dans le dispositif. L'extraction la plus élevée parmi les adsorbants testés a été obtenue en utilisant de la zéolite et du graphène comme adsorbants.

### 5.2.2 Optimisation des paramètres d'extraction et de contre-extraction pour les adsorbants simples et mixtes

Les conditions adoptées sont énumérées dans le tableau 5.1. Dans ces conditions, le pourcentage d'EE utilisant du graphène était : MET (13,9 %), BUF (15,3 %), PHEN (5,03 %) et PROP (9,13 %). Le % d'EE a été calculé à partir de la surface de pic obtenue par CLHP. L'équation est la suivante :

$$\% EE = [(P_{finale} - P_{initial}) / P_{initial}] \times 100 \quad (5.1)$$

où  $P_{initial}$  est la surface de pic d'origine (standard) et  $P_{finale}$  est la surface de pic après désorption.

Pour la zéolithe, le % EE était : MET (7,57 %), BUF (17,0 %), PHEN (28,8 %) et PROP (39,2 %). Dans les conditions optimales, les facteurs d'enrichissement (FE) pour le graphène était : 4,42, 4,76, 1,49 et 1,71 pour MET, BUF, PHEN et PROP, respectivement, tandis que pour les zéolithes le sont: 3,07, 7,12, 11,5 et 14,9, respectivement. Des mélanges de graphène et de zéolite comme adsorbant ont ensuite été mis à l'essai afin d'améliorer l'extraction pour les médicaments qui ne sont pas bien extraits lorsqu'un seul adsorbant est utilisé (p. ex. pour PHEN et PROP lorsqu'on utilise du graphène et MET lorsque la zéolite est utilisée pour extraire).

Tableau 5.1: Résumé des conditions adoptées pour la méthode bar- $\mu$ -SPE-HPLC utilisant du graphène et de la zéolite comme adsorbants.

Conditions	Graphène	Zéolithe	Zéolithe: Graphène
Solvant de conditionnement	ACN	ACN	ACN
pH de l'échantillon	10	3	6
Volume de l'échantillon (mL)	10	10	10
Quantité d'adsorbant (mg)	10	25	7:3
Vitesse de rotation (tr/min)	800	800	800
Temps d'extraction (min)	90	120	120
% NaCl	0	0	0
Solvant de désorption	0.1 M IP in IPA	0.1 M IP in ACN	7: 3 (ACN: IPA) + 0.1 M IP
Temps de désorption (min)	30	30	30
Volume du solvant de désorption (mL)	0.6	0.6	0.6

### 5.2.3 Validation des méthodes

La validation de la méthode a été effectuée par dopage d'échantillons d'urine sans drogue (l'analyse à blanc a été effectuée avant dopage) en utilisant un adsorbant simple ou mixte. Pour les adsorbants simples, la méthode proposée utilisant le graphène comme adsorbant montre une large gamme de plages linéaires avec  $R^2$  allant de 0,9870 à 0,9971. La LD et la LQ obtenues se situaient respectivement dans la plage (126-269  $\mu\text{g L}^{-1}$ ) et (420-896  $\mu\text{g L}^{-1}$ ). Pour la zéolithe, la courbe d'étalonnage de 30 à 1000  $\mu\text{g L}^{-1}$  avait un  $R^2 > 0,9924$ . La LD calculée variait de 62,2 à 126  $\mu\text{g L}^{-1}$  et la LD de 207 à 422  $\mu\text{g L}^{-1}$ . Pour les adsorbants mixtes, tous les analytes étaient bien corrélés ( $R^2 > 0,99$ ). Le tableau 5.2 énumère les paramètres analytiques, la précision et la récupération obtenus pour l'adsorbant mixte.

Tableau 5.2: Paramètres analytiques de la méthode CLHP à l'aide d'un adsorbant mixte pour la méthode bar- $\mu$ SPE-HPLC

Développement de méthodes	Analytes			
	MET	BUF	PHEN	PROP
Plage de linéarité, $\mu\text{g L}^{-1}$	17-1000	17-1000	30-1000	50-1000
$R^2$	0.9993	0.9960	0.9937	0.9942
LOD, $\mu\text{g L}^{-1}$	33.7	82.5	107	106
LOQ, $\mu\text{g L}^{-1}$	112	275	357	355
Précision, % RSD	4.99-8.28	6.27-8.87	5.73-9.01	5.87-9.12
Taux de recuperation, %	75.1-85.4	72.8-84.6	109-116	97.0-116

**Conclusion :** Une nouvelle technique de bar- $\mu$ -SPE avec adsorbant mixte (graphène et zéolite) pour l'extraction de composés polaires et non polaires a été développée. L'utilisation d'un seul sac en PP a été jugée satisfaisante. Les extraits sont compatibles avec la CLHP et peuvent donc être analysés directement. Toutefois, la sensibilité de la méthode n'est pas aussi bonne que celle des autres méthodes.

## 6. CONCLUSION GÉNÉRALE ET RECOMMANDATIONS FUTURES

### 6.1 Conclusion

La technique EMLLE est basée sur le transfert de masse d'analytes d'intérêt par l'application d'une différence de potentiel entre ITIES. L'application du champ électrique peut se faire soit avec un potentiostat soit par un gradient de concentration d'un ion commun dans les deux phases. Lorsqu'un potentiel fixe a été appliqué au système biphasique à l'aide d'un potentiostat pendant 15 minutes pour extraire les médicaments cationiques, la comparaison du nombre de moles extraites avec le nombre de moles détectées a montré une perte de 84,2 % d'analytes. La perte se situe au niveau de la collecte de la phase organique après extraction sous potentiel. La collecte doit se faire sous potentiel appliqué pour empêcher que les drogues extraites ne soient désextraites spontanément. Ce travail devra être poursuivi avec une cellule électrochimique au design optimisé.

Un gradient de concentration de l'ion tétraméthylammonium entre les deux phases est capable de créer un potentiel dans le système biphasique sans potentiostat. L'utilisation de 0,001 mM TMA<sup>+</sup> en milieu aqueux et de 10 mM TMA<sup>+</sup> en DCE permet d'imposer le potentiel suffisant à l'extraction complète des médicaments cationiques sur l'interface. En utilisant des conditions optimales, les médicaments cationiques biguanidiques ont été extraits à près de 100 % et presque enrichis 60 fois. Le PROP est bien extrait, mais mal désextrait en raison de sa hydrophobie. De plus, nous avons démontré que cette méthode peut être appliquée aux échantillons d'urine.

La deuxième méthode de préparation des échantillons que nous avons évalués a été le développement du bar- $\mu$ -SPE. Parmi plusieurs adsorbants étudiés, des résultats prometteurs ont été obtenus avec du graphène et de la zéolite. Le graphène a été étudié en raison de sa très grande surface spécifique, tandis que la zéolite a le potentiel d'agir comme tamis moléculaire pour piéger les analytes ciblés. Pour augmenter leur capacité d'extraction, un mélange de graphène et de zéolite a été utilisé comme adsorbant dans le sac PP. L'utilisation de mélanges adsorbants, après les optimisations, améliore l'extraction du MET mais pas les autres. L'extraction est également améliorée par rapport à celle du graphène. L'EF pour tous les adsorbants est compris entre 1,49 et 14,9, ce qui est typique pour les adsorbants solides.

Entre les deux approches de préparation de l'échantillon, l'EMLLE est supérieure à la méthode LOD est significativement inférieure à celle obtenue avec la méthode bar- $\mu$ -SPE. Le temps d'analyse est également plus court et ne nécessite aucun réactif IP. De plus, la sélectivité peut être réglée en fonction du transfert de potentiel appliqué.

## ABSTRACT

Conventional sample preparation methods for the determination of polar compounds such as liquid-liquid extraction (LLE) and solid phase extraction (SPE) are generally not effective because of their multiple steps, low recovery and high consumption of organic solvents. Thus, this thesis deals with the development of new sample preparation methods, i.e., electrochemically modulated liquid-liquid extraction (EMLLE) and bar-micro solid phase extraction (bar- $\mu$ -SPE) to determine selected pharmaceutical compounds, i.e., metformin (MET), buformin (BUF), phenformin (PHEN), and propranolol (PROP) having varied lipophilicity in biological samples. In the EMLLE method, the aid of electric field was utilized to extract the pharmaceutical compounds across the interface between two immiscible electrolyte solutions (ITIES). ITIES formed when two bulk solvents aqueous phase (lithium chloride) and organic phase (1,2-dichloroethane), both containing electrolytes are brought into contact. Transfer potential for each analyte was analysed by voltammetry. The trend of transfer potential followed their lipophilicity; propranolol < phenformin < phenyl biguanide < metformin. Extraction of the analytes was performed by applying fixed potential to the biphasic system using potentiostat for 15 mins. The extraction performance was poor. Design of another ITIES cell and imposing interfacial potential by chemical polarization was done to enhance the extraction performance of this method. Thus, the EMLLE technique based on application of interfacial potential due to the presence of different concentrations of tetramethylammonium ion ( $\text{TMA}^+$ ) as common ion in each phase was studied. The optimum extraction conditions for this method are,  $[\text{TMA}^+]_o = 10 \text{ mM}$ ,  $[\text{TMA}^+]_w = 0.001 \text{ mM}$ ,  $V_{org} = 2 \text{ mL}$ ,  $pH_{sample} = 9$ , rotation speed = 900 rpm, extraction time = 600 s. The optimised parameters for back-extraction are:  $[\text{TMA}^+]_{back} = 50 \text{ mM}$ ,  $V_{final} = 0.1 \text{ mL}$ ,  $pH_{back} = 2$ . Nearly 100 % extraction of targeted analytes was achieved, and the enrichment factor obtained was up to ~ 60 for biguanide compounds. In the bar- $\mu$ -SPE method, adsorbent and a tiny metal rod was placed in a polypropylene membrane bag. Among the various adsorbents studied, graphene and zeolite showed some potential. Thus, extraction conditions were optimised for each adsorbent and adsorbent mixture. Despite the optimisations, the extraction was low (5.03-39.2 %). Nevertheless, enrichment factors of 1.49 -14.9 were obtained. Both proposed methods were applied to the determination of the analytes in urine. On the whole, the newly proposed methods are simple and markedly reduced consumption of organic solvents.

## RÉSUMÉ

Les méthodes classiques de préparation d'échantillons pour la détermination de composés polaires, telles que l'extraction liquide-liquide (LLE) et l'extraction en phase solide (SPE), ne sont généralement pas efficaces en raison de multiples étapes, d'une faible récupération et d'une consommation élevée de solvants organiques. Cette thèse traite du développement de nouvelles méthodes de préparation d'échantillons, à savoir l'extraction par voie liquide-liquide modulée électrochimiquement (EMLLE) et l'extraction bar-micro en phase solide (bar- $\mu$ -SPE) afin de déterminer les composés pharmaceutiques metformine (MET), buformine (BUF), phénformine (PHEN) et propranolol (PROP). Dans la méthode EMLLE, un champ électrique a été appliqué pour extraire les composés pharmaceutiques ionisés à travers l'interface entre deux solutions électrolytiques non miscibles (ITIES). Des ITIES se forment lorsque deux solvants en vrac en phase aqueuse (chlorure de lithium) et en phase organique (1, 2-dichloroéthane), contenant l'électrolyte, sont mis en contact. Le potentiel de transfert pour chaque analyte a été analysé par voltamétrie. Le potentiel de transfert varie avec leur lipophilie ; propranolol < phénformine < phényl biguanide < metformine. L'extraction des analytes a été réalisée en appliquant un potentiel fixe au système biphasique où l'aide d'une potentiostat pendant 15 minutes a donné des résultats médiocres. Une autre cellule de mesure et un potentiel interfacial obtenu par polarisation chimique ont été mis en œuvre pour améliorer les performances d'extraction de cette méthode. Ainsi nous avons étudié la technique EMLLE basée sur l'application d'un potentiel interfacial due à la présence de différentes concentrations en ion tétraméthylammonium ( $\text{TMA}^+$ ) en tant qu'ion commun à chaque phase. Les conditions optimales d'extraction pour cette méthode sont les suivantes :  $[\text{TMA}^+]_o = 10 \text{ mM}$ ,  $[\text{TMA}^+]_w = 0,001 \text{ mM}$ ,  $V_{org} = 2 \text{ mL}$ ,  $pH_{échantillon} = 9$ , vitesse de rotation = 900 rpm, temps d'extraction = 600 s. Les paramètres optimisés pour la rétro-extraction sont les suivants :  $[\text{TMA}^+]_{retour} = 50 \text{ mM}$ ,  $V_{final} = 0,1 \text{ mL}$ ,  $pH_{retour} = 2$ . Les analytes ciblés ont été extraits à près de 100% et le facteur d'enrichissement obtenu jusqu'à environ 60 fois pour les biguanides. Dans le procédé bar- $\mu$ -SPE, (un adsorbant et une tige métallique ont été placés dans un sac à membrane en polypropylène). Parmi divers adsorbants étudiés, le graphène et une zéolite se sont révélés intéressants. Ainsi, les conditions d'extraction ont été optimisées pour ces deux adsorbants seuls et en mélange. Malgré les optimisations, l'extraction bas (5,03-39,2 %). Néanmoins, des facteurs d'enrichissement de 1,49 à 14,9 ont été obtenus. Les deux méthodes proposées ont été appliquées à la détermination des analytes dans l'urine. Dans l'ensemble, les méthodes nouvellement proposées sont simples et réduisent considérablement la consommation de solvants organiques.